Development and Characterization of a Hybrid Biocomposite Material for Automobile Application

A thesis submitted in partial fulfilment of
the requirements for the degree of

Doctor of Philosophy

in

Mechanical Engineering

by

Mohit Mittal
2K16/Ph.D/ME/48

Under the supervision of

Prof. (Dr.) Rajiv Chaudhary
Department of Mechanical Engineering

Delhi Technological University, Delhi 110042

June, 2020

Department of Mechanical Engineering

Delhi Technological University, Delhi – 110042 (India)

CANDIDATE'S DECLARATION

I hereby declare that the work which is being presented here entitled, ***"Development and Characterization of a hybrid biocomposite material for automobile application"*** in partial fulfilment for the award of the degree of Ph.D submitted in the Mechanical Engineering Department at Delhi Technological University, Delhi (India) is an authentic record of my own work under the supervision of Prof. (Dr.) Rajiv Chaudhary. The matter presented in this dissertation has not been submitted by me in full or in part to any other University/Institute for the award of Ph.D degree.

I hereby further declare that in case of any legal dispute in my Ph.D dissertation, I will be solely responsible for the same.

Mohit Mittal Date: 21.06.2020

Student Registration Number: 2K16/Ph.D/ME/48

This is to certify that the above statement made by the candidate is correct to the best of our knowledge.

Dr. Rajiv Chaudhary
Supervisor and Professor
Delhi Technological University, Delhi

ABSTRACT

Environmental pollution, depletion of raw materials, high consumption of energy during the stage of material processing and high cost of raw & semi-finished materials are the major problems now a days. To get rid of all these problems, we will require utilizing progressively renewable resources based biocomposite materials in non-structural and structural applications. In recent years, the biocomposites are gaining popularity in automotive, aerospace, building & construction, packaging, and medical applications. For successful usage of biocomposites in the above-mentioned fields, it becomes necessary to design the material in such a way that it exhibits high strength with good resistance to flame propagation and moisture sorption. The thermo-mechanical properties of hybrid biocomposites are far better than the pure single fiber biocomposites and comparable to the synthetic fiber strengthened composites. Therefore, the major objective of this study is to fabricate a high performing hybrid biocomposite material.

The critical factors which significantly influence the characteristics of a hybrid composite are such as - inherent features of matrix and reinforcement, filament length, content, orientation, fiber-matrix adhesion, and morphology of the system. In this context, experimental studies have been carried out and presented in this dissertation. To determine the optimum fibers layering pattern, the various hybrid boards [Bilayer (Pineapple/Coir (P/C)); Trilayer (Pineapple/Coir/Pineapple (PCP), Coir/Pineapple/Coir (CPC)); and Intimately Mixed (IM)] were developed and characterized for flammability, viscoelastic properties, and water absorption behavior. The experimental observations revealed that the CPC material possesses higher resistance to burning and moisture absorption than the other patterns. Furthermore, the trilayer CPC composite has lower 'C' value, higher E', and the greater value of activation energy. As compared with PCP and bilayer (P/C) composites, the intimately mixed (IM) has a lower rate of burning, absorbs less water, the higher value of T_g, and broad width of tan δ peak.

In order to select the hybrid biocomposites over traditional materials, it becomes necessary to reinforce it with optimum fiber length and content. In this regard, sixteen samples of PALF/Epoxy and COIR/Epoxy composites of varying fiber volume content (17%, 23%, 34%, and 43%) and length (10, 15, 20, and 25 mm) were

made and characterized. Moreover, the impact of filament content (17%, 23%, 34%) on the viscoelastic behavior of composites has also been investigated. The experimental results proved that the optimum fiber content for PALF/Epoxy and COIR/Epoxy composites is 34% and 23% respectively.

Finally, an experimental study was performed in order to examine the impact of an alkaline treatment with relative reinforcement content on the mechanical properties and biodegradability of PALF/COIR based hybrid material. To accomplish the desired objectives, the biocomposite sheets were fabricated at 11 levels of COIR fiber loading (0, 10, 20, 30, 40, 50, 60, 70, 80, 90, 100 vol.%) with fixed total fiber content (40 vol.%). The physical and mechanical characteristics of developed specimens have been determined according to ASTM standard. The total of four samples for each specimen was tested and their average value was reported. The results showed that the P50-C50 hybrid composite exhibits the best set of mechanical properties and absorbs 62% and 32% less water than the pure PALF/Epoxy and COIR/Epoxy respectively. The mechanical strength and biodegradability of an epoxy thermoset were increased by the incorporation of cellulosic fibers which results in easy and smooth adoption of epoxy-based composite for the fabrication of interior components of an automobile.

PLAGIARISM

I declare that this thesis is my own work. I have appropriately referenced the work of other people that I have used. I have not and will not allow anyone to copy my work with the intention of passing it as his or her own work.

Mohit Mittal

Student Registration Number: 2K16/Ph.D/ME/48

Dedication

To my parents.....you raised me up.

ACKNOWLEDGMENT

I would like to express my sincere gratitude and appreciation to my supervisor, Prof. (Dr.) Rajiv Chaudhary for the valuable guidance, sage advice, encouragement, and support he provided all through my Ph.D programme. I would also like to thank Prof. (Dr.) R.C. Singh for his valuable comments and suggestions. I express my sincere thanks to Dr. Roli Purwar for her assistance. My appreciation goes to the staff in the Department of Mechanical Engineering who assisted me in so many ways. I would like to thank Central Scientific Instruments Organisation, Chandigarh (India) for providing me the characterisation facility.

I am deeply indebted to my family for guiding and encouraging me in applying for this Doctoral program. I extend my gratitude to all PhD students of Mechanical Engineering at Delhi Technological University, Delhi. I would like to sincerely thank Prof. (Dr.) Rajiv Chaudhary once again for providing me an opportunity to pursue PhD under his guidance. My parents and wife receive my deepest gratitude and love for their dedication and support. I have been fortunate to have many friends who cherish me and I thank them all for their support.

To my wife (Kanchan), I extend my gratitude. You have always been there cheering me up and standing by my side through good times and bad. I would also like to thank my dear parents, daughter (Divisha), sister (Mukta), and brother (Manish).

ABBREVIATIONS

PALF	-Pineapple leaf fiber
COIR	-Coconut husk fiber
PLA	-Polylactic acid
PHA	-Polyhydroxyalkanoates
PF	-Phenol formaldehyde
HDPE	-High density polyethylene
PVC	-Poly vinyl chloride
MOE	-Modulus of elasticity
NFRC	-Natural fiber reinforced composite
SFRCs	-Synthetic fiber reinforced composites
UPE	-Unsaturated polyester
KF	-Kenaf fiber
TPU	-Thermoplastic urethane
CD	-Cow dung
NBR	-Nitrile butadiene rubber
NaOH	-Sodium hydroxide
BC	-Bacterial Cellulose
RTM	-Resin transfer molding
CTE	-Coefficient of thermal expansion
DMTA	-Dynamic mechanical thermal analysis
TTI	-Total time to ignition
PHR	-Peak heat release rate
MLR	-Mass loss rate
CLS	-Coconut leaf sheath
UF	-Urea formaldehyde
LDI	-Lysine diisoyanate
IM	-Intimately mixed
GPG	-Glass/Pineapple/Glass
T_g	-Glass transition temperature
GF	-Glass fiber
V_f	-Volume fraction
SEBS	-Styrene ethylene butylene styrene

MA	-Maleic anhydride
BC	-Bamboo charcoal
Wt	-Weight
OPEFB	-Oil palm empty fruit bunch fiber
J_w	-Woven jute fiber
E’	-Storage modulus
GMT	-Glass mat thermoplastic
ABS	-Acrylonitrile butadiene styrene`
PP	-Polypropylene
DP	-Degree of polymerization
deg	-Degree
TGA	-Thermogravimetric analysis
FTIR	-Fourier transform infrared spectroscopy
XPS	-X-ray photoelectron spectroscopy
ESEM	-Environment scanning electron microscope
DMA	-Dynamic mechanical analysis
HF	-Hemp fiber
PA	-Polyamide
MAHgPP	-Maleic anhydride grafted polypropylene
EP	-Epoxy
PE	-Polyethylene
PO	-Polyolefin
DGEBA	-Diglycidyl bisphenol A
TETA	-Triethylene tetraamine
SEM	-Scanning electron microscopy
ASTM	-American society of testing and materials
UL-94V	-Underwriters laboratory-94 vertical
UL-94HB	-Underwriters laboratory-94 horizontal burning
kV	-Kilovolt
PMCs	-Polymer matrix composites
UTM	-Universal testing machine
kgf	-Kilogram force
-OH	-Hydroxyl
DTG	-Derivative thermogravimetric

SCB	-Sugar cane bagasse
BPS	-Banana pseudo stem
C=O	-Carbonyl
CF-EP	-Coir fiber-epoxy composite
PF-EP	-Pineapple fiber-epoxy composite
E''	-Loss modulus
T_P	-Peak decomposition temperature
CF	-Coir fiber
PF	-Pineapple leaf fiber
R_m	-Residual mass
Tan δ	-Damping factor
V_c	-Volume of composite
V_f	-Volume of fibers in a composite
CPC	-Coir/Pineapple/Coir
PCP	-Pineapple/Coir/Pineapple
P/C	-Pineapple/Coir
l/d	-Aspect ratio
g/cc	-Gram per centimetre cube
HRm	-Rockwell hardness at m scale
SMC	-Sheet molding compound
PS	-Polystyrene
xGnP	-Graphene nanoplatelets
GFRP	-Glass fiber reinforced plastic
SiC	-Silicon Carbide
Al_2O_3	-Alumina
PBS	-Polybutylene succinate
BF	-Banana fiber
SG	-Snake grass
EMS	-Epoxidized methyl soyate
µm	-Micrometer
MPa	-Mega Pascal
GPa	-Giga Pascal
APS	-Ammonium Persulphate
PMCs	-Polymer matrix composites

LIST OF FIGURES

LIST OF TABLES

TABLE OF CONTENTS

LIST OF PUBLICATIONS

Journal Publications

I. **Mittal M** and Chaudhary R (2019) Experimental investigation on the mechanical properties and water absorption behavior of randomly oriented short pineapple/coir fiber reinforced hybrid epoxy composites *Mat. Res. Express*. 6(1), http://doi.org/10.1088/2053-1591/aae944.

II. **Mittal M** and Chaudhary R (2019) Biodegradability and mechanical properties of Pineapple leaf/Coir fiber reinforced hybrid epoxy composites *Mat. Res. Express*. 6(4), http://doi.org/10.1088/2053-1591/aaf8d6.

III. **Mittal M** and Chaudhary R (2018) Effect of fiber content on thermal behavior and viscoelastic properties of PALF/Epoxy and COIR/Epoxy composites *Mat. Res. Express*. 5, http://doi.org/10.1088/2053-1591/aae274.

IV. **Mittal M** and Chaudhary R (2018) Experimental study on the water absorption and surface characteristics of alkali treated pineapple leaf fibre and coconut husk fibre *Int. J. Appl. Eng. Res.* 13, 12237-43.

V. **Mittal M** and Chaudhary R (2018) Development of PALF/Glass and COIR/Glass fiber reinforced hybrid epoxy composites *J. Mat. Sci. Surf. Eng.* 6(5), 851-861, http://doi.org/10.jmsse/2348-8956/6-5.1**.**

VI. **Mittal M** and Chaudhary R (2019) Experimental study on thermal behavior of untreated and alkali-treated pineapple leaf fiber and coconut husk fiber *Int. J. Appl. Sci. Eng.* 76(1), 01-16, http://doi.org/10.30954/2322-0465.1.2019.1.

VII. **Mittal M** and Chaudhary R (2018) Effect of alkali treatment on the water absorption of pineapple leaf fiber *Int. J. Tech. Innov. Mod. Eng. Sci.* 12(4), 300-305**.**

VIII. **Mittal M** and Chaudhary R (2019) Effect of layering pattern on flammability and water absorption behavior of Pineapple leaf/Coir fiber-reinforced hybrid epoxy composites *J Mat. Sci.* 7(1), 44-54**.**

IX. **Mittal M** and Chaudhary R (2017) Effect of Glass Fiber on the Mechanical Properties of Hybrid Biocomposites: A Review *Int. J. Res. Appl. Sci. Eng. Tech*. 5, 937-947, http://doi.org/10.22214/ijraset.2017.10134.

X. **Mittal M** and Chaudhary R (2017) Effective Approach to Overcome the Problem of Thermal Degradability in NFRC is Flame Retardants: A Review *Int. J. Res*. 4, 544-556.

XI. **Mittal M** and Chaudhary R (2017) Factors affecting the Performance of Biocomposites, *Int. J. Res*. 4, 749-758.

XII. **Mittal M** and Chaudhary R (2017) Effect of Fiber Surface Treatment on Mechanical Properties of Biocomposites: A Review Int. J. Res. Appl. Sci. Eng. Tech. 5, 1992-2005, http://doi.org/10.22214/ijraset.2017.10292.

XIII. **Mittal M** and Chaudhary R Effect of layering pattern and fiber hybridization on viscoelastic properties of randomly oriented short pineapple and coir fiber-reinforced epoxy composites *J. Mech. Eng. Sci.* **(Under peer –review).**

Conference Papers

I. **Mittal M** and Chaudhary, R (2018) Effect of alkaline treatment on the thermal stability of pineapple leaf fibers *International Conference on Advanced Production and Industrial Engineering* DTU, Delhi.

II. **Mittal M** and Chaudhary R (2016) Optimization of Interfacial adhesion between natural fiber and polymer resin: A Review *International Conference on Advanced Production and Industrial Engineering* DTU, Delhi.

III. Jain V, **Mittal M**, and Chaudhary R (2020) Design optimization and analysis of car bumper with implementation of hybrid biocomposite material *8th International Conference Fusion of Science and Technology* (ISFT) YMCA, Faridabad.

IV. **Mittal M** and Chaudhary R (2020) Effect of fiber length and content on the mechanical properties of pineapple leaf fiber reinforced epoxy composites *International Conference on Advances in Material Science & Mechanical Engineering* (ICAMSME), Andhra Pradesh (India).

Book Chapters

I. **Mittal M** and Chaudhary R (2019) Effect of fiber length and content on mechanical and water absorption behavior of coir fiber-epoxy composite *Adv. Eng. Res. Appl.* 11, 80-100.

II. **Mittal M** and Chaudhary R (2019) Experimental study on the water absorption and surface characteristics of alkali-treated pineapple leaf fiber and coconut husk fiber *Adv. Eng. Res. Appl.* 11, 101-115.

CHAPTER 1 - INTRODUCTION

"Depletion of petroleum resources, persistence of plastics in the environment, concerns over global climatic change and shortage of landfill space has spurred efforts to find new materials that are more compatible with the environment"

This thesis is concerned with the development of a biocomposite material that offers a path to achieve a constructive equilibrium among economy, ecology, and technology. It also depicts the significance of lignocellulosic fibers as strengthening agent in polymer based material.

1.1 Motivation and Background

The idea of making composite materials comes from their attractive and tailor-made properties. Such materials often result in lightweight structures at low cost which leads to increase their usage in various parts of our lives and for the manufacturing of highly sophisticated machines such as automobiles, aerospace structures, electronic components, railway coaches, and mechanical systems like pressure vessels, brakes, drive shafts, tanks, and flywheel, etc.

A composite is a multiphase material, displays the noteworthy mixing of properties that can't be achieved by the ordinary amalgams, earthenware production, and polymeric materials. The synthetic filaments like glass, carbon, aramid, aluminium oxide, boron strands, and so on are broadly utilized in polymer based materials because of their high strength & hardness, wear obstruction, and high toughness. However, these filaments have significant disadvantages in terms of supportability, eco-effectiveness, and green science. Therefore, it gets important to supplant the conventional fibers with characteristic ones in polymer composites.

The exhaustion of oil assets and expanding ecological mindfulness constrained the researchers to move their consideration from engineered strands to natural filaments [1-2]. The regular fibers possess wide varieties of advantageous features such as low price and density; serious explicit mechanical properties; excellent acoustic, thermal, and electrical insulating properties; non-abrasive to molding and mixing equipment; carbon dioxide sequestration; sustainability, biodegradability and recyclability [3-4]. Among a wide range of cellulosic fibers (vegetable strands, creature strands, reused strands, and mineral strands), the plant-based are generally used in composite world.

They offer a genuine answer for supplant the normally utilized engineered fibers, as a result of their great mechanical properties, rich accessibility and issue free removal. [5-6]. The cellulosic fibers (wood or non-wood types) consist of bundles of fibrils that are held together by binding agents (predominantly lignin and hemicellulose). The properties of fibers are significantly reliant on the number of fiber cells, cell wall thickness, microfibrillar angle, cellulose content, molecular structure, and cellulose crystallinity index [7-8].

Among all the plant-based fibers (kenaf, jute, coir, flax, sisal, banana, bagasse, pineapple leaf fiber, etc.), the coconut husk (COIR) and pineapple leaf (PALF) have significant potential to be employ as strengthening additive in fiber or powder form [9-10]. According to the statistical database (2016) of the "Food and Agriculture Organization", the total production of coconut and pineapple fruit in the whole world is 59 and 25.8 million tonnes respectively [11]. Therefore, the challenging job is to reduce their waste disposal in landfill areas and to utilize them efficiently.

The PALF and COIR are multi-cellular fibers, extracted from the leaves of pineapple (*Ananas-comosus*) and the husk of coconut fruit (*Cocos-nucifera*) respectively. The PALF contains high cellulose (70%-85%) while COIR contains high lignin (40-45%) content which results in PALF shows high tensile and flexural properties whereas the COIR shows high impact strength [12]. Moreover, the COIR fiber exhibits good resistance to salt, water, microbial, and fungus attack. So to combine their properties synergistically, it becomes necessary to incorporate both kinds of fiber in the same polymer matrix which can lead to the formation of multifunctional biocomposite material. Such kind of multi fibers reinforced polymeric materials are commonly called “Hybrid composites”. To the best of my knowledge, there has been no report on hybrid composite which was reinforced with PALF and COIR fibers.

The incorporation of more than one kind of reinforcement in a particular resin leads to the high strength material with improved fracture toughness, and better creep & fatigue properties. Many works in the literature report the positive attributes of fiber hybridization. The failure of one kind of fiber can be overcome by the hybridization with a suitable type of other fiber. In most of the cases, the hybrid composite possesses comparable performance to that of synthetic fiber-reinforced material. A

high-performance structural material can be developed at a low cost by employing the hybridization concept [13-14].

Biocomposites offer a way to accomplish eco-accommodating material in the 21st century. However, the need to produce 100% bio-based materials alternative for oil based isn't prompt. Biocomposites that contain a noteworthy substance of bio-based materials can currently accomplish this at a moderate cost-execution proportion to rival oil based materials. The selection of thermoset polymer as a matrix resin leads to the high performing structural material for outdoor applications [15]. The epoxy is an appropriate matrix for use in primary construction and marine industry. This was because of its high mechanical and electrical properties; good resistance to chemicals, moisture, and environmental degradation; low viscosity with easy processing; and good adhesive properties.

The most profitable property of epoxies is their low shrinkage during cure which minimizes internal stresses. As compared with thermoplastic polymers, the thermosets have better fire retardancy. Polymers such as epoxy, polyester, and phenolics formed char during pyrolysis which acts as a heat barrier between the heat source and the lower surface of a polymer. These aspects propel the researchers to select thermoset polymer as a matrix resin [16]. Among all the matrix resins (thermoset, thermoplastic starch, and polyolefin's), the epoxy system offers the best performance of all and shows improved adhesive properties which makes it a competitive material as a matrix.

Despite large number of advantageous properties of lignocellulosic fibers, they are far from an easy selection in structural applications. It was due to their hydrophilic nature, low thermal stability during processing, high variability in their properties, and poor interfacial adhesion with synthetic polymers [17-19]. To overcome these problems, it becomes necessary to alter the surface chemistry of natural fibers using the chemical treatment process. In order to accomplish this, the chemical processes such as alkali treatment, acetylation, methylation, permanganate treatment, cyanoethylation, etc. are widely used. Among all the methods, the alkaline treatment is a cost-effective modification technique to improve the fiber-matrix compatibility [20-21].

1.2 Purpose of the Study

The central purpose was to develop and characterize the PALF/COIR fiber reinforced hybrid epoxy composite for automobile applications.

1.3 Aim of the Study

The primary aim is to develop a high-performance biobased material for the automobile sector which is consistent regarding new enactment executed by the Indian government.

The specific objectives are as follows:

- To evaluate the thermal and water absorption behavior of PALF and COIR fibers.
- To investigate the effect of mercerization on surface chemistry, surface morphology, thermal stability, and hydrophilic behavior of cellulosic fibers.
- To determine the influence of fiber span and loading vol.% on mechanical characteristics of PALF-Epoxy and COIR-Epoxy composites.
- To examine the influence of fiber volume fraction on thermal stability and viscoelastic behavior of developed composites.
- To evaluate the impact of relative fiber content on physical, mechanical, and biodegradation characteristics of PALF/COIR hybrid composites.
- To examine the effect of fibers layering pattern on flammability, viscoelastic characteristics, and water uptake capacity of strengthened composites.
- To examine the influence of mercerization on biodegradability of hybrid material.
- To study the biodegradability of biocomposites in the natural soil environment.

1.4 Delimitations of the Study

- Both fibers (PALF and COIR) were collected from Kerala (India) only.
- The matrix resin is not a “green bio-resin”.
- Manual hand lay-up technique was used to synthesize the biocomposite materials which may lead to the non-uniform wetting of fibers.

1.5 Division of the Work

This work is divided into six main chapters:

Chap. 1 shows the motivation for doing research in the field of biocomposites. It includes the drawbacks of synthetic fiber-reinforced composites (SFRCs) and the positive attributes of biocomposites. It also presents the main objectives and delimitations of the study.

Chap. 2 presents a survey of past research outlining fiber reinforced polymer composites. It includes the work on hybrid composites, development of biocomposites and its applications. A review on natural fibers is mentioned, in specific pineapple leaf and coir fibers. The impact of several parameters on the properties of composites is also reported in this chapter.

Chap. 3 consist the research design and methodology. It incorporates the detail depiction of raw materials, fabrication and chemical treatment techniques, and hypothesis behind the test.

Chap. 4 discusses the experimental results obtained after the testing of natural fibers and their composites.

Chap. 5 includes the possible uses of developed hybrid biocomposite in automobile application.

Chap. 6 will present conclusions based on the significant findings. It also includes the suggestions for future work in this field.

CHAPTER 2 - LITERATURE REVIEW

In the recent chapter, a survey of the past research work is presented. This chapter includes the classification, composition, properties, and structure of natural fibers and matrix material. It also presents the studies on hybrid biocomposites and accounts the impact of different parameters influencing the performance of biocomposites examined by various researchers. In the finishing segment, the information gap in prior examinations and the targets of the present research work is illustrated.

2.1 Introduction

Composite materials have been utilized for a considerable length of time going back to around 2500 years ago. Throughout the most recent years, there has been an expanded utilization of composites in many of our modern technologies and this was because of their numerous profitable properties [22]. Mathews and Rawlings reported that the composites possess low solidity, high specific strength, and abrasion opposition characteristics which make it attractive in aviation, underwater, and transportation industries. [23].

It is a multiphase material that displays a considerable share of the properties of both constituents' phases. The two main constituents are matrix material (polymer) and reinforcement [24]. The mechanical response of composite material is the aggregate impact of reinforcing fibers and matrix resin (Fig. 2.1). Generally, it is made artificially as opposed to one that occurs naturally. There are also a number of composites that occur in nature. For example, Bone is a composite of the strong protein collagen and the hard apatite substance.

The composite materials are using in immense variety of applications ranges from day to day common uses to highly sophisticated machines such as automobiles, aerospace structure, electronic components, railway coaches, and combustion engines. It advertises a multibillion-dollar business market and 31% of this is ruled by the automotive sector (Fig. 2.2) [25]. Mapleston [26] reported that the automakers were first sawed the potential of biocomposite material over conventional materials to use in interior components of an automobile.

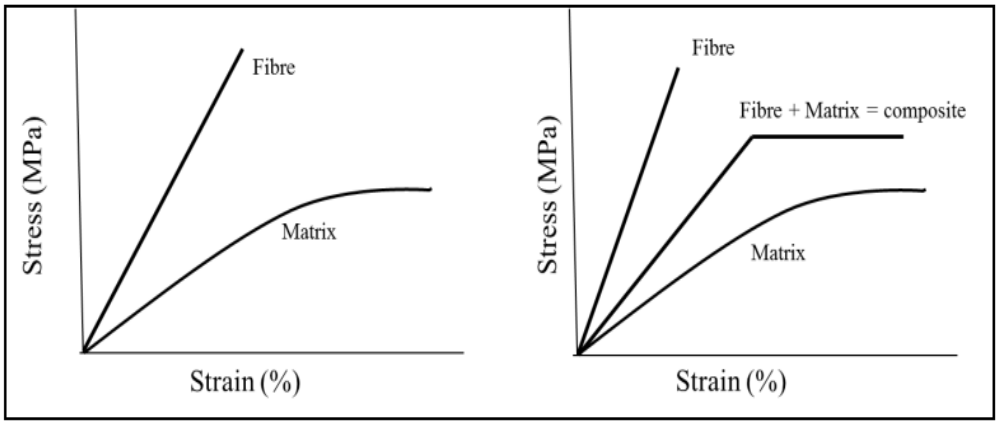

Fig. 2.1: Aggregate impact of loading fiber to the matrix

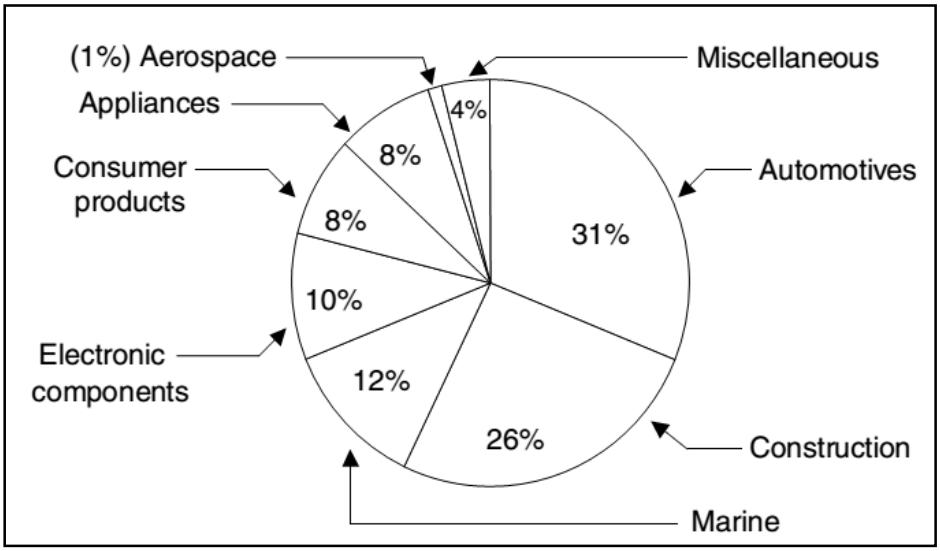

Fig. 2.2: Fiber strengthened composites utilized in various applications

2.2 Biocomposites

Biocomposite is a material made from natural fiber and oil inferred polymers or biopolymers (Fig. 2.3). G. Koronis *et al.* [27] reported that the biodegradability is a major problem to successfully employ green composites (100% biodegradable) in automobile body panels. Therefore, to produce 100% bio-originated material as a substitute for synthetic materials is not instant. The partially biodegradable materials can fight with oil inferred polymers at an affordable cost-performance ratio.

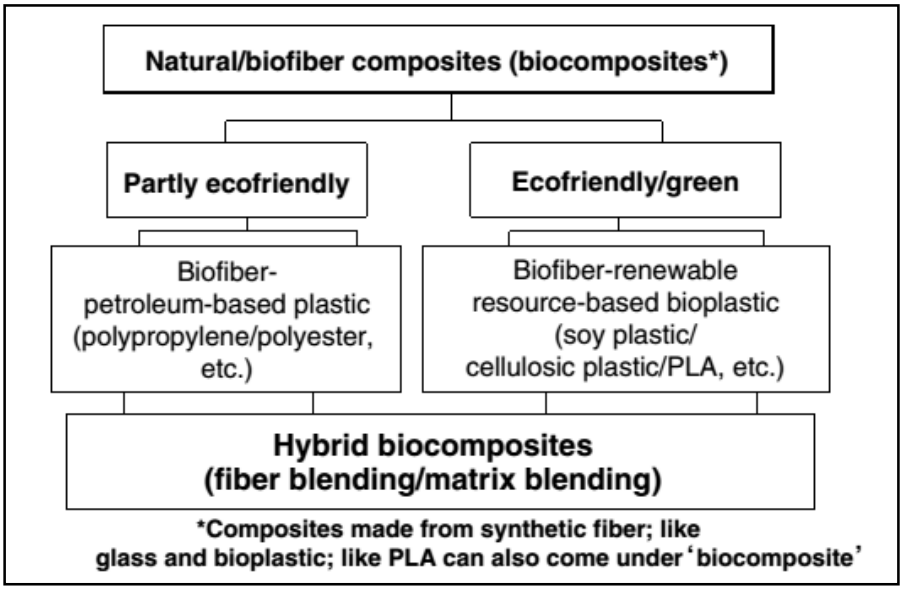

Fig. 2.3: Organization of biocomposites

Wedin *et al.* [28] stated that the biocomposites based on synthetic polymers can be a viable alternative to glass fiber reinforced plastics (GFRPs). Mohanty *et al.* [29] stated that the natural fiber filled thermoset composites shows comparable mechanical performance to GFRP. According to Mohanty *et al.* [30], biocomposites are the material of the 21st century and be a fractional answer for some worldwide natural issues. A few analysts have added to the information bank of biocomposites. Mohanty *et al.* [31] reviewed the opportunities and challenges associated with the application of biocomposite materials in engineering applications. H. M. Akil [32] reviewed the kenaf fiber filled composites regarding their market, fabricating techniques, and overall properties. Mohanty *et al.* [33] have reviewed NFRCs and reported that the straw fibers obtained from rice, wheat, and corn can be used as very inexpensive reinforcement for biocomposites. S. Kalia [34] presented a book on lignocellulosic composite materials. G. George *et al.* [35] have reviewed the properties and applications of green composites. A.N Nakagaito *et al.* [36] investigated the thermo-mechanical properties of biocomposites. L.T Drzal *et al.* [37] reviewed the different aspects of biocomposite materials as a substitute to oil-based composites for automobile sector. Fowler *et al.* [38] reviewed the technology, limitations, barriers, and drives of biocomposite material.

Fig. 2.4 illustrates the tri-cornered approach for designing the high performance biocomposites. Mohanty *et al.* [39] reported that a suitable blend of biofibers can make a composite of excellent tensile and flexural properties with better impact

toughness. R. Malkapuram *et al*. [40] stated that the performance of a composite is notably affected by the interfacial interaction between constituent elements. They reviewed a range of surface treatment techniques for the improvement of fiber-matrix interaction.

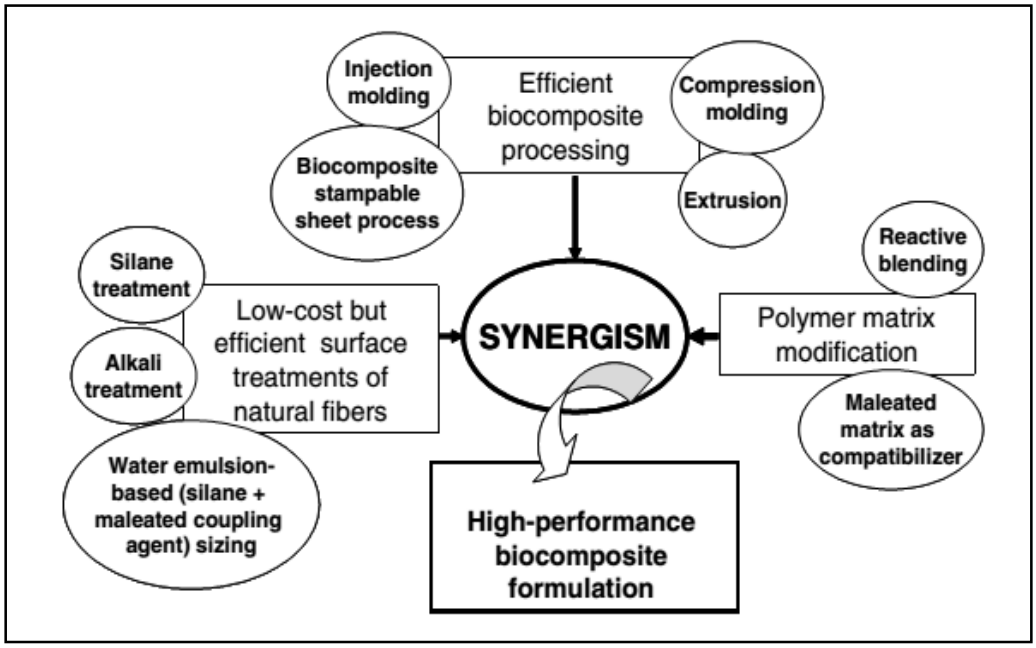

Fig. 2.4: Tri-corner approach in designing the high-performance biocomposites

2.2.1 Application of Biocomposites

The biocomposite materials are utilized in a wide assortment of applications (Fig. 2.5). F. Namvar *et al.* [41] reported that the biocomposites are used in biomedical applications, for example, medicate/quality conveyance, tissue designing, orthopedics, and restorative orthodontics. The report of Daimler Chrysler showed that the biocomposites are extensively used in making interior components of an automobile [42]. Automakers will see potential in biocomposites [43-44]. According to Broge [45], the biocomposites can diminish the mass of automobile parts and lower the power required for construction by 80% as compared to glass composites.

Numerous European enterprises are eco-driven; particularly the car ventures are attempting to make each segment recyclable. All the significant vehicle makers in Germany exploit NFRCs in interior applications such as boot lining, side and back door panel, seat backs. In 2000, Audi propelled A2 midrange vehicle in which entryway trim boards were made of flax/sisal reinforced PU composite. These boards not just an amazingly low mass but also of high-dimensional stability. Daimler

Chrysler has utilized flax and hemp rather than glass strands [46]. The Mercedes-Benz firstly used NFRC in the production of exterior components. However, the uses of biocomposites are mainly limited to low strength interior components.

Biocomposites can also be used as an alternative to building materials, especially as wood substitutes. Satyanarayana *et al.* [47] reported that the coir/polyester composite has received considerable attention for the formation of post office boxes, helmets, bunker houses, and roofing sheets. The Coir/Phenolic composite can be used for the manufacture of flush door shutters.

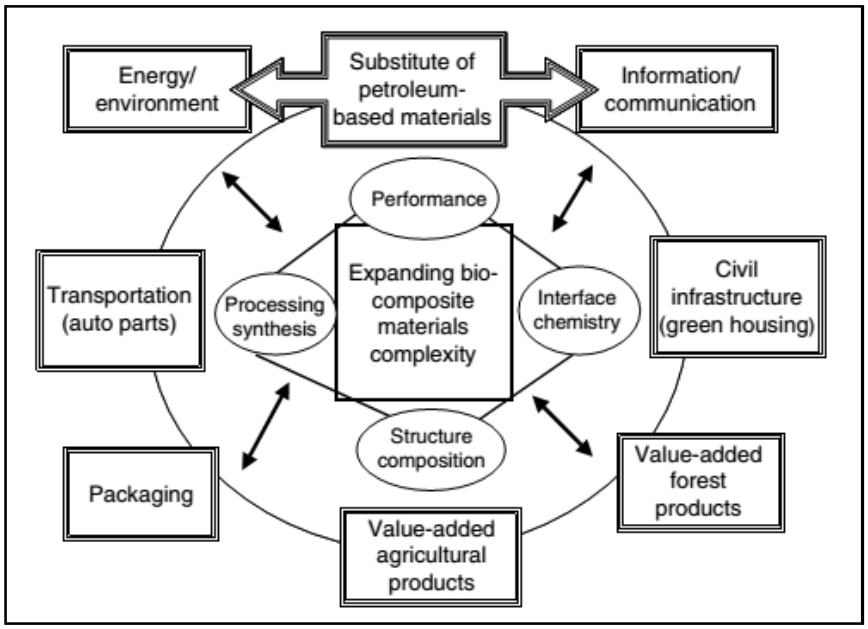

Fig. 2.5: Real-world applications of biocomposite materials

2.2.2 Mechanical Behavior of NFRCs

Misra *et al.* [48] observed that the tensile strength of plastic was increased by 150% after the incorporation of 50 wt% jute fiber. S. Ozturk *et al.* [49] stated that the optimum reinforcement volume in Kenaf/PF and Fibrefrax/PF materials is 43% and 36% respectively. C.U Maheshwari *et al.* [50] explored the impact of fiber modification and loading % on the mechanical behavior of tamarind strengthened UPE material and reported on that the composite of 25 wt% treated fiber has superior mechanical performance as compared to the other compositions. N. Venkateshwaran *et al.* [51] stated that the optimal fiber span and content for Banana/Epoxy are 15 mm & 16 wt% respectively. X. Zhao *et al.* [52] stated that the tensile properties of HDPE polymer were increased appreciably by the addition of only 10 wt% sisal fibers.

Mohanty *et al.* [53] have made Bamboo fiber-reinforced-HDPE composites by injection molding technique and reported the elevation in mechanical strength with the increase of reinforcement content up to 30 wt%. V. Alvarez *et al.* [54] determined the optimum fiber volume fraction in sisal fiber based composites in terms of the mechanical properties. J.L Leblanc *et al.* [55] reported that the complex modulus of PVC was improved by the incorporation of green coconut strands. Sezgin *et al.* [56] stated that the tensile, bending, and impact strengths of Jute-Polyester were enhanced by 25%, 100%, and 340% respectively with the increase of jute fabric plies from four to eight. M.C.N Yemele *et al.* [57] checked the impact of black spruce bark filler on the mechanical performance of Bark/HDPE material. G. Romhany *et al*. [58] revealed the critical improvement in the rigidity of starch plastic by the incorporation of 40 wt% flax fiber. A. Sbiai *et al*. [59] considered the impact of fiber length on the performance of date palm fiber/epoxy material and revealed that the composite of short strands has higher strength than the long filaments. The mechanical properties of an epoxy polymer were increased significantly after the loading of short date palm fibers. W. Mohamed *et al*. [60] evaluated the performance characteristics of Mengkuang strengthened natural rubber composites. G. Rajeshkumar *et al*. [61] analyzed the impact of filler content (0%, 10%, 20%, 30%, 40%, and 50%) and size (300 μm particles, 10mm, 20mm, 30mm) on characteristics of phoenix sp. strengthened epoxy material and observed that the composites of 40% fiber volume possess maximum strength. Among all the samples, the composites of 300 μm particle possess excellent impact toughness and the lowest water absorption. C. Capela *et al.* [62] revealed that short fiber is an effective reinforcement in strengthening and toughening the polymeric materials. K. Kumar *et al*. [63] considered the viscoelastic characteristics of Malvaceae strengthened UPE composites. J. Margem *et al*. [64] checked the potential of Malva strands as reinforcement in polymer matrix composites and reported on that the flexural rupture strength of an epoxy matrix was improved linearly with an enlarge of reinforcement content up to 30 vol%. MK Gupta *et al*. [65] have reviewed the viscoelastic characteristics of NFRCs in their review article. Y.A. El-Shekeil *et al*. [66] explored the impact of fiber loading (20%, 30%, 40%, and 50%) on the thermo-mechanical behavior of Kenaf/PU material and reported on that the composite of 30% fiber content exhibited an optimum set of mechanical properties. S. Varghese *et al.* [67] researched the impact of reinforcement weight percentage, direction, and interfacial

grip on the viscoelastic feature of natural rubber based strengthened composites. M. Botev *et al*. [68] have examined the thermo-mechanical properties of Basalt-PP materials. M.S Teja *et al*. [69] analyzed the impact of SiC filler addition (0%, 5%, and 10%) on performance of Sisal/UPE material and observed that the composite with 10% SiC exhibits 2.53 and 1.73 times greater tensile and impact strength respectively than the composite of without SiC. K.L Pickering *et al.* [70] stated that the properties of composites is significantly influenced by the chemical treatment of fiber, relative fiber-matrix volume content, and curing time of matrix resin. C. Ganesan *et al*. [71] compared different types of fibers (sawdust, straw, rice husk, and bagasse) and found that the sawdust fiber-based materials have better strength than the other strengthened ones. Y. A. El-Shekeil *et al*. [72] focussed the impact of filler wt% on mechanical characteristics of PVC/TPU/KF material and found the reduction in tensile strength and strain, while elevation in tensile modulus with the increase of kenaf fiber content. Ray *et al*. [73] evaluated the viscoelastic behavior of Jute/Vinyl Ester and observed the increment in E' with the elevation of jute wt.%. Furthermore, the glass transition temperature (T_g) of vinyl ester resin was moved to a elevated temperature with the augment of fiber volume fraction. M. Yusefi *et al.* [74] confirmed the enhancement in flexural properties of PLA polymer after the incorporation of cow dung (CD) particles. Moreover, the incorporation of cow dung led to an overall decline in the thermal stability of the biocomposites. KMD Mazharuddin *et al*. [75] have prepared and characterized the composite materials (Rose Madder/Epoxy and Silk Orchid/Epoxy) with different fiber weight (5, 10, 15, 20 gms) and reported the increment in their impact strength with the increase of filler weight fraction. M. Assarar *et al*. [76] considered the role of water aging on mechanical features of flax filled material and reported on that the tensile strength was reduced, whereas the tensile modulus and failure strain were not affected significantly after water aging. J. Giancaspro *et al.* [77] have developed the biocomposite board by using sawdust fibers and investigated for compression and flexural strength.

Even a lot of study has been done in the field of biocomposites but very few works are available on PALF and COIR filled thermoset composites. A.L Leao *et al*. [78] have reviewed the various aspects of pineapple leaf fiber and reported that the fiber has significant potential to reinforce thermoplastics and thermosetting polymers for

developing low cost and lightweight composites. U. Wisittanawat *et al*. [79] observed the increment in tear and tensile strength of NBR to 100kN/mm and 10 MPa respectively by the loading of 30% pineapple leaf fiber. A. Kalapakdee *et al*. [80] considered the mechanical properties of specially aligned PALF strengthened composites and noticed the considerable rise in their tear strength and stiffness with the amplification of PALF content. O.O Daramola *et al.* [81] reported that the tensile strength, MOE, and moisture sorption of PALF/UPE were increased with the enhance of PALF wt.%. The optimum bending properties were obtained at 20 wt% PALF content. M. Bohra *et al*. [82] examined the impact of strand vol.% (5%, 15%, and 25%) on the characteristic of PALF filled HDPE material and observed the reduction in tensile strength and hardness with enhance of PALF content. D. Verma *et al*. [83] have checked the capability of COIR as strengthening filler in composite materials. P. Naveen *et al*. [84] reported that the coir fibers can be utilized in non-structural and structural applications. Rout *et al*. [85] declared the significant rise in strength of UPE matrix by the incorporation of 25 wt% coir fiber. P. Pradeep *et al*. [86] reported that the palm-based composite has superior properties and can be utilized for the fabrication of lightweight high strength automobile parts. N.P.G. Suardana *et al*. [87] checked the impact of mercerization on the water sorption affinity of coir filled PLA material. They found that the NaOH treated ones absorb more water which caused its tensile and flexural strength dropped drastically. G. Das *et al*. [88] checked the role of fiber parameters on the performance of Coir/Epoxy material. S. Nallusamy *et al.* [89] assessed the mechanical properties of bone and seashell powder reinforced coir fiber composites. G. Das *et al*. [90] examined the physical and mechanical characteristics of Coir/Epoxy composite filled with Al_2O_3 particulates.

2.2.3 Thermal and Moisture Sorption Properties of NFRCs

BA Muralidhar [91] observed the reduction in thermal stability of epoxy polymer after the inclusion of flax woven and knitted preforms. The woven preform reinforced composite has higher storage modulus than the knitted one. Y.Z Wan *et al.* [92] concluded that the presence of bacterial cellulose (BC) nanofibres improves the tensile properties and resistance to moisture absorption of starch polymer. A. Singh *et al*. [93] stated that the tensile properties of CF-HDPE material were reduced in humid environment. E. Osman *et al*. [94] checked the role of filler weight fraction

and temperature (25 ^{0}C and 50 ^{0}C) on the moisture uptake capacity of Kenaf-PE composites. E. Munoz *et al*. [95] reported that the flax fiber/bio-epoxy composite developed by the RTM process has significant ability to be employed in outdoor applications. K. Padal *et al.* [96] reported that the jute nanofiber improves the crystallization temperature and thermal degradation temperature of epoxy matrix. Y. Nishitani *et al*. [97] reported that the hemp fibers are very effective to improve the thermal and mechanical characteristics of plant-derived polyamide 1010 polymeric resin. A. Nakagaito *et al.* [98] studied the thermo-mechanical properties of biocomposites based on micro-fibrillated cellulose. Y. Song *et al*. [99] examined the thermal and viscoelastic properties of woven hemp strengthened PLA material and reported that the twill weaved hemp fabric composite exhibits better thermal, mechanical, and viscoelastic behavior than the plain-woven hemp composite. M.J. John *et al.* [100] evaluated the viscoelastic properties of Flax/PP material and observed the increment in thermal stability and storage modulus of polypropylene by the incorporation of flax fiber. P. Niu *et al*. [101] stated the positive shift of onset temperature and maximum decomposition temperature of polypropylene matrix to a higher value by the incorporation of hemp fiber. C. Costa *et al*. [102] also discussed the viscoelastic characteristics of NFRCs. M. Salazar *et al.* [103] declared the increment in tensile strength, bending strength, and T_g of epoxy resin by the incorporation of nonwoven industrial fique fiber mats. M. Tajvidi *et al*. [104] considered the influence of fiber weight fraction, fiber type, compatibilizer, and heating rate on thermogravimetric characteristics of cellulosic fillers strengthened HDPE material. M. Tajvidi *et al*. [105] compared the thermal stability of various natural fibers (wood flour, kenaf, rice hulls, and newspaper) filled PP composites.

2.2.4 Flammability of Biocomposites

Flammability is a censorious matter particularly in the area of change where little spaces make fires a recognizable danger. The flammability of composite material is different from the components and is greatly depends on the structure of composite and adhesion between the reinforcement and matrix. Hshieh *et al.* [106] and Brown *et al.* [107] stated that the certain combinations have lower flammability, whereas others may higher than their components. W.D. Schindler *et al*. [108] stated that the flammability of composites is a consequence of the "scaffolding effect" where the liquid decomposition products from the polymer are held in contact with the heat

source by the fiber support. Helwig *et al*. [109] investigated the flammability of Flax/PP material. Borysiak *et al*. [110] observed that the composites had a shorter TTI, lower PHR, and MLR as compared to unfilled polypropylene. Kandola *et al*. [111] stated that the burning behavior of a composite not just a component of the properties of resin and reinforcement but also depends on the synergistic or antagonistic effects between them. K.N. Bharath *et al*. [112] considered the flammability of CLS fiber strengthened phenol formaldehyde composites and reported on that the 5% NaOH treated composite requires more oxygen to burn than the untreated composite material. After an alkaline treatment, the mass loss and rate of flame propagation were decreased. Waldman *et al*. [113] stated that the improved compatibilization between constituent elements direct the augment of thermal solidity and activation energy for decomposition. Albano *et al*. [114] found that the acetylated composite exhibits higher thermal stability than the untreated Sisal-Polyolefin one.

Flammability of a material is highly affected by the fire intensity or incident heat flux. Fig. 2.6 illustrated the stages of a typical fire [115-117]. C.R. Rajeesh *et al*. [118] reported that the flammability, flame penetration, and rate of burning of medium density coir fiber board were decreased after the chemical treatment with an aqueous solution containing borax and boric acid. Suardana *et al*. [119] stated the improvement in thermal stability of biocomposites by the incorporation of flame retardants. As compared to thermoplastics, the thermoset matrix resin exhibits better fire retardancy and this was because of its highly cross-linked network structure. According to Mark *et al*. [120] and Mouritz *et al*. [121], the polymers undergo thermal-oxidative decomposition on exposure to heat which results in the generation of hydrocarbons, non-combustible residues, solid particles (smoke), and toxic volatiles. During thermal-oxidative decomposition, the combustible gases combine with oxygen which results in the formation of reactive $\mathbf{H^{\cdot}}$ and $\mathbf{OH^{\cdot}}$ radicals. These are engaged in further disintegration and the supported burning of the polymer. In most of the thermoset polymers, a significant amount of physical transformation occurs before melting such as glass transition; thermal decomposition; change in viscosity, thermal and electric conductivity, density, and modulus [122]. Polymers such as epoxy, polyester, and phenolics can form char during pyrolysis which act as

a hindrance between the heat source and polymer. These aspects propel the researchers to select thermoset polymer as a matrix resin.

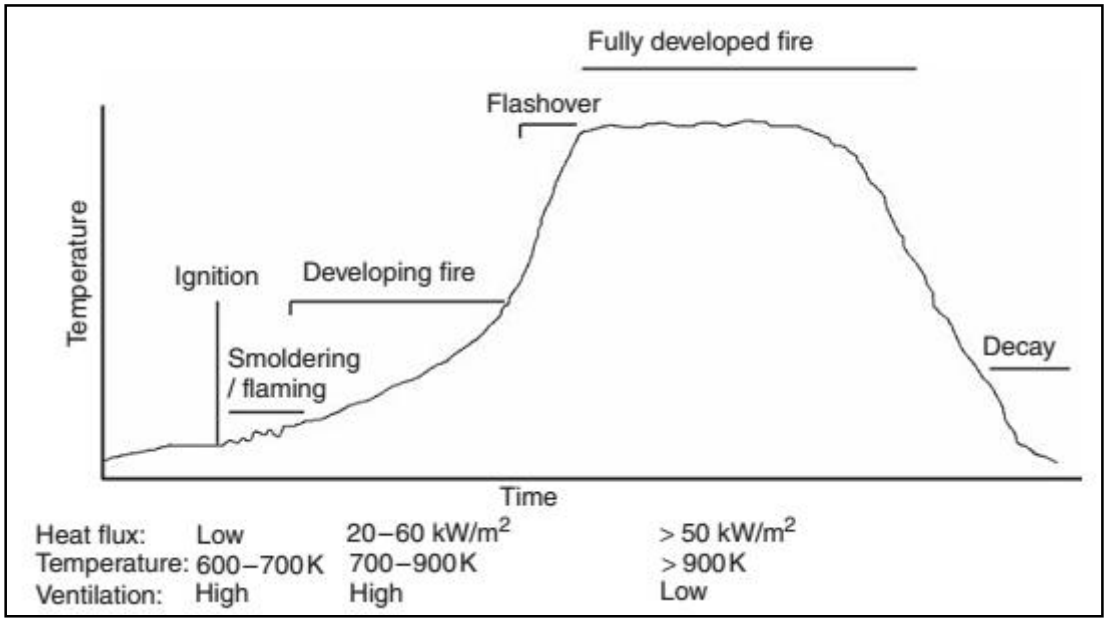

Fig. 2.6: The stages of a typical fire and some fire properties at various stages

2.2.5 Biodegradation of Biocomposites

Environmental policies set the boundary conditions for industries and commercial market regarding the maximum utilization of biodegradable material. Furthermore, people are also looking for those materials which can biodegrade at the end of product life-cycle. Therefore, the researchers and technologists are putting their efforts to develop a high-performance material based on lignocellulosic fibers. The natural fiber-reinforced composites (NFRC's) have an adequate potential to supplant synthetic materials in a wide variety of engineering applications because of their exceptional features such as biodegradability.

Biocomposites are equipped for experiencing mostly or completely deterioration principally through the enzymatic activity of microorganisms. However, to create green polymeric materials as a substitute for oil based materials isn't quick. Therefore, the optimum solution is to develop a material that contains a significant content of biobased materials which shows an affordable cost-performance ratio. The life pattern of compostable biodegradable materials is shown in Fig. 2.7. Several analysts have investigated the biodegradability of NFRCs. T. Fakhrul *et al*. [123] reported that the small addition (5%) of wood sawdust and wheat flour in the

polypropylene matrix results in a considerable improvement in biodegradability of a polymer. The most pronounced biodegradation was exhibited in brine solution and burial in moist soil conditions. H. Takagi [124] studied the biodegradability of hemp fiber reinforced starch-based biocomposites and reported on that the biodegradation of bio-resin was considerably amplified by the inclusion of Manila hemp fiber. This was due to the rapid degradation at the interface between hemp fiber and resin as well as preferential water transportation through internal cavities in hemp fiber. R. Kumar *et al*. [125] have studied the biodegradation of woven and nonwoven flax fiber reinforced PLA composites with amphiphilic additives and reported on that the composites in presence of mandelic acid have accelerated degradation with 20-25% weight loss after 50-60 days. K.N. Bharath *et al*. [126] studied the biodegradability and swelling characteristics of areca fiber and maize powder reinforced urea-formaldehyde (UF) composites and reported on that the composites were decomposed at a much slower rate after the loading of areca fiber and maize powder. The areca fibers possess better resistance to moisture as compared to the wood-based particleboard. S.H. Lee *et al*. [127] analyzed the impact of lysine diisocyanate (LDI) on the biodegradability and thermal stability of PLA/BF and PBS/BF materials and concluded that the biocomposites with LDI exhibit higher resistance to enzymatic degradation and thermal decomposition than the biocomposites of without LDI. N. Pons *et al.* [128] investigated the biodegradation of Glass/PLA material. Z.N. Azwa *et al*. [129] have considered the degradability of NFRCs in their review article.

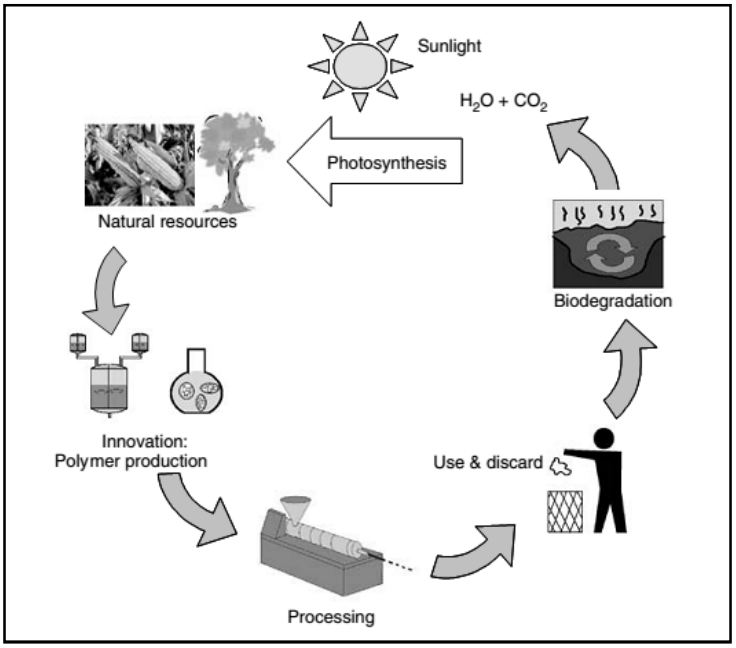

Fig. 2.7: The life cycle of biodegradable materials

2.3 Hybrid Composites

The best way of regulating the properties and performance of composite material is to reinforce hybrid fibrous fillers within a single matrix. It can allow for their expansion in application areas. Hybrid fiber composite is a blend of at least two unique strands either common or engineered in matrix resin. N.K. Sinha *et al*. [130] stated that the benefits of one sort of reinforcement could supplement what is inadequate in the other. As an outcome, equalization in price and performance could be accomplished by appropriate material structure. MJ John *et al*. [131] reported that the performance characteristics of a hybrid composite are primarily reliant upon the length of individual strands, relative fiber volume content, orientation, arrangement, and the degree of intermingling of fibers. In majority of the cases, the mechanical strength of NFRCs was enhanced by the hybridization with glass fibers [132-133]. Ghosh *et al*. [134] discussed the viscoelastic characteristics of Jute/Glass strengthened epoxy based hybrid material. Pothan *et al*. [135] studied the DMA characteristics of Banana/Glass filled polyester material.

Numerous works are available in literature which concerns the characteristics of hybrid material. M. Rahman *et al*. [136] considered the impact of reinforcement weight fraction on the performance properties of Banana and PALF strengthened polypropylene hybrid material. Arumugaprabu *et al*. [137] observed that the strength of a material based on Palmyra waste was improved after the loading of coir fiber. The hybrid composite consists of 40% Palmyra fiber and 60% Coir fiber exhibits the maximum affinity of water absorption. M.J. Sharba *et al*. [138] evaluated the influence of strand patterns on the performance characteristics of Glass/Kenaf filled hybrid material. They found that the woven type composite has low fatigue sensitivity with better static and fatigue strength than the other composites. M.J. Sharba *et al*. [139] studied the impact of relative weight proportion of kenaf and glass fibers [30/70 (H1), 45/55 (H2), and 70/30 (H3)] on the mechanical behavior of hybridized material and observed that the H1 possess better set of mechanical properties than the others. A. Atiqah *et al*. [140] evaluated the impact of relative filler vol.% and NaOH treatment on the properties of Kenaf/Glass filled polyester based material and observed that the treated composite of 15/15 (v/v) composition exhibits maximum mechanical strengths than the other composites. A.L. Fong *et al.* [141] checked the mechanical performance of sugarcane bagasse fiber and nano-

silica filled thermoset material. R. Manoj *et al.* [142] examined the mechanical behavior of hybrid E-glass filled polyester material. H.P.S Khalil *et al*. [143] analyzed the role of coconut shell nano-particles on the performance characteristics of kenaf/coconut strengthened vinyl ester material. N. Nurazzi *et al*. [144] analyzed the performance properties of sugar palm yarn/glass filled polyester material and observed that the specimens of 40 wt% fibers with a ratio of 50:50 exhibits optimum set of mechanical properties. R. Shrivastava *et al*. [145] analyzed the properties of Coir/Glass filled thermoset material and observed the expansion in mechanical strength by the incorporation of glass strand mat. Furthermore the composite of 10 mm span possesses better mechanical properties than the 15 mm. V.K. Bhagat *et al*. [146] examined the performance characteristics of Coir/Glass strengthened epoxy based material. L. Devi *et al*. [147] analyzed the effect of temperature (28, 60, and 90 ^{0}C), surface treatments, and hybrid pattern on the moisture sorption of PALF/Glass strengthened UPE material. F. Cheng *et al.* [148] concluded that the strength and modulus of coir strengthened material were increased considerably after the incorporation of glass fabric. V.S. Uppin *et al*. [149] found that the addition of cellulose results in the enhancement in fracture robustness of Glass-Epoxy material and it was due to the fiber bridging action. S.K. Saw *et al*. [150] analyzed the impact of layering pattern on the mechanical behavior of Jute/Coir strengthened epoxy novolac material. TP Sathishkumar *et al*. [151] characterized the snake grass/banana & snake grass/coir fiber composites and reported on that the SG/B and SG/C composites exhibits maximum strength at 20% and 25% V_f respectively. P.N. Khanam *et al*. [152] examined the role of fibre geometry and alkaline action on the mechanical features of Coir/Silk polyester based material. S. Nunna *et al*. [153] reviewed the mechanical characteristics of cellulosic strands based hybrid materials. C. Kakou *et al*. [154] analyzed the mechanical properties of coir and oil palm fiber strengthened HDPE material. L. Zhang *et al*. [155] reported that the mixture of rice straw and coir fiber has noteworthy potential to be used in manufacture of particleboard composites at low cost. S. Siddika *et al*. [156] evaluated the influence of total fiber vol.%, relative fiber ratio, and alkaline action on the performance properties of Jute-Coir strengthened PP based material. R. Siakeng *et al*. [157] examined the impact of relative fiber volume content on the thermal stability of COIR/PALF strengthened PLA composites and reported on that the C1P1 hybrid composite (1CF:1PALF) possess highest thermal stability than the other

compositions. M. Ramesh *et al*. [158] analyzed the mechanical and moisture sorption behavior of banana-carbon fiber strengthened hybrid material. J. Alexander *et al*. [159] reported that the Basalt/Sisal filled epoxy based material better properties than the sisal/glass one which results that it can be used in aircraft structural applications. M. Idicula *et al*. [160] considered the impact of layering pattern on viscoelastic behavior of Banana/Sisal fiber filled polyester material and reported that the intimately mixed and bilayer composite possess higher stiffness and damping property than the other composite samples respectively. S.S. Chee *et al*. [161] have developed 3 types of composites [kenaf (K)/epoxy, bamboo (B)/epoxy, and bamboo charcoal (BC)/epoxy] by hand lay-up technique and concluded on that the BC/Epoxy composite exhibits higher thermal stability than the K/Epoxy and B/Epoxy. Moreover, the K/Epoxy composite has better dynamic mechanical properties with the highest complex modulus than the others. B. Baghaei *et al*. [162] reported the positive hybridization effect obtained by the combination of hemp and lyocell fibers in PLA polymer. IS Aji *et al*. [163] characterized the kenaf/pineapple reinforced material and reported on that the composite of fiber ratio 1:1 (Kenaf and PALF) possess maximum tensile strength and modulus, whereas the K3P7 composite (Kenaf: PALF = 3:7) absorbs least amount of moisture than the other samples. B. Bakri *et al*. [164] examined the influence of relative fiber volume fraction on the mechanical characteristics of coir/agave strengthened epoxy material and reported that the composite of 15:15 fiber volume fraction exhibits higher tensile and flexural properties than the other composites of fiber volume fraction-10:20, 20:10. R. Yahaya *et al*. [165] stated that the moisture sorption and thickness swelling of Kenaf/Kevlar composite was increased by the amplification of kenaf volume fraction. Akash *et al*. [166] assessed the flammability and moisture sorption affinity of sisal/coir filled epoxy material. M. Jawaid *et al*. [167] declared that the hybridization of EFB with jute strands leads to the increased $E^{'}$ and thermal stability of epoxy based hybrid composites. Furthermore, T_g of the polymeric resin was shifted to a elevated value by the addition of reinforcing fibers. M.R. Mansor *et al*. [168] stated that the kenaf fiber is the paramount candidate to prepare hybrid composite for automotive application. M.M. Davoodi *et al*. [169] declared that the kenaf/glass filled epoxy composite has comparable mechanical properties to the glass mat thermoplastic (GMT) which confirms its potential to be used in an automotive structural application. M.S. Sreekala *et al*. [170] corresponds the loading impact of

EFB fillers on the performance characteristics of EFB/Glass filled hybrid material and reported that the impact strength was improved with considerably lower density by replacing the glass fiber with EFB. S. Mishra *et al*. [171] considered the mechanical performance of PALF/Glass and Sisal/Glass fiber strengthened hybrid polyester composites and concluded the improvement in mechanical strength by the incorporation of glass fiber. The optimum loading of glass fiber for PALF/Glass and Sisal/Glass hybrid composites is 8.6 and 5.7% respectively. R. Burgueno *et al*. [172] reported that the biocomposite sheet developed by the incorporation of industrial hemp, chopped glass, woven jute, and unidirectional carbon fabrics in polyester resin exhibits excellent strength, stiffness, and dimensional stability which leads to its utilization for structural application. N. Ranganathan *et al*. [173] examined the influence of viscose filler volume fraction on fracture toughness and fatigue life of Jute/Viscose fiber reinforced polypropylene based hybrid composites and reported on that the fracture toughness (K_{IC}) and fatigue life were improved significantly by the addition of 10 wt% viscose fibers. M. Kaiser *et al*. [174] stated that the impact strength of natural fiber reinforced PLA composites was improved by more than 50% after the loading of 3 wt% nanoclay. M.M. Davoodi *et al.* [175] stated that the kenaf/glass hybrid epoxy composite can be used for making the automotive structural components. V.S. Chevali *et al*. [176] noticed the diminution in mechanical strength of ABS polymer after the incorporation of sunflower hull and dried grain fibers. M. Haq *et al*. [177] conclude that the inclusion of hemp strands in a blend of UPE, EMS and nanoclay results in a novel multifunctional biocomposite material having a balanced combination of stiffness and toughness and can be used in structural and transportation applications. R. Murugan *et al*. [178] evaluated the mechanical characteristics of woven glass/carbon fabric filled epoxy composites. R. Ranjan *et al*. [179] characterized the banana/sisal reinforced PLA material and reported that the mercerized composites have higher mechanical strength of than the untreated ones. M. Jawaid *et al*. [180] considered the chemical behavior of OPEFB/Jute filled hybrid material and reported the improvement in dimensional and chemical stability with the increase of jute fiber volume fraction. M. Jawaid *et al*. [181] reviewed the cellulose/synthetic fiber reinforced hybrid composites in their review article.

2.4 Natural Fibers

History has seen several endeavours to incorporate cellulosic fibers in various parts of the world. The combination of natural fibers with polymer matrices is gaining attention over the last decade. A broad classification of plant-based natural fibers is represented schematically in Fig. 2.8.

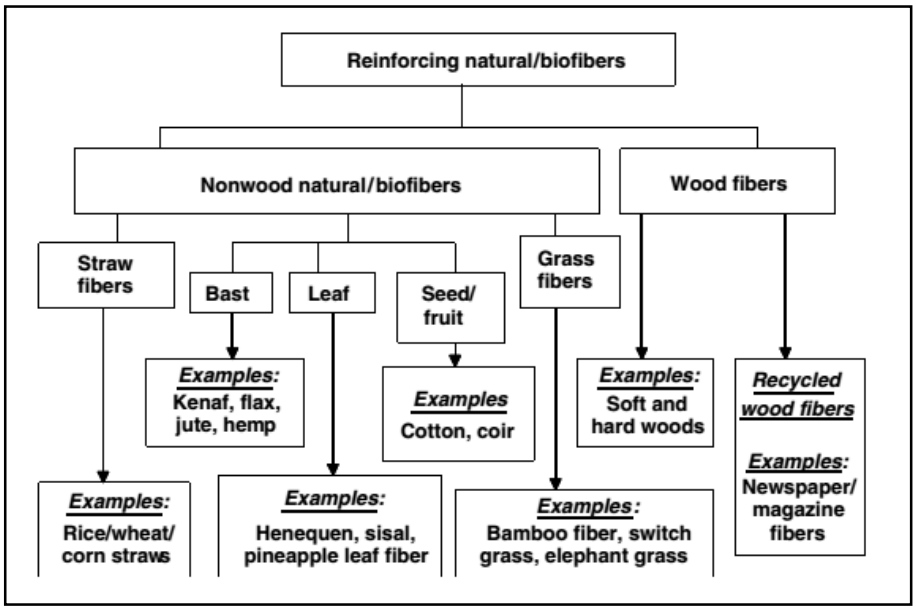

Fig. 2.8: Organization of natural fibers

Natural filaments are presently developing as possible choices to glass fiber for an assortment of utilizations, for example, vehicle parts, building structures, and rigid packaging materials. The upsides of natural filaments over manufactured ones are listed below:

- Renewable and sustainable plant fiber resource
- Recyclable and biodegradable
- Weight saving
- Cost-saving
- Abundant supply which is accessible in many regions of the world
- Low energy requirement for production
- Carbon dioxide sequestration
- Non-abrasive and good formability
- cheaper as compare to synthetic fibers
- Exhibit excellent thermal and acoustic properties

Due to their wide varieties of advantageous properties, scientists and technologists are doing a lot of efforts to utilize natural fibers in value-added applications. The various applications of natural fibers, depending upon fiber length are reported in Fig. 2.9.

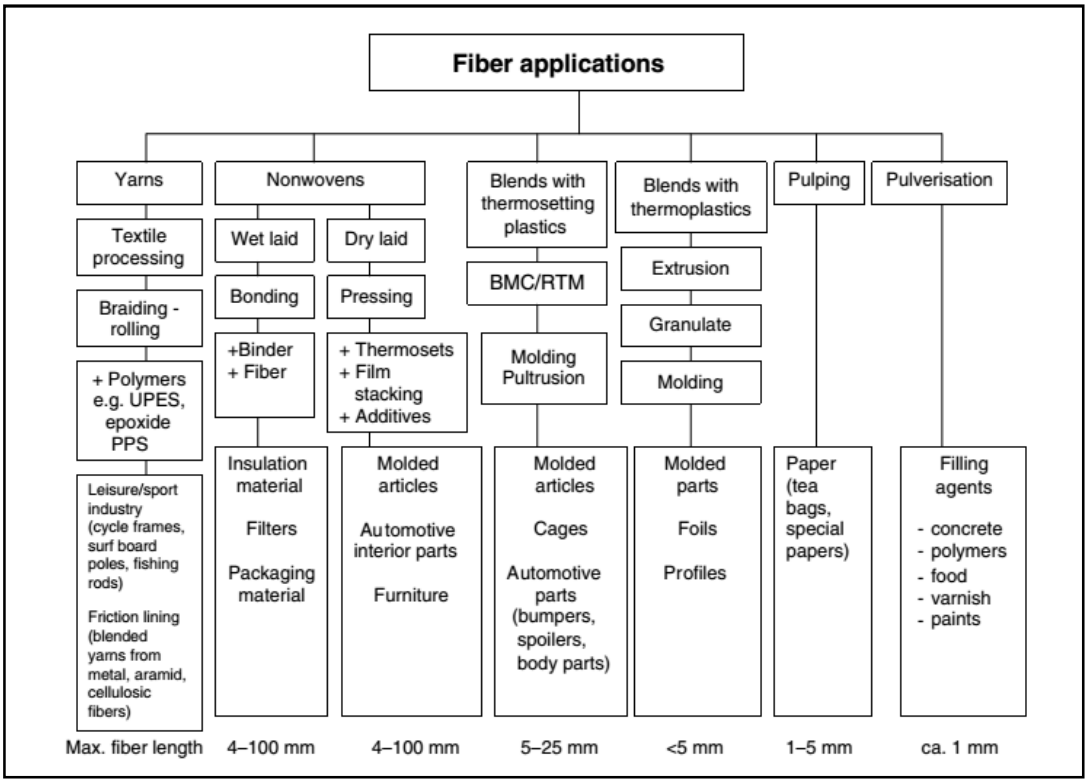

Fig. 2.9: Applications of common filaments

2.4.1 Composition and Structure of Natural Fibers

The chemical composition (Table 2.1) and the structure of plant strands are highly complicated. They are comprised of cellulose, hemicellulose, lignin, waxes, and water-soluble compounds [182].

Table 2.1: Chemical composition (in wt.%) of plant-based strands

Fiber	Cellulose	Hemicelluloses	Lignin	Pectin	Moisture level	Microfibrillar angle (deg)
Kenaf	42-61	19.9	7-14	2-6	-	-
Ramie	66.6-78.4	12.3-17.6	0.7-0.8	1.8	6.9-18	7.5
Hemp	65-72	16.4-23.7	2.9-6.1	0.8	5.8-14	2-6.2
Sisal	66-78	10-14	10-14	10	10-22	10-22
Nettle	86	-	-	-	11-17	-
Jute	60-72.7	14.5-19.8	10-15	0.4	11.9-14.4	8
Henequen	78.1	3-9	12.7	-	-	-
Coir	30-45	0.13-0.22	41-49	2-6	9	32-51
Banana	60-65	11.5	6	-	9-13	-

Abaca	51-66	-	12-17	3.1	3-13	-
Oil palm mesocarp	61	-	12	-	-	43
PALF	72-84	-	4-11.8	-	10.9	13
Palm EFB	64	-	18	-	-	44
Cereal straw	38-45	15-31	12-20	8	-	-
Flax	72	18.3-20.1	2.5	2.2	7-11	5-10
Cotton	80-94	4.9		0-2	7.74-8.2	

Cellulose is a straight macromolecule comprises of D-anhydroglucose ($C_6H_{11}O_5$) rehashing elements attached by β-1,4-glycosidic connections (Fig. 2.10). Each rehashing unit contains three hydroxyl bunches (-OH) and these gatherings form intermolecular and intramolecular hydrogen bonds. The synthetic structure of cellulose from various regular filaments is same yet the level of polymerization (DP) differs. The mechanical properties of fiber are fundamentally reliant on the DP. The measure of cellulose in normal filaments can vary contingent upon the species and age of the plant. Cellulose is impenetrable to solid salt and oxidizing operators anyway it is adequately hydrolyzed by acids to water-solvent sugars.

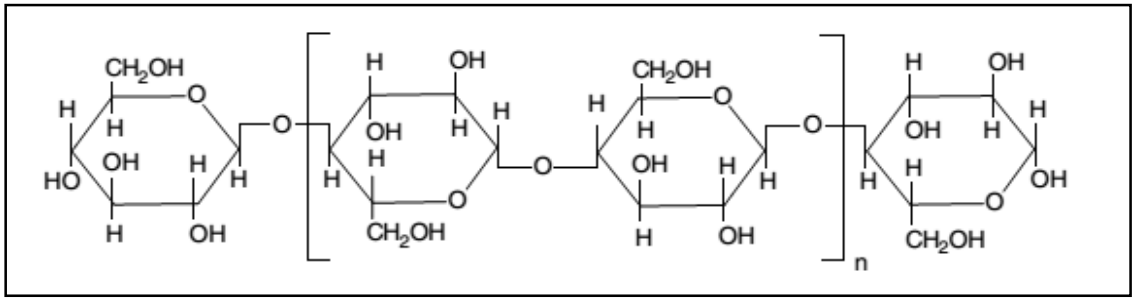

Fig. 2.10: Cellulose structure

Lignin is a complex, 3-dimensional compound of aliphatic and aromatic constituents that provides stiffness to the plants. The structure of lignin (Fig. 2.11) illustrates that it is extremely aromatic in nature. It is amorphous and hydrophobic in nature having T_g of around 90 ^{0}C. The mechanical strength of plant fiber is correlated to the distribution of lignin between hemicellulose and cellulose.

The plant fiber is usually of a 1 to 50 mm length and a 10-50 µm diameter. Fig. 2.12 illustrates that the structure of plant fiber is like microscopic tubes in which cell walls surrounding the center lumen [183]. The cell wall in fibers is developed of few layers: the principal cell wall is the initial film set down during cell development, and the minor wall (S) further comprises of 3 films (S1, S2, and S3). The microfibrils are

rooted in cell walls with hemicellulose and lignin matrix. The external cell wall is permeable and practically the entirety of the non-cellulose mixes. Lumen is the section that creates the problem of poor absorbency, poor wettability, and other undesirable textile properties [184-185].

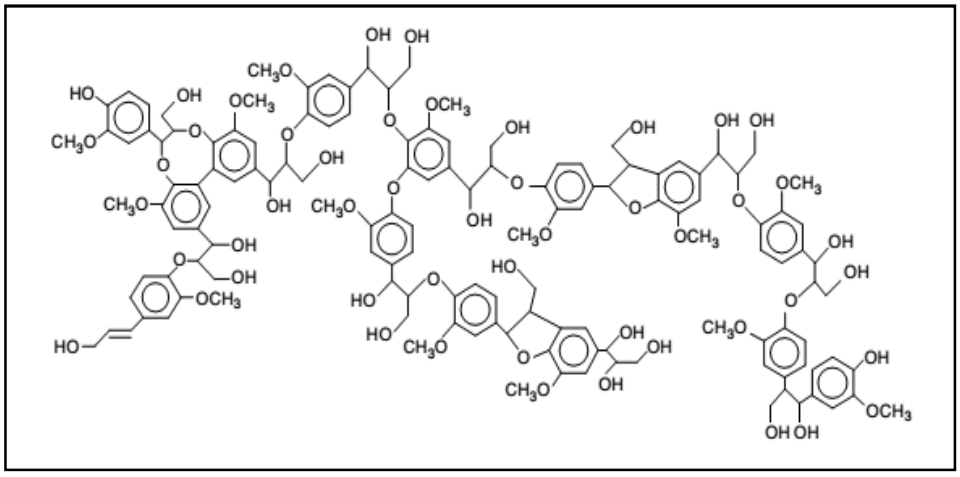

Fig. 2.11: Lignin structure

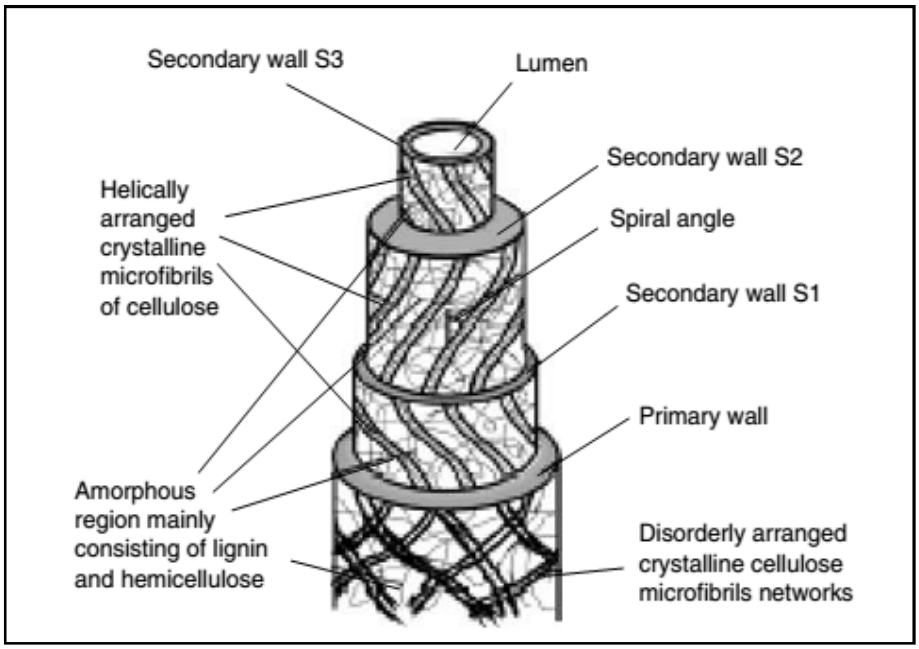

Fig. 2.12: Organization of a single cellulose strand

2.4.2 Limitations of Natural Fibers

Inspite of their wide range of profitable properties, the natural fibers have some limitations which are mentioned below:

- High moisture absorption
- Low microbial resistance and susceptible to rotting

- Low thermal stability
- Non-uniformity and variability of dimensions
- Variability in physical and mechanical properties
- Decomposition in alkaline solution

D.N. Saheb *et al.* [186] stated that the effectiveness of natural fibers as a reinforcement is greatly diminished by its hydrophilic character and the lack of satisfactory linkage with the matrix material. Moreover, natural fibers can be subjected to thermal degradation during composite processing. Therefore, it is practically significant to understand and prevent the water absorption and thermal decomposition process of natural fibers.

2.4.3 Water Absorption of Natural Fibers

One of the most differences between natural fibers and glass fibers is their response to humidity. In humid conditions, natural fibers absorb high level of moisture which results in the structural alteration and evolution in mechanical properties of fibers jointly with the composites in which they are fitted in [187-189]. B.M. Pejic *et al*. [190] evaluated the individual role of hemicelluloses and lignin on the moisture sorption of hemp fibers and observed on that the moisture sorption and water retention power of hemp fiber was increased and decreased respectively after the removal of hemicellulose, while lignin removal decreases the moisture sorption and increase the water retention ability of hemp fibers. Frederick *et al.* [191] stated that the coir has least moisture sorption affinity as compared to other cellulosic fibers. Nakamura *et al.* [192] concluded that the water sorption by cellulosic fibers was decreased with the increase in crystallinity of cellulose. Davies and Bruce [193] reported that the hemicellulose is primarily responsible to store moisture in humid environmental conditions. A. Stamboulis *et al*. [194] examined the moisture uptake characteristics of flax strand in various humidity conditions. Xie Yanjun *et al*. [195] evaluated the moisture sorption behavior of cotton, filter paper, flax, hemp, jute, and sisal fibers in their research article. A. Bismark *et al.* [196] also checked the hydrophilic feature of flax, hemp, and cellulosic fibers using the zeta potential method.

2.4.4 Thermal Behavior of Natural Fibers

Another restrictive variable for the exploitation of lignocellulosic fillers in composite materials is their low thermal stability. Wielage *et al.* [197] reported that the processing temperature of natural fibers should be limited to 200 ^{0}C in turn to avoid degradation of fibers. N. Stevulova *et al.* [198] investigated the thermal behavior of cellulosic fibers (wood pulp and waste paper) using TGA technique. Varma *et al.* [199] compared the thermal stability of natural and chemically treated coir fibers. D.A. Motari *et al.* [200] evaluated the thermal decomposition yield and the activation energy of bagasse under CO_2/O_2 and N_2/O_2 atmospheres and reported that the activation energy of bagasse was increased by 90% when N_2 is replaced by CO_2. S. Ndazi *et al.* [201], A. Rachini *et al.* [202] declared that the major decomposition of rice husk fiber occurs at 351.5 ^{0}C, and natural hemp fiber at 312 ^{0}C due to decomposition of α-cellulose.

Thermogravimetric analysis (TGA) is one of the most popular and widely used techniques to analyze the decomposition process of solid material; kinetic analysis of de-volatilization; and to study the effects of heating rate, temperature, pressure, atmosphere gas, gas flow rate, biomass composition, and particles size on mass loss of a sample [203]. Yao Fei *et al.* [204] examined the thermal decomposition kinetics of 10 types of cellulosic fibers using TGA. The decomposition of natural fibers occurs in two to three stages based on the type and chemical composition of fiber. Na Lu *et al.* [205] stated that the hemp fiber can decompose in two steps, starting with the loss of moisture around 100 ^{0}C followed by successive breakdown of hemicellulose, cellulose, and lignin in the range of 150-400 ^{0}C. J. Elammaran *et al.* [206] reported that the temperature of 10 wt% mass loss of betel nut-polyester composites was shifted from 110 ^{0}C to 120 ^{0}C after 5 wt% of alkaline treatment.

2.4.5 Fiber Surface Modification

The quality of fiber-matrix interface is one of the most important factors that can control the performance of a composite material. So as to accomplish optimum performance of the biocomposites, a satisfactory extent of linkage between the cellulosic fillers and the matrix material is preferred. Therefore, the fiber surface has to be customized in turn to encourage linkage. The chemical treatments have achieved a great level of success for improving the fiber-matrix adhesion [207].

2.4.5.1 Mercerization

Mercerization is an effective & low-cost surface modification method for cellulosic fibers. Its efficiency relies upon the type and concentration of the alkaline solution, time of treatment, and temperature. The reaction between sodium hydroxide (NaOH) and natural fibers occurs as shown below:

$$NaOH + OH\text{-}Cell \longrightarrow H_2O + Cell - O^-Na^+ + \text{Surface impurities}$$

The alkaline modification of cellulosic filaments promotes the partial subtraction of hemicelluloses, lignin, and waxes present on the surface which leads to the change in morphology and chemical composition [208-209]. The leaching of these compounds enhances the availability of sites for the cellulose-matrix interaction. M.S. Sreekala *et al.* [210] reported that the globular pultrusions present in the untreated fiber were disappeared after an alkali-treatment for 48 h which results in the formation of a large number of voids.

The alkaline treatment of fibers may result in:

- Improved interfacial mechanical Linkage.
- Enhance the amount of feasible reaction sites.

2.4.5.2 Chemical Action on the Cellulosic Fibers and their Composites

Several reports concerning the chemical treatment of fibers are available in the literature. P. Ramadevi *et al*. [211] checked the impact of NaOH of different concentrations (5%, 10%, 15%, and 20% NaOH) on water uptake capacity of abaca fiber and reported on that the moisture absorption was diminished with the increase of an alkali concentration. Abaca fibers treated with 20% alkali solution resisted up to 67% moisture absorption than the untreated fibers. A. Bismarck *et al*. [212] determined the impact of several surface modification techniques (dewaxing, alkali treatment, methyl methacrylate grafting) on thermal stability, moisture sorption, and surface morphology of sisal and coir fibers and found the increment in thermal stability of fibers by alkali treatment and grafting with methyl methacrylate. The treatment of coir fiber results in an increase in water absorption since all treatments affect the protective layer at the fiber surface. N. Sgriccia *et al*. [213] characterized the surface of untreated and alkali-treated hemp and kenaf fibers using FTIR, XPS,

and ESEM. K. Ramanaiah *et al*. [214] examined the impact of alkali modification (5% NaOH) on the thermo-mechanical behavior of sansevieria green fiber. Samal and Bhuyan [215] have characterized the functionality of acrylonitrile grafted pineapple leaf fibers. Ray *et al*. [216] evaluated the mechanical properties of chemically treated jute fibers. A. Rachini *et al*. [217] reported the order of thermal stability for untreated and chemically treated hemp fiber: NaOH treated fibers> silane-treated fibers> solvent extracted fibers (water/ethanol mixture, 20/80 v/v)> untreated hemp fibers. C.U Maheswari *et al*. [218] have compared the tensile and flexural strength of untreated, alkali-treated, silane treated, and alkali silane treated tamarind fiber reinforced polyester composites and reported on that the alkali silane treated composite has highest tensile and flexural strength. S.C Venkateshappa *et al*. [219] declared that the mechanical strengths of Areca/Epoxy material were increased with the increase of curing time, fiber-matrix weight ratio, and alkali treatment. D. Shanmugam *et al.* [220] reported that the mercerization leads to the improvement in E' and T_g of Palmyra/jute strengthened polyester composite. T.J Chung *et al*. [221] noticed the increment in storage modulus of Kenaf/PLA composite after the acetylation of kenaf strands. J.K Pandey *et al.* [222] stated that the surface modification of cellulose whiskers can overcome the compatibility challenges with synthetic polymer matrices. T. Doan *et al.* [223] declared the improvement in mechanical strength of Jute/PP composites by the addition of 2 wt% maleic anhydride grafted polypropylene (MAHgPP). Franco *et al*. [224] reported the increment in mechanical strength of HDPE-henequen composite after the treatment with NaOH followed by silane. E. Lopez *et al*. [225] reported that the surface treatment led to better fiber distribution and a more uniform composite morphology. T. Chung *et al*. [226] stated that the sufficient acetylation of kenaf would effectively improve the bonding with the PLA matrix. P.J. Jandas *et al*. [227] examined the influence of surface modificatios (NaOH, APS, and Si69) on performance characteristics of Banana/PLA material. K. Panyasart *et al*. [228] investigated the impact of surface treatments on the performance of PALF strengthened polyamide 6 material. Na Lu *et al*. [229] stated that the degradation temperature of Hemp/PLA was augmented from 330 ^{0}C to 340 ^{0}C after an alkaline treatment of hemp fiber. S. Oza *et al*. [230] evaluated the role of chemical treatments (Alkali, silane, and acetic anhydride) on the thermal stability of hemp-PLA composites and reported that the composite consists of acetic anhydride modified hemp fiber has elevated thermal

stability than the other ones. E. Jayamani *et al*. [231] considered the impact of mercerization on performance characteristics of Betelnut/Polyester material. K. Zhang *et al*. [232] examined the impact of NaOH modification on the performance of Bamboo/Epoxy and reported the higher thermal stability of 6 wt% NaOH treated than the other ones. P. Niu *et al.* [233] evaluated the impact of various pairing agents (PP-MAH, SEBS-MAH, and POE-MAH) on mechanical properties and thermal stability of Hemp/PP material. H.P.S. Khalil *et al*. [234] confirmed that the chemical alteration of kenaf strands using anhydride propionic and succinic anhydrides results in the decrease in contact angle of kenaf bast leading to the good adhesion characteristics with matrix resin system. R.K. Mishra *et al*. [235] evaluated the mechanical behavior of untreated and chemically modified Jute-Coir strengthened epoxy based material. G. Goud *et al*. [236] observed that the strength and stiffness of Roystonea regia-epoxy composite were increased after an alkali treatment of fibers.

2.4.6 Pineapple Leaf Fibers

Pineapple leaf fiber (PALF) is one of the waste materials in agribusiness division which is obtained from the leaves of pineapple plant and its development is considerable (around 91,000 ha) in India. As indicated by the measurable database (2016) of "Food and Agriculture Organization", the total creation of pineapple in the entire world is 25.8 million of tons. After banana and citrus, pineapple (Ananas comosus) is one of the most fundamental natural products on the planet and is to a great extent developed in tropical nations. Economically, pineapple organic products are significant and its leaves are being utilized for creating common strands. The fiber is extracted by hand scratching in the wake of whipping the leaves to break the thick tissue or after a retting procedure that in part ferments and soften the leaves.

PALF is a multi-cell lignocellulosic fiber. The fiber is of fine quality and its structure is without mesh. It is white in shading, smooth and gleaming as silk. Fig. 2.13 depicts the local pineapple plant and pineapple leaf filaments. It comprises basically of cellulose (70-82%), polysaccharides and lignin. It can be utilized as a raw material in the textile and non-textile industries and has significant potential to replace expensive and non-renewable synthetic fibers.

Fig. 2.13: Mature pineapple plant (left) and pineapple leaf fibers (right)

2.4.7 Coir Fibers

Coir filaments are acquired from the husk encasing the product of coconut palm (Fig. 2.14), which is a side-effect of the copra extraction process. The strands are to a great extent delivered in tropical zones of Asia like Philippines, India, Sri Lanka, and Malaysia. In any case, India and Sri Lanka are the principle creating nations. By and large, from 100 coconuts 7.5 to 8.2 kg of strands can be acquired. Generally, they are acquired by the water retting process. During the retting of the husks, the coir strands are mollified and can be effortlessly decorticated.

Coir has high lignin (40-45%) yet low cellulose content which makes it increasingly stable under a wide scope of temperature, humid natural conditions, and under the activity of microbial and growth assault. Because of their capacity to endure water immersion for a considerable length of time without deteriorating, they find numerous applications. Coir is one of the toughest plant strands as a result of which they are widely used as seat cushions in the automotive industry. From the above discussion, we can note the following points:

- PALF contains high cellulose content (70-82%) and less value of spiral angle (14^0) which results that they possess high tensile strength and stiffness with low impact toughness.
- COIR contains low cellulose content (32-43%) and high value of spiral angle ($30\text{-}49^0$) which results in high impact strength.

Therefore, to consolidate their properties synergistically, it gets important to reinforced PALF and COIR strands in the same polymer matrix. Hybridization of

stiffer and low elongation fiber with the high strain to failure fiber can prompts to the high-performance composite material.

Fig. 2.14: Coconut tree (left) and coir fibers (right)

2.5 Polymer Matrices

As we already mentioned in section 2.1 that the biocomposites comprise natural fibers and synthetic or bio-resin. Synthetic resins are either thermoplastics or thermosets. This work is restricted to the exploit of thermosetting polymer.

2.5.1 Thermosetting Polymers

Thermosetting polymers are comprised of large molecules, with repeating structural units of monomers that experience irreversible curing. These are shaped from a chemical reaction in situ, where the resin and hardener are blended in proper proportion to form a hard, infusible product. At room temperature, thermosets are found in liquid form which empowers trouble-free loading of fibers or other substances before being cured. In contrast to thermoplastics, thermosets won't become fluid again whenever warmed. Although over a specific temperature called as glass transition temperature (T_g), their mechanical properties will change significantly. Holbery [237] reported that thermosets are commonly used in the composite industry. Most of basic parts are made with three principle sorts of thermosetting polymer, to be specific polyester, vinyl ester, and epoxy [238].

Among all thermosetting polymers, epoxies generally outperform regarding mechanical properties, adhesive, and thermal properties which caused their wide acceptance as a primary construction material in the automotive and aerospace

sectors. Epoxy resin is effectively cured at any temperature from 5 ^{0}C to 150 ^{0}C, contingent upon the sort of curing agent. The idealized structure of typical epoxy is depicted in Fig. 2.15.

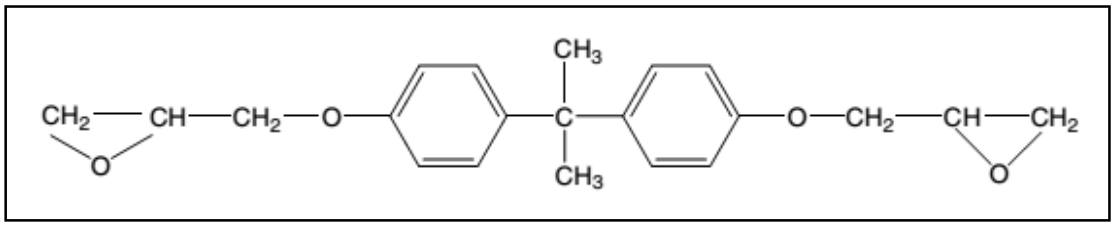

Fig. 2.15: Idealised structure of a typical epoxy

The epoxy molecules are competent to handle both mechanical and thermal stresses which result it possesses very good stiffness, toughness, and heat resistant properties. The other beneficial property of epoxies is their low contraction during cure which results in the surface contacts set up between the liquid resin and the adherends are not disturbed during the cure. During curing, the epoxy resins lead to very little rearrangement and no volatile by-products being evolved.

2.6 Summary

In this chapter, the previous research works on biocomposites were studied and it is clear that the performance of composite depends on the types of fiber and matrix, fiber geometry (length and diameter), fiber-matrix interfacial interaction, fibers layering pattern and their orientation, etc. It has been found that the natural fibers are gaining interest within the automobile engineering. Several researchers have utilized fibers hybridization concept but no research work has been done till now which accounts for the hybridization of PALF and COIR fibers. The review on their chemical composition and properties showed that the PALF and COIR fibers are ideal agricultural waste having significant potential to combine together in a single polymer matrix and form a biocomposite material that could be employed for automotive application.

The subsequent section will offer the research design and methodology applied for the research work.

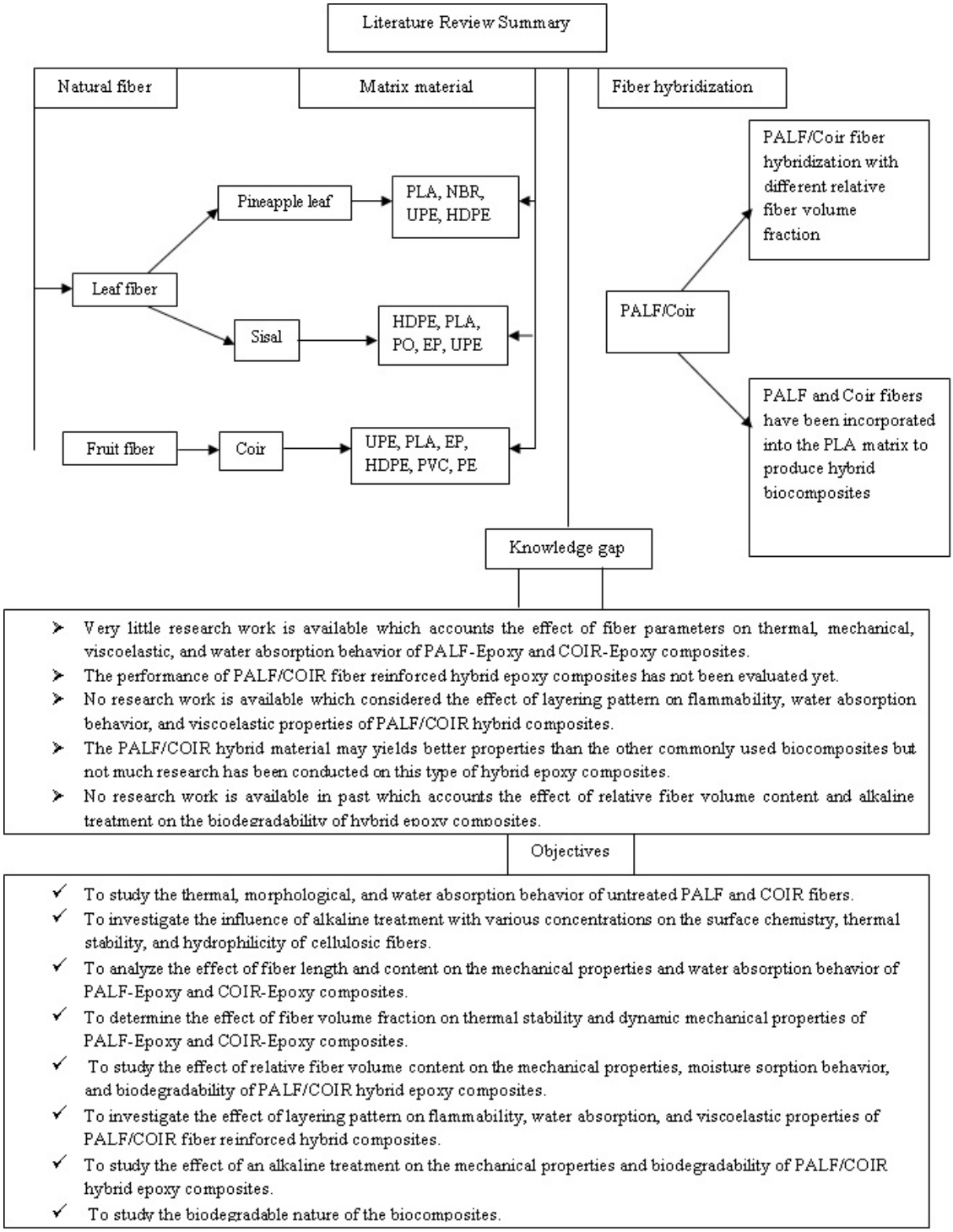

Fig. 2.16: Schematic representation of literature review

CHAPTER 3 - RESEARCH DESIGN AND RESEARCH METHODOLOGY

3.1 Introduction

To accomplish the research targets, a quantitative methodology was utilized, where the examination was directed by gathering the exploratory information that was then investigated with unprejudiced realities. The literature review that was led in the beginning period of the research gives the fundamental establishment to research and more importantly knowledge gap in this area. Fig. 3.1 outlines the design of an experiment.

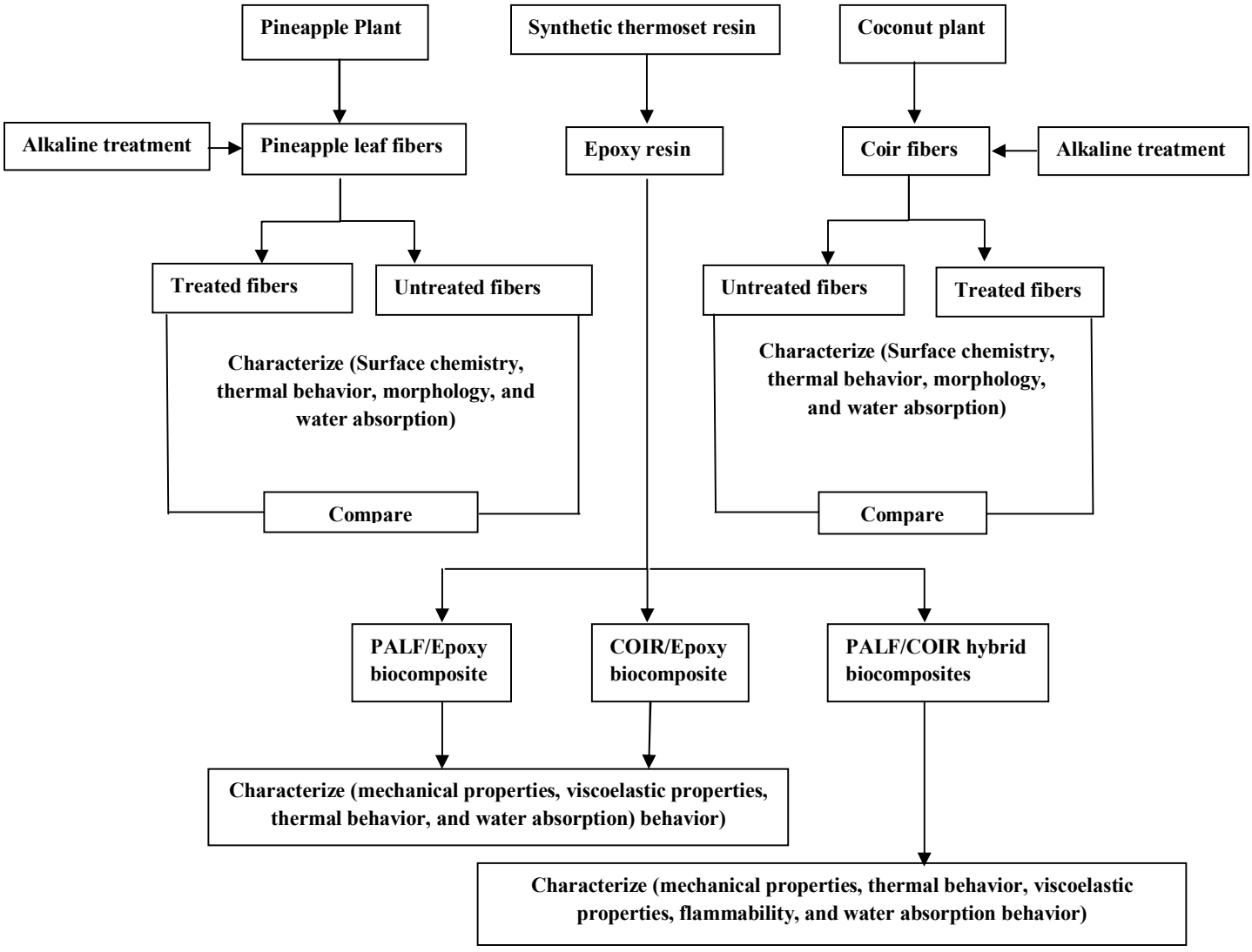

Fig. 3.1: Chart of the research plan

This chapter outlines the materials used for the development of composites followed by the experimental segment discussing the procedure for the preparation of biocomposites. The characterization techniques used and their basic procedure are also mentioned in this chapter.

3.2 Materials

The medium viscosity epoxy resin [DGEBA (diglycidyl bisphenol-A); LY 556; density: 1.16 g/cm^3; average molecular weight (M_n): 2300 g/mol] and hardener [TETA (triethylene tetraamine); HY 951; density: 0.95 g/cm^3; average molecular weight (M_n): 146.23 g/mol] were procured from M/s Sakshi Dies and Chemicals, Delhi (India). The chemical reaction involved during the curing process of an epoxy thermoset is illustrated in Fig. 3.2. The lignocellulosic pineapple leaf fiber (PALF, *Ananas-comosus*) and coconut husk fiber (COIR, *Cocos-nucifera*) were obtained from M/s Go Green Products, Chennai (India). The strands were washed under tap run to expel the residue and polluting influences and dried in sunlight for 3 days. The SEM micrograph of untreated fibers and the typical properties of an epoxy thermoset are shown in Fig. 3.3 and Table 3.1 respectively.

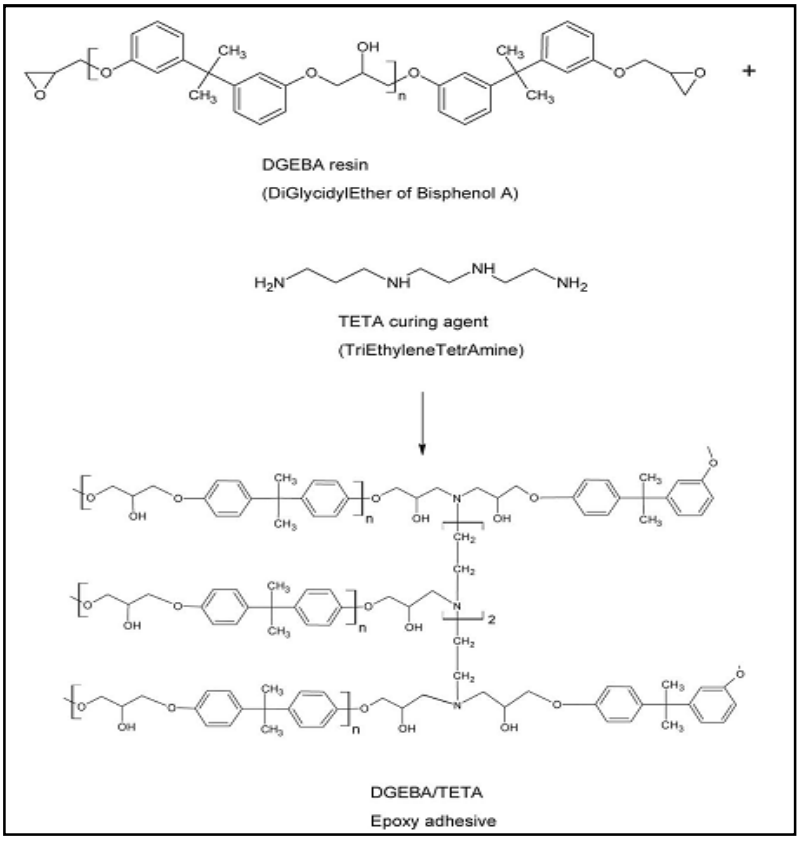

Fig. 3.2: Curing reaction between epoxy resin (DGEBA) and hardener (TETA)

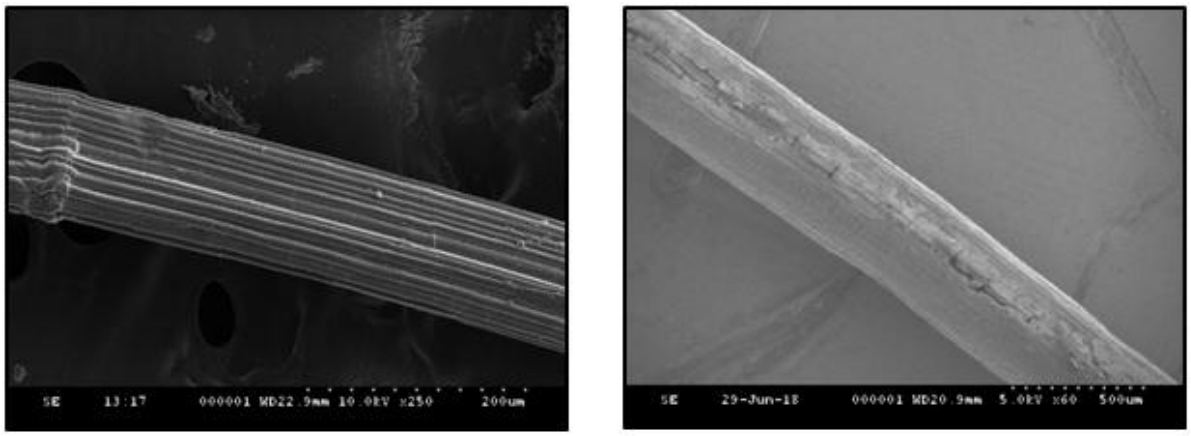

Fig. 3.3: SEM images of (a) Untreated PALF (b) Untreated COIR fiber

Table 3.1: Properties of an epoxy matrix

The appearance of liquid resin	A clear pale yellow
Density (Kg/m^3)	1200-1250
Viscosity at 25^0C (cps)	550
Tensile strength (MPa)	11.14
Tensile modulus (GPa)	0.48
Flexural strength (MPa)	25.29
Flexural modulus (GPa)	1.53
Max. Elongation (%)	4.2-5.6
Impact strength (kJ/m^2)	1.2
Flashpoint	$> 200^0C$

(Authors observations)

3.3 Experimental Methodology

This section explains the methodology used for 1) preparation of biocomposites 2) alkaline treatment of cellulosic fibers. At last, the instruments used for the characterization will be detailed.

3.3.1 Alkaline Treatment of Cellulosic Fibers

To enhance the interfacial contact between cellulosic strands (PALF and COIR) and thermoset resin, the generally utilized chemical treatment known as '*mercerization*' was employed. At first, the cellulosic strands were separated from the pith, clean in tap water, and dried in daylight for 3 days to evacuate the surface contaminations and consumed water particles. The cleaned and dried filaments were immersed in various concentrated solution of alkali (2%, 4%, 6%, 8%, and 10%) for 24 hrs at room

temperature, followed by the treatment with 2 wt.% acetic acid (CH_3COOH) solution and then rinsed in distilled water to control the pH level at 7. The neutralized wet fibers were dried again for 24 hrs at room temperature and then followed by oven drying at 70 ^{0}C until the constant weight was obtained.

3.3.2 Fabrication of Composites and Sample Preparation

The hand lay-up molding technique was employed to impregnate and compound the cellulosic fibers with an epoxy thermoset resin in an open mold cavity of dimensions 200 mm X 100 mm X 4 mm. The epoxy resin (DGEBA) was thoroughly mixed with a curing agent (TETA) in a necked round glass flask through mechanical stirrer at room temperature (approx 30 ^{0}C) for 10 minutes. Before using the polymeric resin for molding, ensure that it was mixed completely with hardener and no air bubbles were present. In all composite samples, the volume of resin and hardener was kept at 2:1 (v/v), while the total fiber content was varied according to the tests performed as illustrated in Table 3.2.

Table 3.2: Total filler content in developed composites

Tests performed	Total fiber content
Mechanical and water absorption tests on Coir-Epoxy and PALF-Epoxy composites	17%, 23%, 34%, and 43%
TGA and DMTA tests on PALF-Epoxy and Coir-Epoxy	17%, 23%, and 34%
Mechanical and moisture sorption tests on PALF/COIR strengthened hybrid material	40%
Biodegradability of hybrid material	40%
DMA test on PALF/Coir hybrid composites	40%

The mold was covered with a Teflon sheet and its surface was sprayed with a releasing agent to prevent the sticking of adhesive polymeric resin [Fig. 3.4 (a)]. Ensure that the distribution of fibers and polymeric resin are uniformed throughout the mold space [Fig. 3.4 (b)-(c)]. During the fabrication of a composite sheet, the air bubbles are abstracted cautiously using a paint steel roller. In the end, closed the mold and then pressed with 35 kg deadweight for 24 hrs curing at room temperature. The specimens for various tests were cut from the molded sheet [Fig. 3.4 (d)] as per ASTM standards, revealed in Fig. 3.5.

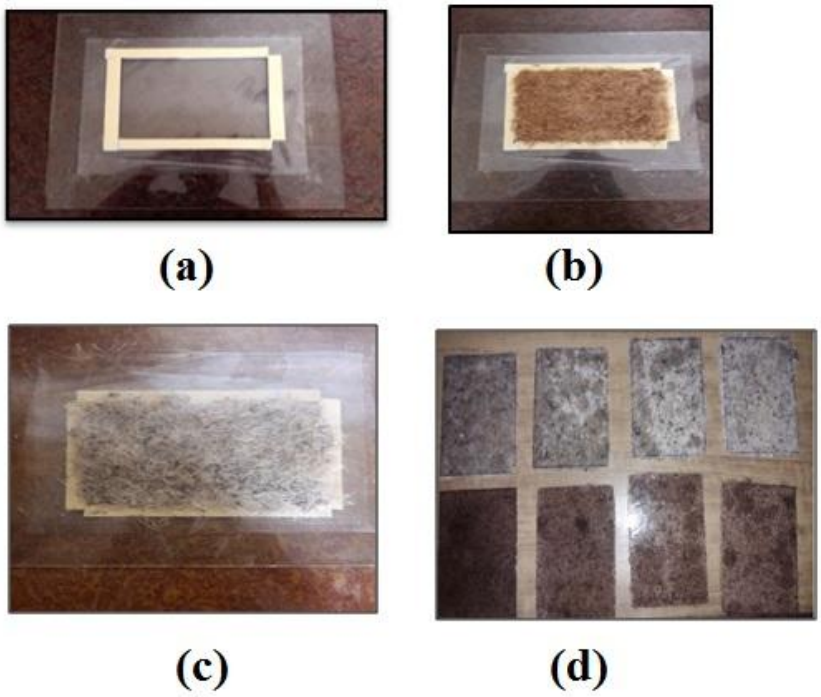

Fig. 3.4: (a) Glass mold covered with a Teflon sheet (b) Mold with Coir-Epoxy compounded material (c) Mold with PALF-Epoxy compounded material (d) Biocomposite sheets – (Top) PALF/Epoxy (Bottom) Coir/Epoxy

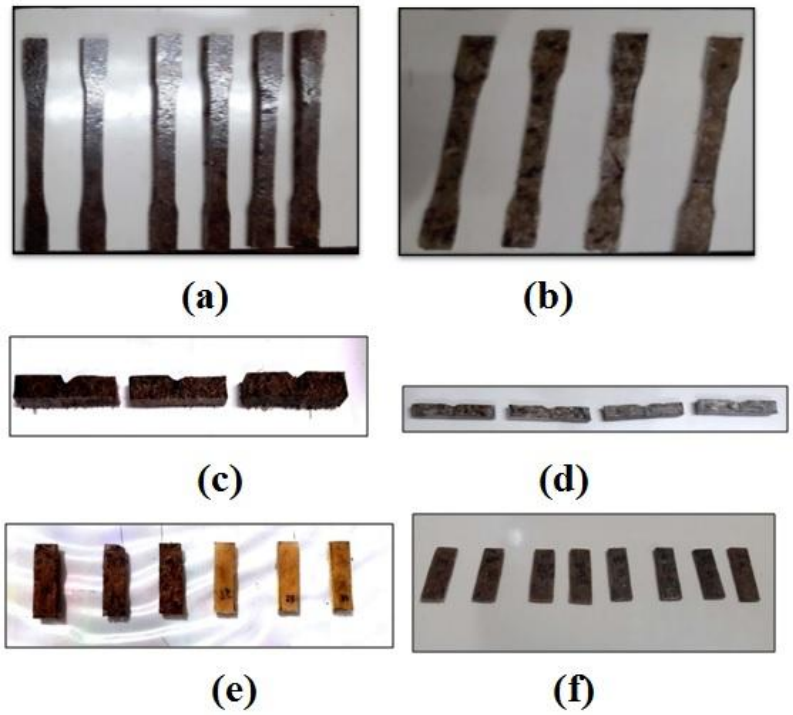

Fig. 3.5: (a) Tensile test specimens of COIR/Epoxy composites (b) Tensile test specimens of PALF/Epoxy composites (c) Impact test specimens of COIR/Epoxy composites (d) Impact test specimens of PALF/Epoxy composites (e) DMA test specimens of COIR/Epoxy and PALF/Epoxy composites (f) Different layered hybrid PALF/COIR biocomposites for DMA test

3.4 Characterization Techniques and Basic Procedure

This section deals with a range of techniques employed for the characterization of natural fibers (PALF and COIR) and their biocomposites. A checklist is specified in Table 3.3.

Table 3.3: Tests performed in this work

Technique	**Reason for test**
FTIR	Examination of surface chemistry
TGA	Find out the thermal degradation temperature
SEM	Examination of surface structure and morphology
Water immersion technique	Density
Water absorption	Moisture uptake
Tensile test	Material strength
Tensile modulus	Measure-stiffness of material
Flexural test	Bending strength
Flexural modulus	Resistance to deformation under load
Impact test	Resistance to impact
Rockwell hardness test	Determination of hardness
Dynamic mechanical analysis	Elastic and viscoelastic properties
Biodegradability test	The disintegration of biocomposite to give CO_2, water, inorganic compounds, and biomass
UL-94V flammability test	Determination of the rate of burning and mass-loss rate in the vertical direction
UL-94HB flammability test	Determination of the rate of burning and mass loss rate in the horizontal direction
Flame penetration test	Determination the time taken for flame penetration to material thickness

3.4.1 FTIR Analysis

FTIR technique [model Perkin Elmer 2000 (Fig. 3.6)] was exploited to examine the surface chemistry of raw and alkaline-treated (2%, 4%, 6%, 8%, and 10%) cellulosic fibers. It was done in Analytical Instrumentation Laboratory, CSIR-CSIO, Chandigarh (India). The FTIR spectrum of each sample was obtained in the range of 400-4000 cm^{-1} and a resolution of 2 cm^{-1}. Approximately 1 g of sample was taken for FTIR measurements.

Fig. 3.6: Perkin Elmer 2000 FTIR spectrometer

3.4.2 TGA Study

The thermal stability of the material was determined using a thermogravimetric analyzer, model Perkin Elmer TGA 4000 (Fig. 3.7). A sample of mass 12 mg was evenly and uniformly distributed in the alumina crucible which was supported by a precision balance. The variation in the mass was monitored and recorded using Perkin Elmer thermal software (Pyris). The temperature range was controlled from 25-700 ^{0}C. The heating rate of 10^{o}C/min was selected for better resolution of transition. TGA of all the samples had done in Central Instrumentation Laboratory, DTU Delhi (India).

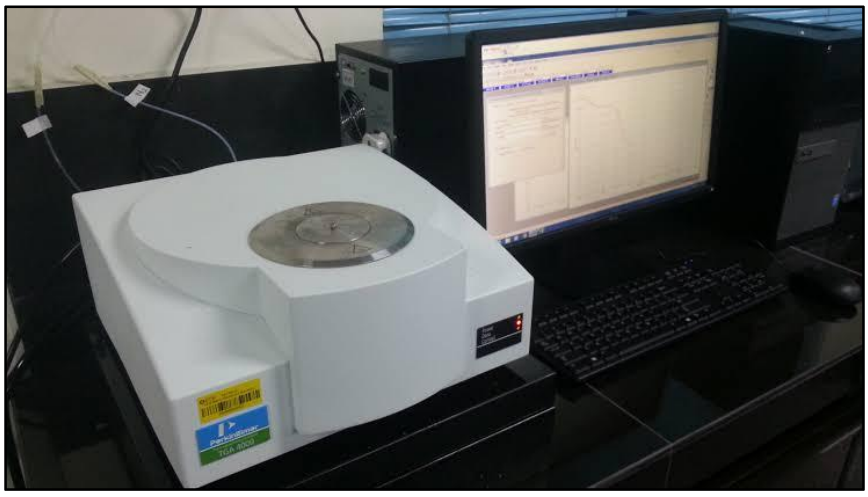

Fig. 3.7: Perkin Elmer TGA 4000 instrument

3.4.3 DMTA Study

DMTA is a powerful technique in the development of composites aiming to establish a significant relationship between microscopic structure and thermo-mechanical properties. The comprehensive knowledge of viscoelastic properties such as stiffness and damping, thermal transition, melting & degradation, and crystallization is important for manufacturing a high-performance polymeric material. DMA method has enormous potential to analyze the elastic and viscous response of polymer composites over a range of temperature, frequency, and time [239]. The stiffness and damping of PMC's can be easily determined in terms of storage modulus (E' or G') and tan δ. Nielson's proposed an equation to find out the damping of composites, based on the proportional contribution of a matrix.

$$\tan \delta_c = \tan \delta_m(1-V_f) \quad (3.1)$$

where $\tan \delta_c$ and $\tan \delta_m$ is the damping value of composite and matrix respectively, and V_f is the volume fraction of reinforcement. The damping behavior is influenced by the type of reinforcing fiber and resin, fiber/matrix interfacial adhesion, the orientation of fibers in a matrix system, fiber length and content, and void content [240-242]. To study the viscoelastic behavior of developed specimens, a dynamic mechanical thermal analyzer, model DMA 8000 [Fig. 3.8] was used which is installed in Central Instrumentation Laboratory, DTU, Delhi (India). Rectangular specimens of dimensions 35mm X 10mm X 2mm were used in double cantilever mode over a temperature range of 25-140 ^{0}C at a rate of 3^{0}C/min. The effect of frequency on E', tan δ, and T_g were also studied at two different frequencies, namely 1 and 5 Hz.

Fig. 3.8: DMA 8000 instrument

3.4.4 SEM Analysis

SEM was employed to examine the surface morphology of PALF and COIR strands. It was performed using a Field Emission Scanning Electron Microscope [FE-SEM, Hitachi 4300 (Fig. 3.9)] at an accelerating voltage of 10 kV in Analytical Instrumentation Laboratory, CSIR-CSIO, Chandigarh (India).

Fig. 3.9: Hitachi S-4300 SEM instrument

3.4.5 Water Absorption

The water absorption test was performed on the cured epoxy matrix, untreated and alkaline treated cellulosic fibers, and their biocomposites according to ASTM D570 standard. Four samples of each composite specimen were submerged in distilled water at room temperature. However, in the case of fibers, water absorption measurement was done in various water samples such as distilled water, river water, and hand-pump water. The pH of water samples was – distilled water: 7.0, river water: 7.67, hand-pump water: 7.42. Initially, dried all the samples in a vacuum oven at 70 ^{0}C for 24 hrs, and then cooled to room temperature. Repeat the drying process until the constant weight was obtained. The weight of dried and wet samples was measured by using a digital highly calibrated weighing machine [0.001 g accuracy, DTU, Delhi (India)]. After every 12 hrs of immersion, the samples were taken out from the water bath and wipe dry to remove redundant water molecules on the surfaces. The weight gain (%) was calculated by using the formula

$$Weight\ gain\ (\%) = \frac{(W_t - W_o)}{W_o} \times 100 \qquad (3.2)$$

where W_t and W_O are the weight of the specimen after immersion time "t" and the oven-dried weight respectively. The mechanism of water diffusion into the PMCs was determined by analyzing the diffusion exponent (n) according to the equation (3.3) and (3.4).

$$\frac{M_t}{M_m} = kT^n \tag{3.3}$$

$$LOG\frac{M_t}{M_m} = LOG(k) + nLOG(T) \tag{3.4}$$

where M_t and M_m are the water absorption at time t and saturation level respectively, k is a constant parameter and n is diffusion coefficient which defines the water diffusion mechanism.

3.4.6 Void and Density Measurement

The hypothetical density of composites is determined according to the equation 3.5 [243].

$$\rho_{theoretical} = \frac{1}{\left[\left(\frac{W_f}{\rho_f}\right)+\left(\frac{W_m}{\rho_m}\right)\right]} \tag{3.5}$$

where W and ρ represents the weight fraction and density respectively. The actual density was calculated as per ASTM D2734. The void content was measured through equation 3.6.

$$Void\ Contents\ (\%) = \frac{\rho_{theoretical} - \rho_{experimental}}{\rho_{theoretical}} \tag{3.6}$$

3.4.7 Mechanical Properties

For the mechanical characterization of developed composites, the tensile, flexural (3 point bending), impact, and hardness tests were performed at ambient temperature using ASTM standard.

3.4.7.1 Tensile Test

The test was executed on fabricated composite specimens using a Table Top Tinius Olsen Horizon H50KS, Universal Testing Machine (Fig. 3.10) in accordance with ASTM D638 standard. The tensile properties (strength, modulus, breaking load, and elongation at break) of composites were measured at room temperature with a crosshead speed of 1 mm/min. The standardized sample was in the dumbbell shape

of 50 mm gauge length, 13 mm width, and 4 mm thickness. The results are reported as an average of four identical test samples.

Fig. 3.10: Tinius Olsen Horizon H50KS Universal Testing Machine

3.4.7.2 Flexural Test

The composite samples of dimensions 80 mm X 15 mm X 4 mm with the span length to depth ratio 20:1 were subjected to a 3-point flexural bending test as per ASTM D790 standard. The flexural test was executed on the above-mentioned UTM at a speed of 3 mm/min. Four similar-sized test specimens were tested in each case and the mean value was reported.

3.4.7.3 Impact Test

In automotive applications, the major concern in the use of NFRCs is their response to impact load. The impact fracture strength of unhybridized and hybridized notched composite specimens was determined using an Izod impact testing machine (Fig. 3.11) as per ASTM D256 standard. The energy absorbed by a specimen was determined using Equation 3.7. The total of four samples for each specimen was tested and their average value was reported.

$$\text{Impact energy} = \text{mass X height X gravity} \quad (3.7)$$

Fig. 3.11 Impact testing machine

3.4.7.4 Rockwell Hardness Test

The hardness of developed specimens was measured as per ASTM D785 standard. The test is performed with a ball indenter ¼" (6.54 mm) with an applied minor and major load of 10 kgf and 100 kgf respectively. Rockwell hardness scale chosen was M scale and it is used for soft or thin materials including plastics. The test was performed four times on similar test specimens and their mean value was reported. The observations are useful to determine relative resistance to indentation.

Fig. 3.12 Rockwell Hardness Testing Machine

3.4.8 Biodegradability

The biodegradability of untreated and alkali-treated composites was studied in natural soil burial condition for 110 days. The specimens were dugout after every 10 days of soil burial, followed by washing in distilled stream and then desiccated at 70^0C for 24 hr. The weight loss (%) was measured using a digital highly calibrated weighing machine (0.001 g accuracy). The total four measurements were taken for each composite specimen and their average values were reported.

3.4.9 Flammability Tests

3.4.9.1 UL-94V Test

The UL-94 vertical (UL-94V) test was performed to measure the flammability of developed specimens. The test specimen is clamped at the upper end and mounted vertically in such a manner that its lower end is 3/8 inch above the Bunsen burner tube (Fig. 3.13). The sample is ignited at the center of its lower end for 10 seconds, replaced and then reapplied for another 10 seconds. The rate of mass loss and time taken for flame propagation in the vertical direction is observed and recorded. The formation of residual char and dripping of flaming particles is carefully observed by the lab technician. To obtain accurate results, a total of four samples for each layered hybrid specimen were tested and their average value was reported.

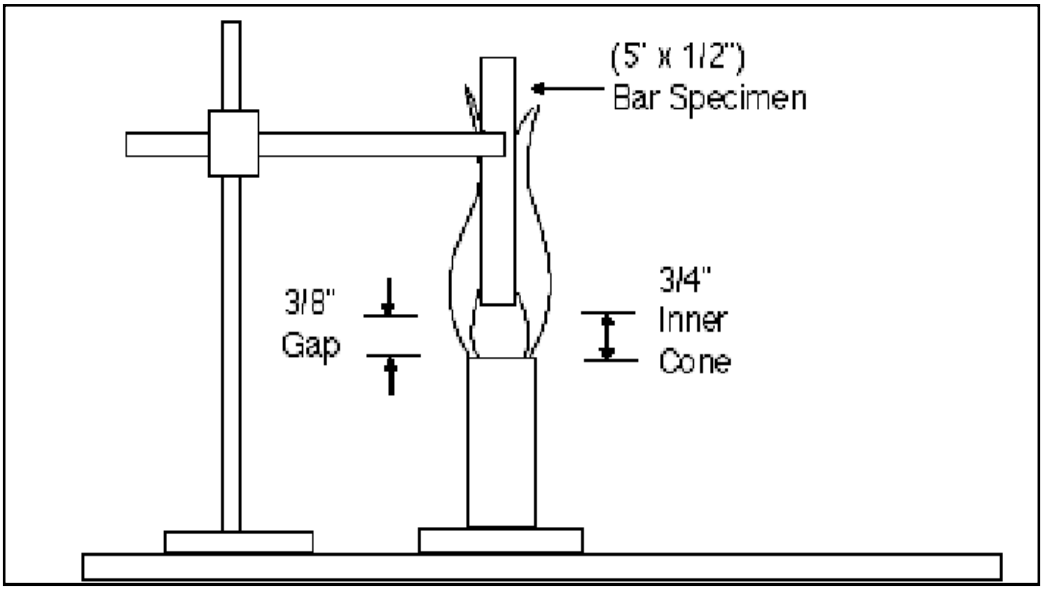

Fig. 3.13: Setup for Vertical Flammability Test

3.4.9.2 UL-94HB test

The Underwriters Laboratories horizontal burning test (UL-94HB) is the easiest and widely used standard to determine the burning rate of plastics and their composites. The typical dimensions of a sample for the horizontal burning test are same as the vertical flammability test. Fig. 3.14 shows the marked specimen (1" and 4" from one end of the specimen), mounted with its long axis horizontally on the stand and a 1" high blue Bunsen flame is applied to the free end of a specimen for 30 seconds. The time for the flame front to travel between the two gauge marks is recorded and measured.

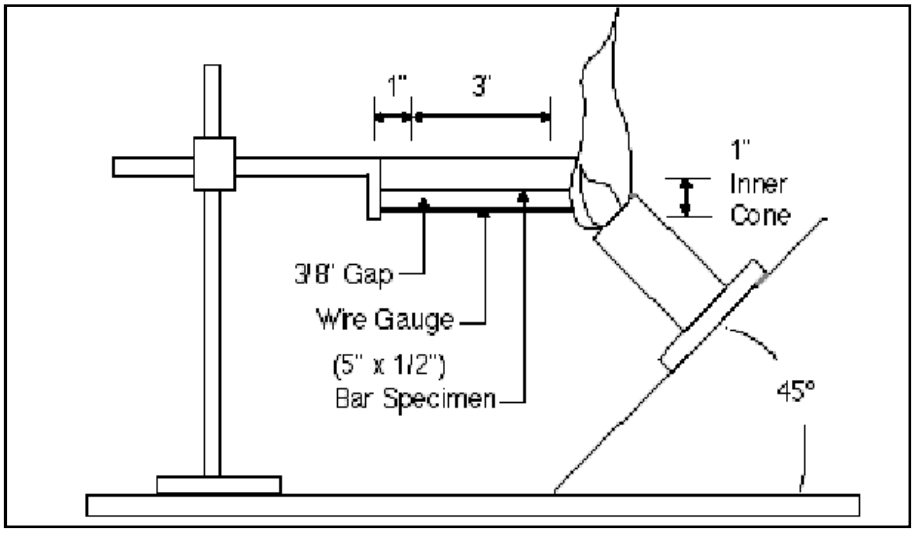

Fig. 3.14: Setup for Horizontal Flammability Test

3.4.9.3 Flame Penetration Test

Flame penetration test was conducted on the developed hybrid composites having dimensions of 125 mm X 70 mm X 12 mm. Fig. 3.15 depicts the specimen, supported 1.5 inches above the nozzle of a blowpipe. The time-lapse for the flame to penetrate the thickness were recorded.

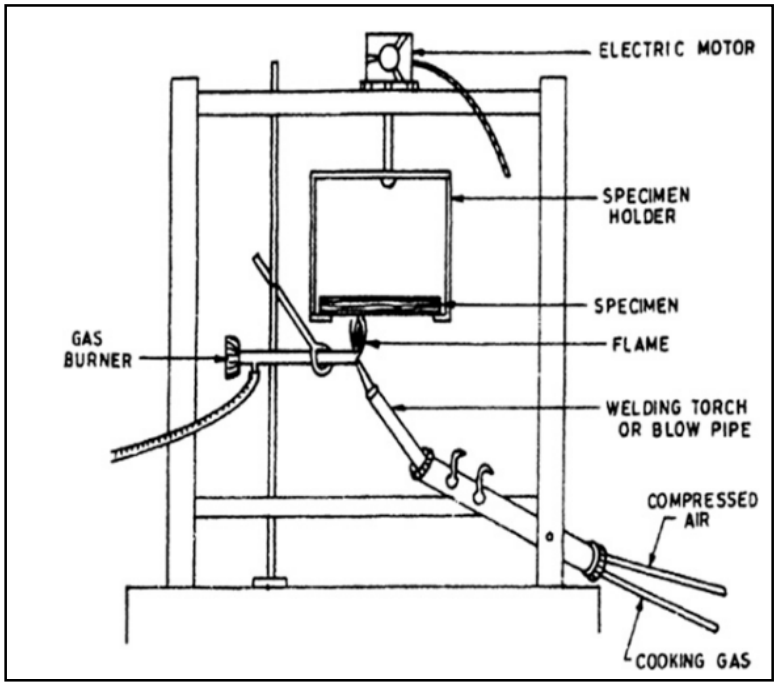

Fig. 3.15: Setup for Flame Penetration Test

3.5 Summary

This section clarified the system utilized in the creation of biocomposite materials and alkaline treatment of lignocellulosic fibers. The materials and characterization techniques used in this study were also reported. The following section discusses the results, obtained after an experimental investigation of cellulosic fibers and their biocomposites.

CHAPTER 4 – RESULTS AND DISCUSSION

4.1 Impact of Alkaline Action on Surface Chemistry, Morphology, Thermal Stability and Water Absorption Behavior of Cellulosic Fibers

The significant factor which controls the effectiveness of reinforcing fibers in a composite material is the interfacial interaction with matrix resin. So, it is required to improve the bonding and compatibility between them. The alkaline treatment is an extensively used technique to modify the surface chemistry of strands which may result the improvement in resistance to moisture sorption and thermal decomposition. In this segment, the impact of mercerization (2%, 4%, 6%, 8%, and 10% of NaOH) on the surface chemistry, thermal stability, and water uptake behavior of PALF and COIR fibers were studied.

4.1.1 FTIR Analysis

The FTIR spectra of COIR and PALF (Fig. 4.1) revealed that the surface chemistry of cellulosic fibers was changed considerably after alkaline action. The intensity at 3300 cm^{-1} and 1000 cm^{-1} (corresponds to the -OH functional group) was increased after alkaline modification and this was because of the removal of waxy and gummy substances. An increase in peak intensity at around 1600-1650 cm^{-1} and 1250 cm^{-1} also assured the elimination of wax, adhesives, pectin, and gummy substances from the fiber surface. The absorption peak at 1745 cm^{-1} was observed in raw fibers but disappears after NaOH treatment. It is related to C=O stretch and confirmed the removal of hemicellulose. The FTIR spectra of untreated PALF and COIR fibers (Fig. 4.2) illustrate that the PALF has a large amount of hydroxyl (-OH) group than the COIR fiber. The broad peak in the region 3200-3500 cm^{-1} is related to the hydroxyl group. The peak at 1244 cm^{-1} is much smaller in PALF than the COIR. This peak specify the C=O stretch of an acetyl group of lignin.

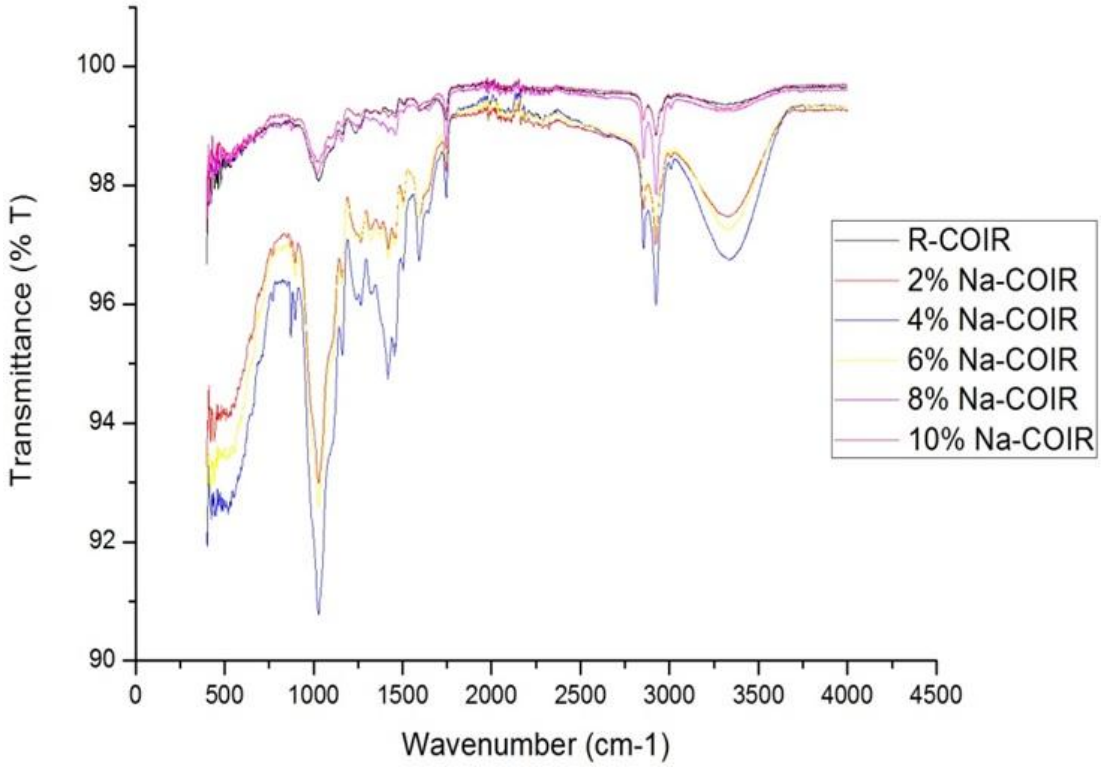

(a)

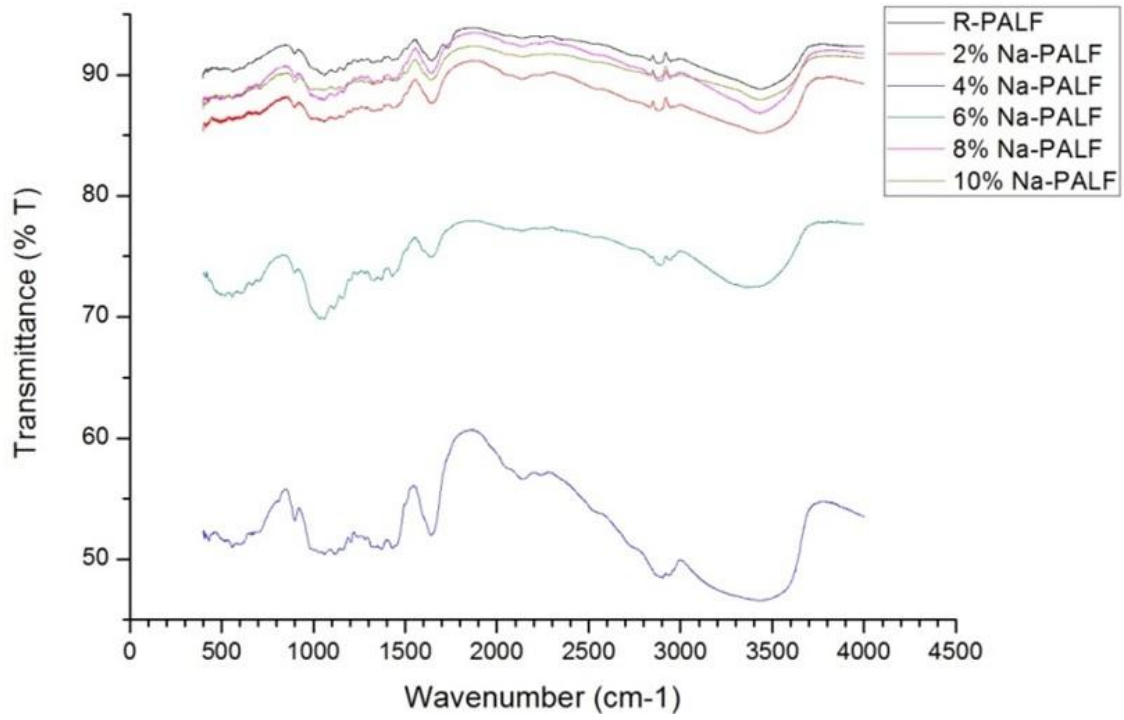

(b)

Fig. 4.1: FTIR of raw and treated fibers (a) COIR (b) PALF

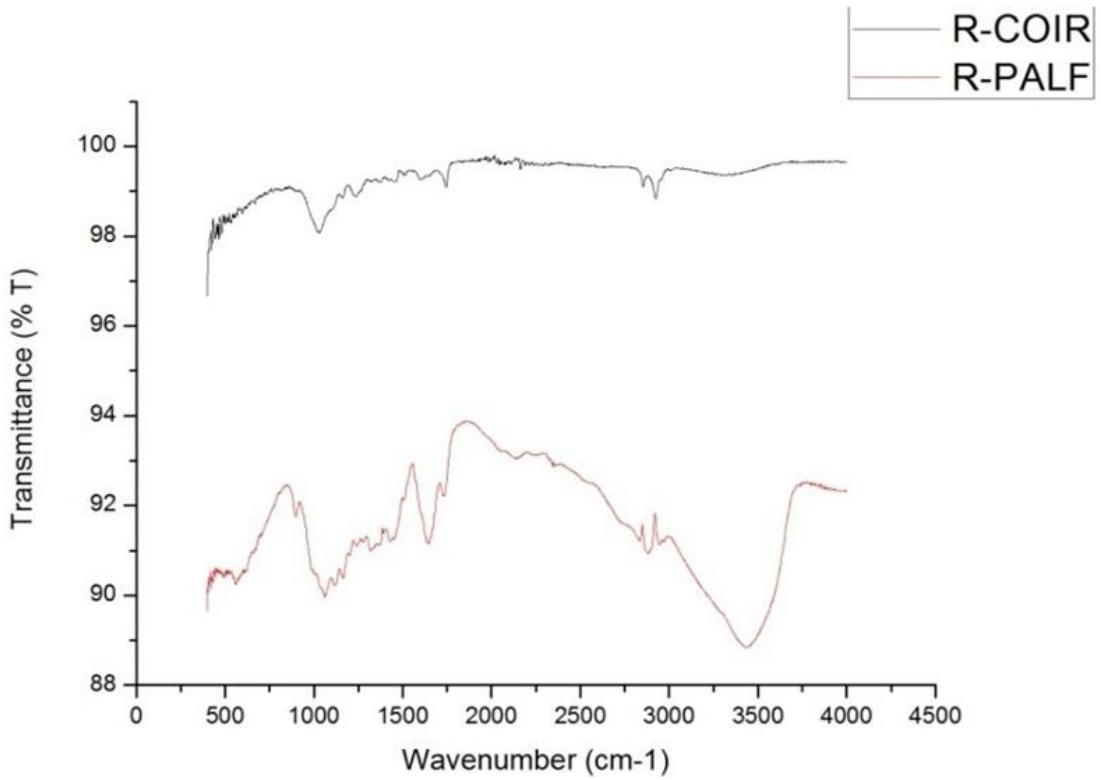

Fig. 4.2: FTIR of COIR and PALF

4.1.2 SEM Analysis

The surface morphology of raw and treated COIR strands is reported in Fig. 4.3 (a)-(f). The raw fiber display "rotten-wood" like appearance in which many holes and cavities are present. The micrograph in the left bottom of Fig. 4.3 (a) revealed the network-like structure that contains longitudinally oriented unit cells held together by binder lignin and fatty-waxy substances. Fig. 4.3 (b) depicts that the surface topography of 2% NaOH treated COIR is much smoother than the untreated fiber. It seems that the fiber surface being roughens again with regularly placed pinholes after the modification with highly concentrated alkali solution [Fig. 4.3 (c)-(f)]. This was because of the incomplete exclusion of waxes, surface residues, and fatty deposits.

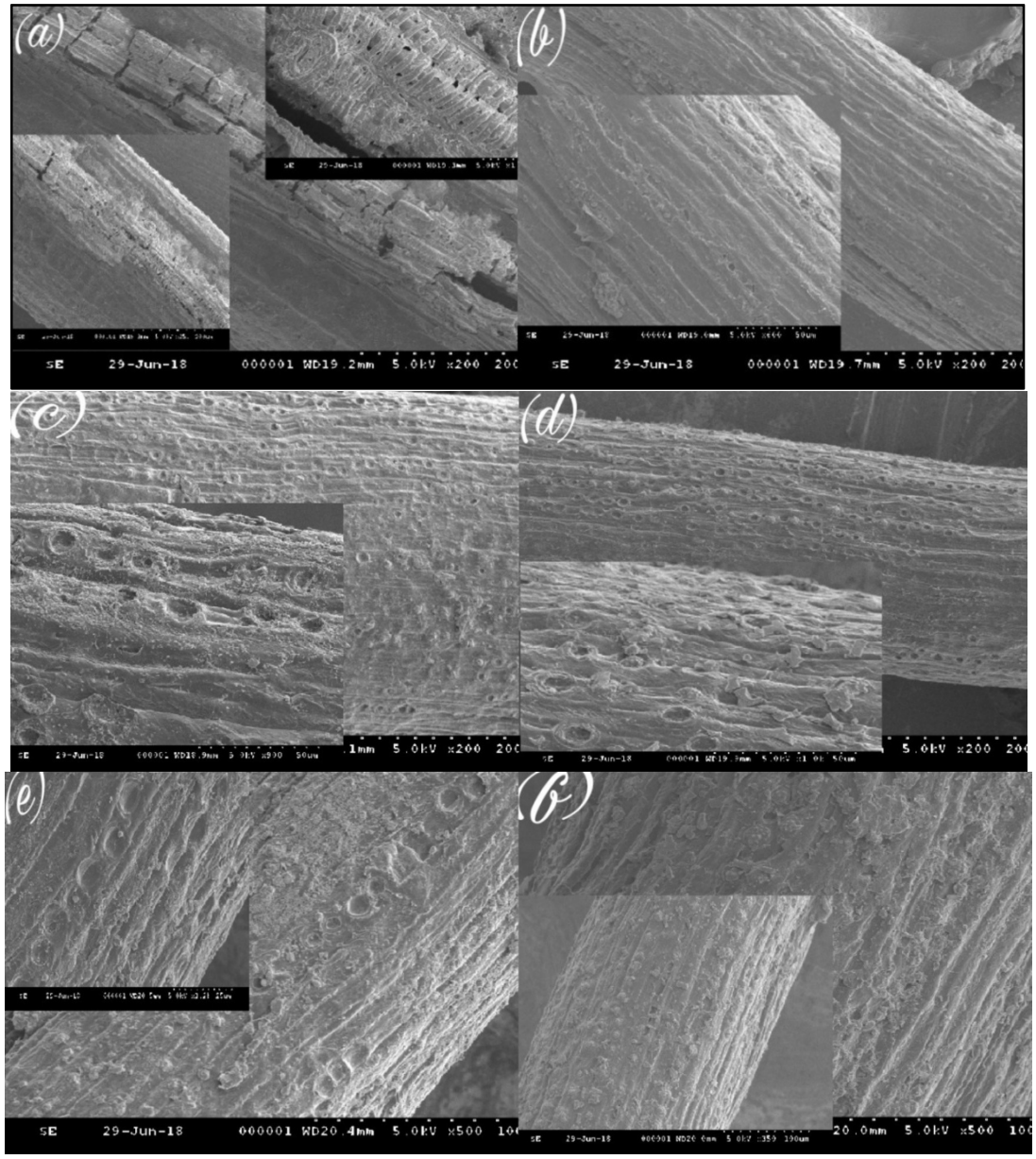

Fig. 4.3: (a) Untreated COIR fiber, plane view (X200), and magnified plane view (X1200). (b) 2% NaOH treated COIR fiber, plane view (X200), and magnified plane view(X400). (c) 4% NaOH treated COIR fiber, plane view (X200), and magnified plane view(X900). (d) 6% NaOH treated COIR fiber, plane view (X200), and magnified plane view(X1000). (e) 8% NaOH treated COIR fiber, plane view (X500), and magnified plane view(X1200). (f) 10% NaOH treated COIR fiber, plane view (X350), and magnified plane view(X500)

Fig. 4.4 (a)-(e) revealed that the PALF has much smoother and continuous morphology than the COIR fibers. Moreover, PALF represents no pin-holes. Similar to the results of COIR, the alkali-treated PALF also has a higher degree of roughness than the untreated one and this was because of the partial removal of hemicellulose and binder lignin. Fig. 4.4 (c)-(f) depicts that the fibrillation and cracks were increased by alkaline treatment of fiber.

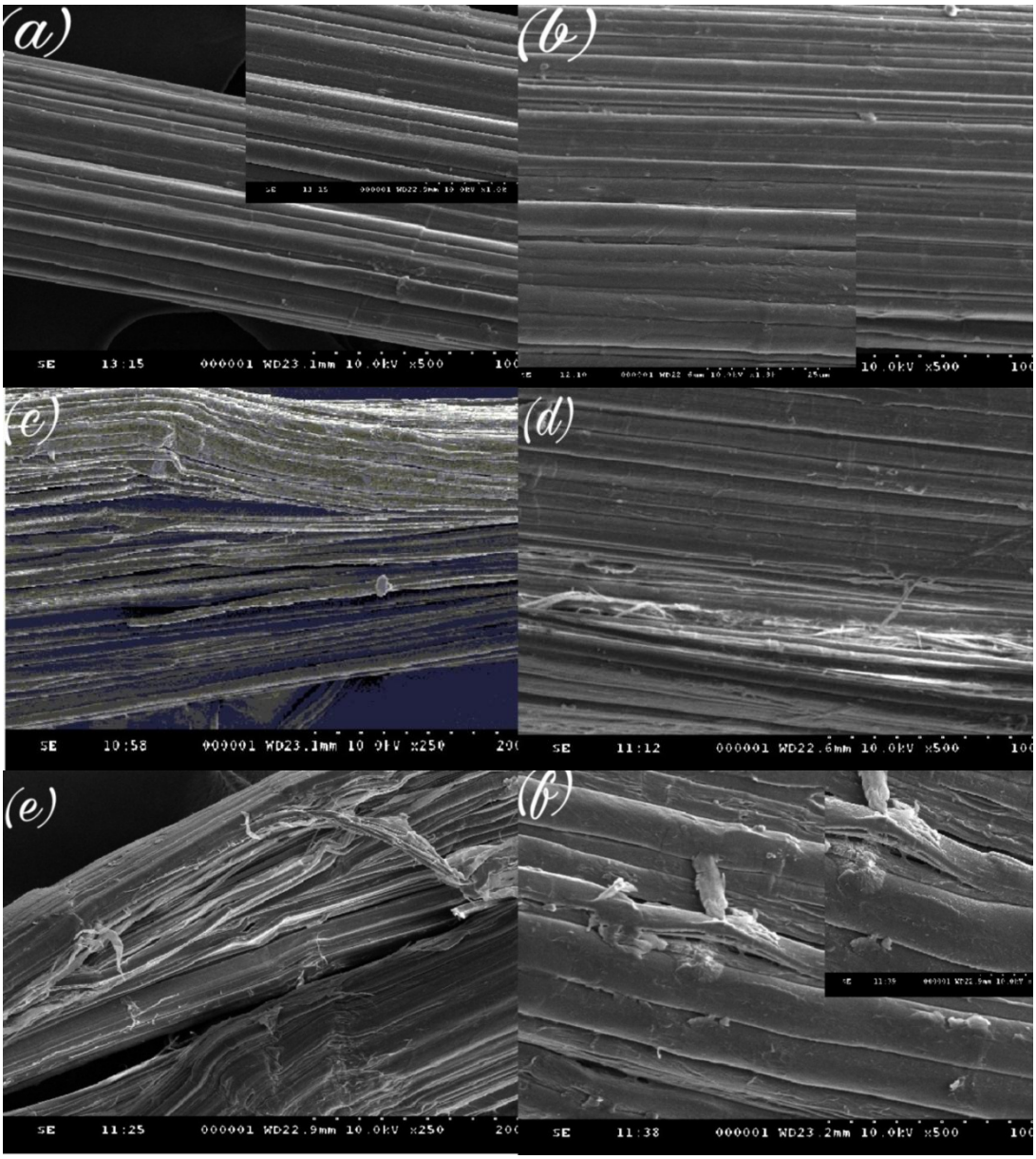

Fig. 4.4: (a) Untreated PALF fiber, plane view (X500), and magnified view (X1000). (b) 2% NaOH treated PALF fiber, plane view (X500), and magnified plane view(X1300). (c) 4% NaOH treated PALF fiber, plane view (X250). (d) 6% NaOH treated PALF fiber, plane view (X500). (e) 8% NaOH treated PALF fiber, plane view (X250). (f) 10% NaOH treated PALF fiber, plane view (X500), and magnified plane view (X1000)

4.1.3 Water Absorption Measurement

The moisture absorption in cellulosic fibers is the main barrier to their successful usage in engineering applications. It leads to the swelling of material, dimensional change, reduction in rigidity of cell wall, and poor strength & stiffness. Therefore, it is highly required to examine the water absorption behavior of COIR and PALF. For accurate estimation of the water absorption behavior, it is required to prepare the

fiber bundles in the same manner. Four replicates were tested and their mean was presented as a result. The bundles of fibers were immersed in containers containing various sources of water (River water, Distilled water, and Hand-Pump water). After every 12 hrs, the fibers were taken out and mopped the excess water from the fiber surface before weighing. Fig. 4.5 revealed that the PALF absorbs more water (7.8%) than the COIR and it is due to the lower O/C ratio in COIR fiber.

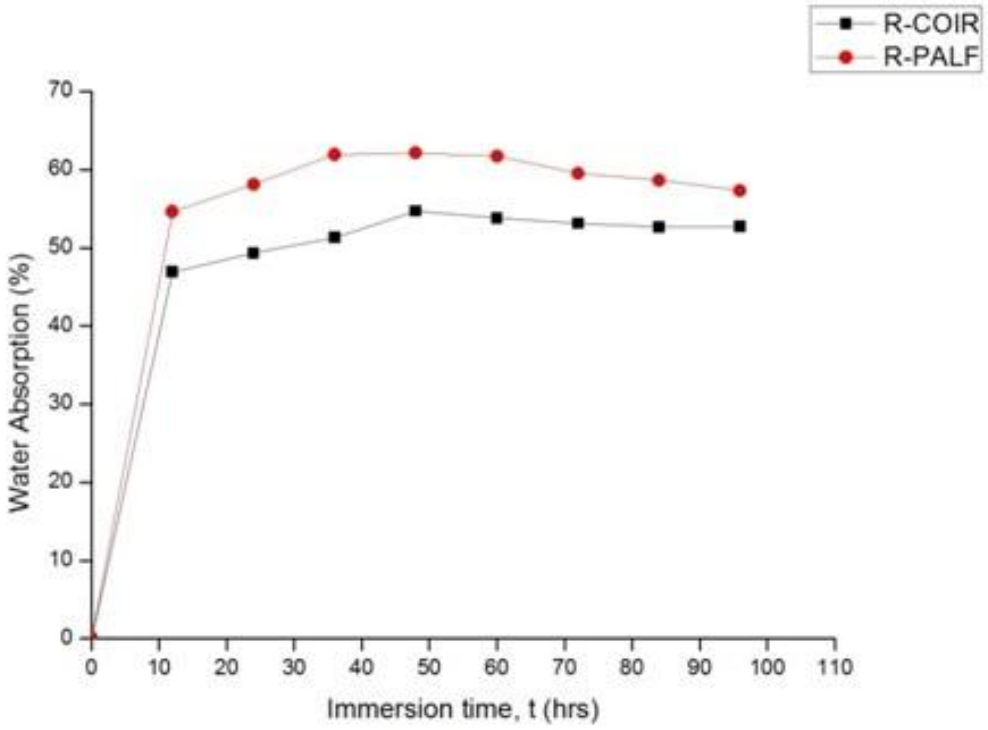

Fig. 4.5: Water absorption behavior of COIR and PALF in distilled water

The untreated PALF and COIR fiber absorb maximum water in distilled water (62.99%) and river water samples (60.6%) respectively. The water absorption is because of the existence of free hydroxyl and ionic functional groups; the presence of a hollow cavity called lumen; and the capillary action of micropores, cavity, crevices, and holes. Fig. 4.6 illustrates the influence of submersion period (**t)** on the moisture sorption of cellulosic fibers in various water samples. It was observed that the moisture sorption is a two-step process; in 1st step, fiber absorbs water up to the saturation level due to the capillary effect and in 2nd step, a diminution in the water absorption due to hydro-elastic property of fiber. The water diffusion and capillary action are more pronounced in alkali-treated fibers than the untreated ones.

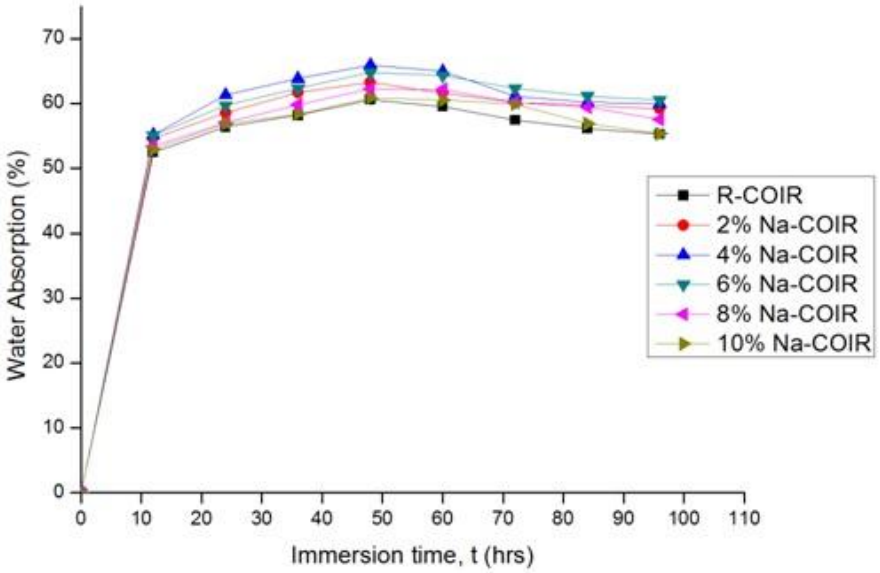
Water Absorption (%)
Immersion time, t (hrs)
R-COIR
2% Na-COIR
4% Na-COIR
6% Na-COIR
8% Na-COIR
10% Na-COIR

(a)

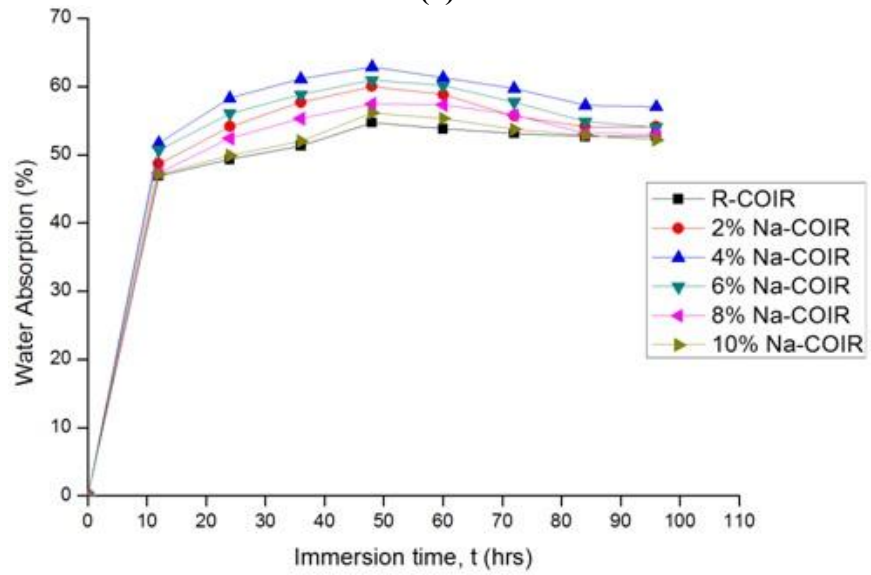
Water Absorption (%)
Immersion time, t (hrs)
R-COIR
2% Na-COIR
4% Na-COIR
6% Na-COIR
8% Na-COIR
10% Na-COIR

(b)

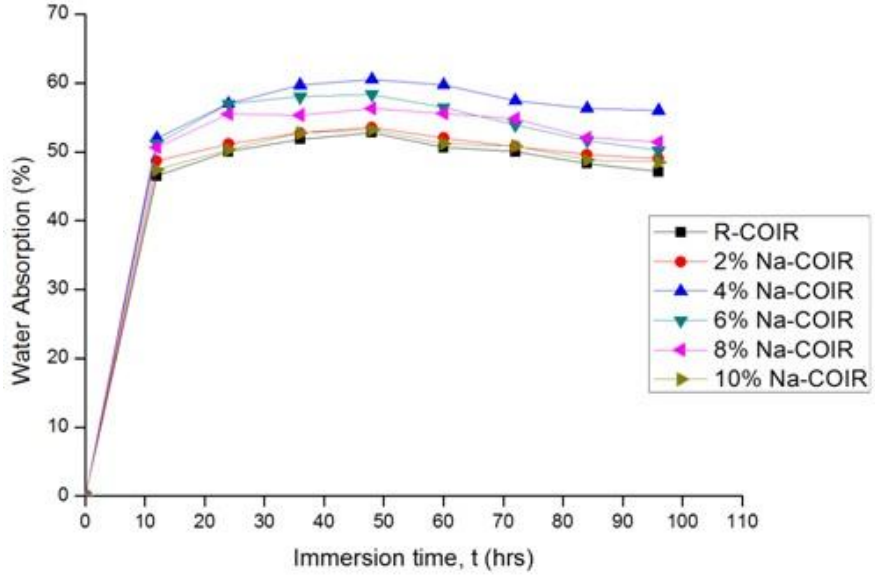
Water Absorption (%)
Immersion time, t (hrs)
R-COIR
2% Na-COIR
4% Na-COIR
6% Na-COIR
8% Na-COIR
10% Na-COIR

(c)

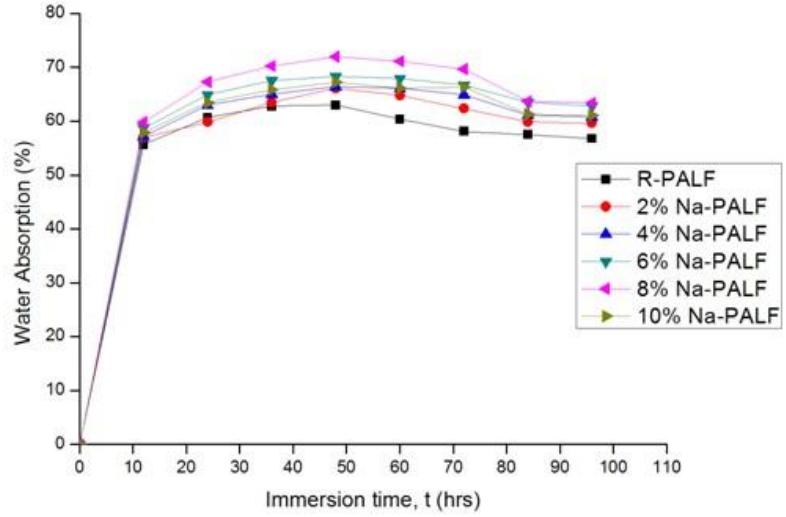

(d)

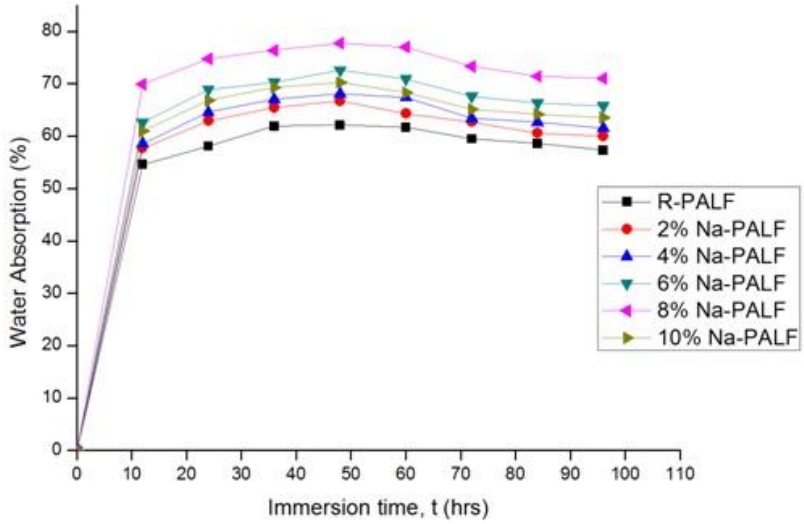

(e)

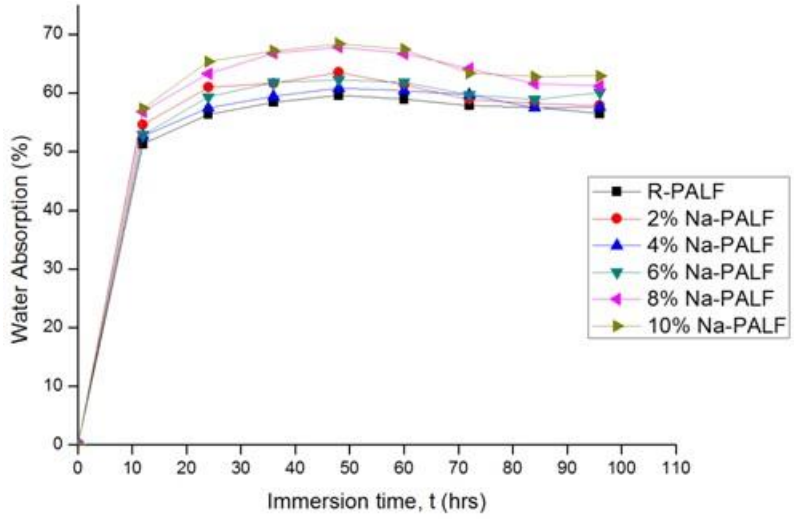

(f)

Fig. 4.6: Influence of submersion period (**t**) on the moisture sorption of untreated and alkali-treated: **(1)** COIR fibers in (a) river water (b) distilled water (c) hand-pump water **(2)** PALF in (d) river water (e) distilled water (f) hand-pump water

Fig. 4.7 depicts the impact of mercerization action on water absorption of COIR and PALF. The moisture sorption was increased considerably after an alkali treatment of fibers and this was because of the partial removal of hemicellulose and lignin. Bismarck *et al.* (2001) also reported the de-waxing and higher accessibility of active functional groups in sisal fiber caused by mercerization [212]. Amongst all the samples of COIR fiber, the 4 wt% NaOH treated one exhibit maximum water uptake. However, in the case of PALF, the 8% NaOH treated fiber possesses maximum water absorption in river (71.96%) and distilled water sample (77.72%). Alkaline treatment results in the removal of pectinous gum, lignin, and hemicellulose which leads to the faster liquid penetration in small, interconnected and uniformly distributed pores.

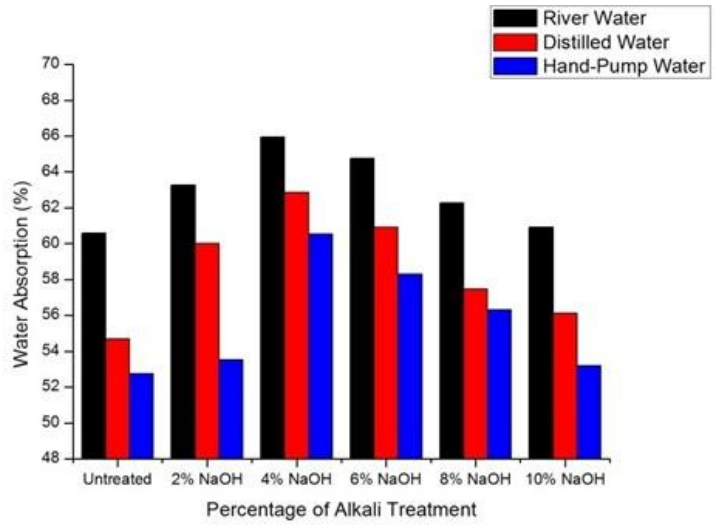

(a)

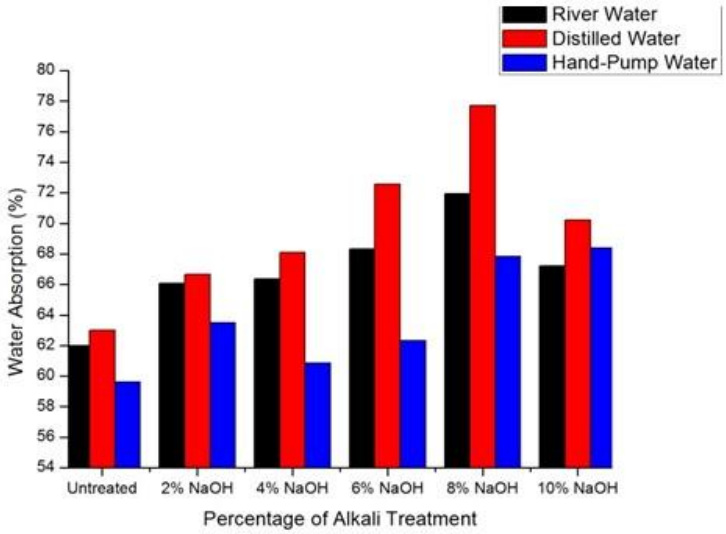

(b)

Fig. 4.7 Impact of mercerization action on the moisture sorption of (a) COIR (b) PALF

4.1.4 Thermal Decomposition of PALF and COIR Fibers

TGA and DTG curves of natural and treated strands are illustrated in Figs. 4.8-4.10 and the corresponding weight loss as a function of temperature is mentioned in Table 4.1 and 4.2. In all cases, the initial decomposition occurs at a temperature between 30 ^{0}C to 185 ^{0}C and it corresponds to the release of bound water and volatile extractives. The PALF exhibits a higher rate of moisture loss than the COIR fiber. The peak temperature related to the moisture loss appears at 48 ^{0}C and 31 ^{0}C for untreated COIR and PALF respectively. From Table 4.2, we can report that the 4 wt% NaOH treated PALF exhibits less weight loss (around 48%) than the untreated fiber. Ndazi *et al.* [244] concluded that the structurally bound water is resistant to complete water removal during drying.

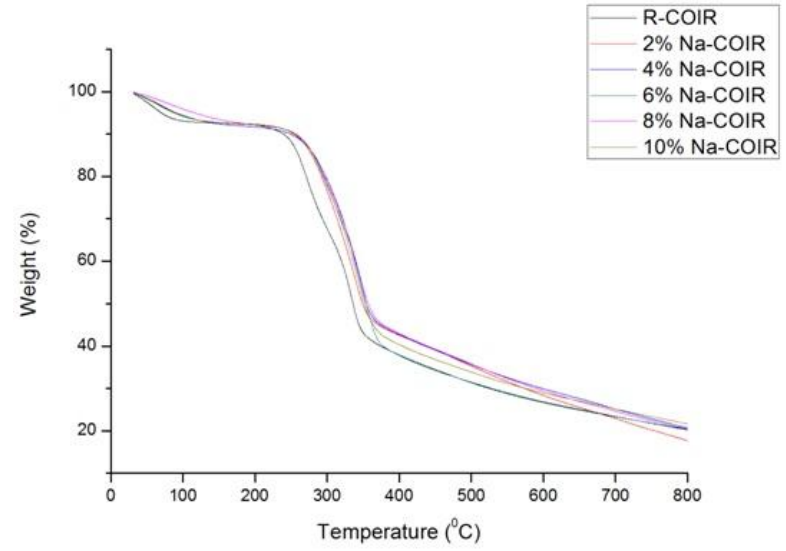

(a)

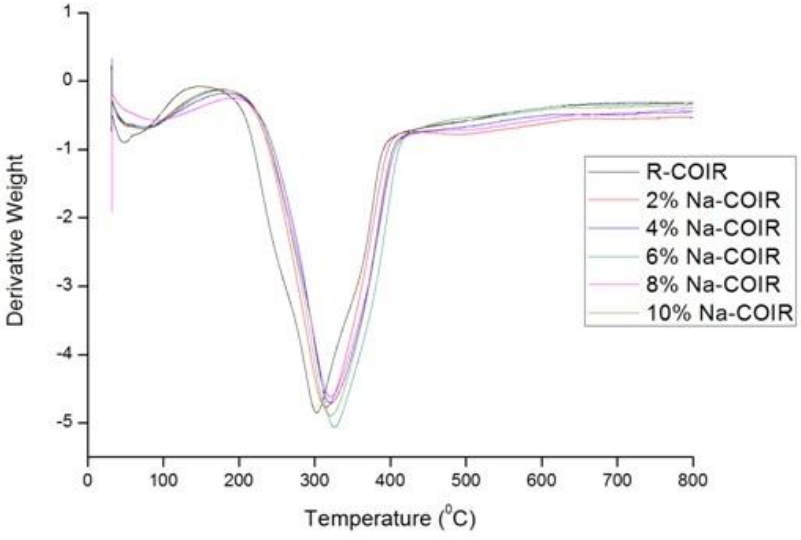

(b)

Fig. 4.8: (a) TGA (b) DTG of raw and alkali-treated coir fibers

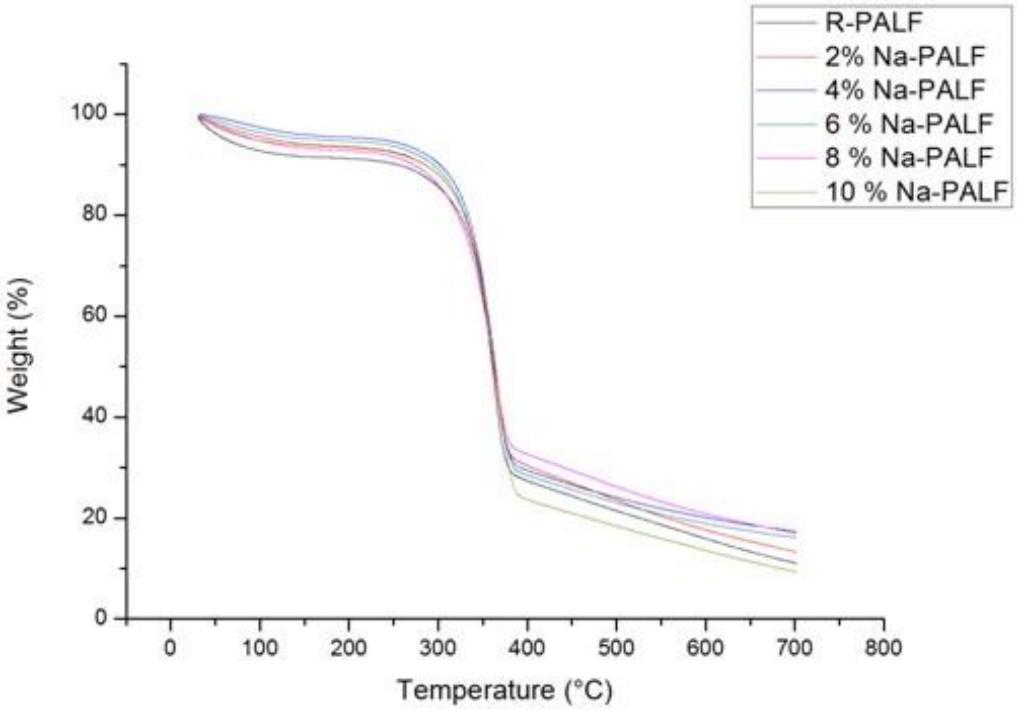

(a)

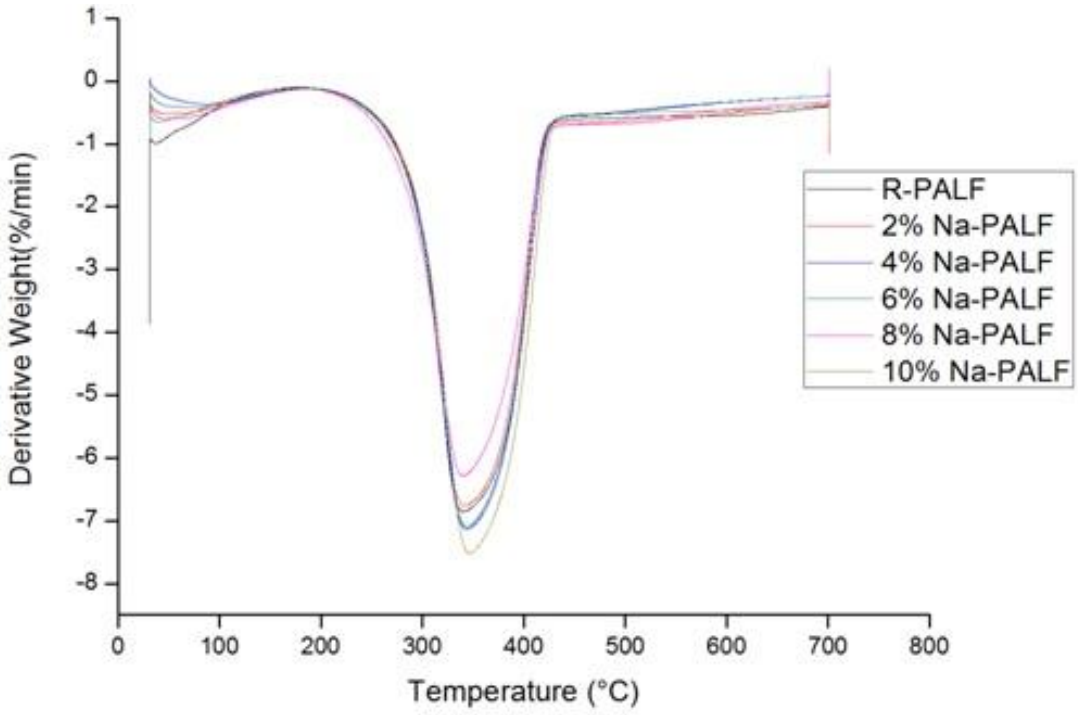

(b)

Fig. 4.9: (a) TGA (b) DTG of raw and alkali-treated PALF

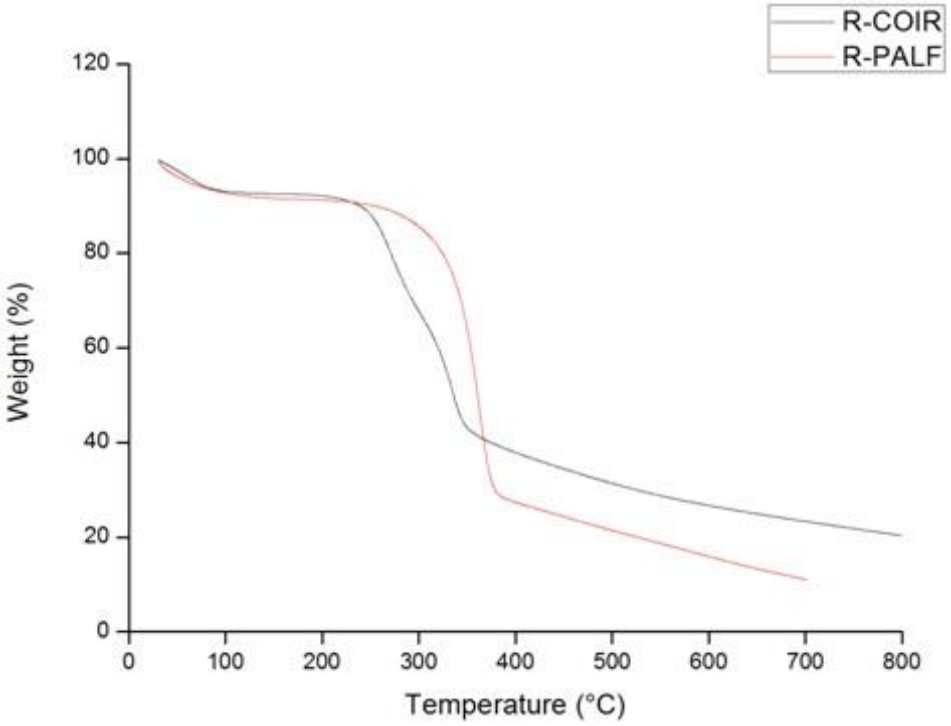

(a)

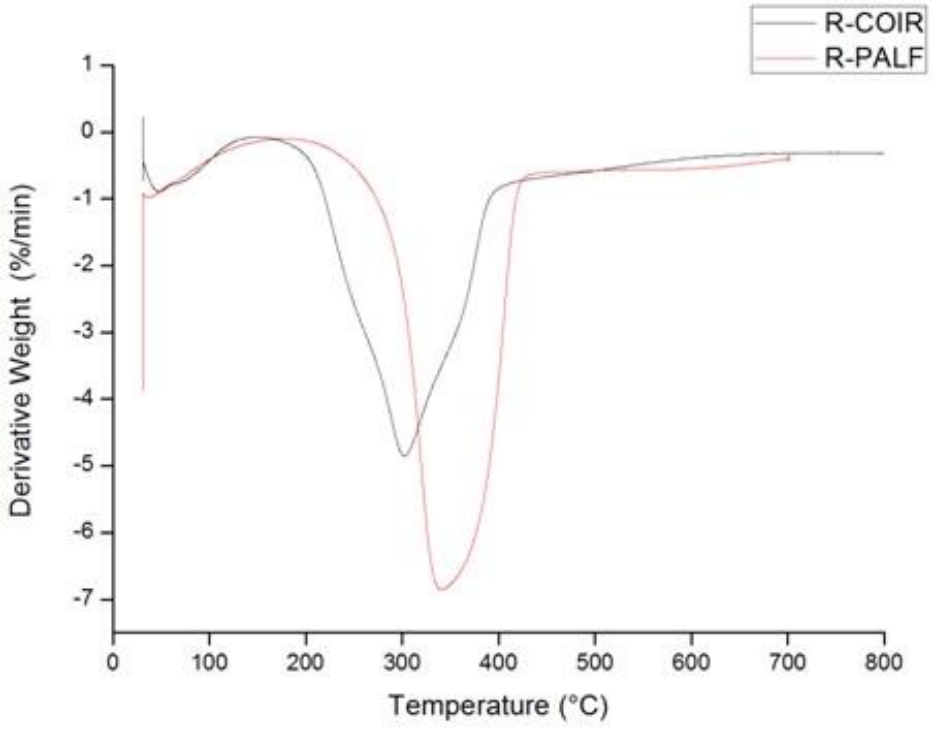

(b)

Fig. 4.10: (a) TGA (b) DTG of COIR and PALF

Tables 4.1 and 4.2 illustrates that the weight loss of cellulosic fibers is negligible below 290 ^{0}C. Moreover, the major mass loss (30-50%) occurs above this temperature and it was due to the degradation of crystalline cellulose. M. Siti. Alwani *et al.* [245] also reported that the major mass loss (30-50%) in SCB, PALF, COIR, and BPS fibers occurred at a temperature above 300 ^{0}C. As the temperature increases, the cellular breakdown of hemicellulose takes place. The hemicellulose decomposition is the first stage of fiber degradation. It was observed that the COIR fibers started to decompose at 150 ^{0}C; however, the PALF decompose at 185 ^{0}C. In both cases, the peak temperature of maximum degradation was shifted to a higher value after alkaline treatment. The 4 wt% NaOH treated COIR fiber exhibits the higher value of peak temperature (about 20 ^{0}C more) than the untreated one and it was due to the elimination of less stable hemicellulose. It was observed that the main degradation peak lies within the temperature range of 290-380 ^{0}C with 50% degradation. The PALF possesses higher total mass loss (around 10%) than the COIR. However, the degradation of PALF occurs at a higher temperature and it was due to the presence of a large amount of cellulose content.

Table 4.1 - TGA of raw and treated coir fibers

Fiber	Temperature Range ^{0}C	Weight Loss (%)	Residual char (%)
R-COIR	0-152.4	7.396	23.359
	152.4-242.85	3.05	
	242.85-352.94	46.49	
2% Na-COIR	0-161.9	7.4	22.94
	161.9-262.01	3.68	
	262.01-361.86	42.73	
4% Na-COIR	0-176.06	8.07	25.135
	176.06-277.08	5.7	
	277.08-363.15	39.39	
6% Na-COIR	0-176.19	7.66	23.409
	176.19-271.44	4.8	
	271.44-376.18	47.29	
8% Na-COIR	0-152.38	6.65	24.64
	152.38-266.72	4.7	
	266.47-376.25	43.43	
10% Na-COIR	0-171.52	7.55	25.15
	171.52-276.12	5.69	
	276.12-361.95	40.92	

Table 4.2 - TGA of raw and treated pineapple leaf fibers			
Fiber	Temperature Range ^{0}C	Weight Loss (%)	Residual Char (%)
R-PALF	0-184.78	8.63	11.103
	184.78-330.4	13.63	
	330.4-382.66	48.75	
2% Na-PALF	0-164.31	6.071	13.356
	164.31-261.85	1.97	
	261.85-361.97	41.98	
4% Na-PALF	0-184.04	4.465	17.34
	184.04-324.15	11.18	
	324.15-376.7	49.59	
6% Na-PALF	0-175.1	5.12	16.14
	175.1-321.7	11.16	
	321.7-378.32	50.57	
8% Na-PALF	0-186.88	7.162	17.01
	186.88-315.15	10.54	
	315.15-378.23	46.56	
10% Na-PALF	0-186.95	6.545	9.386
	186.95-326.09	12.03	
	326.09-382.54	54.058	

Lignin is the most thermally stable component of cellulosic fiber and this was attributed to its highly cross-linked complex aromatic structure. Mackay and Nassar [246] reported that the thermal stability of lignocellulosic fibers is in the order: lignin>α-cellulose>hemicellulose. Lignin starts to decompose at a lower temperature (typically 160-175 ^{0}C) as compared to cellulose but it decomposes slowly under the whole temperature range and its temperature extends as high as 900 ^{0}C. According to Paiva *et al.* [247], the decomposition of lignin occurs in a wider temperature range than the cellulose and hemicellulose components. After 700 ^{0}C, the remaining mass in COIR was higher than the PALF and this was attributed to the presence of a large amount of lignin compound in COIR fiber. It was observed that the 4 wt% NaOH treated COIR and PALF fibers possess higher residual mass than the untreated one and it was due to the slow rate of chemical decomposition reaction and dominance of the formation of condensed cellulose as the solid residue.

Table 4.3 and 4.4 illustrates the DTG results of raw and chemically modified strands. On account of raw COIR, the two decomposition peaks at 228 ^{0}C and 302 ^{0}C at the rate of 1.475 and 4.852 %/min correspond to the breakdown of hemicellulose and cellulose components. The rate of hemicellulose decomposition is more prominent in untreated fibers (PALF and COIR) than the alkali-treated. It was observed that the

PALF exhibits a higher rate of decomposition than the COIR fiber. Thus from DTG results, we can conclude that the alkaline treated fibers possess degradation peak at a higher temperature than the untreated fibers.

Table 4.3 - DTG of raw and treated coir fibers		
Fiber	**Temperature ^{0}C**	**Rate of Weight Loss (%/min)**
R-COIR	48.43	0.897
	228.43	1.475
	302.56	4.852
2% Na-COIR	72.47	0.697
	243.35	1.162
	314.3	4.774
4% Na-COIR	73.61	0.67
	250.13	1.156
	321.74	4.708
6% Na-COIR	74.43	0.428
	252.74	0.565
	325.9	5.061
8% Na-COIR	90.80	0.571
	252.96	1.413
	321.09	4.62
10% Na-COIR	72.77	0.693
	258.48	1.719
	321.95	4.894

Table 4.4 - DTG of raw and treated pineapple leaf fibers		
Fiber	**Temperature ^{0}C**	**Rate of Weight Loss (%/min)**
R-PALF	31.16	1.47
	310.82	3.54
	341.58	6.85
2% Na-PALF	46.37	0.52
	247.81	0.49
	341.52	6.75
4% Na-PALF	85.79	0.37
	308.69	3.39
	343.43	7.13
6% Na-PALF	70.83	0.43
	302.33	2.73
	343.12	7.091
8% Na-PALF	46.49	0.60
	300.08	2.71
	339.72	6.28
10% Na-PALF	39.7	0.65
	313.05	3.66
	346.85	7.51

4.2 Impact of Fiber Span and Content on the Mechanical Characteristics of PALF/Epoxy and COIR/Epoxy Composites

The geometrical dimensions (length and diameter) and the volume content of reinforcing filaments greatly affect the performance of FRCs. To elevate the inherent strength of polymers and their probability of being selected as compared to the traditional materials, it is extremely required to reinforce it with an optimum fiber length and content. In this regard, sixteen samples of PALF/Epoxy and COIR/Epoxy composites with altering fiber volume content (17%, 23%, 34%, and 43%) and length (10 mm, 15 mm, 20 mm, and 25 mm) were made using the manual lay-up method. The designation and composition of the specimens are reported in Table 4.5. The tensile, flexural, impact and moisture sorption tests were conducted at room temperature as per ASTM standard.

Table 4.5: Description of the CF-EP specimens

Designation	Composition
EP	Epoxy (100 vol.%)
17(10)CF-EP	Epoxy (83 vol.%) + Coir fiber (17 vol.%) (fiber length of 10 mm)
17(15)CF-EP	Epoxy (83 vol.%) + Coir fiber (17 vol.%) (fiber length of 15 mm)
17(20)CF-EP	Epoxy (83 vol.%) + Coir fiber (17 vol.%) (fiber length of 20 mm)
17(25)CF-EP	Epoxy (83 vol.%) + Coir fiber (17 vol.%) (fiber length of 25 mm)
23(10)CF-EP	Epoxy (77 vol.%) + Coir fiber (23 vol.%) (fiber length of 10 mm)
23(15)CF-EP	Epoxy (77 vol.%) + Coir fiber (23 vol.%) (fiber length of 15 mm)
23(20)CF-EP	Epoxy (77 vol.%) + Coir fiber (23 vol.%) (fiber length of 20 mm)
23(25)CF-EP	Epoxy (77 vol.%) + Coir fiber (23 vol.%) (fiber length of 25 mm)
34(10)CF-EP	Epoxy (64 vol.%) + Coir fiber (34 vol.%) (fiber length of 10 mm)
34(15)CF-EP	Epoxy (64 vol.%) + Coir fiber (34 vol.%) (fiber length of 15 mm)
34(20)CF-EP	Epoxy (64 vol.%) + Coir fiber (34 vol.%) (fiber length of 20 mm)
34(25)CF-EP	Epoxy (64 vol.%) + Coir fiber (34 vol.%) (fiber length of 25 mm)
43(10)CF-EP	Epoxy (57 vol.%) + Coir fiber (43 vol.%) (fiber length of 10 mm)
43(15)CF-EP	Epoxy (57 vol.%) + Coir fiber (43 vol.%) (fiber length of 15 mm)
43(20)CF-EP	Epoxy (57 vol.%) + Coir fiber (43 vol.%) (fiber length of 20 mm)
43(25)CF-EP	Epoxy (57 vol.%) + Coir fiber (43 vol.%) (fiber length of 25 mm)

4.2.1 Mechanical Behavior of PALF/Epoxy

4.2.1.1 Impact of Reinforcement Length and Volume Fraction on Tensile Characteristics of PALF/Epoxy

Fig. 4.11 revealed that the tensile strength and stiffness were increased with the enlarge of PALF span and content up to 15 mm and 34 vol.%. Further loading of fibers leads to the reduction in tensile properties of composite materials and it may be due to the agglomeration and inadequate wetting of strands. The accumulation of strands results in non-uniform stress distribution and poor stress transfer from matrix to fibers. The composite consists of 34 vol. % of fiber with 15 mm length has carried maximum tensile load (1954.68 N) than the others. Amongst all the developed materials, the composite of 25 mm fiber length with 43% fiber volume content yields minimum tensile strength (5.1 MPa) and modulus (0.62 GPa). As from the results, it is clear that at an intermediate level of fiber loading, the stress distribution is uniform and fibers effectively participate to carry the load.

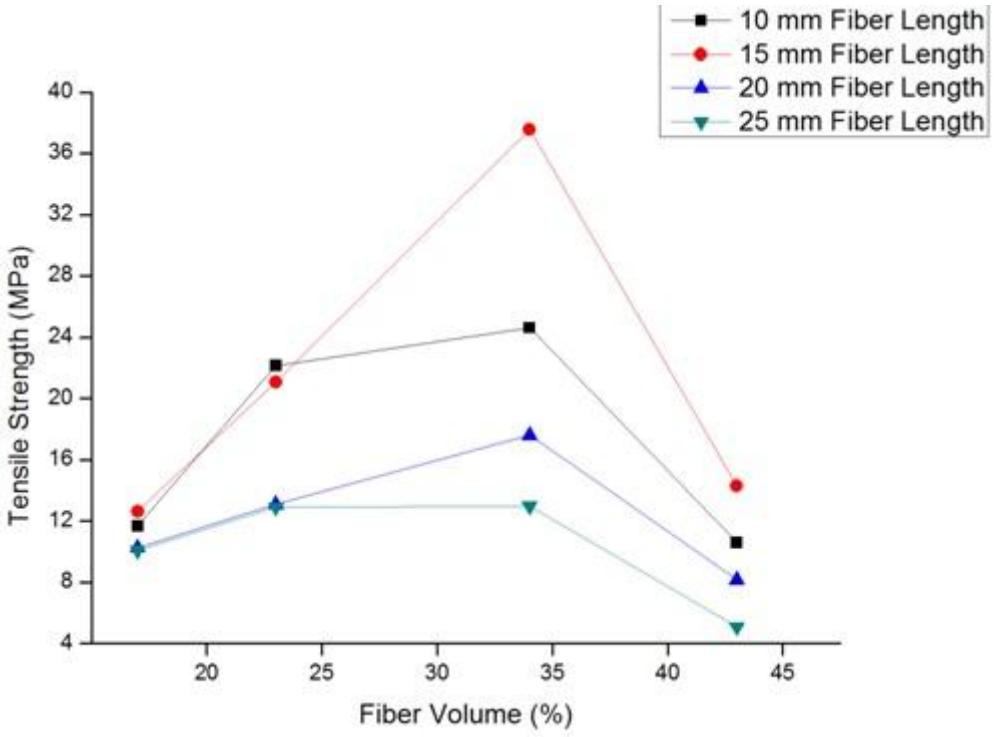

(a)

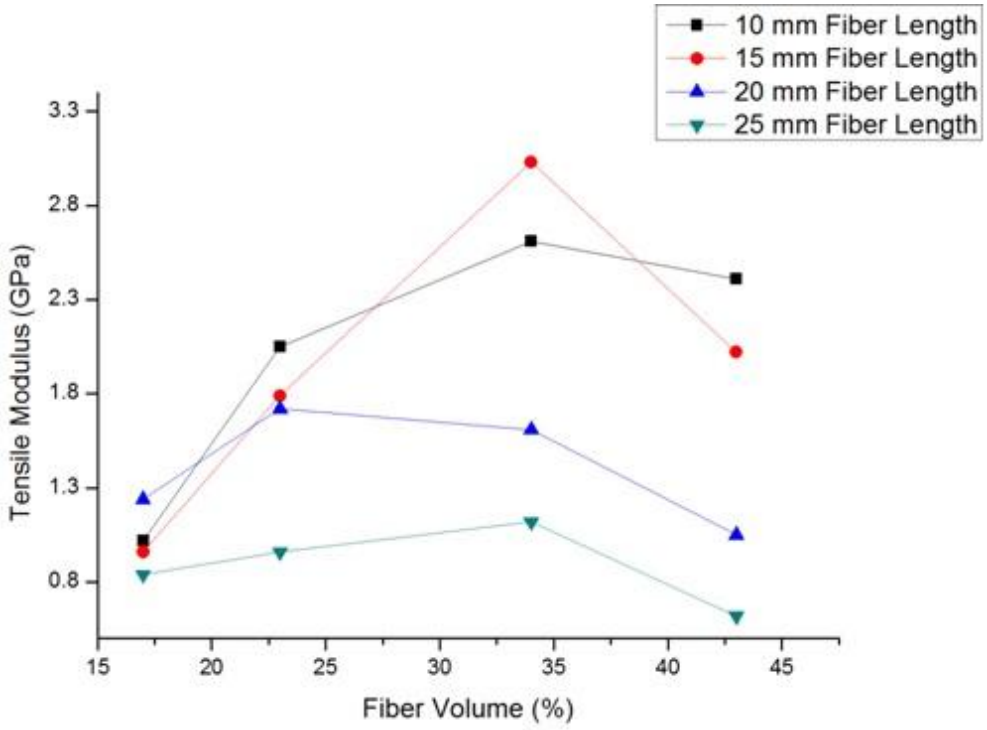

(b)

Fig. 4.11: Impact of reinforcement length and content on tensile properties of PALF/Epoxy

4.2.1.2 Impact of Reinforcement Length and Content on Flexural Characteristics of PALF/Epoxy

The flexural test was performed on PALF/Epoxy composites according to ASTM D790 criterion and the observations are illustrated in Fig. 4.12. The composite consists of 34% fiber has higher bending strength and stiffness than the other ones. The composite with 15 mm fiber length and 34 vol. % fiber content carried maximum bending load (227.6 N). In flexural testing, the upper end of a specimen is subjected to a compressive force, lower-end faced tensile load, and the axisymmetric plane is subjected to a shear load. The maximum deflection (5.05 mm) was observed at 43% fiber content and it was due to the fiber pull action at higher fiber loading. The flexural properties are calculated by using the formulas:

$$\sigma_f = \frac{3FL}{2wt^2} \tag{4.3}$$

$$Flexural\ strain = \frac{6st}{L^2} \tag{4.4}$$

$$Flexural\ modulus = \frac{L^3F}{4swt^2} \tag{4.5}$$

Where S = Measured deflection, L = Length of specimen

The 17% fiber-reinforced composite has minimum flexural strength and this was because of the insufficient loading of reinforcing fibers in an epoxy matrix. The flexural strength was reduced with the increase of fiber content from 34% to 43% and it was due to the improper wetting of fiber with a thermoset resin.

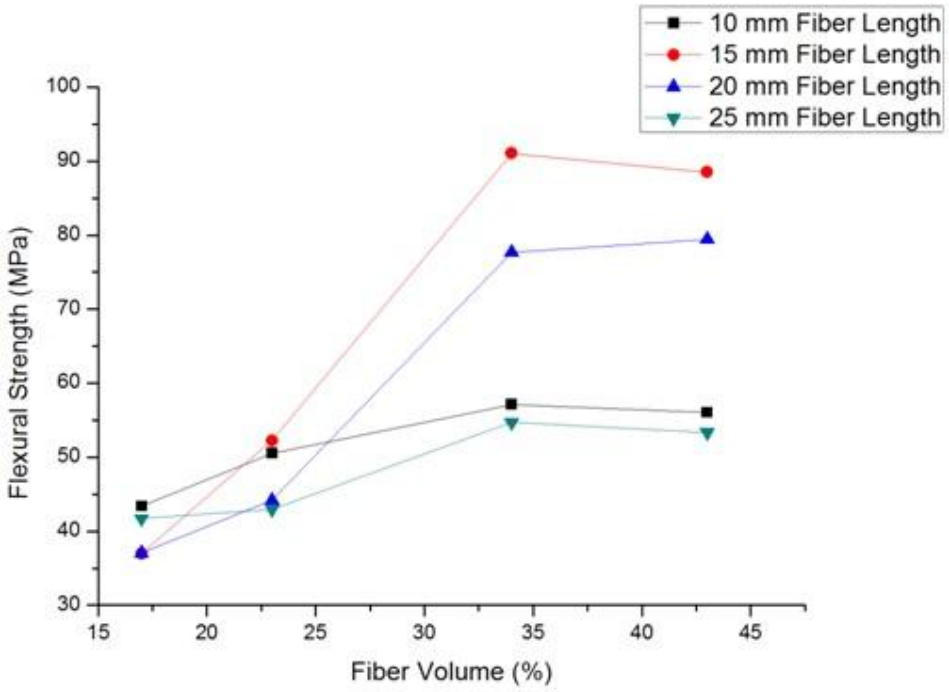

(a)

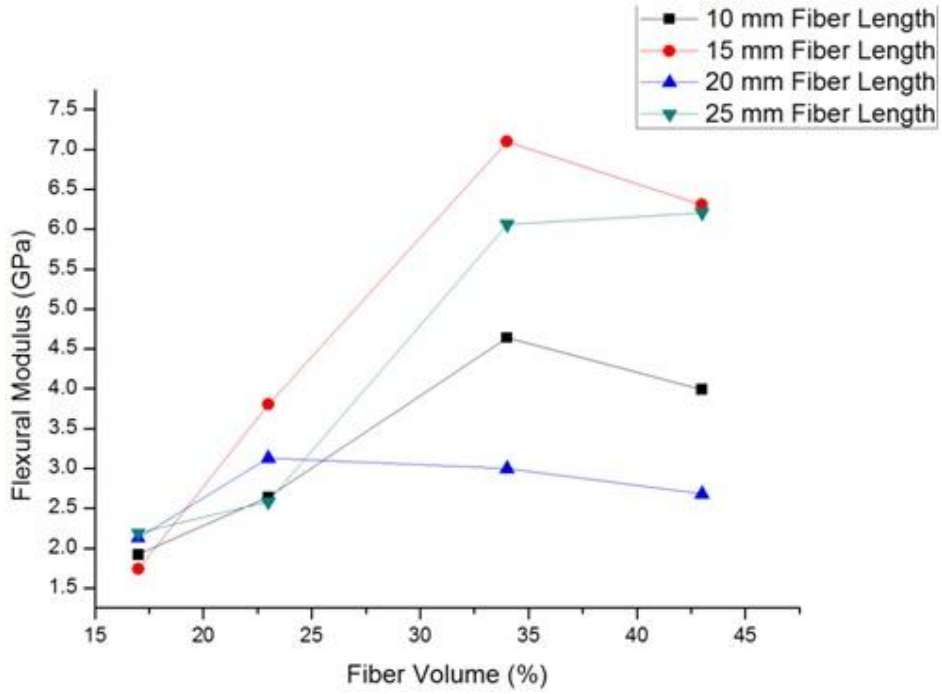

(b)

Fig. 4.12: Impact of reinforcement length and content on bending properties of PALF/Epoxy

4.2.1.3 Impact of Reinforcement Length and Content on Impact Strength of PALF/Epoxy

The strength of composites under impact loading has relatively lower value than the metals. To make an accurate estimation of impact toughness, the total 4 test run was performed and their results are illustrated in Fig. 4.13 and Table 4.8. In majority of the cases, the strength was improved with enhance of fiber content and it shows the transition from brittle to ductile behavior. The average value of impact strength at a low level of PALF loading (17 vol. %) is much lower than the high volume of fiber content (43%) and it was due to the phenomena of fiber fracture in spite of fiber pull out at a low level of fiber loading. When fiber content is low, the fiber pull out mechanism does not play a lead role in energy absorption and the fiber deformation is small. The maximum impact strength is 3.15 J/m at 25 mm fiber length with 43% fiber content.

Table 4.8: Impact test results of PALF/Epoxy composites

Sr. No	Fibre Length (mm)	Fibre Vol.%	Test 1	Test 2	Test 3	Test 4	Average Value of impact strength (J/m)
1	10	17	1.61	1.61	1.76	1.82	1.7
2		23	1.72	1.62	1.89	1.93	1.79
3		34	2.23	2.05	2.89	2.89	2.51
4		43	2.34	2.01	2.73	2.67	2.43
5	15	17	1.93	1.84	2.08	2.13	1.99
6		23	2	1.9	1.97	1.86	1.93
7		34	2.71	2.68	2.75	2.83	2.74
8		43	2.91	3.08	3.07	3.11	3.04
9	20	17	2.04	2.31	2.22	2.07	2.16
10		23	1.97	2.04	2.01	2.04	2.01
11		34	2.05	2.18	2.42	2.34	2.24
12		43	2.73	2.84	2.77	3.03	2.84
13	25	17	2.13	2.34	1.78	2.11	2.09
14		23	2.02	2.07	2.02	1.97	2.02
15		34	2.88	2.67	2.91	2.91	2.84
16		43	3.01	2.91	3.47	3.24	3.15

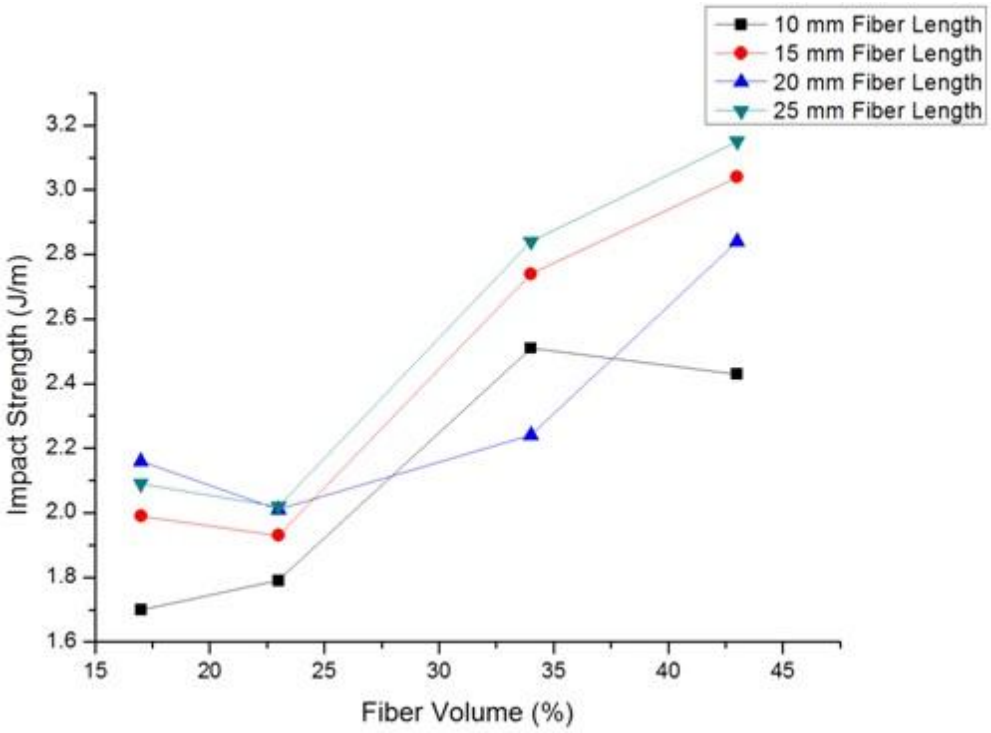

Fig. 4.13: Impact of reinforcement span and vol.% on the impact strength of PALF/Epoxy

4.2.2 Moisture Sorption of PALF/Epoxy

The moisture sorption behavior of composites is illustrated in Figs. 4.14-4.15. The water uptake capacity of composites was amplified by the increase of filament span and content. The specimen of 25 mm fiber length with 43% PALF content exhibits maximum water absorption (around 9%). The composites absorb water monotonically with immersion time and become stable after 12 hrs. In all cases, the composites of 25 mm fiber length have highest affinity of water absorption. This might be due to the growth of void spaces by the incorporation of long cellulosic fibers. Composites usually obey Fickian's diffusion mechanism and it depends on the relative mobility of penetrant (water molecules) and polymer segments. The water sorption constants (n and k) of different samples were obtained from fitting of experimental data into the equation 3.4. The diffusion coefficients and mechanism of different composite samples are presented in Table 4.9.

Table 4.9: Moisture sorption constants and diffusion mechanism of the PALF/Epoxy

Fibre Vol.%	Fibre Length (mm)	Diffusion exponent (n)	Intercept (k)	Type of diffusion mechanism
17	10	0.73	0.194	Non-Fickian Diffusion (0.5<n<1.0)
	15	0.8	0.187	
	20	0.71	0.216	
	25	0.81	0.167	
23	10	0.85	0.11	
	15	0.95	0.1	
	20	0.93	0.11	
	25	0.84	0.16	
34	10	0.46	0.214	Less Fickian Diffusion (n<0.5)
	15	0.51	0.179	Fickian Diffusion (n=0.5)
	20	0.5	0.18	
	25	0.8	0.134	Non-Fickian Diffusion (0.5<n<1.0)
43	10	0.84	0.135	
	15	0.77	0.14	
	20	0.76	0.149	
	25	0.79	0.147	

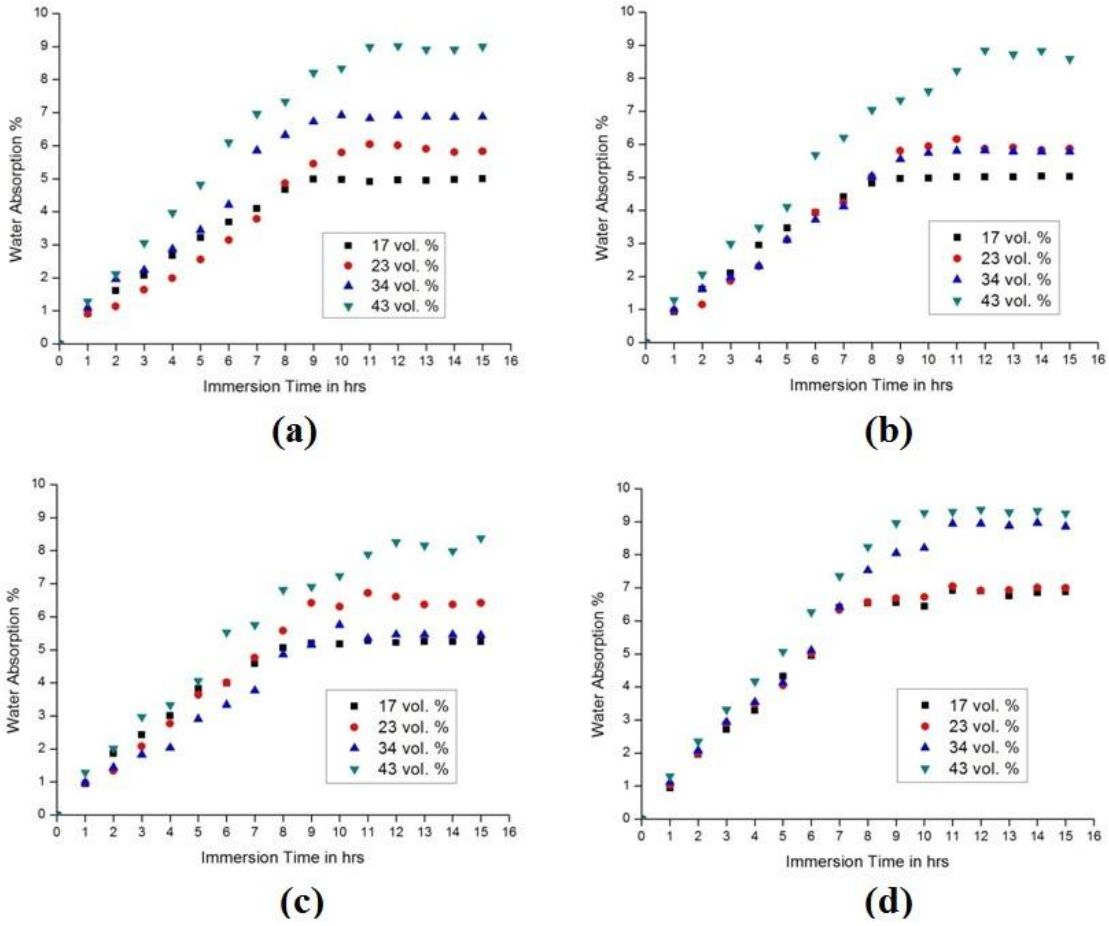

Fig. 4.14: Impact of reinforcement content on moisture sorption of PALF/Epoxy; Fiber length – (a) 10 mm (b) 15 mm (c) 20 mm (d) 25 mm

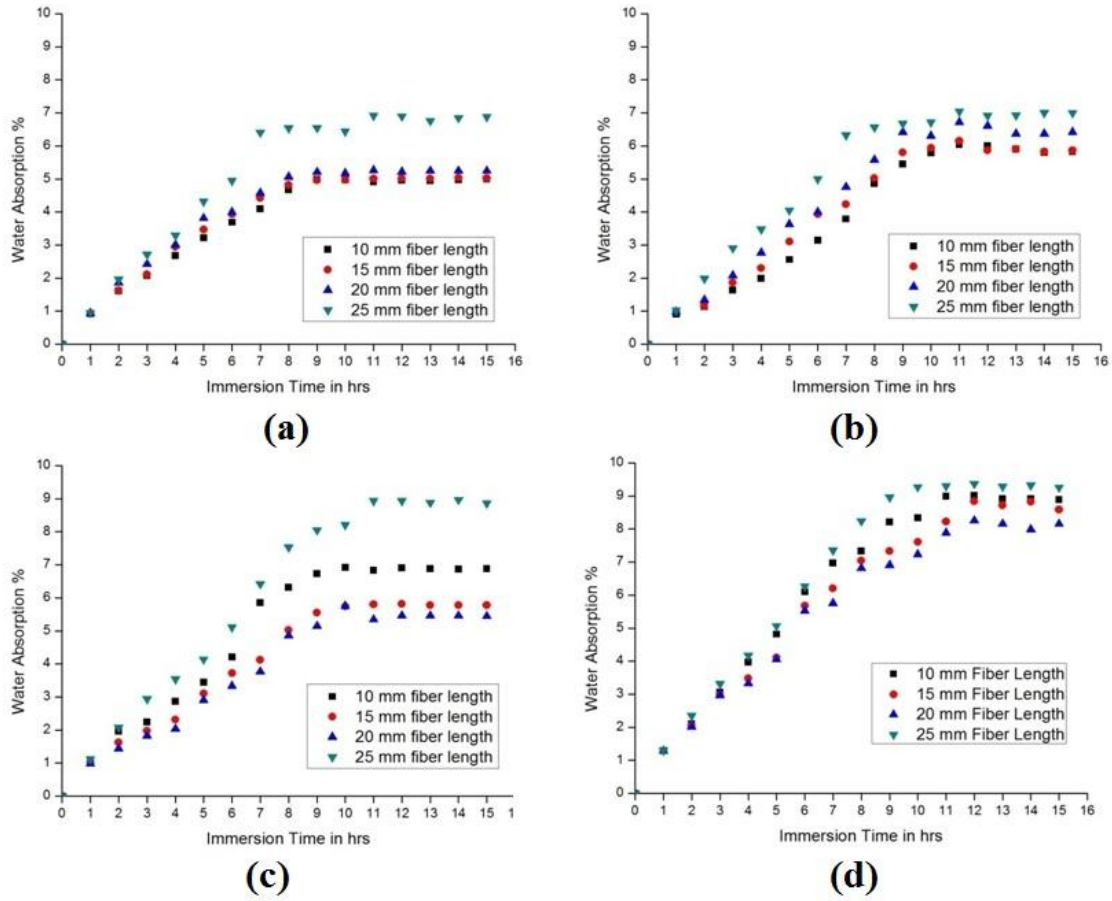

Fig. 4.15: Impact of reinforcement length on moisture sorption of PALF/Epoxy; Fiber content – (a) 17 vol.% (b) 23 vol.% (c) 34 vol.% (d) 43 vol.%

4.2.3 Mechanical Characteristics of COIR/Epoxy

4.2.3.1 Impact of Reinforcement Length and Content on Tensile Characteristics of COIR/Epoxy

Fig. 4.16 illustrates that the strength of composites was improved with enhance of filament length and content up to 15 mm and 23 vol.%. Further addition of fiber leads to the reduction in strength and it may be due to the agglomeration, poor dispersion, and inadequate wetting of strands with a polymeric resin. The maximum tensile strength of CF-EP composite is 19.23 MPa. It was found that the reinforcement geometry plays a significant job to affect the properties of FRCs. The tensile strength was less in the case of long fibers (20-30 mm) and it was attributed to the folding, entanglement, and improper bonding of fibers with unfolded ones. Fig. 4.16 (b) revealed that the modulus of CF-EP was increased with the increase of fiber content. The maximum tensile modulus (2.3 GPa) was obtained for a 20 mm length with 34% fiber volume content.

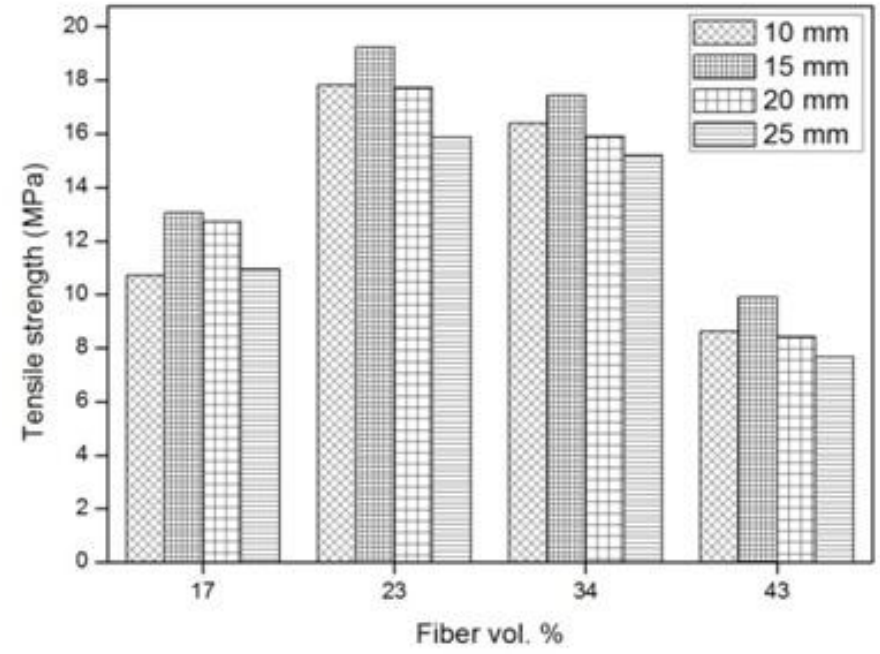

(a)

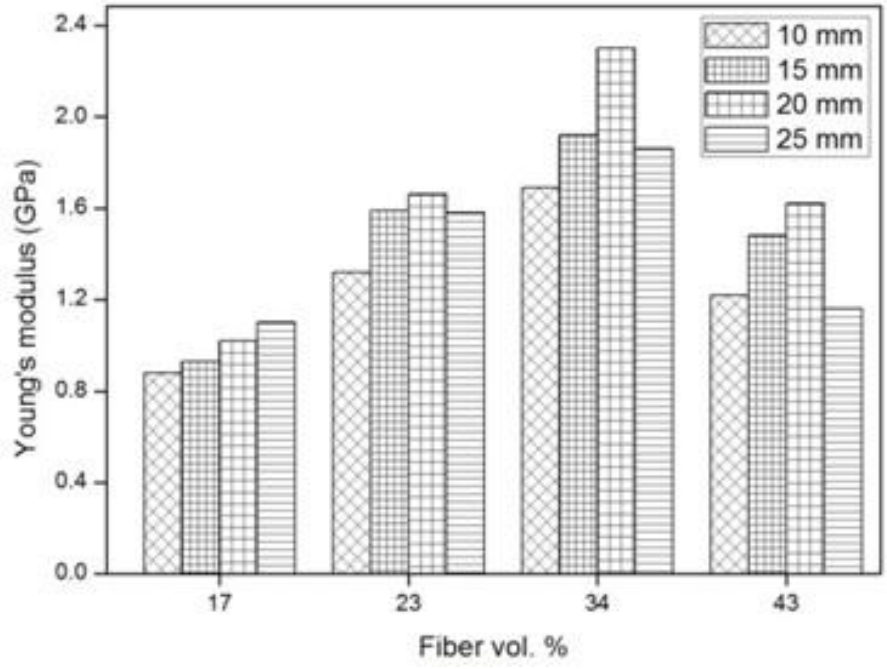

(b)

Fig. 4.16: Impact of reinforcement length and content on Tensile Properties of CF-EP

4.2.3.2 Impact of Reinforcement Length and Content on Flexural Behavior of COIR/Epoxy

Fig. 4.17 revealed the flexural properties of CF-EP which confirms that the bending strength was increased with the increase of fiber span and volume content up to 20

mm and 23 vol.% respectively. Further increase of fiber length and content caused the reduction in bending strength and it might be due to the curling of long fibers, increment in void density, and poor dispersion of fibers in the matrix resin. The highest bending strength and modulus are 31.87 MPa and 2.41 GPa for 23(20)CF-EP and 34(20)CF-EP composites respectively.

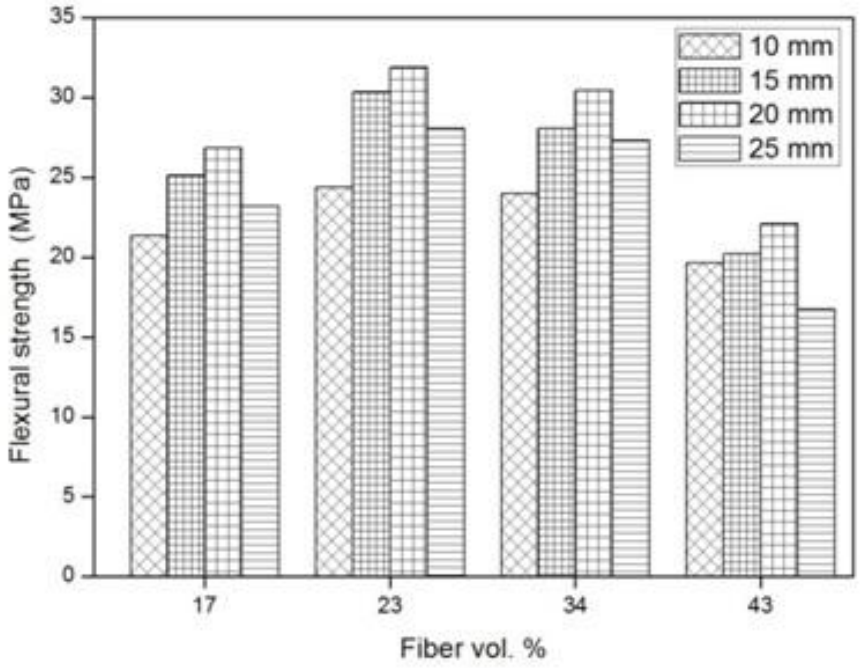

(a)

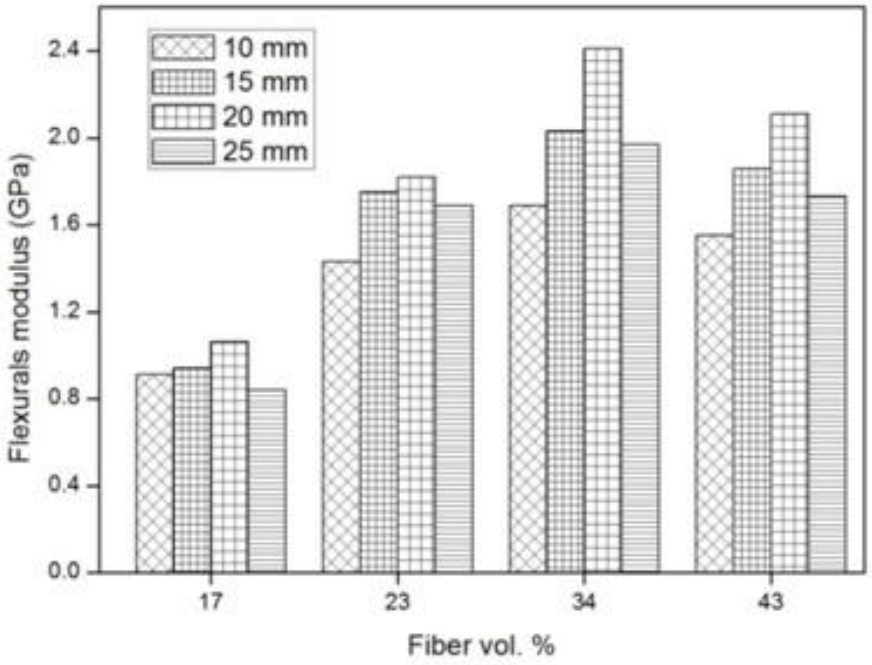

(b)

Fig. 4.17: Impact of reinforcement length and volume content on bending properties of CF-EP

4.2.3.3 Impact of Reinforcement Length and Content on Impact Strength of COIR/Epoxy

Fig. 4.18 illustrated the role of reinforcement length and volume on the impact strength of CF-EP. The impact strength was improved with the increase of fiber volume content. Irrespective of fiber length, the maximum impact strength was obtained with 43% fiber. The impact strength of PMC's basically relies upon the kind of fiber and polymer, geometrical shape and size of the fiber, and fiber-matrix adhesion. It is worth noting that the resistance to impact loading was increased with the increase of fiber length. Moreover, the composite consists of 20 mm long fibers with 43% fiber volume content possess the maximum value of impact strength (11.33 kJ/m^2) than the other ones.

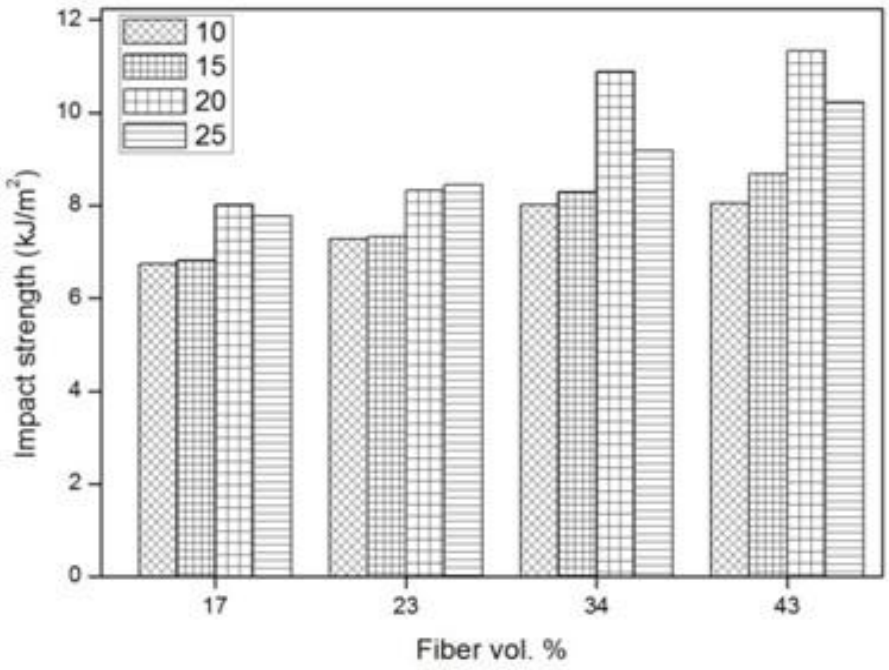

Fig. 4.18: Impact of reinforcement span and vol.% on the impact strength of CF-EP

4.2.4 Impact of Reinforcement Length and Content on the Moisture Sorption Behavior of COIR/Epoxy

The moisture uptake behavior of CF-EP composites is presented in Figs. 4.19-4.20. The water absorption was increased from 1.8% to 5.32% with the increase of fiber volume content from 17% to 43%. Previous work (A. Singh *et al*. [93], G. Rajeshkumar *et al*. [61], G. Das *et al*. [88], V.K Bhagat *et al*. [146]) have also reported the similar results. The composites absorb water with immersion time and become saturated after 360 hrs. The maximum amount of water absorption at the saturation level is tabulated in Table 4.10. From the experimental data, we can report

that the variation in fiber length at the constant value of fiber content not much influence the water absorption capacity of composites.

Table 4.10: Maximum water absorption for CF-EP composites

Fiber length	Coir fiber volume content (%)			
	17	**23**	**34**	**43**
10	1.80	2.45	4.74	5.31
15	1.81	2.46	4.75	5.32
20	1.81	2.46	4.75	5.32
25	1.80	2.47	4.76	5.32

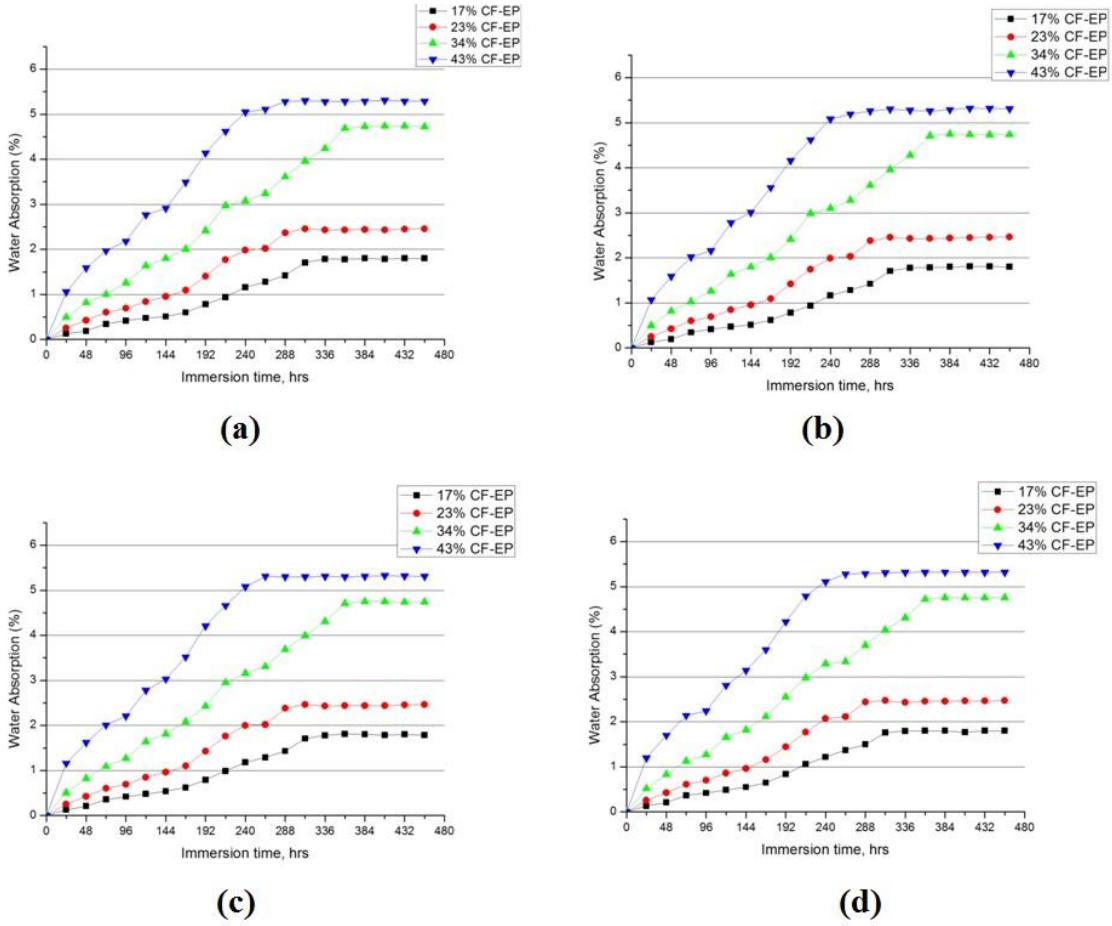

Fig. 4.19: Impact of reinforcement content on water absorption of COIR/Epoxy; Fiber length – (a) 10 mm (b) 15 mm (c) 20 mm (d) 25 mm

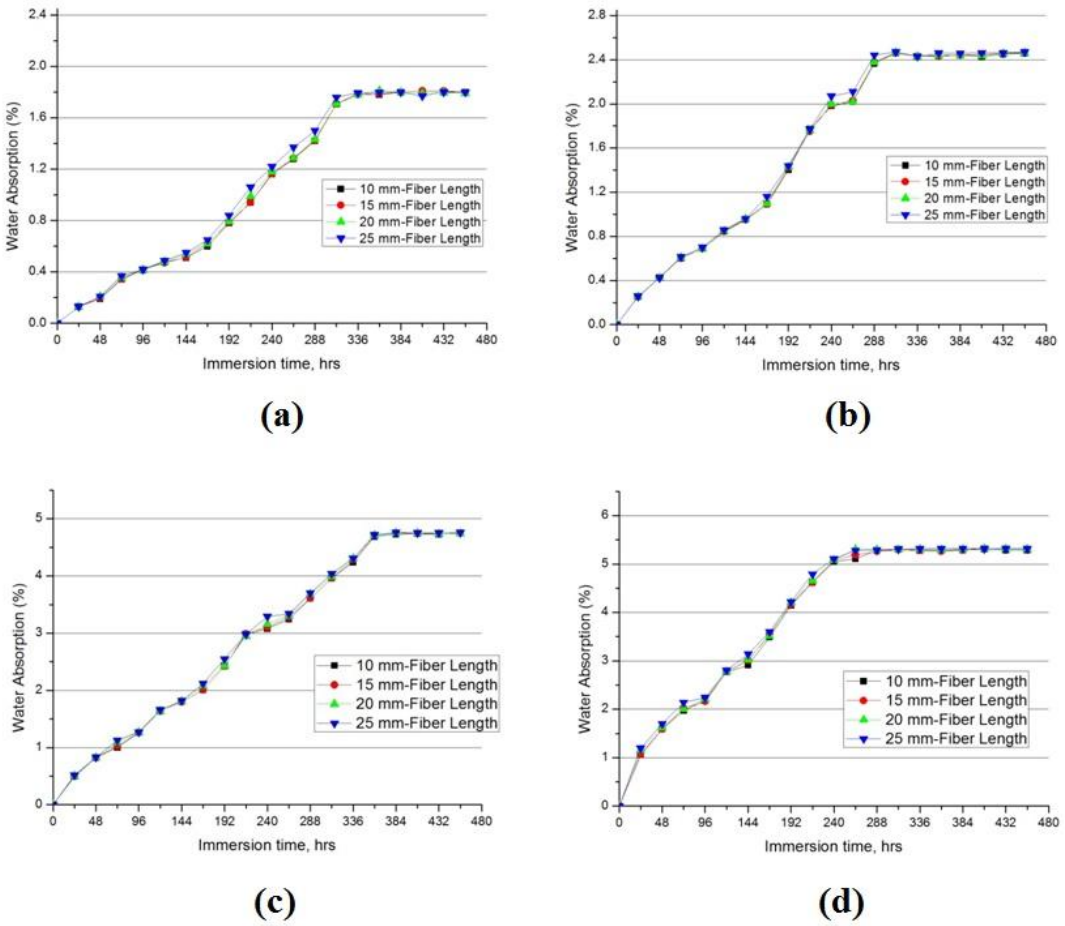

Fig. 4.20: Impact of reinforcement length on water absorption of COIR/Epoxy; Fiber volume content – (a) 17% (b) 23% (c) 34% (d) 43%

4.2.4.1 Impact of Moisture Sorption on the Mechanical Characteristics of CF-EP

The impact of moisture sorption on the mechanical characteristics of CF-EP is illustrated in Figs. 4.21-4.22. The strength and stiffness of material were reduced after the immersion in water. The tensile strength of wet samples-17(20)CF-EP, 23(20)CF-EP, 34(20)CF-EP, and 43(20)CF-EP was found to be lower than the dry composite samples by 10.54%, 15.16%, 29.32%, and 37.02% respectively. This was attributed to the swelling of fibers, the formation of voids, and poor stress transfer from the matrix to the reinforcement. A similar trend has also been reported in coir fiber reinforced polyethylene composites [93]. The flexural strength follows the same path as tensile strength and also showed reduction in wet composites-17(20)CF-EP, 23(20)CF-EP, 34(20)CF-EP, and 43(20)CF-EP by 8.45%, 8.75%, 10.31%, and 21.15% respectively than the dry composites of the same composition. The tensile and flexural modulus of 43(20)CF-EP composite exhibits the maximum reduction after immersion in water for 456 hrs. Fig. 4.22 clearly shows that the

impact strength of composites was improved considerably after the moisture absorption and this may be due to the domination of fiber pull-out mechanism than the fiber fracture.

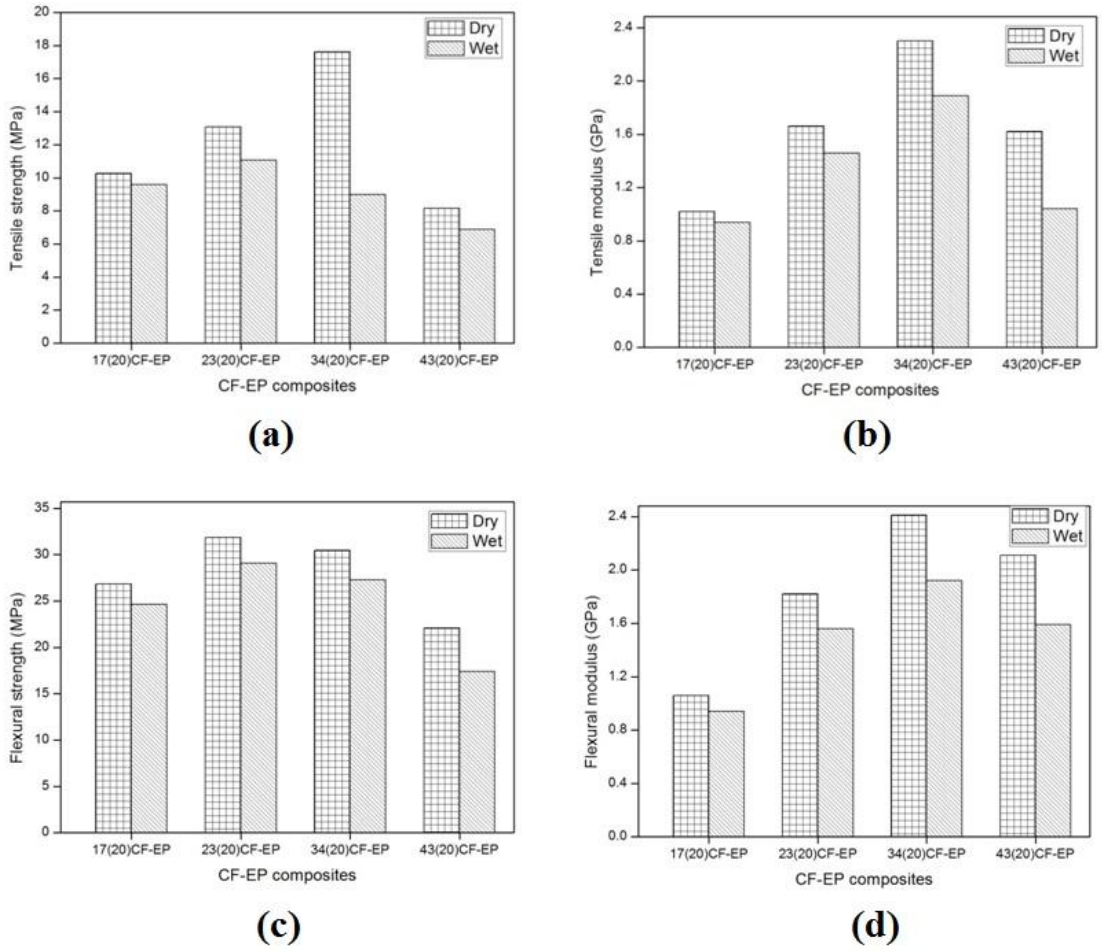

Fig. 4.21: Impact of moisture sorption on tensile and flexural behavior of CF-EP

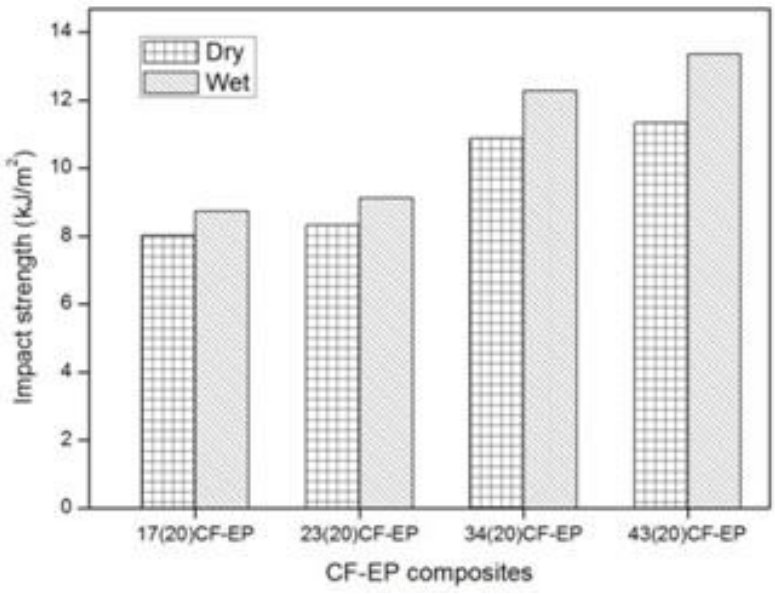

Fig. 4.22: Impact of moisture sorption on the impact strength of CF-EP

4.3 Impact of Reinforcement Volume on Thermal Behavior and Viscoelastic Characteristics of PALF/Epoxy and COIR/Epoxy Composites

The comprehensive cognition of the thermal and viscoelastic behavior of polymeric material is highly significant in order to determine the structure-property relationship for various applications. The prime goal of this section was to analyze the impact of reinforcement volume fraction on the thermo-mechanical characteristics of strengthened material. In this regard, randomly oriented chopped fibers of length 20 mm with varying fiber volume content (17%, 23%, and 34%) were used as reinforcement in an epoxy polymer matrix for the development of coir fiber-epoxy and pineapple leaf fiber-epoxy composites. The description of manufactured composites is presented in Table 4.11. The effect of frequency and temperature on the E', E'', tan δ, and T_g is also reported in this section. TGA and DMTA techniques are used to characterize polymer-based composite materials.

Table 4.11: Designation and composition of coir fiber-epoxy (CF-EP) and pineapple leaf fiber-epoxy (PF-EP) composites

Designation	Composition
EP	Epoxy (100 vol.%)
17 CF-EP	Epoxy (83 vol.%) + Coir fiber (17 vol.%)
17 PF-EP	Epoxy (83 vol.%) + Pineapple leaf fiber (17 vol.%)
23 CF-EP	Epoxy (77 vol.%) + Coir fiber (23 vol.%)
23 PF-EP	Epoxy (77 vol.%) + Pineapple leaf fiber (23 vol.%)
34 CF-EP	Epoxy (64 vol.%) + Coir fiber (34 vol.%)
34 PF-EP	Epoxy (64 vol.%) + Pineapple leaf fiber (34 vol.%)
34 CF-EP (1)	Epoxy (64 vol.%) + Coir fiber (34 vol.%) (frequency: 1 Hz)
34 CF-EP (5)	Epoxy (64 vol.%) + Coir fiber (34 vol.%) (frequency: 5 Hz)
34 PF-EP (1)	Epoxy (64 vol.%) + Pineapple leaf fiber (34 vol.%) (frequency: 1 Hz)
34 PF-EP (5)	Epoxy (64 vol.%) + Pineapple leaf fiber (34 vol.%) (frequency: 5 Hz)

4.3.1 Thermogravimetric Analysis

The thermal decomposition curve of cellulosic fibers and their composites was recorded in Figs. 4.23-4.24. All the samples exhibit three steps of mass loss. The first step is the loss of absorbed moisture and volatile content in the range of 6-8.4 wt.%, up to 150 ^{0}C. The second and third decomposition step exists at 190-300 ^{0}C and 300-400 ^{0}C, corresponds to the loss of major constituents of natural fibers such as hemicellulose, cellulose, and lignin. Table 4.12 shows that the decomposition temperature of virgin epoxy resin was increased by the loading of coir and pineapple

leaf fibers. The peak decomposition temperature (T_P) of the epoxy matrix was increased from 371.96 ^{0}C to 379.59, 386.03, and 377.45 ^{0}C, after the incorporation of 17, 23, and 34 vol.% of coir fiber respectively. A similar result was also reported in the case of pineapple leaf fiber (Table 4.12). The maximum rate of thermal degradation (peak height in DTG curves) of epoxy resin was reduced by 14% and 12% after the loading of 34% coir and pineapple leaf fiber respectively. This was attributed to the higher restrictions in the debonding of molecular chains. TGA and DTG curves for coir and pineapple leaf fiber distinctly revealed their lower thermal stability as compared to the virgin epoxy and fiber-matrix composites. Table 4.12 also depicts that the degradation of PALF occurs at a higher temperature than the COIR fiber. It was due to the presence of more crystalline cellulose in PALF than the COIR. Among all the fabricated composites, the composite containing 23% fiber volume content shows maximum thermal stability. This was because of the strong linkage between reinforcement and resin, less void content, and good wettability of fibers with the matrix resin. From Table 4.12, it was cleared that the major degradation of CF, PF, CF-EP, and PF-EP composites occur in the range of temperature 300-400 ^{0}C and it was due to the decomposition of α-cellulose. Yang *et al*. [248] reported that the presence of a carbonyl group (C=O) in hemicellulose be the cause of its lower thermal stability than α-cellulose, and lignin. Lignin was the most thermally stable component of natural fiber but it starts to decompose at a lower temperature (typically 160-175 ^{0}C) compared to cellulose. According to Paiva et al. the decomposition of lignin occurred in a wider temperature range compared to cellulose and hemicellulose [247]. Table 4.13 revealed that after 700 ^{0}C, the residual mass (R_m) was increased caused by the enhance of fiber vol.% in an epoxy matrix. The coir strands has maximum residual mass (23.36%) at 700 ^{0}C. It was attributed to the presence of more lignin content in coir.

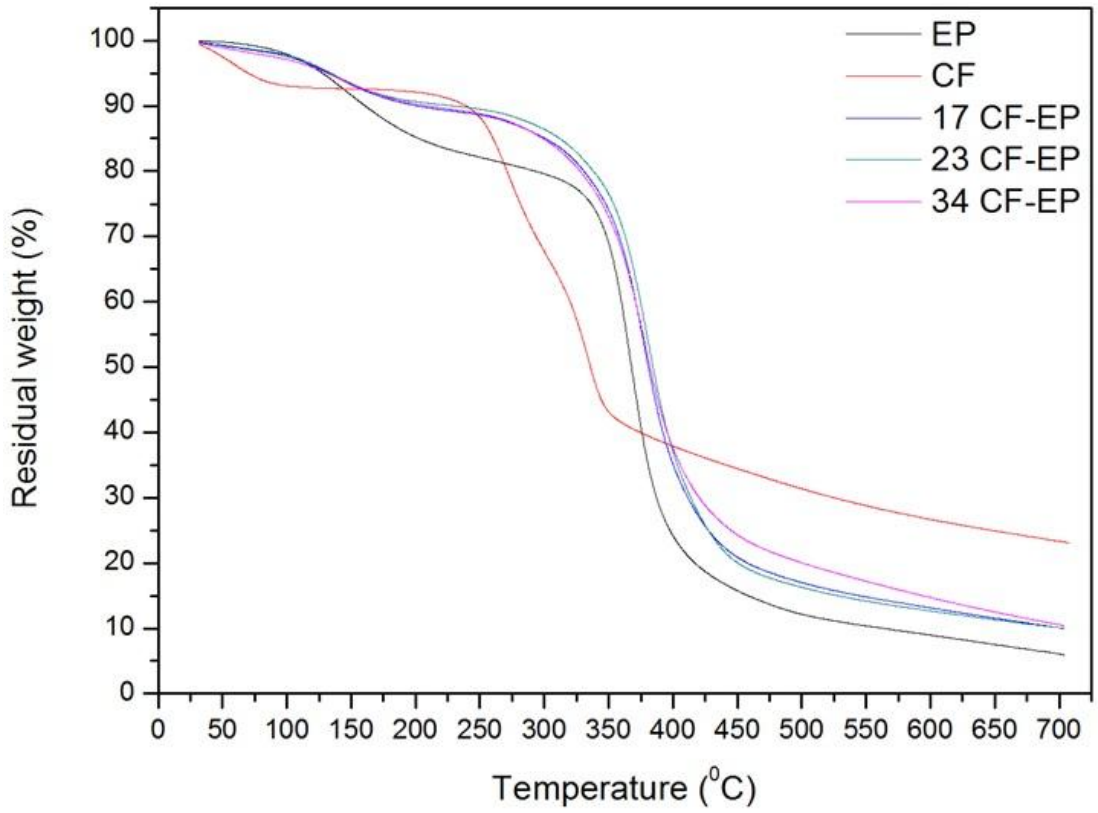

(a)

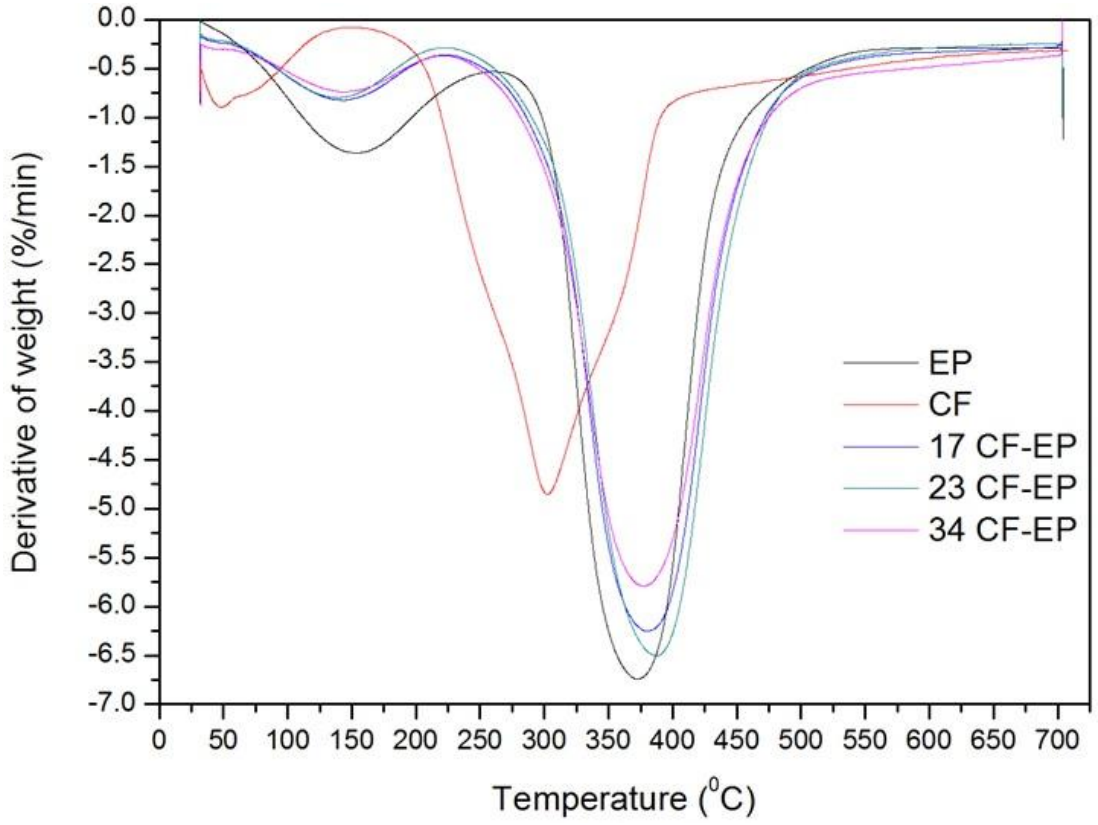

(b)

Fig. 4.23: (a) TGA (b) DTG of virgin epoxy, coir fiber, and coir fiber-epoxy composites

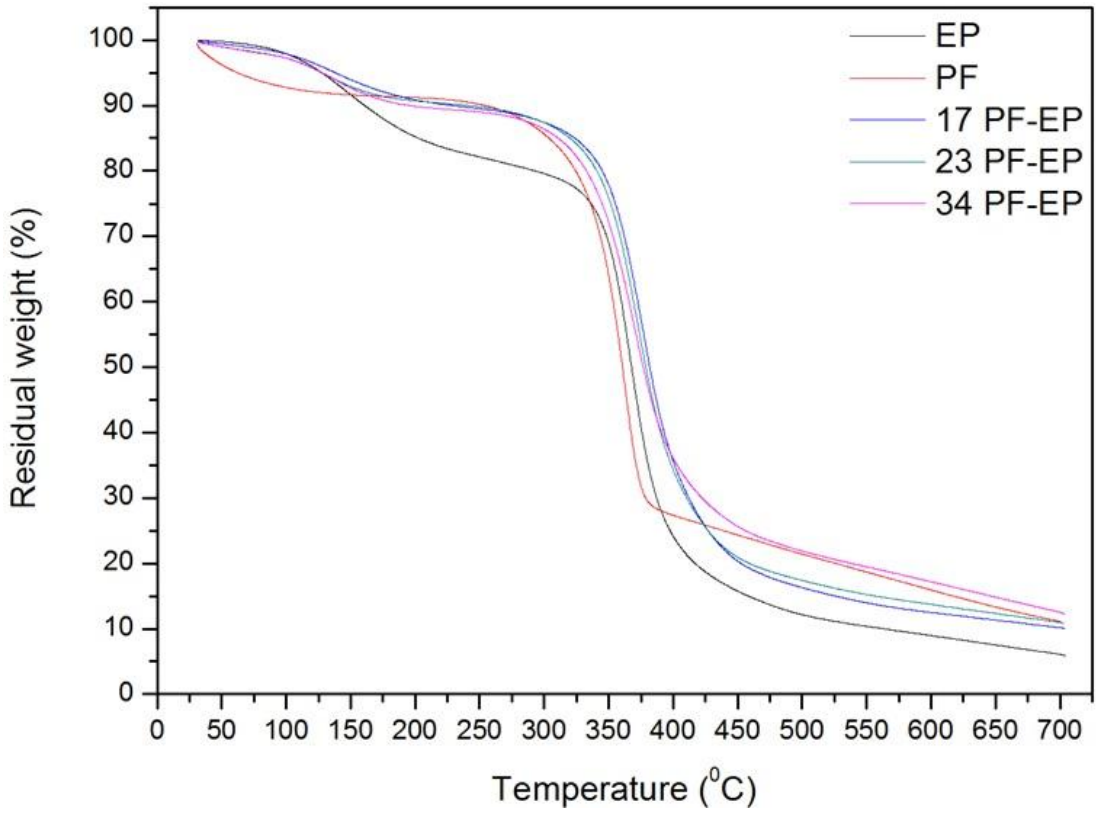

(a)

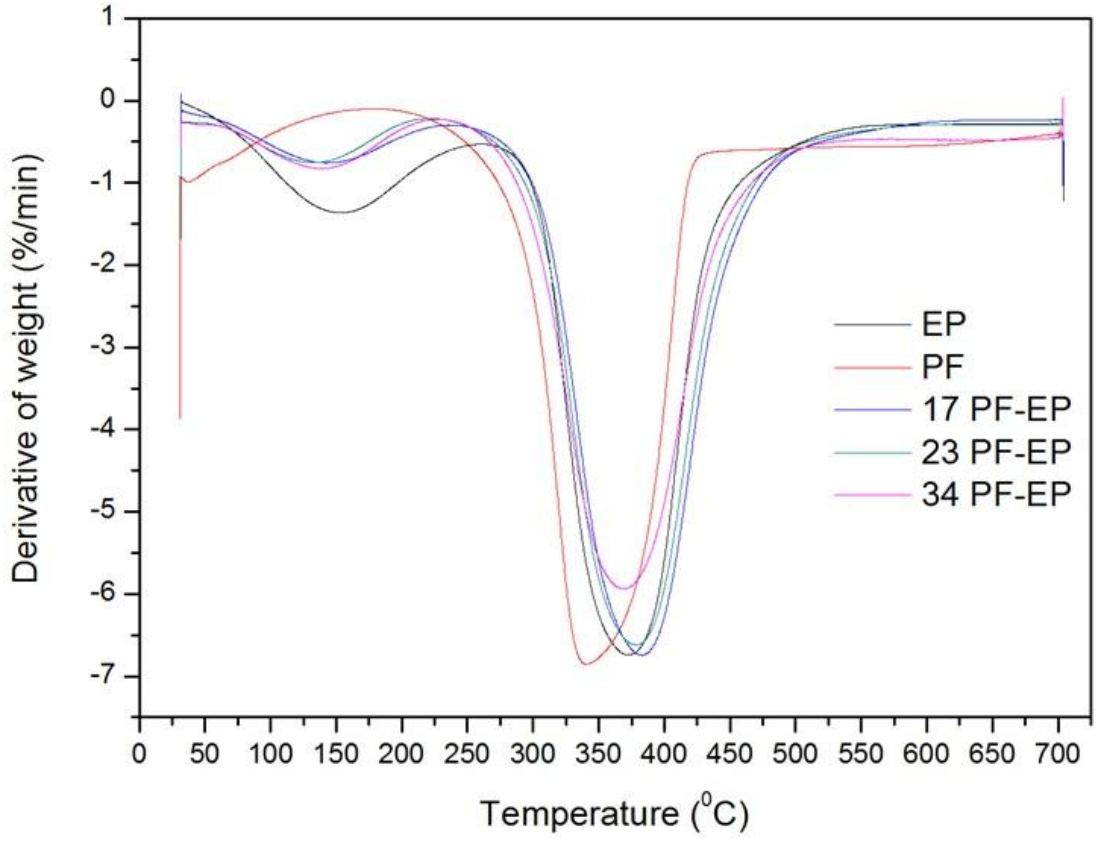

(b)

Fig. 4.24: (a) TGA (b) DTG of virgin epoxy, pineapple leaf fiber, and pineapple leaf fiber-epoxy composites

Table 4.12: Thermal degradation temperature for virgin epoxy, coir fiber, pineapple leaf fiber, coir-epoxy, and pineapple leaf fiber-epoxy composites

Composites	$T_{5\%}$ (^{0}C) [1]	$T_{10\%}$ (^{0}C)[1]	$T_{30\%}$ (^{0}C)[1]	$T_{50\%}$ (^{0}C)[1]	T_P [2]	Peak height (%/min)	Peak width
EP	127.61	160.79	348.33	367.69	371.96	6.74	93.49
CF	69.85	239.12	293.55	335.83	302.56	4.85	121.48
17 CF-EP	132.42	201.16	358.13	380.79	379.59	6.24	101.69
23 CF-EP	134.19	229.2	362.82	384.48	386.03	6.5	101.53
34 CF-EP	131.37	209.08	356.37	382.08	377.45	5.79	104.94
PF	62.28	254.48	343.47	360.66	340.38	6.85	91.69
17 PF-EP	137.98	228.73	362.15	381.84	382.87	6.74	99.15
23 PF-EP	127.87	241.71	358.72	383.8	377.77	6.62	99.72
34 PF-EP	127.77	195.63	353.22	376.77	368.65	5.9	101.91

[1] Decomposition temperature of 5%, 10%, 30%, and 50% weight loss respectively; [2] Peak decomposition temperatures

Table 4.13: Weight loss and residual mass percentage for virgin epoxy, coir fiber, pineapple leaf fiber, coir-epoxy, and pineapple leaf fiber-epoxy composites

Composites	RT-150^{0}C	190-300^{0}C	300-400^{0}C	R_m (%)
EP	8.38	6.6	55.44	6.12
CF	7.39	24.56	29.85	23.36
17 CF-EP	6.75	5.36	49.98	10.11
23 CF-EP	6.57	4.56	49.39	10.12
34 CF-EP	6.65	5.82	47.36	10.56
PF	8.38	5.68	58.29	11.1
17 PF-EP	6.07	3.9	51.76	10.18
23 PF-EP	7.1	3.54	53.08	10.97
34 PF-EP	7.32	3.8	50.33	12.53

R_m= Residual mass at 700^{0}C

4.3.2 Dynamic Mechanical Thermal Analysis

The performance of a FRC greatly depend on the characteristics of fiber and polymer, the interfacial bond strength between them, and the aspect ratio, orientation, distribution, and volume content of the fiber. DMTA is one of the most significant and effective techniques to characterize the viscoelastic behavior of composites with respect to temperature, time, and frequency of oscillation.

4.3.2.1 Effect of fiber content on the storage modulus (E') of CF-EP and PF-EP composites

The stiffness of composite material is mainly affected by the loading of reinforcing fibers. Fig. 4.25 revealed the impact of reinforcement volume with temperature on E'

of the coir fiber-epoxy and pineapple leaf fiber-epoxy composites. In both cases, E' was improved with the increase of filler volume fraction over the entire temperature range. This was attributed to the hindrance in molecular mobility, the formation of more covalent bonds at the fiber-matrix interface, and the interference of molecular chains which results in slow down the stress relaxation process. Previous research work (Ornaghi *et al*. [249], Obaid *et al*. [250], Idicula *et al*. [160]) have also reported the same effect. It was observed that the E' of neat polymer and polymer-based composites was reduced dramatically on passing through the dynamic glass transition temperature (T_g). Table 4.14 and Fig. 4.25 revealed that the samples of 34 vol. % of fibers have higher stiffness at room temperature and elevated temperature as compared to all other samples. This enormous behavior can be explained in terms of the higher fiber-matrix interfacial adhesion, rigidity of polymer chains, and restrictions to the deformability and viscous flow of the matrix. The storage modulus (E') of 17 PF-EP and 23 PF-EP composites has almost the same value. The modulus curves depict the higher E' values of all PF-EP composites than the CF-EP and this was because of the strong adhesion between the pineapple leaf fibers and neighboring polymeric chains. The effectiveness of reinforcement to increase the stiffness of base polymer resin can be determined by a coefficient 'C' such as

$$C = \frac{{E'_G}/{E'_R}^{Composite}}{{E'_G}/{E'_R}^{Resin}} \tag{4.6}$$

where E'_G and E'_R are the storage modulus in the glassy and rubbery phase respectively. The higher value of C indicates the poor effectiveness of fiber to elevate the modulus. Usually, filled systems have lower C values as compared to the unfilled matrix polymer. Table 4.14 shows the calculated effectiveness coefficient 'C' (30-130^{0}C) for both types (CF-EP and PF-EP) of composites. The C value for 34 vol.% pineapple leaf fiber-reinforced composite is minimum amongst all the composites. The value of C is highly increased with the increase of PALF content from 17% to 23% in PF-EP composites. In coir fiber composites, the 23% fiber volume content is the most effective amount to reinforce epoxy polymer.

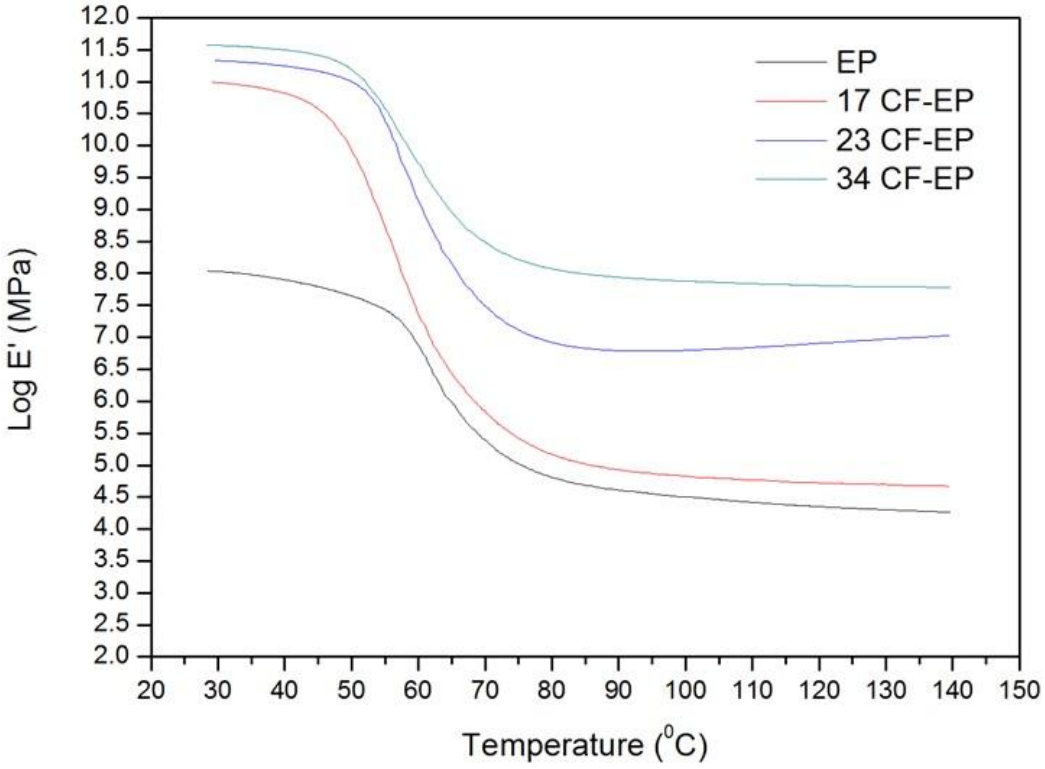

(a)

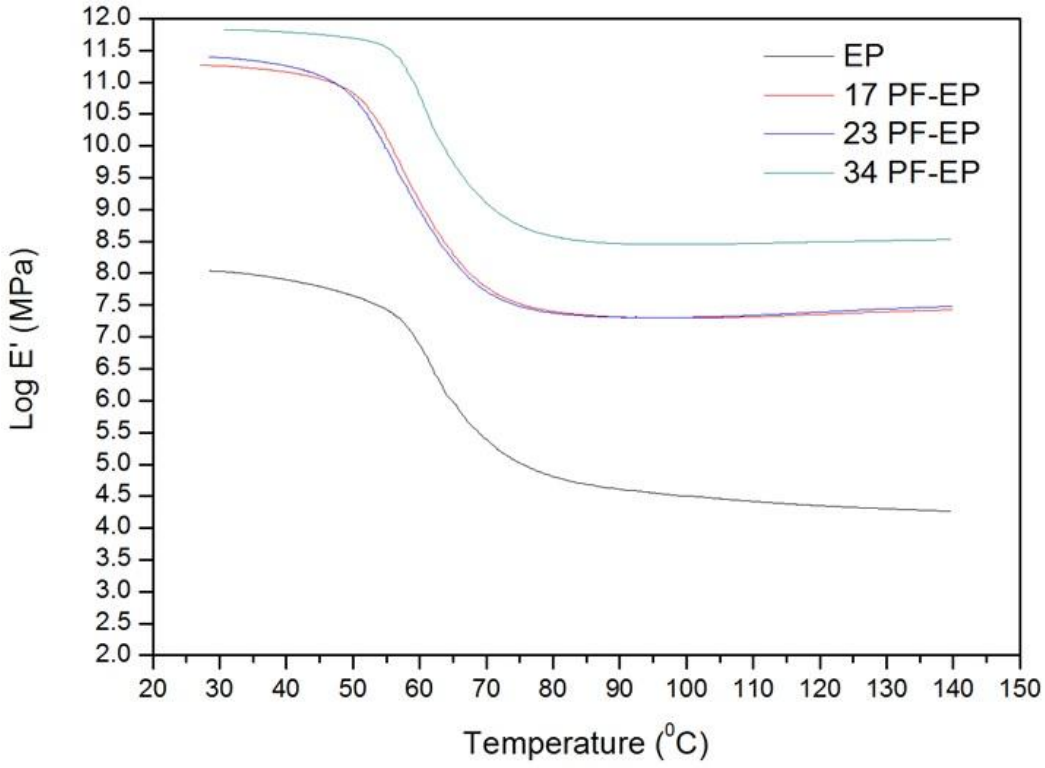

(b)

Fig. 4.25: Impact of reinforcement volume with temperature on storage modulus of (a) CF-EP (b) PF-EP composites at a frequency of 1 Hz

Table 4.14: Values of effectiveness coefficient 'C', tan δ peak height and width, glass transition temperature (T_g), loss modulus (E'') curves peak height, and E' values for coir fiber-epoxy and pineapple fiber-epoxy composites

Composites	C	tan δ peak height	tan δ peak width	T_g from Tan δ_{max} (^{0}C)	Log E'' Peak height (MPa)	T_g from E'' (^{0}C)	E' value (Pa) at 50^{0}C	E' value (Pa) at 70^{0}C
EP	-	0.82	19.84	52.95	8.79	47.1	2.092E + 09	1.524 E +08
17 CF-EP	12.96	0.76	16.11	69.8	9.14	61.36	2.001E + 10	2.245E + 08
23 CF-EP	1.88	0.45	19.09	72.5	5.5	65.8	5.975E + 10	1.22E +09
34 CF-EP	2.38	0.41	23.33	63.5	9.15	54.5	7.356E +09	3.709E +09
17 PF-EP	1.15	0.69	18.43	63.72	9.02	54.38	5.037E +10	1.841E +09
23 PF-EP	39.58	0.73	19.08	62.9	9.2	52.17	4.715E +10	1.773E +09
34 PF-EP	0.66	0.53	17.22	66.1	9.58	60.08	1.196E +11	6.315E +09

4.3.2.2 Effect of Fiber Content on the Loss Factor (tan δ) of CF-EP and PF-EP Composites

The variation in loss factor (tan δ) with fiber content and temperature for CF-EP and PF-EP composites is shown in Fig. 4.26. The temperature at which the tan δ curve shows a peak is called the dynamic glass transition temperature (T_g). It was observed that the unfilled polymer has lower T_g (52.95 ^{0}C) than the CF-EP and PF-EP composites. This shift of tan δ peak to the higher temperature was because of the interphase interaction between the reinforcing filler and molecular chains. In context to the glass transition temperature, 23% and 34 vol.% are the optimum fiber content for coir fiber-epoxy and pineapple leaf fiber-epoxy composites respectively. The peak width and peak height values are also given in Table 4.14. As expected, the value of tan δ peak height was reduced after the incorporation of fibers in an epoxy matrix. Amongst all samples, a shorter and wider peak was obtained in the case of 34 CF-EP. This was credited to the better allocation of the fillers in resin that leads to an inhibition of the relaxation process and the improvement in rigidity of polymeric chains. Fig. 4.26 (a) revealed that the peak height and width of 23 CF-EP composite and 34 CF-EP composites were approximately the same, but the value of 'C' and T_g are more favorable in the case of 23 vol.% coir fiber-reinforced composite. In PF-EP composites, the damping peak height was increased from 0.69 to 0.73, and T_g was decreased from 63.72 to 62.9 ^{0}C, with the increase of fiber content from 17% to 23%. This may be due to the more interfacial area and large frictional forces which leads to more energy dissipation to overcome the friction. From Table 4.14, it can be concluded that the COIR/Epoxy composites possess a relatively higher value of T_g than the PALF/Epoxy composites. This was because of the porous morphology of coir fiber which results in better wetting action by the capillary effect.

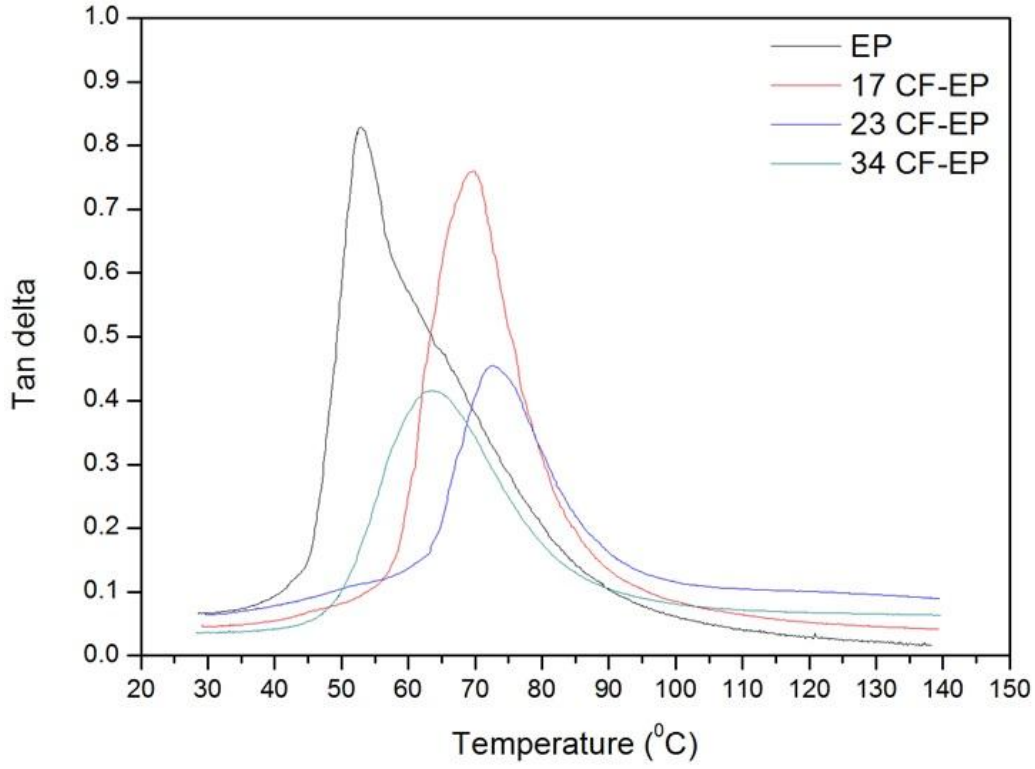

(a)

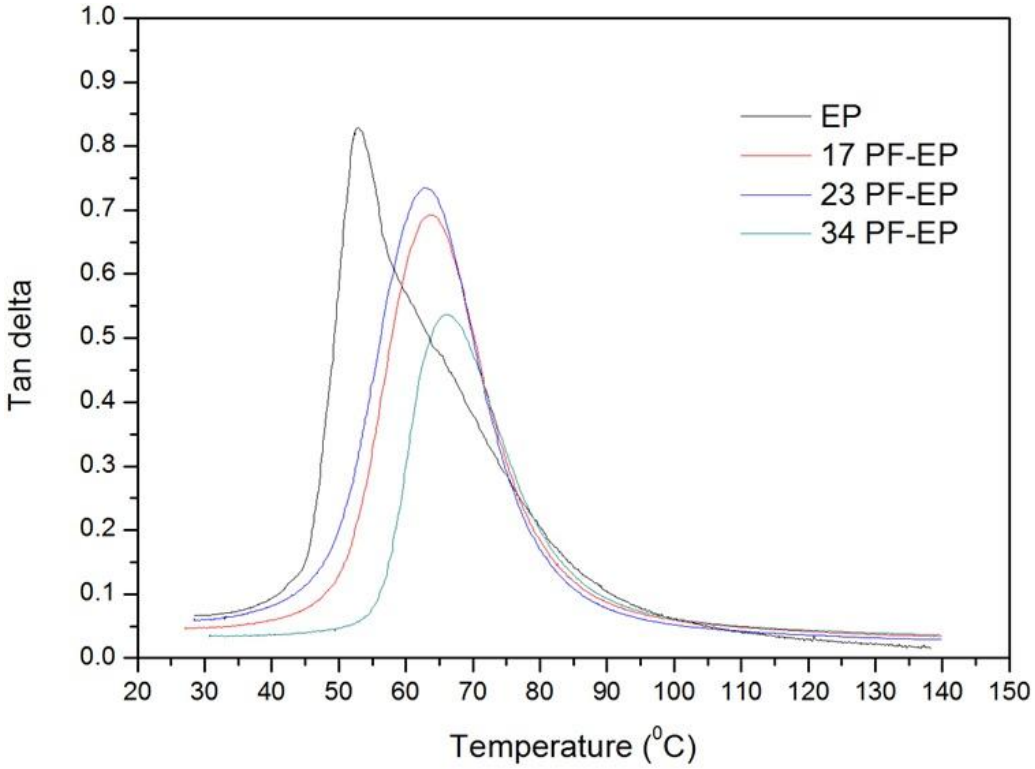

(b)

Fig. 4.26: Impact of reinforcement volume with temperature on tan δ of (a) CF-EP (b) PF-EP composites at a frequency of 1 Hz

4.3.2.3 Effect of Fiber Content on the Loss Modulus (E'') of CF-EP and PF-EP Composites

The impact of fiber content with temperature on the viscous response (loss modulus, E'') of CF-EP and PF-EP composites was recorded in Fig. 4.27. The temperature corresponding to the peak of E'' represents T_g, at which the maximum energy dissipation occurred in the form of heat. The loss modulus (E'') peak height and T_g values are mentioned in Table 4.14. The elevation of peak height and the shifting of T_g to the higher temperature were observed with the increase of fiber content. This was because of the increment in the heterogeneity of polymer matrix, and recoverable viscoelastic deformation at higher concentration. All E" curves attained a peak (maximum energy dissipation) and decrease to a lower value at a higher temperature (above T_g), due to the free molecular motion. Fig. 4.27 revealed that the effect of fibers is more prominent at a higher temperature (above T_g). Table 4.15 shows that the T_g obtained from the peak of E" curve was lower than that of the damping factor (tan δ) curve. The E" value (MPa) of 34 vol.% fiber-reinforced composite is considerably greater than the 17% and 23% fiber composites at a higher temperature. This result confirmed the higher activation energy required to mobile the polymer chains in the case of 34% strengthened material.

Table 4.15: Comparison of T_g obtained from the tan δ and loss modulus curve

Composites	**T_g from tan δ_{max} (^{0}C)**	**T_g from E'' (^{0}C)**	**Comment**
EP	52.95	47.1	The glass transition temperature (T_g) is not a well-defined temperature for a thermodynamic phase transition. It depends on the experimental conditions (velocity or frequency used and cooling or heating rate). The T_g value obtained from E'' was lower (5-10^{0}C) than the value obtained from tan δ_{max}. It can be defined by using the definition: Tan δ is the fraction of E" to E' which does not have the same maximum as E" by itself. The glass transition is a range of behavior where material softens.
17 CF-EP	69.8	61.36	
23 CF-EP	72.5	65.8	
34 CF-EP	63.5	54.5	
17 PF-EP	63.72	54.38	
23 PF-EP	62.9	52.17	
34 PF-EP	66.1	60.08	

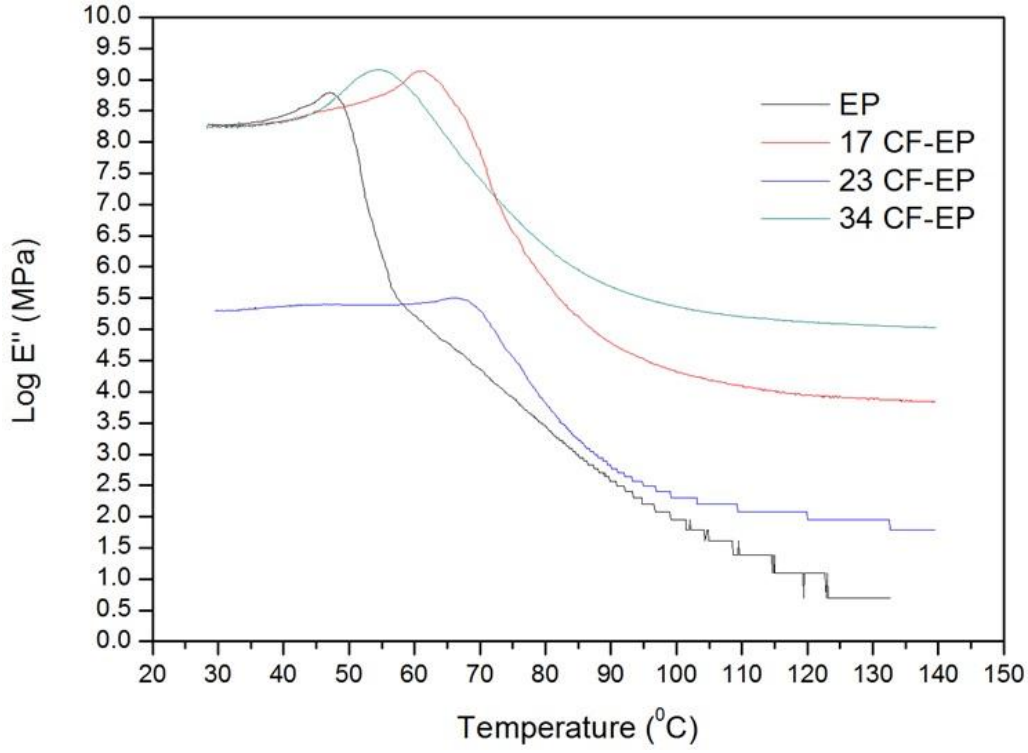

(a)

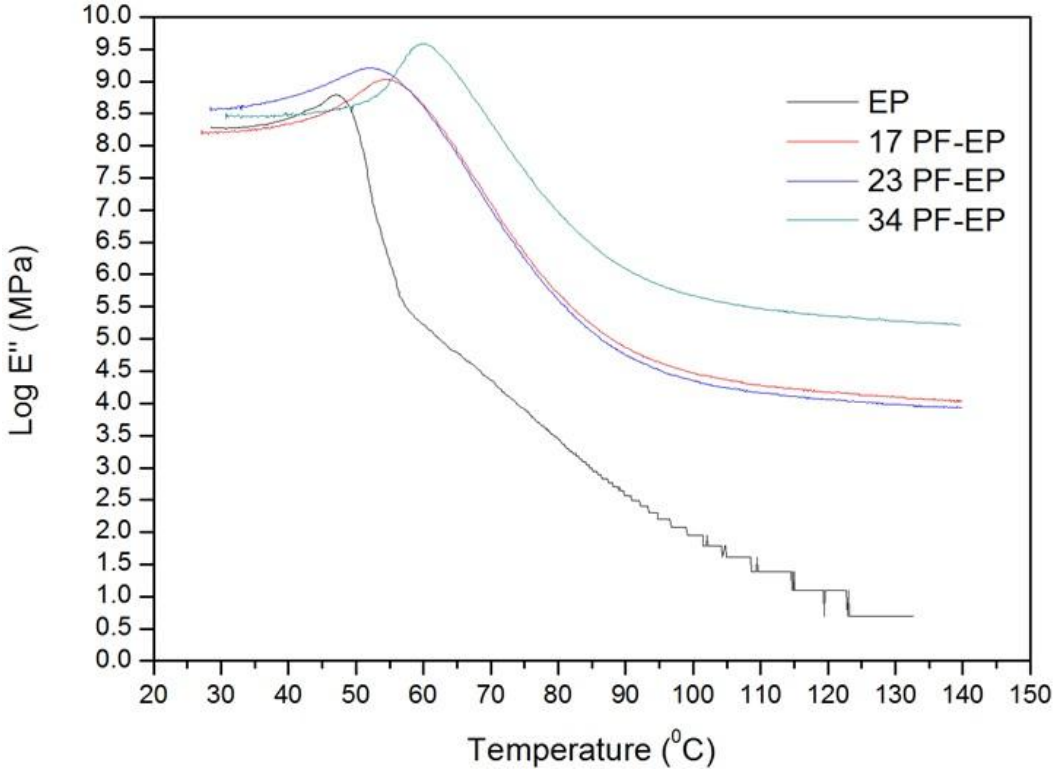

(b)

Fig. 4.27: Impact of reinforcement volume with temperature on the loss modulus of (a) coir fiber-epoxy (b) pineapple leaf fiber-epoxy composites at a frequency of 1 Hz

4.3.2.4 Effect of Frequency

For characterizing the viscoelastic behavior of composite material, the frequency of oscillation plays a vital role. The stiffness and damping behavior of a material is a function of frequency at which the load is applied. Fig. 4.28 present the impact of frequency with temperature on E' and tan delta of 34 CF-EP and 34 PF-EP composites. It observed that the storage modulus (E') was reduced with the increase of oscillation frequency. Usually, the stiffness of a polymeric material is increased with the increase of frequency (short time). But, in this case, the reverse effect was observed. This surprising result may be due to the increased molecular-molecular interactions and entanglements of the polymeric chains over the time. As seen in Table 4.16, we can report that the glass transition temperature and the tan δ peak height of 34 CF-EP were increased with the increase of frequency. This behavior confirmed the good damping power of manufactured composites at a higher frequency.

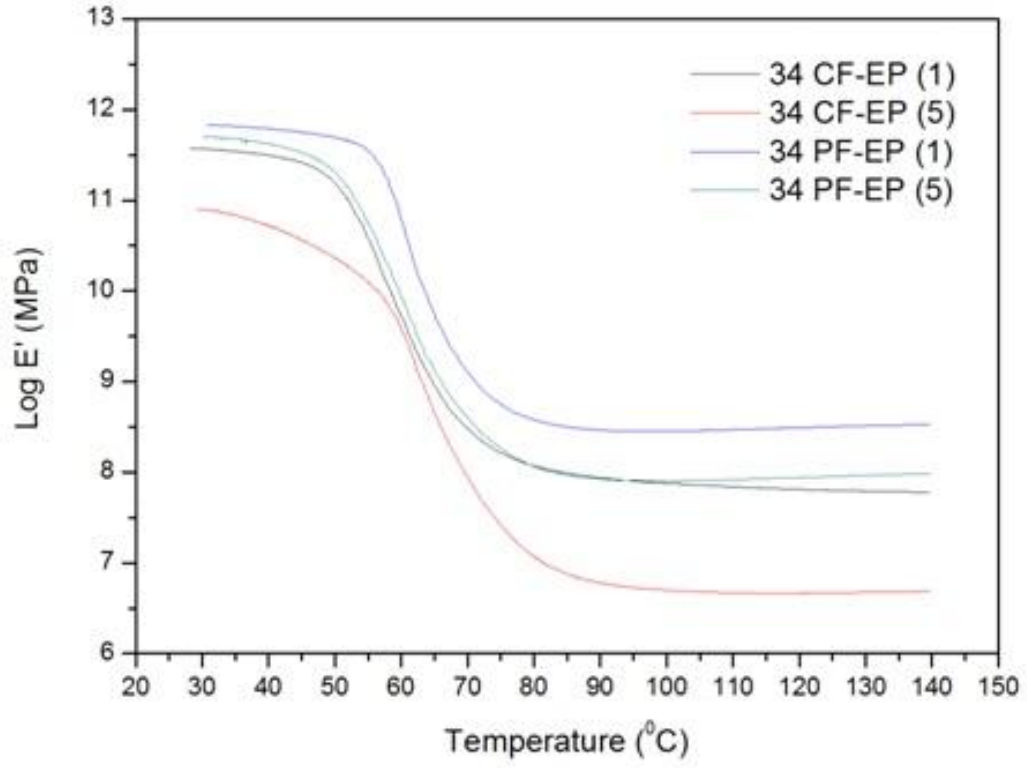

(a)

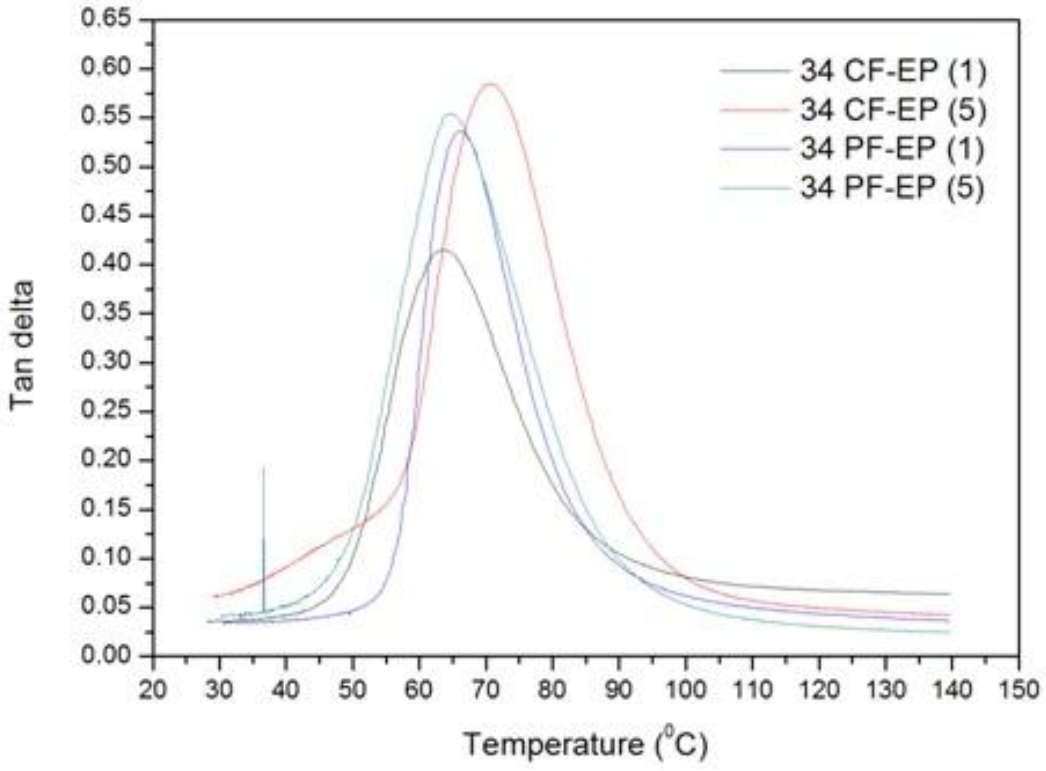

(b)

Fig. 4.28: Impact of frequency on (a) storage modulus (b) loss factor (tan δ) of the 34 CF-EP and 34 PF-EP composites as a function of temperature

Table 4.16: Effect of frequency on T_g, tan δ peak and width values, and E' (storage modulus) of 34 vol.% fiber-reinforced composites

Composites	T_g	tan δ peak height	tan δ peak width	E' value (Pa) at 50^0C	E' value (Pa) at 70^0C
34 CF-EP (1)	63.5	0.41	23.33	7.356E +09	3.709E +09
34 CF-EP (5)	70.8	0.58	22.61	3.164E +10	2.822E +09
34 PF-EP (1)	66.1	0.53	17.22	1.196E +11	6.315E +09
34 PF-EP (5)	64.8	0.55	23.28	8.167E +10	5.416E +09

4.3.2.5 Cole-Cole Plot

In order to understand the structural/property relationship, the Cole-Cole plots are widely used. The effect of fiber content on the dielectric relaxation of a polymer can be analyzed by using the Cole-Cole plot. Fig. 4.29 depicts the Cole-Cole plots of unfilled epoxy and filled epoxy systems with coir fiber and pineapple leaf fiber respectively. The nature of the plot is an important tool to determine the homogeneity of the system. J. Ferry *et al*. [239] reported that the homogenous polymeric systems should indicate a semicircular plot. As seen in Fig. 4.29, where the log E'' values are plotted as a function of log E', the Cole-Cole plots for all the

composites are imperfect circles. It was observed that the extent of plot imperfection was increased, with the increase of fiber content. Even, an unfilled epoxy polymer shows a large amount of heterogeneity. The 17 PF-EP and 23 PF-EP composites show a similar Cole-Cole plot. This result confirmed that both composites have almost the same degree of homogeneity.

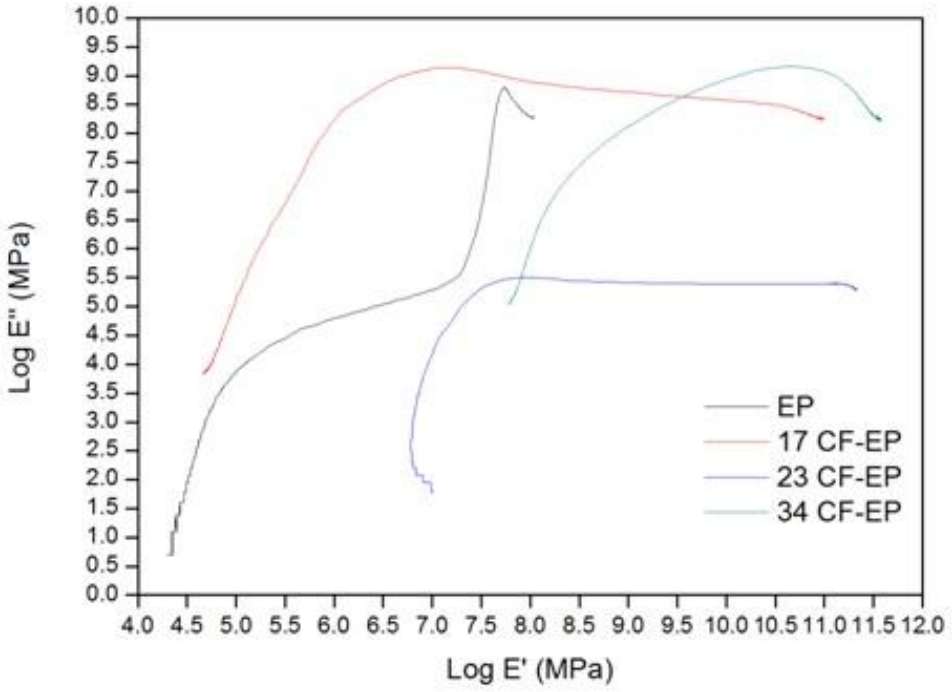

(a)

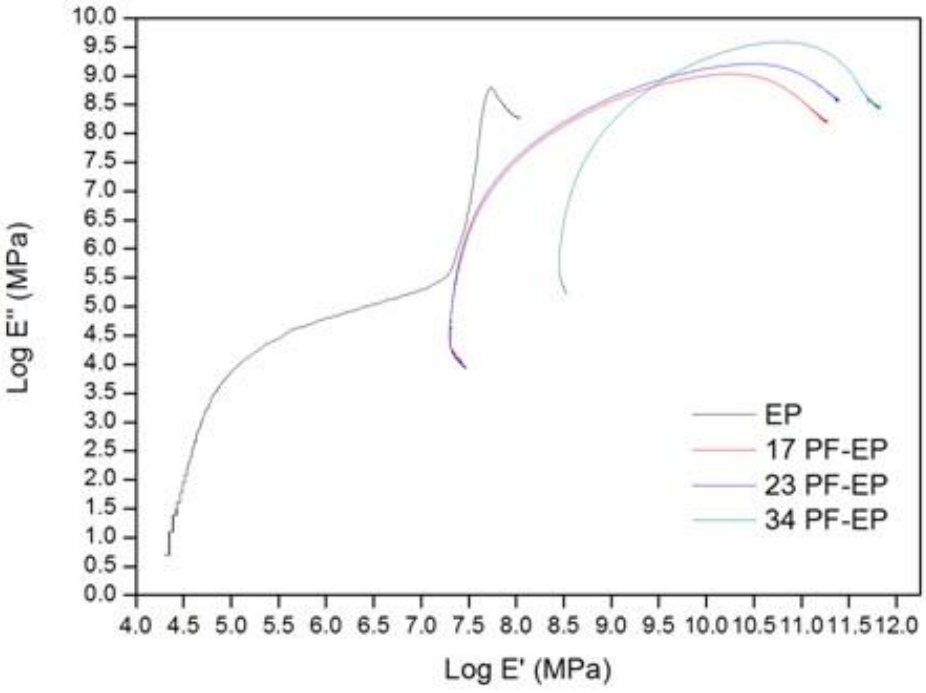

(b)

Fig. 4.29: Cole-Cole plots of the (a) Coir fiber-epoxy (b) pineapple leaf fiber-epoxy composites

4.4 Impact of Fibers Layering Pattern on Performance Characteristics of PALF/COIR Hybrid Epoxy Composites

For successful employment of NFRCs in structural applications, it gets important to make the composite so that it hinders fire spread and moisture sorption. In addition, the detailed characterization of viscoelastic properties is a critical step in the development of polymer-based composite materials. In this regard, this section deals with the impact of layering pattern on the flammability, viscoelastic behavior, and moisture sorption of PALF/COIR strengthened epoxy based material. The different layered hybrid composites [bilayer (pineapple/coir); trilayer (pineapple/coir/pineapple, coir/pineapple/coir); and intimately mixed (shown in Fig. 4.30)] were prepared by hand lay-up technique, keeping the volume ratio of pineapple and coir 1:1 and the total fiber volume content 0.40 V_c. The designation of developed composites for the DMA test is shown in Table 4.17. To characterize the flammability and hydrophilicity of developed materials, the UL-94V, UL-94HB, flame penetration, and moisture sorption tests were performed. Dynamic mechanical thermal analysis (DMTA) test method has also been employed to quantify the dynamic behavior of manufactured composites.

Table 4.17: Designation of PALF/COIR hybrid epoxy composites

Designation	**Details**
EP	Neat Epoxy resin
CF-EP (1)	Coir fiber-Epoxy composite (frequency 1 Hz)
PF-EP (1)	Pineapple leaf fiber-Epoxy composite (frequency 1 Hz)
CPC (1)	COIR/PALF/COIR hybrid composite (frequency 1 Hz)
PCP (1)	PALF/COIR/PALF hybrid composite (frequency 1 Hz)
Bilayer (P/C) (1)	Bilayer (PALF/COIR) hybrid composite (frequency 1 Hz)
IM (1)	Intimately mixed hybrid composite (frequency 1 Hz)
CPC (5)	COIR/PALF/COIR hybrid composite (frequency 5 Hz)
PCP (5)	PALF/COIR/PALF hybrid composite (frequency 5 Hz)
Bilayer (P/C) (5)	Bilayer (PALF/COIR) hybrid composite (frequency 5 Hz)
IM (5)	Intimately mixed hybrid composite (frequency 5 Hz)

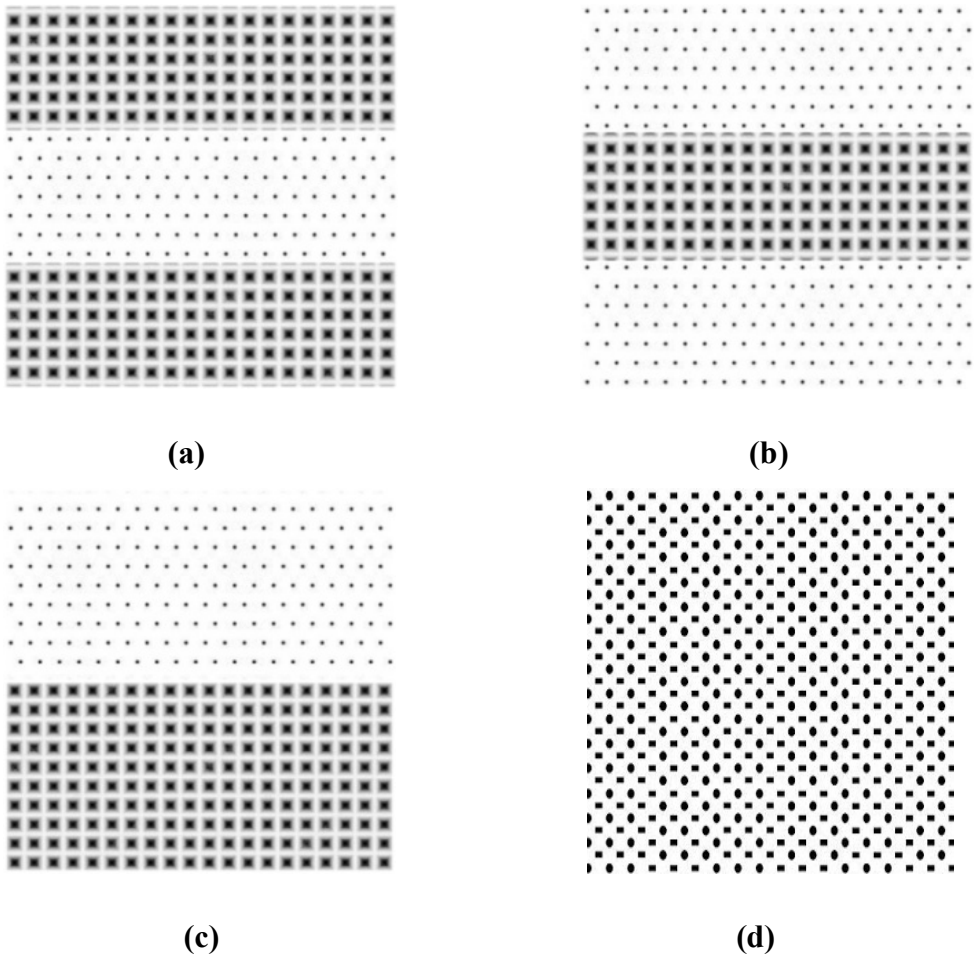

Fig. 4.30: Different Layered Hybrid Composite Boards (a) PCP, (b) CPC, (c) Bilayer (P/C), (d) IM

4.4.1 Impact of Layering Pattern on the Flammability of PALF/COIR Material

The fire retardant behavior of unfilled epoxy and fibers filled epoxy composites was investigated by employing the flammability tests (UL-94V and UL-94HB) and flame penetration test. The experimental results showed that the flammability of developed biocomposites is higher than the virgin epoxy thermoset. Moreover, the cellulosic fibers (PALF and COIR) filled hybrid composites exhibit a shorter time for flame penetration from bottom to top surface as compared to an epoxy polymer. These negative outcomes of NFRCs can be explained by the scaffolding effect of fiber which leads to an uninterrupted contact between decomposition products of polymer and heat source. Lignocellulosic fibers support fire and have a lower activation energy than the thermosetting resin. Compared to a neat epoxy matrix, the developed hybrid composites exhibit a higher mass-loss rate (MLR) and shorter time to ignition (TTI). The ability of hybrid composites to retard flame is not only dependent on the

type of matrix and reinforcing fibers, but also is a function of orientation and distribution of fibers, the relative volume content of matrix and fiber, and the interfacial interaction between fiber-matrix and fiber-fiber. Figs. 4.31 to 4.33 illustrate the effect of layering pattern on the rate of burning (mm/min), mass loss rate (gm/min), and flame penetration time (min) of composites. The flame retardancy of hybrid material is greatly depends on the nature of skin and core material. The PCP hybrid composite (pineapple as skin and coir as a core material) has lower resistance to flame spread than the CPC hybrid material (coir as skin and pineapple as a core material). This was due to the the presence of high lignin (40-45%) and low cellulose content (32-43%) in COIR results in the formation of more char at the surface which yields higher resistance to thermal-oxidative decomposition and poor heat conduction to core PALF material. Amongst all the different layered hybrid composites (PCP, CPC, Bilayer (P/C), and IM), the CPC material possess maximum time (41 min) for Bunsen flame penetration from bottom to top surface. The PCP and Bilayer (P/C) hybrid composites exhibit a value of 27 and 24 min respectively, failed to meet the minimum requirement of 30 minutes (15t/6 = 30 min, t = 12 mm) for the fire-resistant material test. The presence of high cellulose content in pineapple leaf fiber generates more flammable volatiles and gases during the thermal decomposition process. In comparison with CPC, the PCP layered hybrid composite consists of higher crystalline cellulose at the surface which formed a higher amount of levoglucosan during combustion that leads to higher flammability. Manfredi *et al*. [251] stated that the thermal decomposition of natural fibers includes the removal of absorbed water molecules; decomposition of hemicellulose, cellulose, and lignin component; formation of volatiles, residual char, and inorganic non-flammable products. It can be observed from UL-94 flammability tests that the intimately mixed hybrid composite exhibits higher resistance to travel flame front from 25.4 mm to 101.6 mm than that of PCP and Bilayer (P/C) composites. The speed of flame spread in a vertical burning test (UL-94V) is more than the horizontal flammability and it was due to the preheating of the samples.

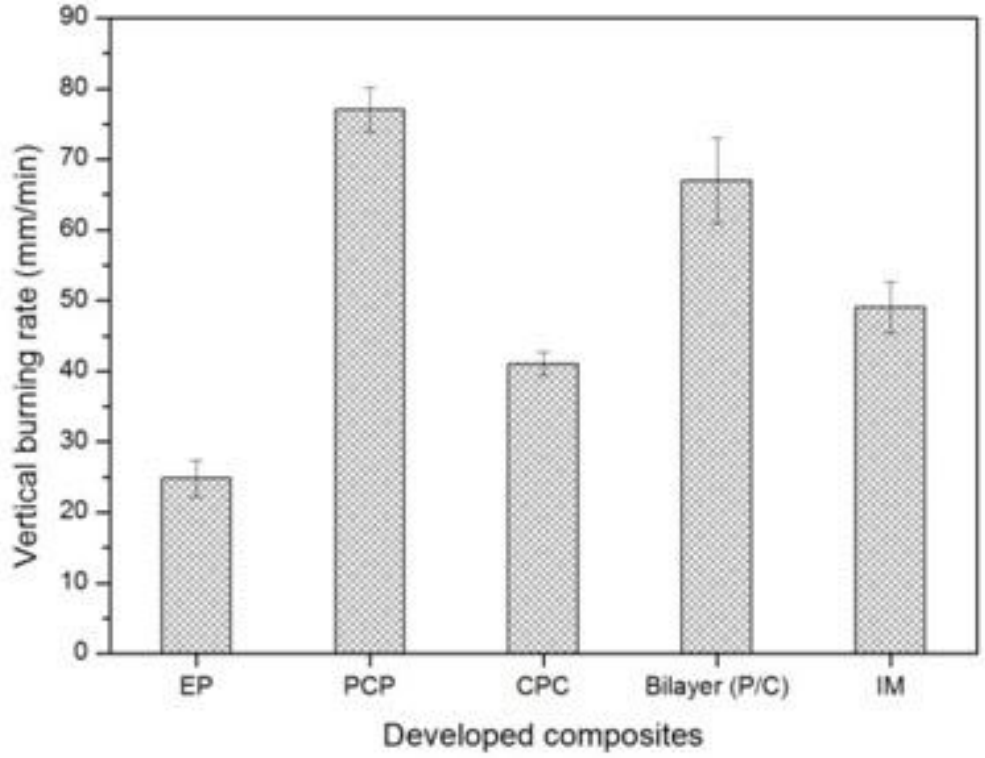

(a)

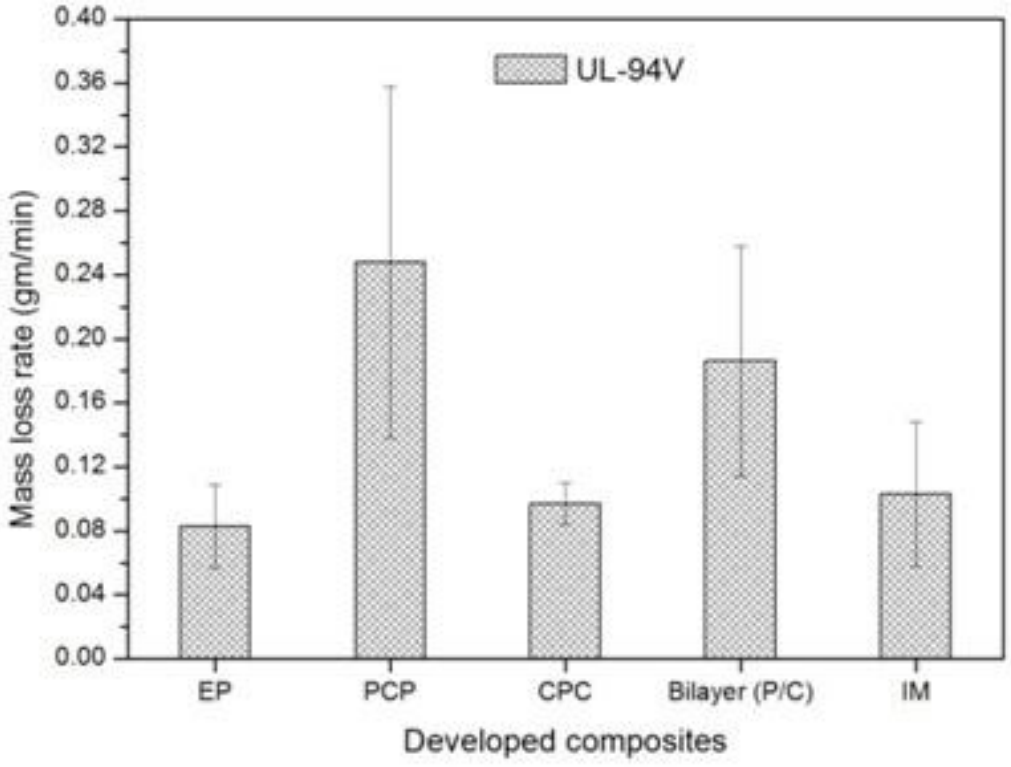

(b)

Fig. 4.31: Impact of layering pattern on (a) Vertical burning rate (b) Mass loss rate

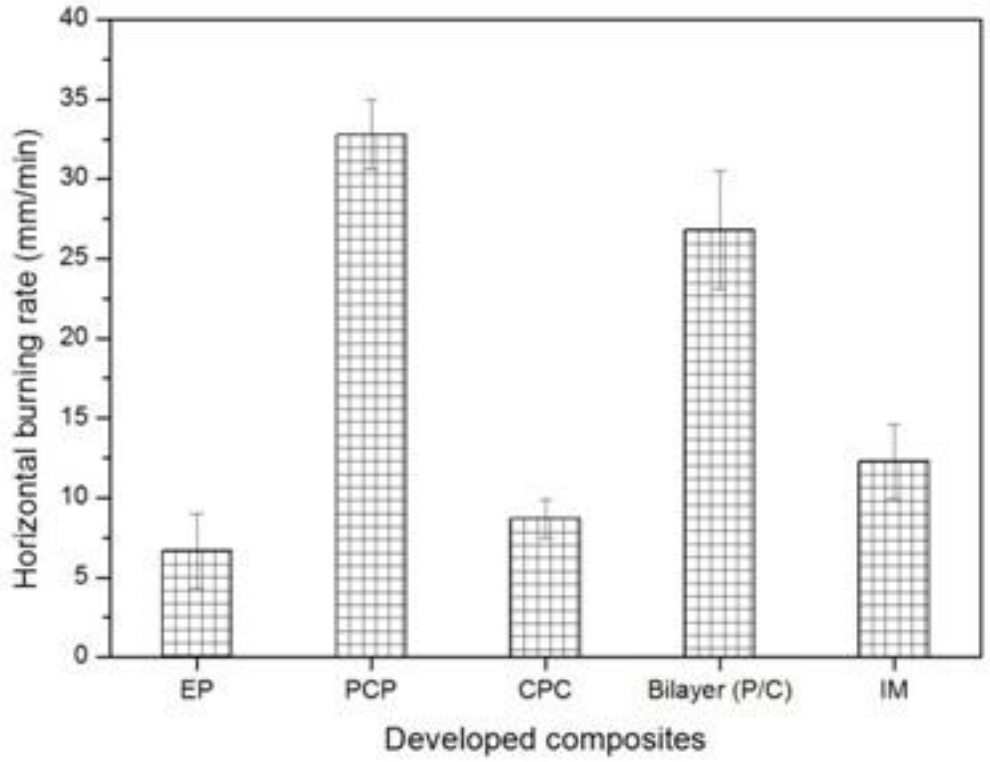

(a)

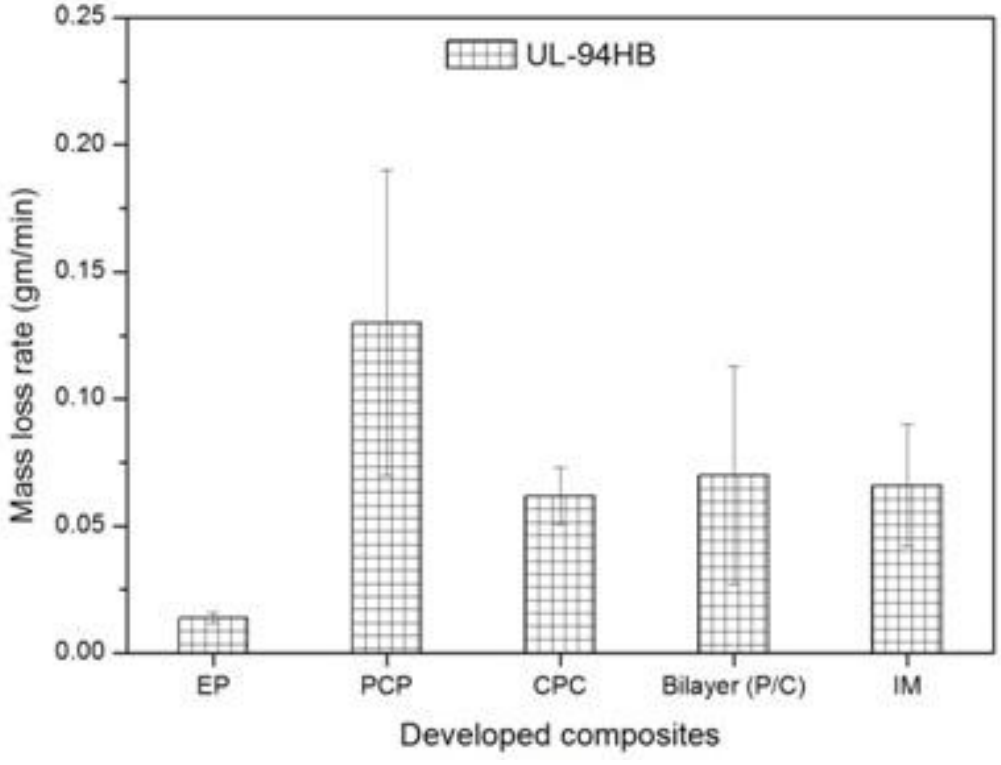

(b)

Fig. 4.32: Impact of layering pattern on (a) Horizontal burning rate (b) Mass loss rate

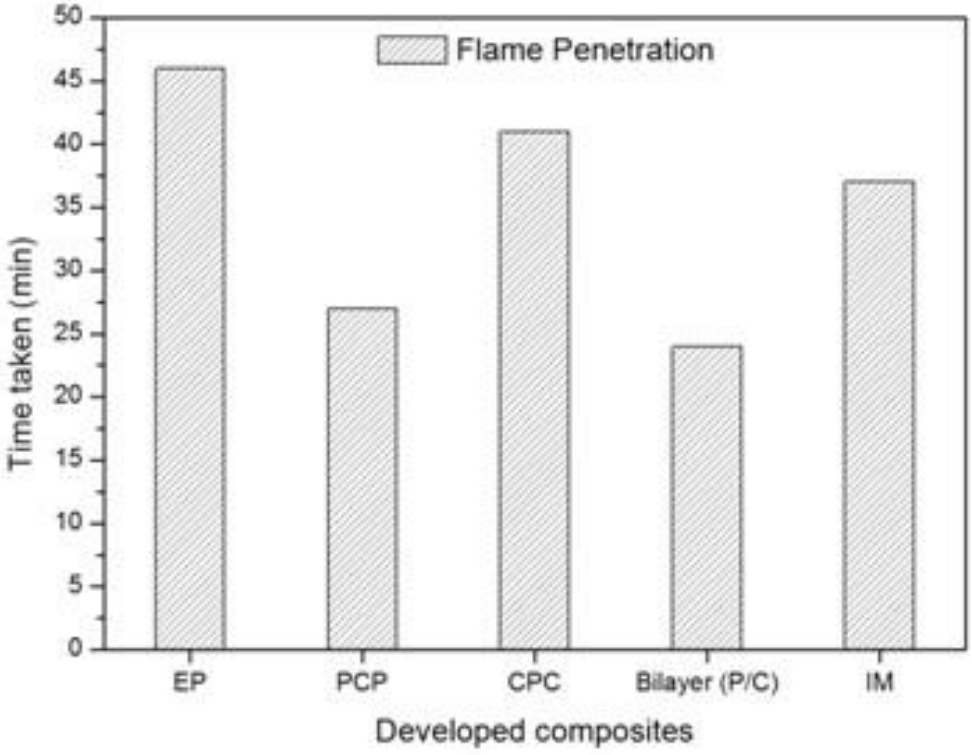

Fig. 4.33: Impact of layering pattern on time taken for flame penetration from bottom to top surface

4.4.2 Impact of Layering Pattern on the Moisture Sorption of PALF/COIR Material

The moisture sorption characteristic of hybrid composites was recorded in Fig. 4.34. The water uptake power of a matrix medium was increased considerably after the incorporation of cellulosic fibers (As expectedly). According to Flory's proposed theory, the diffusion of water molecules in polymers is due to the presence of cavities and micro-pores between polymeric chains. The gaps are generated at the interfacial region that results in penetration of water droplets inside the polymer. From the test results, we can conclude that the ability of polymer composites to absorb moisture in a humid environment greatly depends on how reinforcing fibers are arranged in a viscoelastic matrix medium. Amongst all the formulated different layered hybrid composites, the CPC material absorbs the least amount of water. This may be due to the occurrence of a large amount of lignin compound on the surface irrespective of cellulose content which yields high impedance to water molecules. The PCP hybrid composite exhibits a higher rate of moisture sorption than the other hybrid specimens [Bilayer (P/C), CPC, Intimately mixed (IM)]. This was attributed to the presence of a larger amount of -OH functional group on the outside of PCP composite which

supports the formation of hydrogen bonds with water molecules. Fig. 4.35 clearly illustrates that the intimately mixed (IM) hybrid composite absorbs 44.32% and 34.87% less water than the PCP and Bilayer (P/C) composite respectively. This was caused by the better dispersion of fibers and improved interaction between constituent elements. Fig. 4.34 revealed that all the composite specimens absorb water sharply up to 60 hrs and become saturated or reached at equilibrium level after 120 hrs.

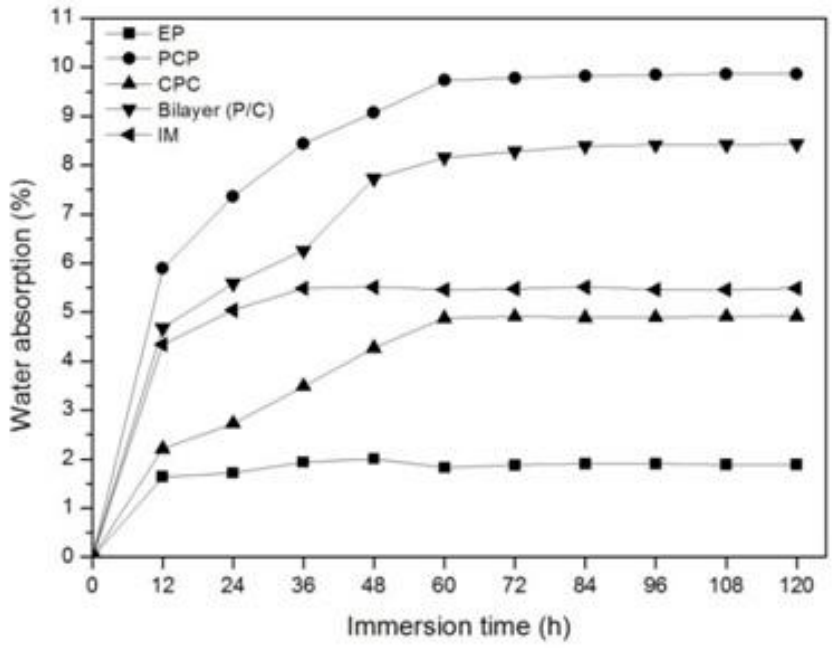

(a)

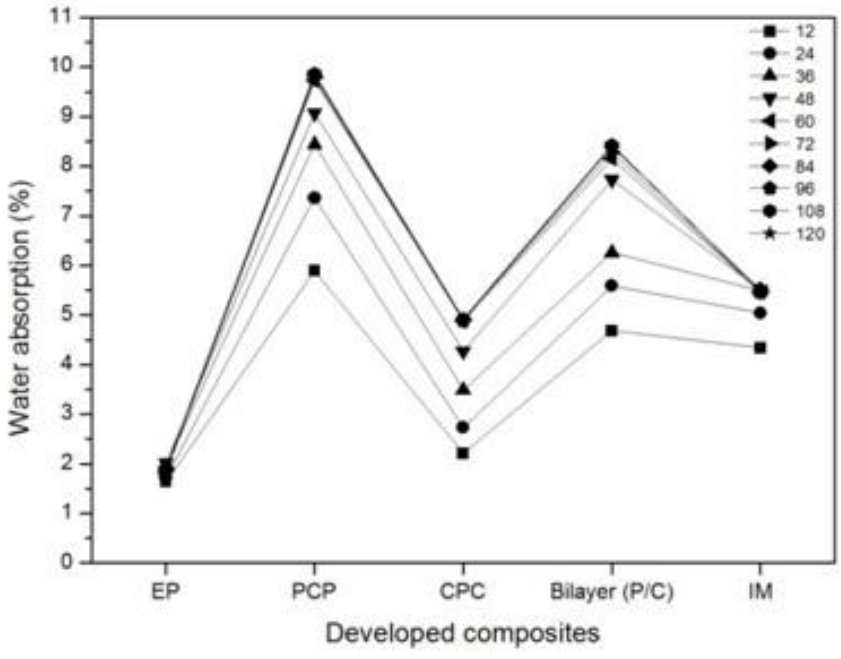

(b)

Fig. 4.34: Moisture sorption behavior of hybrid materials as a function of (a) Immersion time (b) Layering pattern

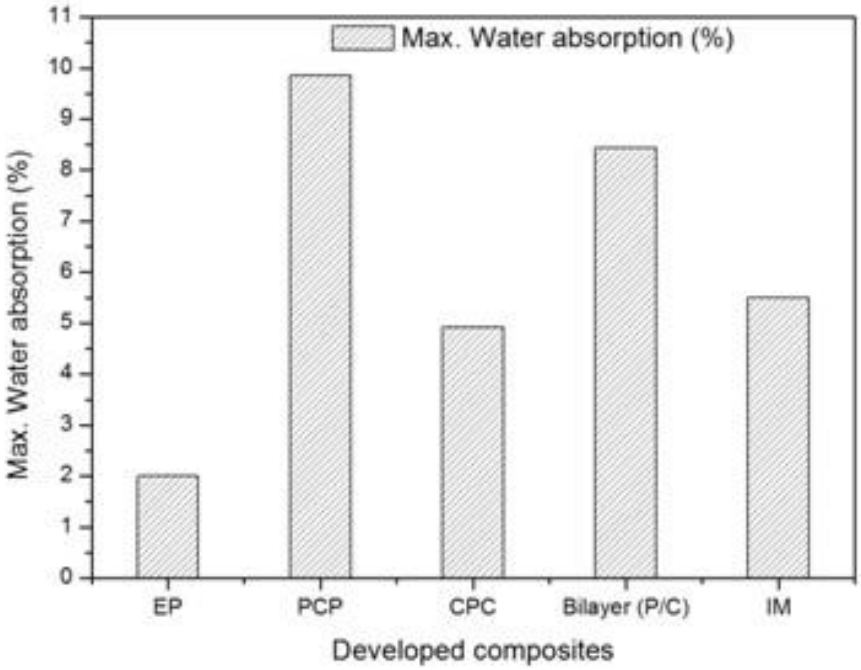

Fig. 4.35: Maximum water absorption of differently layered hybrid composites

4.4.3 DMA of Hybrid Composites

The performance of a polymer composite material under a range of temperature, frequency, and time can be accurately assessed by using DMTA technique. The viscoelastic behavior of FRCs is a function of the nature of reinforcing fiber and polymer matrix; the aspect (l/d) ratio, orientation, and distribution of the fiber; fiber to matrix volume content ratio; and the interfacial interaction between them. DMA test results which are reported in this section concerns the impact of layering pattern and fiber hybridization on the viscous and elastic response of PALF/COIR fiber reinforced epoxy-based composites.

4.4.3.1 Impact of Layering Pattern and Fiber Hybridization on the Storage Modulus (E') of PALF/COIR Strengthened Hybrid Material

The modulus curve provides information about the viscoelastic rigidity and energy storage ability of a composite material. The reinforced fibers and fillers play an active role to greatly affect the modulus of polymeric materials. Fig. 4.36 illustrates that the storage modulus (E') of a virgin epoxy matrix was increased by the incorporation of stronger and stiffer PALF and COIR fibers. This behavior can be verbalized in terms of higher restrictions on the chain movement. Irrespective of the fiber layering pattern, the stiffness of CF-EP composite is significantly improved by

the loading of PALF in equal volume content [PALF: COIR = 1:1 (v/v); V_f= 0.4 V_c]. This was due to the synergistic compatibility between both types of cellulosic fibers. Amongst all the different layered hybrid composites, the bilayer (P/C) and trilayer CPC have higher value of storage modulus below and above 70 ^{0}C (T_g) respectively. The effectiveness of various layered reinforcements can be determined in terms of coefficient 'C' (mentioned in equation 4.6). The higher value of constant C signifies the poor effectiveness of fiber to increase the modulus. Usually, filled systems have lower C values than the unfilled polymer. Table 4.18 present the measured values of effectiveness coefficient 'C' (30-120 ^{0}C) for developed specimens. The CPC composite has lower C value than the other hybridized composites and it was due to the better interfacial interaction at the fiber-matrix interface, higher wetting ability of COIR, less void content, and the construction of more covalent linkages. The 'C' value of CF-EP composite (0.7048) was reduced by the incorporation of pineapple leaf fiber. It confirms the synergistic compatibility between PALF and COIR fiber. Fig. 4.36 revealed that the bilayer (P/C) and intimately mixed hybrid composites possess the same E' value at T_g. But at a higher temperature (above T_g), the E' values of bilayer composite were significantly greater than the intimately mixed one.

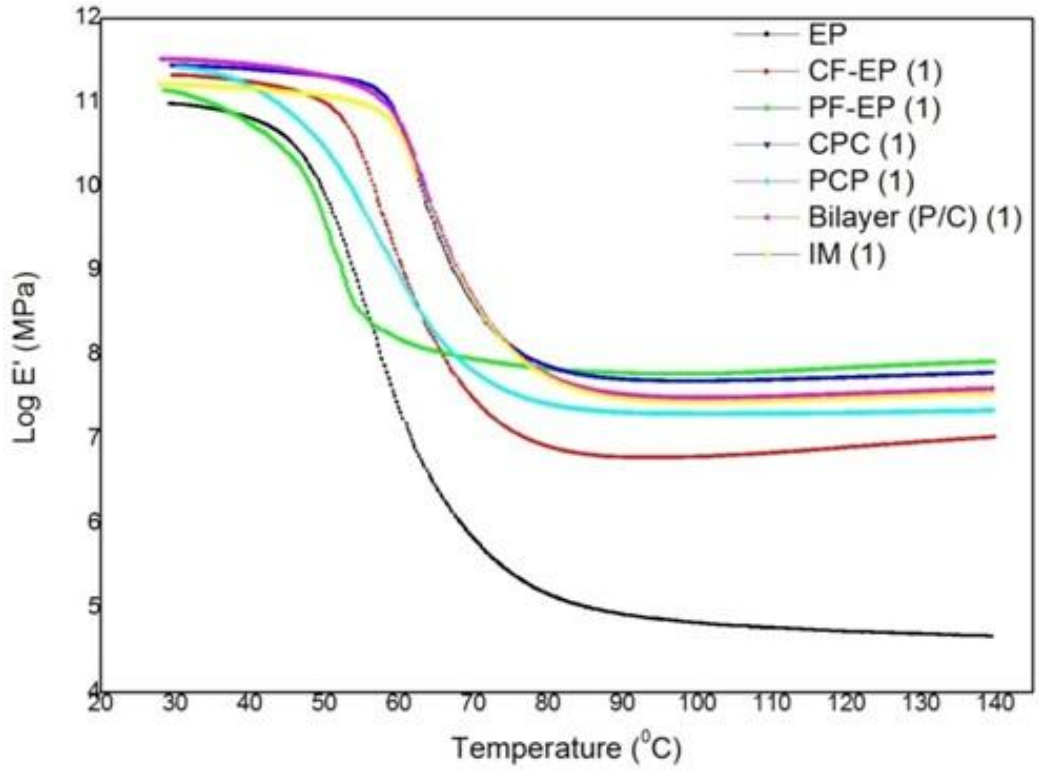

Fig. 4.36: Impact of layering pattern and fiber hybridization on E' of composites at a frequency of 1 Hz

Table 4.18: Values of the effectiveness coefficient 'C', tan δ peak height and width, glass transition temperature (T_g), E'' peak height, E' and E'' values at different temperature for virgin epoxy, pure coir fiber-epoxy, pineapple leaf fiber-epoxy, and the different layered hybrid composites

Composites	C	T_g from tan δ_{max} (^{0}C)	tan δ peak width	tan δ peak height	T_g from E'' (^{0}C)	Log E'' Peak height (MPa)	Log E' (30^{0}C)	Log E' (50^{0}C)	Log E' (70^{0}C)	Log E' (90^{0}C)	Log E' (120^{0}C)	Log E'' (50^{0}C)	Log E'' (70^{0}C)
P	-	61.2	23.66	0.8283	44.3	8.79	10.98	9.6	5.83	4.93	4.72	8.78	5.29
CF-EP	0.7048	64.9	20.39	0.76	55.88	9.14	11.33	10.99	7.45	6.79	6.91	8.71	7.021
PF-EP	0.6089	62.9	19.08	0.73	52.17	9.205	11.12	9.9	7.95	7.79	7.85	9.16	7.021
CPC	0.635	68.51	17.12	0.63	61.56	9.206	11.45	11.32	8.61	7.73	7.75	8.12	8.12
PCP	0.67	62	27.52	0.43	49.24	9.138	11.42	10.46	7.81	7.33	7.32	8.99	6.71
Bilayer	0.656	70	18.64	0.63	62	9.130	11.51	11.33	8.68	7.54	7.54	8.46	8.22
IM	0.643	70	20.13	0.58	62.23	8.928	11.22	11.08	8.64	7.49	7.49	7.92	8.09

4.4.3.2 Impact of Layering Pattern and Fiber Hybridization on tan δ of PALF/COIR Strengthened Hybrid Material

The tan δ value indicates the damping ability or impact resistance of a material. It provides indirect information about the stiffness, internal structure, interfacial characteristics, and the morphology of a composite sample. Fig. 4.37 presents the tan δ curve of unhybrid and hybrid composites and revealed that the curve goes on increasing with temperature and attains a peak value (phase transition region), followed by the reduction due to the free movement of molecular chain segments. The increment in tan δ peak corresponds to the greater mobility of small groups and chain segments. From Table 4.18, we can report that the virgin epoxy matrix occupies a higher value of tan δ_{max} than the reinforced polymer composites. This was because of the restricted motion of polymeric chains after the incorporation of fibers. Amongst all the developed hybrid composites, the PCP composite exhibits a wider and shorter tan δ peak. The hybrid effect of PALF and COIR fibers can be better understood in terms of T_g. The T_g of CF-EP was increased from 64.9 ^{0}C to 68.51 ^{0}C and 70 ^{0}C after the hybridization with pineapple leaf fiber in CPC and bilayer (P/C) arrangements respectively. In comparison to the CPC hybrid composite, the bilayer and intimately mixed composites have a higher value of T_g. In addition to this, the peak width and height of both hybrid composites (Bilayer and IM) were found to be more and equal to or less than the CPC respectively. This was due to the better distribution of fibers within the polymer matrix and effective stress transfer from matrix to fibers without the matrix cracking. The positive displacement of T_g value

represents the reinforcement effectiveness in an epoxy thermoset resin. Concerning this statement, the intimately mixed (IM) fibers have a higher ability to reinforce polymers and this was because of its highest T_g, lower peak height, and broader tan δ peak. The better performance of intimately mixed banana/sisal material based on polyester resin was reported by M. Idicula *et. al* [160].

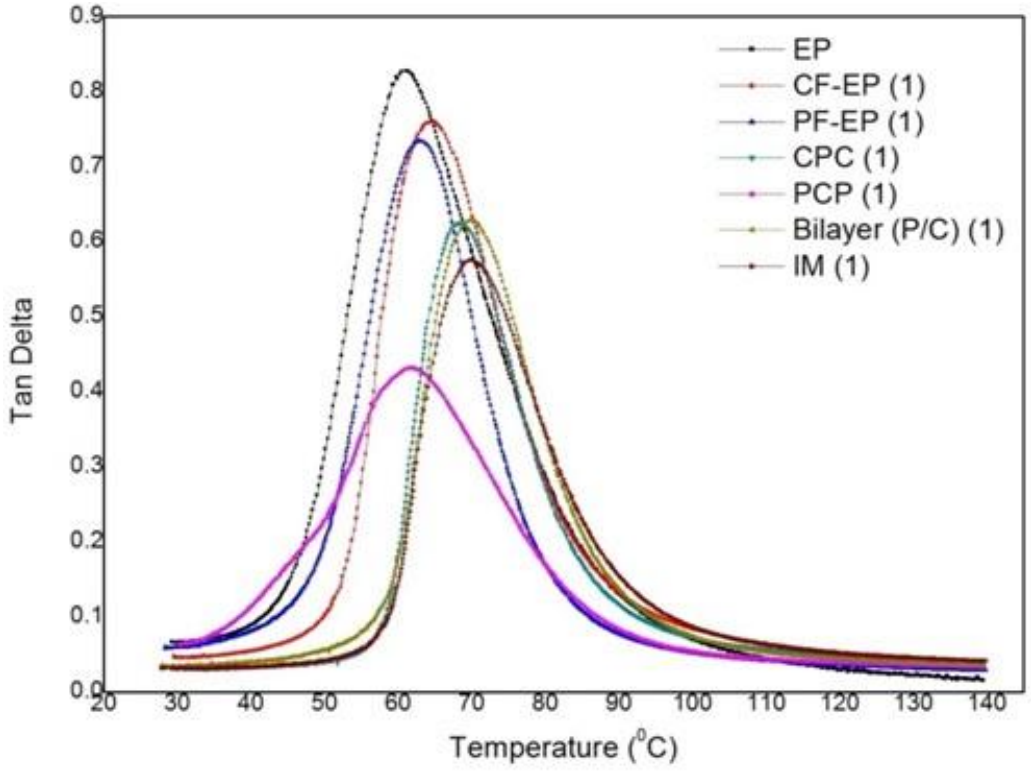

Fig. 4.37: Impact of layering pattern and fiber hybridization on tan δ of fabricated composites at a frequency of 1 Hz

4.4.3.3 Impact of Layering Pattern and Fiber Hybridization on E'' of PALF/COIR Strengthened Hybrid Material

The DMA parameter-"loss modulus (E'')" can be defined as the viscous response of polymer-based materials which is 90^0 out of phase component and represents the capability of a material to dispel energy as heat. The loss modulus (E") curve for virgin epoxy and epoxy-based composites is illustrated in Fig. 4.38. At high temperature (above T_g), the E" of epoxy thermoset matrix was significantly increased by the incorporation of reinforcing fibers. It confirmed the prominent effect of fibers to elevate the frictional force at the fiber-matrix interface which leads to a higher dissipation of energy. The peak of E" corresponds to the maximum energy loss at the T_g of the system. Similar to the tan δ curves, the loss modulus curves also drop down to lower values beyond T_g. This decrement is due to the free movement of polymer

chain segments. From Table 4.18, we can report that the T_g (obtained from E'' curve) of a neat thermoset resin was increased by the addition of reinforcing fibers (PALF and COIR). It was attributed to the inhibition in the chain relaxation process, rigidity of polymer chain segments, and elevation in heterogeneity within the composite material. The phase transition temperature (T_g) of CF-EP and PF-EP was positively shifted to a higher temperature after the hybridization of PALF and COIR. The glass transition temperature obtained from E" curves is lower as compared to the values resulted from the tan δ curve. The intimately mixed composite has highest value of T_g, followed by bilayer, CPC, and PCP hybrid ones.

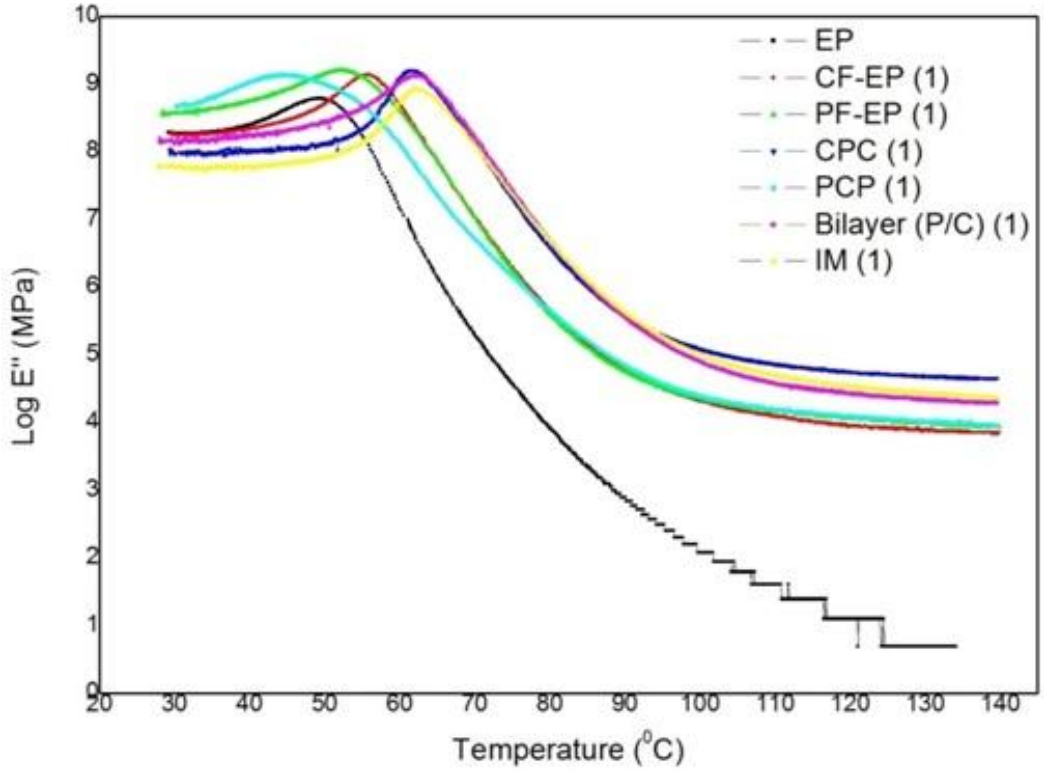

Fig. 4.38: Impact of layering pattern and hybridization on E'' of fabricated composites at a frequency of 1 Hz

4.4.3.4 Impact of Frequency

To fully characterize the viscoelastic properties of polymer-based composites, it is highly required to analyze the effect of frequency on E', E'', tan δ, and T_g. Fig. 4.39 revealed the variation in E' of hybrid composites with a special reference of frequency and temperature. In all cases, the storage modulus (E') was increased with the increase of the frequency of oscillation from 1 Hz to 5 Hz. This experimental result follows the same line of action as in the previous research work [Pothan *et. al* [252], Romanzini *et. al* [253]]. Both the static and dynamic modulus was found to be

decreased over a long time and it was because the internal molecular rearrangement takes place to overcome the localized stresses. The modulus values were found to be dramatically reduced from 55 ^{0}C to 110 ^{0}C. Fig. 4.40 shows that the damping ratio (tan δ) is greatly influenced by the frequency of oscillation. At high frequency (5 Hz), the tan δ_{max} and T_g were shifted to the higher value. The tan δ peak and its corresponding temperature (T_g) is linked with the process of partial loosening of the polymeric structure and the cross-linkage density. As seen in Table 4.19, the peak width of tan δ curve becomes broader with the increase of frequency from 1 Hz to 5 Hz and it was due to the morphological rearrangement of chain segments which upshot the inhibition of polymer relaxation process. Similar to tan δ curve analysis, the peak of loss modulus curve (E") was displaced to the higher temperature with step-up of frequency (shown in Fig. 4.41 and Table 4.19). The response of the viscoelastic materials may vary with temperature and oscillation frequency. Therefore, it becomes significant to plot a three-dimensional thermogram which represents the combined effect of frequency and temperature on the damping ratio of the manufactured polymer-based composite material. Fig. 4.42 revealed the 3D thermogram in which peaks of different composite samples are visible.

Table 4.19: Impact of frequency on T_g, tan δ peak height and width, and E'' peak height for all hybrid composites

Composites	T_g from tan δ_{max} (^{0}C)	tan δ peak height	tan δ peak width	T_g from E'' (^{0}C)	Log E'' peak height (MPa)
CPC (1)	68.51	0.63	17.12	61.56	9.206
CPC (5)	70.1	0.656	20.91	62.55	9.577
PCP (1)	62	0.43	27.52	49.24	9.138
PCP (5)	68.16	0.528	25.99	54.5	9.35
Bilayer (P/C) (1)	70	0.63	18.64	62	9.130
Bilayer (P/C) (5)	73.7	0.622	22.88	63.08	9.212
IM (1)	70	0.58	20.13	62.23	8.928
IM (5)	73.36	0.619	24.19	62.35	9.28

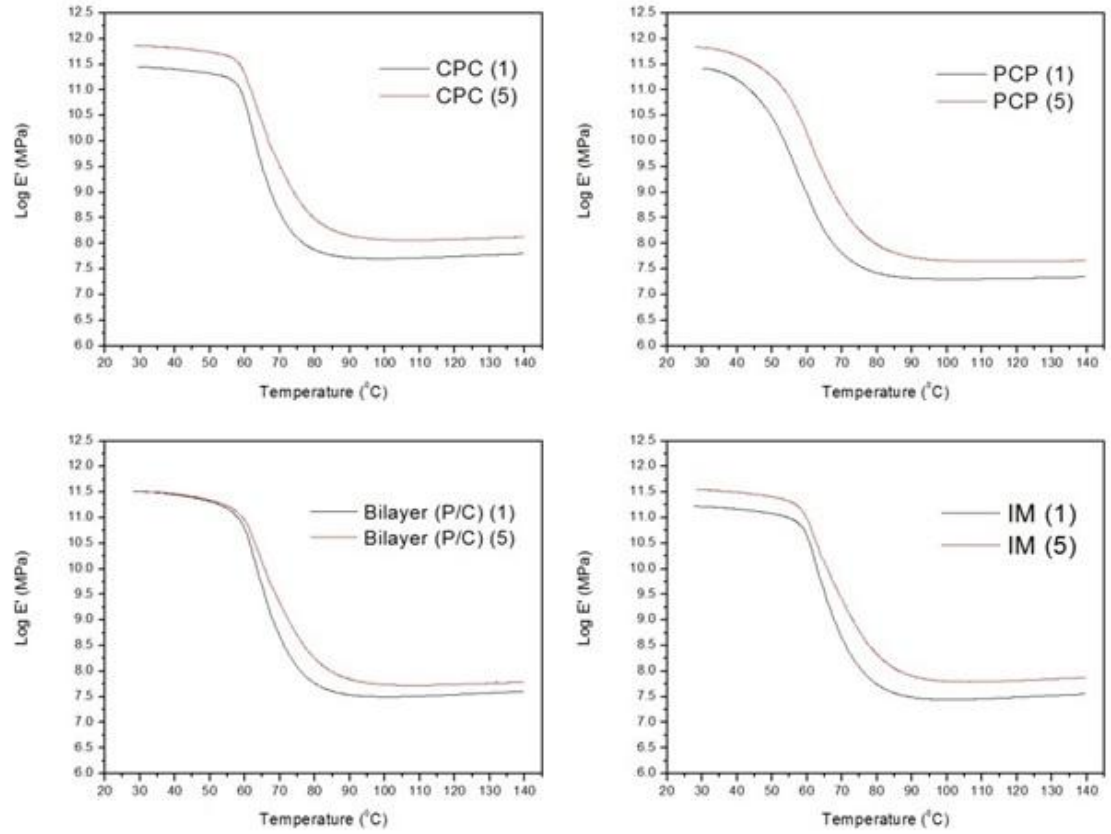

Fig. 4.39: Impact of frequency with temperature on E' of fabricated hybrid materials

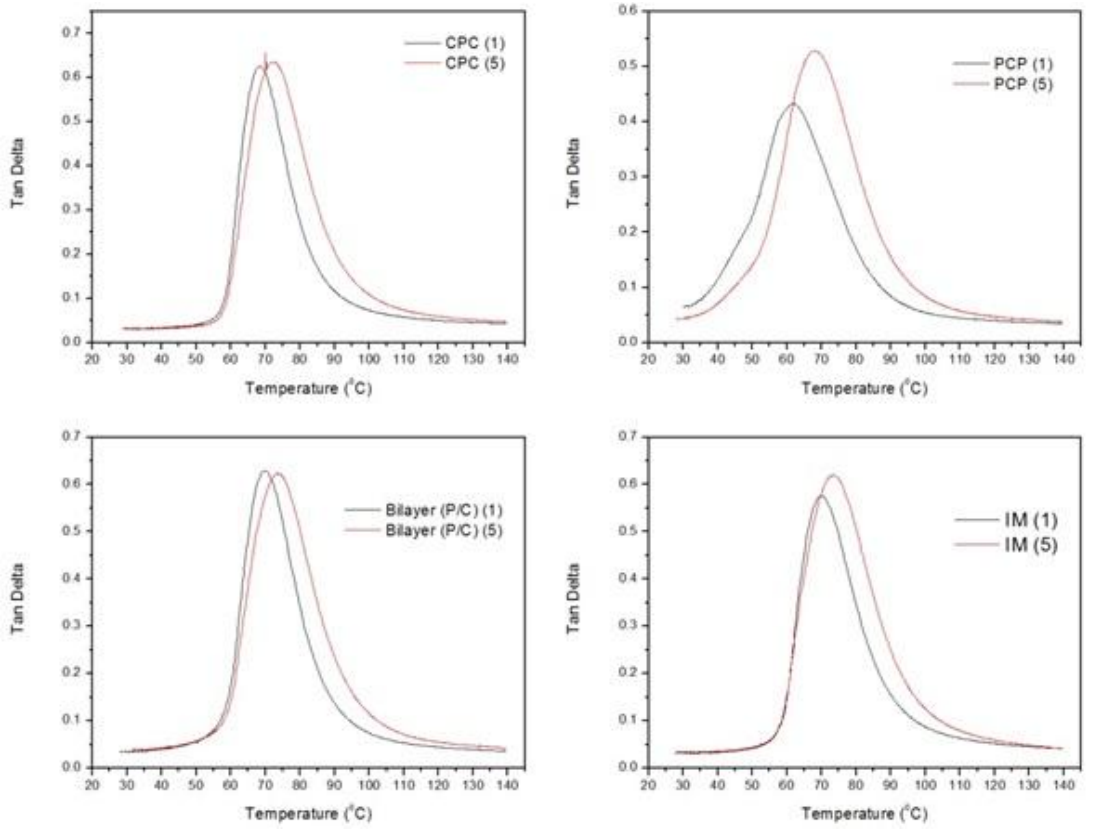

Fig. 4.40: Impact of frequency with temperature on tan δ of fabricated materials

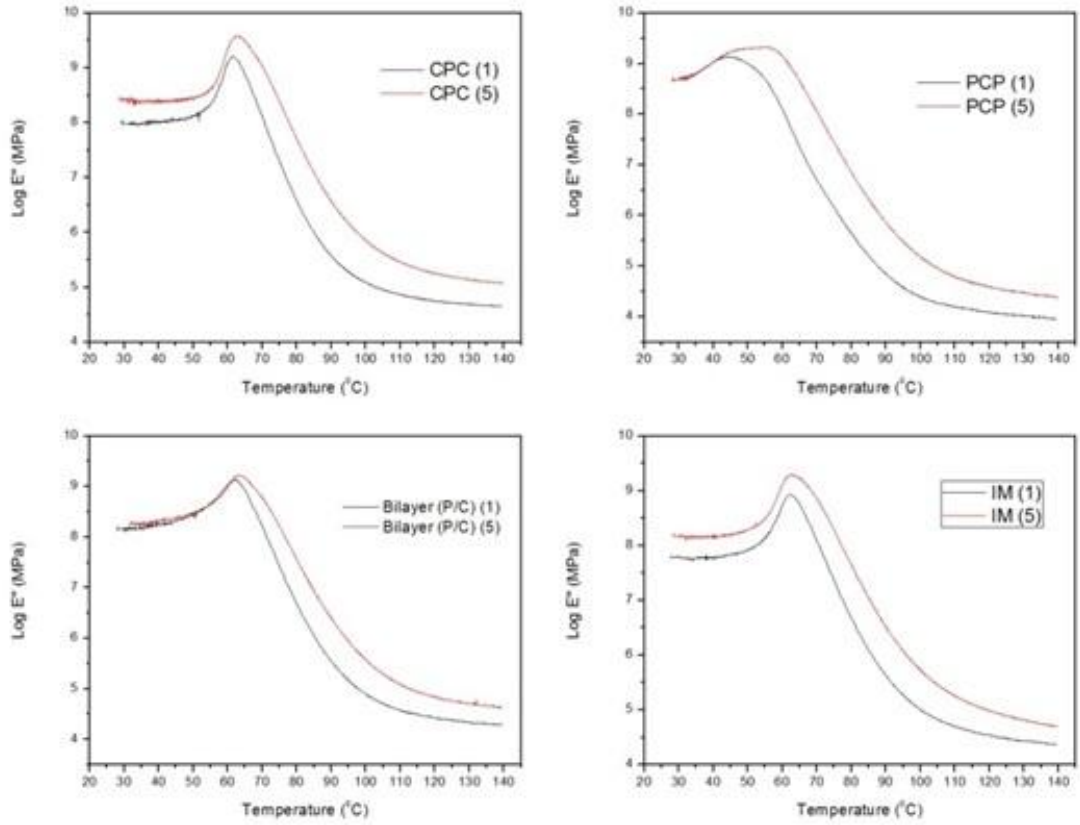

Fig. 4.41: Impact of frequency with temperature on E'' of fabricated materials

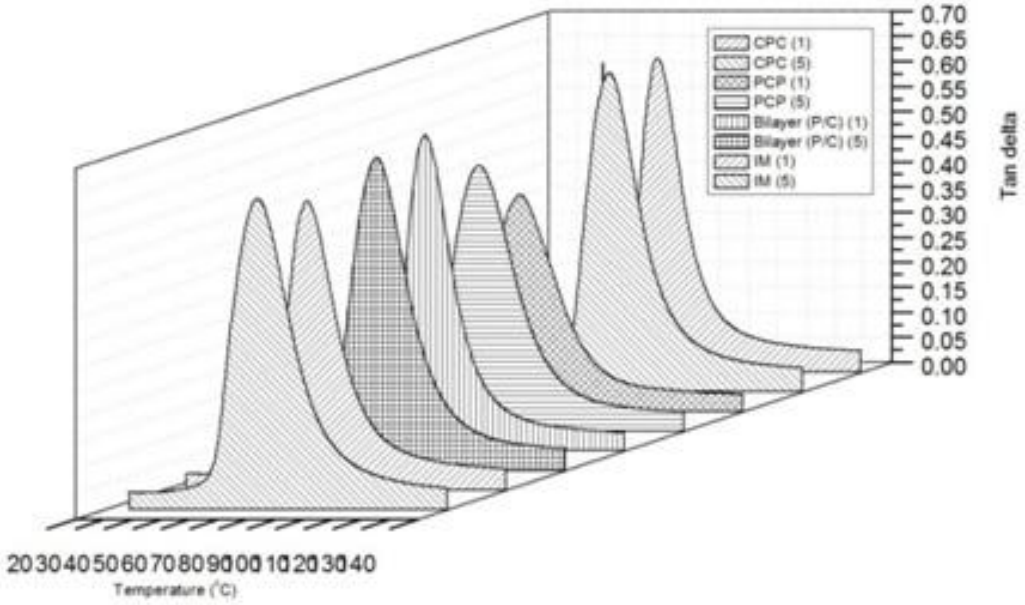

Fig. 4.42: Three-dimensional thermogram of different layered PALF/Coir hybrid materials

4.4.3.5 Activation Energy for Phase Transition

The energy required for the switching of phase from glassy state to rubbery state in the composite material can be easily and accurately measured by using the Arrhenius equation

$$f = f_0 \exp\left(-\frac{E}{RT}\right) \tag{4.7}$$

The calculated activation energy for the different layered hybrid epoxy specimens is mentioned in Table 4.20. The CPC and PCP hybrid composites have the highest and least value of activation energy.

Table 4.20: Activation energy for the different layered hybrid composites

Hybrid composites	Activation energy (kJ/mole)
CPC	40.54
PCP	9.179
Bilayer (P/C)	18.65
IM	20.45

4.4.3.6 Cole-Cole Plots

Cole-Cole plot signifies the fiber-matrix interaction at the interface and the heterogeneity or non-uniform diffusion of reinforcement in the polymeric system. The Cole-Cole plot of a homogenous system is reported as a smooth semi-circular arc whereas the heterogeneous system displays irregular or imperfect semicircles. The dielectric relaxation and viscoelastic response can never be predicted by a single tan δ peak. Therefore, it is particularly important to understand the structure-property relationship using Cole-Cole plot. Fig. 4.43 revealed the plots at a frequency of 1 Hz and 5 Hz. The Cole-Cole plot of EP was significantly changed and leads to a higher degree of imperfection by the addition of reinforcing fibers. This was evident in the greater heterogeneity among all hybrid composites. The curve of the PCP hybrid composite reveals the less heterogeneity in an epoxy thermoset matrix, proposed the poor fiber-matrix adhesion. The shape of the Cole-Cole curves for IM, CPC, and bilayer composites pointed towards the good fiber-matrix interfacial adhesion.

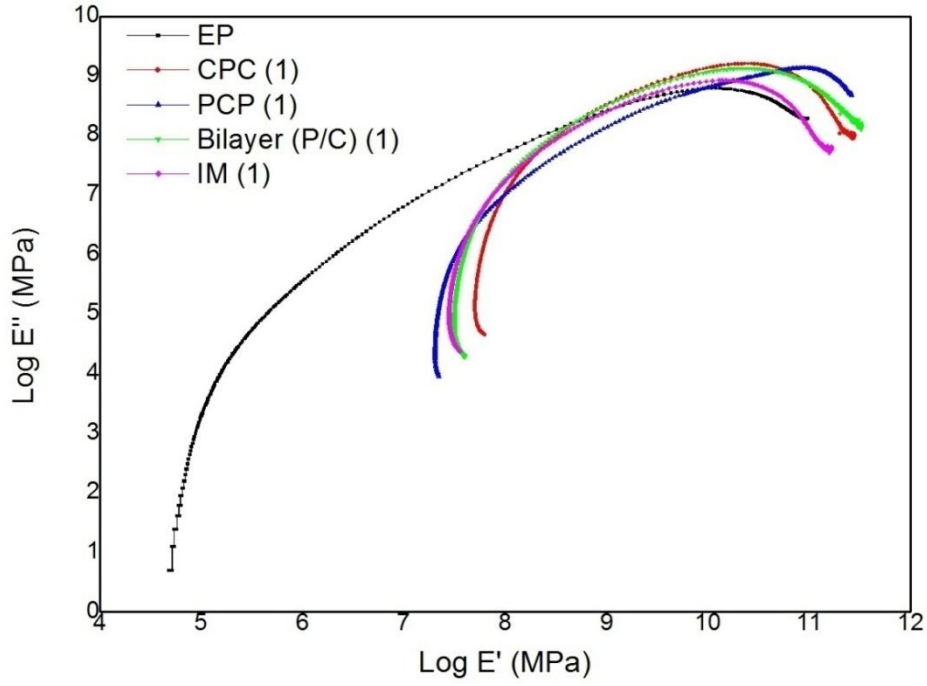

(a)

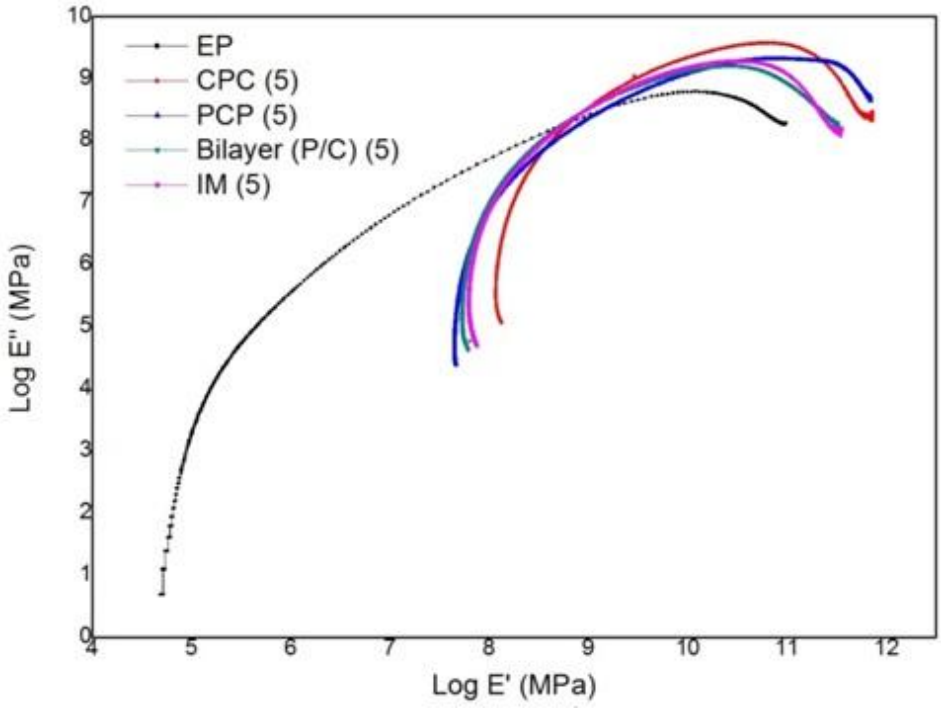

(b)

Fig. 4.43: Cole-Cole plots of neat epoxy and hybrid composites at a frequency of (a) 1 Hz (b) 5 Hz

4.5 Mechanical Characterization of PALF/COIR Strengthened Hybrid Material

To elevate the progressive utilization of NFRCs in structural applications, it is extremely required to heighten their properties by using the hybridization tool. In most of the cases, the performance of hybrid material strengthened with cellulosic

filaments is comparable to the synthetic fiber-reinforced composites. Therefore in this section, the mechanical and moisture sorption characteristics of hybridized PALF/COIR specimens have been explored. The biocomposite sheets consist of randomly oriented and intimately mixed short fibers (20 mm in length) were fabricated by employing the hand lay-up technique at 11 levels of COIR fiber loading (0, 10, 20, 30, 40, 50, 60, 70, 80, 90, 100 vol.%) with fixed total fiber content (40 vol.%). The designation and composition of developed specimens are shown in Table 4.21. The mechanical properties and water uptake behavior of various formulated composites have been studied according to ASTM standard. The total of four samples for each composite specimen was tested and their average values were reported.

Table 4.21: Designation and composition of PALF/COIR fiber reinforced hybrid epoxy composites

Designation	Composition
EP	Epoxy matrix (100 vol.%)
P100	Epoxy (60 vol.%) + Pineapple leaf fiber (40 vol.%) + Coir fiber (0 vol.%)
P90-C10	Epoxy (60 vol.%) + Pineapple leaf fiber (36 vol.%) + Coir fiber (4 vol.%)
P80-C20	Epoxy (60 vol.%) + Pineapple leaf fiber (32 vol.%) + Coir fiber (8 vol.%)
P70-C30	Epoxy (60 vol.%) + Pineapple leaf fiber (28 vol.%) + Coir fiber (12 vol.%)
P60-C40	Epoxy (60 vol.%) + Pineapple leaf fiber (24 vol.%) + Coir fiber (16 vol.%)
P50-C50	Epoxy (60 vol.%) + Pineapple leaf fiber (20 vol.%) + Coir fiber (20 vol.%)
P40-C60	Epoxy (60 vol.%) + Pineapple leaf fiber (16 vol.%) + Coir fiber (24 vol.%)
P30-C70	Epoxy (60 vol.%) + Pineapple leaf fiber (12 vol.%) + Coir fiber (28 vol.%)
P20-C80	Epoxy (60 vol.%) + Pineapple leaf fiber (8 vol.%) + Coir fiber (32 vol.%)
P10-C90	Epoxy (60 vol.%) + Pineapple leaf fiber (4 vol.%) + Coir fiber (36 vol.%)
C100	Epoxy (60 vol.%) + Pineapple leaf fiber (0 vol.%) + Coir fiber (40 vol.%)

4.5.1 Void and Density Measurement

The density of developed hybrid specimens is reported in Table 4.22. The density of epoxy thermoset was decreased with increase in void content (%) by the incorporation of lightweight cellulosic fibers. The compactness of a material is not only a function of the types of constituent elements but also depends on the interfacial bond strength between them. The density of hybrid composites was amplified with the increase of coir content. This was because of the higher density of

coir fiber as compared to the pineapple leaf fiber. The volume of emptiness was decreased by enlarge of coir fiber volume up to 50% of total fiber volume. Amongst all the developed composites, the P50-C50 composite exhibits the minimum value of void fraction. The addition of coir fiber beyond $0.5V_f$, the density of cavities and holes was increased, leading to an increase of void volume fraction. As compared to the pure PALF/Epoxy composite, the COIR/Epoxy composite has a higher density and lower value of void content. This was because of the higher density and porous surface morphology of coir fiber which leads to entrapment of viscoelastic matrix medium inside the coir fibers through capillary action. The presence of large number of voids may results in poor fatigue strength, immense potential to moisture sorption, and increased variation in mechanical properties. The void formation in polymer composites can be the result of poor compression during the consolidation of fiber-matrix composite in a mold.

Table 4.22: Void content, theoretical density, and true density of hybrid composites

Composites	Theoretical Density (g/cc)	Experimental density (g/cc)	Void content (%)
EP	1.3	1.25	3.84
P100	1.08	1.006	6.85
P90-C10	1.112	1.051	5.48
P80-C20	1.134	1.08	4.76
P70-C30	1.142	1.109	4.55
P60-C40	1.163	1.112	4.38
P50-C50	1.182	1.154	2.36
P40-C60	1.20	1.148	4.57
P30-C70	1.218	1.163	4.51
P20-C80	1.237	1.169	5.49
P10-C90	1.244	1.194	4.02
C100	1.253	1.16	5.69

4.5.2 Mechanical Properties

To quantify the reinforcing ability of PALF, COIR, and PALF/COIR hybrid fiber in an epoxy thermoset polymer resin, the mechanical tests were performed on pure pineapple-epoxy, coir-epoxy, and pineapple/coir fiber reinforced hybrid epoxy composites.

4.5.2.1 Tensile Behavior

The tensile characteristics of developed specimens are revealed in Fig. 4.44. The strength and stiffness of cured epoxy thermoset (shown in Table 3.1) were increased

by the incorporation of PALF and COIR fiber. The positive reinforcing effect of PALF and COIR fibers on tensile properties of an epoxy matrix can be observed in Table 4.23. It was observed that the PALF/Epoxy composite possesses 61.2% and 49.5% elevated strength and stiffness than the COIR/Epoxy composite respectively. This was because of the better inherent tensile properties of PALF than the COIR fiber. Moreover, the diameter and microfibrillar angle of PALF is less than that of COIR fiber that leads to the higher surface area and reinforcement effectiveness of PALF than COIR. The tensile response of COIR/Epoxy was improved by the hybridization with pineapple leaf fiber. Fig. 4.49 makes clear that even the addition of 0.2 V_f (20% of the total fiber volume) pineapple leaf fiber in coir-epoxy composite, the tensile strength was increased from 12.34 MPa to 22.97 MPa. From the tensile test, we can conclude that the P50-C50 hybrid composite containing relative volume fraction of two fibers PALF: COIR = 1:1 has maximum tensile strength and stiffness. The strength of PALF/Epoxy was improved by 16.74% by the incorporation of COIR fiber in equal volume content as PALF. This is due to the synergistic compatibility between pineapple leaf fiber and coir fiber and it is evident that the poor elongation at break (%) of PALF fiber can be overcome by the positive hybridization with high strain to failure COIR fiber. Moreover, the hybridization of a polymer matrix with optimum relative fiber volume improves the adhesion characteristics at the fiber surface. Previous research works [Sathishkumar *et al*. [151], C.A Kakou *et al*. [154], V.K Bhagat *et al*. [146], Siddika *et al.* [156]] were also reported the similar result. Fig. 4.49 depicts the diminution in strength of hybrid material with the further addition of PALF beyond 50% of total fiber volume ($V_f = 0.4V_c$). This was attributed to the poor dispersion of fiber and an increase of void spaces. At a very high concentration of PALF in hybrid composites, the processing is poor and fibers get agglomerated with an improper orientation which results in packing defects and rapid crack propagation.

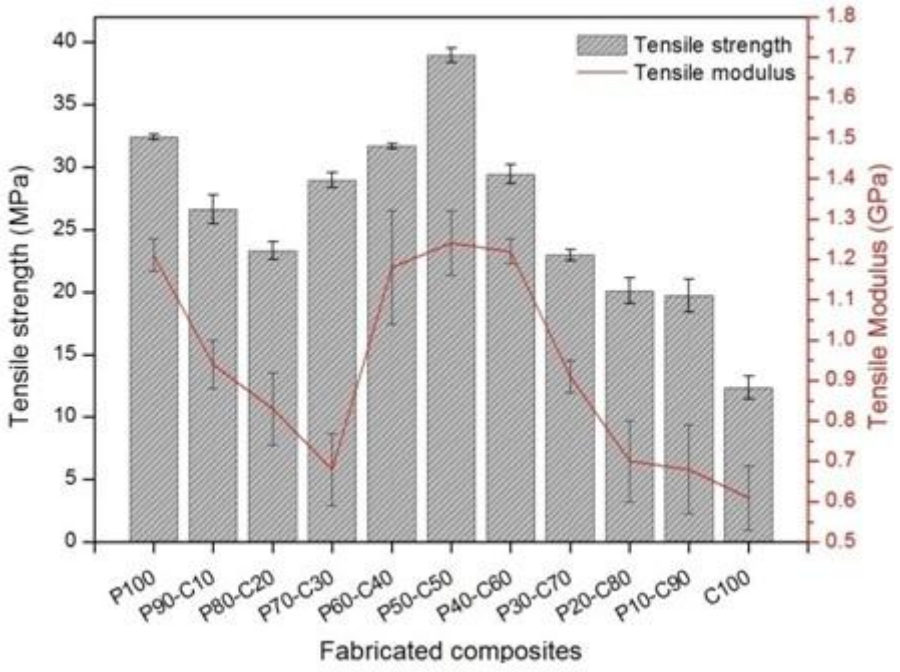

Fig. 4.44: Tensile properties of fabricated composites as a function of coir fiber volume content

4.5.2.2 Flexural Behavior

The bending strength of the developed hybrid specimens was determined using a Tinius Olsen H50KS, universal testing machine. Table 4.23 shows that the flexural strength of epoxy thermoset matrix was improved by the addition of PALF and COIR fibers. Fig. 4.45 depicts the variation in flexural properties of PALF/COIR hybrid material as a function of coir fiber volume fraction. The bending strength of pure COIR/Epoxy was significantly improved by the incorporation of pineapple leaf fiber, up to 50% of total fiber volume. The maximum flexural strength of 102.81 MPa is obtained for P50-C50 hybrid composite. The step-up of flexural strength by 23.44% and 77.03% was observed between the P100 to P50-C50 and C100 to P50-C50 composites respectively. This was because of the increased shearing resistance of fibers and effective stress transfer from the matrix to reinforcing fibers at this particular relative fiber volume content. Flexural strength is a combined effect of tensile, shear, and compressive strength. During the three-point bending test, the lower end of composite material experiences tensile stress, upper end faced compressive stress, and the axisymmetric plane is subjected to a shear load. The flexural strength of a composite material almost follows a similar pattern as tensile strength. Similar to tensile strength, the flexural strength is also decreased with the further loading of pineapple leaf fiber from 0.5 V_f to 0.9 V_f. The flexural strength

was rapidly amplified with the increase of PALF content from 0.3 V_f to 0.5 V_f. This behavior is due to the synergistic compatibility between PALF and COIR in P40-C60 and P50-C50 composites. Moreover, an optimum balance between strength, stiffness, and ductility was obtained as a result of a balanced combination of PALF and COIR fiber in a viscoelastic epoxy thermoset medium. However, the hybrid composite P60-C40 possess a higher value of flexural modulus than the P50-C50 composites. It was due to the little more accumulation of stiffer and stronger pineapple leaf fiber which results to restrict the plastic deformation.

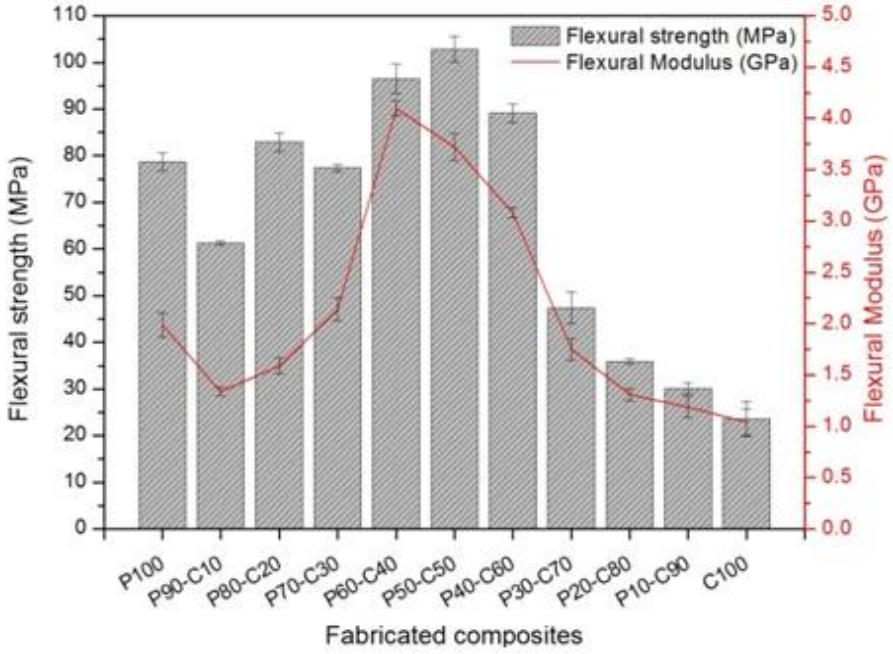

Fig. 4.45: Bending characteristics of fabricated specimens

Table 4.23: Percentage change in mechanical properties of epoxy matrix after the incorporation of PALF and COIR

Specimens	Tensile strength (MPa)^{IM}	Tensile modulus (GPa)^{IM}	Bending strength (MPa)	Bending modulus (GPa)	Impact strength (kJ/m^2)^{IM}
P100	65.63	60.33	67.86	23.11	57.29
P90-C10	58.15	48.93	58.7	14.17^{DC}	66.19
P80-C20	52.2	42.16	69.48	3.77	74.63
P70-C30	61.51	29.41	67.31	28.5	77.01
P60-C40	64.83	59.32	73.79	62.68	84.59
P50-C50	71.39	61.29	75.4	58.87	86.63
P40-C60	62.12	60.65	71.62	50.32	86.28
P30-C70	51.5	47.25	46.63	12.57	83.02
P20-C80	44.6	31.42	29.57	16.79^{DC}	84.96
P10-C90	43.53	29.41	16.09	28.57^{DC}	85.54
C100	9.72	21.31	7.11^{DC}	47.11^{DC}	86.11

^{IM} Improvement (%), ^{DC} Reduction (%)

4.5.2.3 Impact Strength

The toughness of a fiber strengthened composite is dependent on the nature of the constituent elements; internal structure and geometry of the composite; interfacial interaction between the reinforcing elements and the matrix; and experimental conditions. To study the effect of pineapple leaf fiber, coir fiber, and hybrid pineapple-coir fiber reinforcement on the impact performance of epoxy thermoset polymer, the fabricated composites were subjected to Izod Impact test as per ASTM D 256 standard. The impact strength of a virgin epoxy matrix (1.2 kJ/m^2) was significantly improved with the incorporation of PALF and COIR fiber (shown in Table 4.23). From Fig. 4.46, it can be reported that the pure COIR/Epoxy composite has 67.47% higher impact strength than that of pure PALF/Epoxy composite. This might be due to the inherent property of coir fiber (large value of spiral angle) and the dominating phenomena of "Fiber Pull-Out" than the "Fiber Fracture" in COIR/Epoxy composite. Moreover, the COIR fiber contains less cellulosic content with porous surface morphology which leads to good interfacial adhesion and wetting of COIR fiber with thermoset epoxy matrix by capillary action. Fig. 4.46 revealed that the strength of PALF/Epoxy was increased by the incorporation of COIR fiber. The hybrid composite (P50-C50) exhibits the maximum value of impact toughness (8.98 kJ/m^2) and it was due to the synergistic combination of properties. The low elongation to failure property of PALF/Epoxy composite can be overcome with the incorporation of high strain to failure-COIR fiber. The strength of a material under impact loading is a function of stiffness and ductility. In the case of PALF/COIR hybrid composite, the inherent strength of pineapple leaf fiber makes a good balance with the ductile nature of coir fiber which leads to the improvement in toughness of developed composites. Amongst all samples, the composite reinforced with an equal volume fraction of coir and pineapple leaf fiber (P50-C50) possess better mechanical properties than the others. This was because of the good interfacial adhesion between fiber and matrix that leads hamper the crack propagation along the interface. It is worth to note that the toughness indicates the amount of energy dissipated in the form of heat during the process of crack initiation, growth, and propagation. In relative to pure COIR/Epoxy composite, the hybrid composite (P40-C60) shows better impact strength. It was attributed to the positive hybridization effect with intercede result (C100<P40-C60>P50-C50). As expected, the hybrid

composites reinforced with optimum relative fiber volume content presents a better impact toughness than that of single fiber reinforced polymer composites.

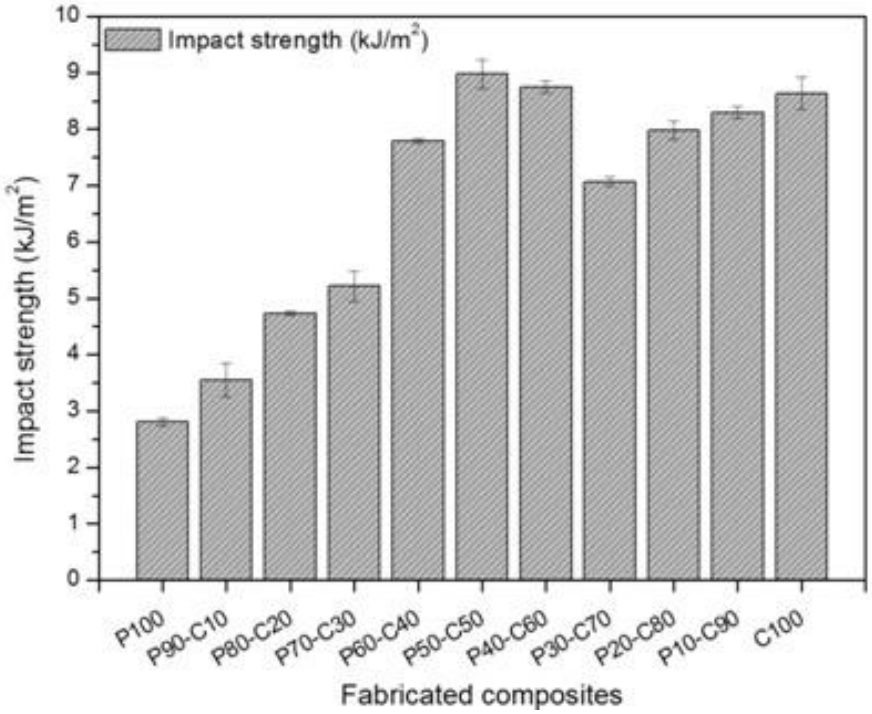

Fig. 4.46: Impact strength of fabricated specimens

4.5.2.4 Rockwell Hardness

The hardness of developed composites was determined using the Rockwell hardness tester and their results are reported in Table 4.24. The pure PALF/Epoxy composite exhibits higher hardness value than the hardness of single COIR/Epoxy composite. This was mainly due to the presence of high cellulose content in pineapple leaf fibers. From Fig. 4.47, it can be concluded that the hardness of a pure COIR/Epoxy was increased by the incorporation of PALF up to 0.6 V_f.. The P60-C40 hybrid composite shows the highest hardness than the other single and hybrid composites. The average value of hardness for P60-C40 hybrid material is 43.26 HRm. It is worth noting that the hardness of an epoxy matrix was significantly increased by the loading of cellulosic fibers.

Table 4.24: Summary of the results of the hardness test for developed PALF/COIR hybrid composites

Composites	Trial 1	Trial 2	Trial 3	Trial 4	Average
EP	32.68	36.14	33.42	32.08	33.58
P100	40.36	38.96	40.07	40.01	39.85
P90-C10	37.77	35.4	37.29	37.21	36.92
P80-C20	38.30	34.18	37.88	38.05	37.10
P70-C30	40.01	39.39	40.21	40.03	39.91
P60-C40	44.96	42.18	42.83	43.08	43.26
P50-C50	42.96	41.18	40.72	41.79	41.66
P40-C60	40.89	40.26	41.31	40.58	40.76
P30-C70	39.27	36.05	38.11	38.92	38.09
P20-C80	36.03	36	36.42	34.19	35.66
P10-C90	35.08	35.68	36.93	36.65	36.09
C100	37.11	36.84	39.95	39.08	38.25

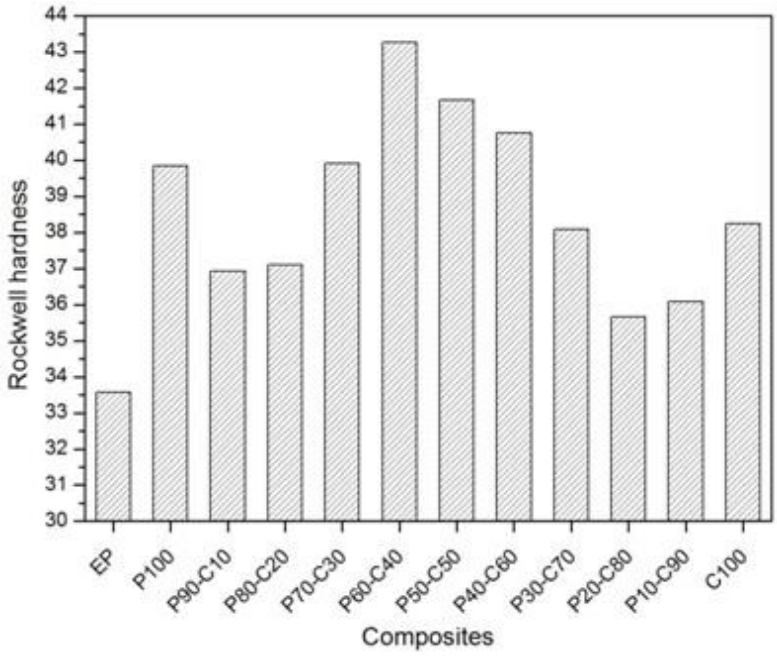

Fig. 4.47: Rockwell hardness of fabricated composites as a function of coir fiber volume content

4.5.3 Water Absorption

Water sorption characteristics of virgin epoxy, pineapple-epoxy, coir-epoxy, and pineapple-coir fiber hybrid epoxy composites were studied with the special reference of immersion time (in hrs) and the relative volume fraction of both types of cellulosic fiber. The water absorption curves for all formulated composites as a function of immersion time and the coir fiber content are illustrated in Fig. 4.48. The virgin thermoset resin absorbs the least amount of water among all the composite

specimens. The moisture uptake ability and dimensional instability of thermoset polymer was increased with the incorporation of cellulosic fibers. The diffusion of water molecules in polymers is due to the presence of micro-gaps and cavities between polymeric chains. According to Flory's proposed theory, the water diffusion in polymer and polymer-based composites are two-step processes. In the 1st step, the penetrant diffuses rapidly to induce elasticity in polymer chains and in the 2nd step, the saturation level (equilibrium absorption) was achieved that leads to the polymer chain relaxation. Fig. 4.48 (a) clearly shows that all the composites absorb water sharply up to 50 hr and reached to the saturation point at 120 hr. The maximum water absorption values (in %) of all the fabricated composites are reported in Table 4.25. It was observed that the pure pineapple-epoxy composite absorbs more water as compared to the coir fiber-epoxy composite. This was attributed to the presence of a large number of -OH functional group on the shell of PALF. Water uptake in NFRC's depends on the inherent sorption power of individual fibers and matrix, fiber length and content, fiber orientation, matrix cracking, and fiber-matrix interfacial adhesion. From Fig. 4.48 (b), it can be concluded that the hybridization of a PALF-Epoxy composite with coir fiber leads to the improvement in resistance to water diffusion. The hybrid composite (P50-C50) has the least affinity to absorb water because of excellent structural integrity, good fiber-matrix interfacial adhesion, and less number of voids, cavities, and micro-pores. In comparison to the pure pineapple leaf fiber-epoxy and coir fiber-epoxy composite, the hybrid composite (P50-C50) absorbs 62% and 32% less amount of water respectively. It indicates that the hybrid fiber reinforcement in the polymer matrix yields more packed structure which leads to the dimensionally stable high strength composite. The penetration of water molecules through the composite materials is mainly occurring by the capillary drive through cracks, voids, and flaws at the interfacial region between reinforcement and resin. The percent water absorption of single coir fiber reinforced epoxy composite is significantly reduced by hybridization with $0.2V_f$ content of pineapple leaf fiber. This may be due to the improved fiber-matrix interaction and better-ordered dispersion of fiber in the matrix resin. In addition to the polymer and fiber swelling, the delamination of the interlayer between the fibers can also be the cause of free voids that leads to an important mechanism for water absorption in the hybrid composites. To understand the kinetics and mechanism of water absorption, the experimental data are fitted into the following generalized equation

$$Log\frac{M_t}{M_m} = Log(k) + nLog(T) \quad (4.8)$$

where M_t and M_m are the water absorption at time t and saturation level respectively, k is a constant parameter and n is the diffusion coefficient. The water sorption constants n and k define the mechanism of water diffusion and the kind of interaction between polymer and water respectively. According to the value of n (n<0.5, n=0.5, 0.5<n<1, n>1), the water diffusion mechanism can be classified into less Fickian, Fickian, Anomalous, and Non-Fickian mechanism respectively. From Table 4.25, we can report that all the composites follow a less Fickian water diffusion mechanism.

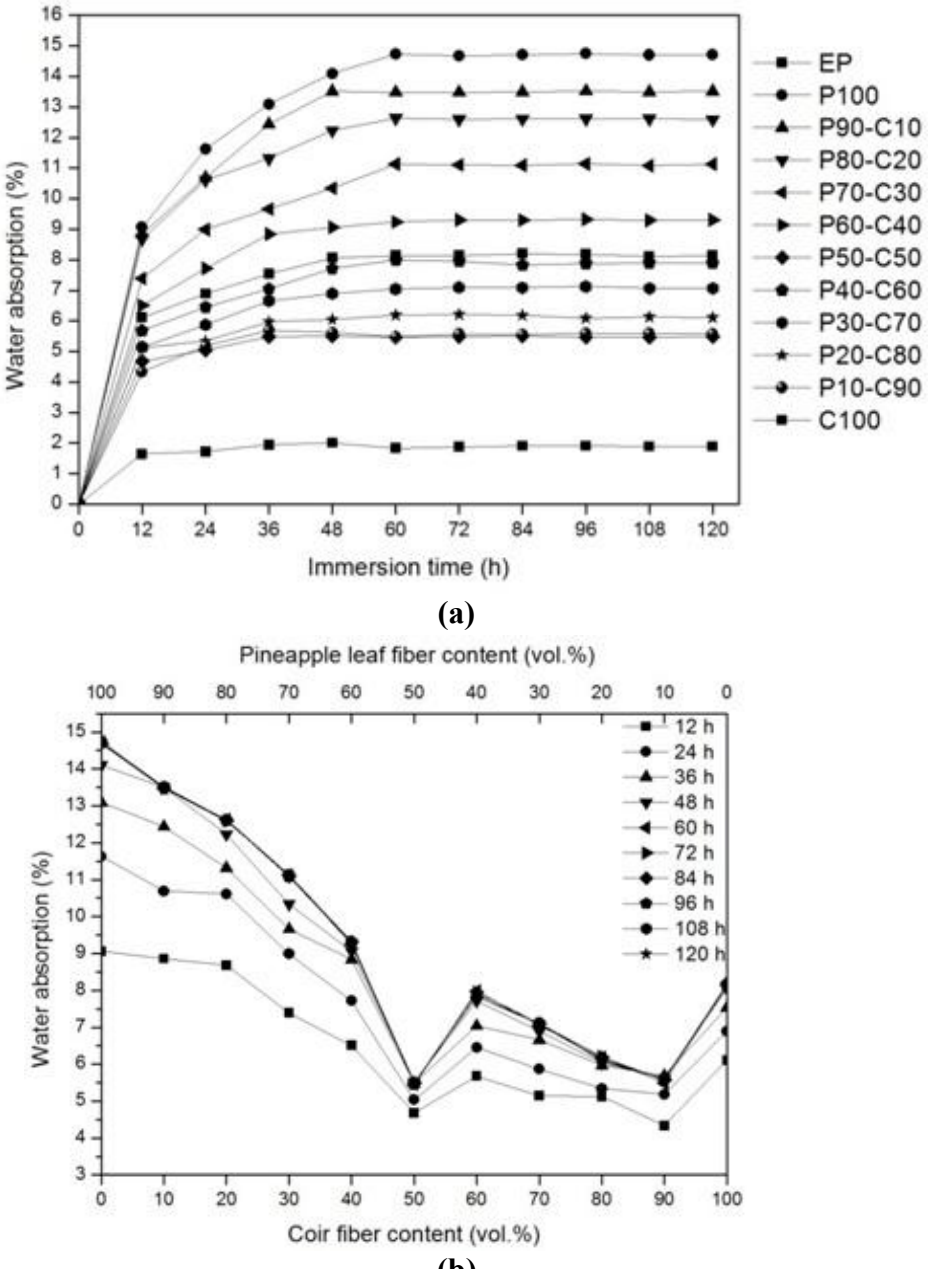

Fig. 4.48: Water absorption behavior of fabricated composites as a function of (a) immersion time (b) coir fiber volume content

Table 4.25: Maximum water absorption, water sorption constants, and diffusion mechanism of the fabricated composites

Composites	Max. WA (%)	Diffusion exponent (n)	Intercept (k)	R^2	Type of diffusion mechanism
EP	2.01	0.14712	-0.65441	0.85839	Less Fickian diffusion
P100	14.75	0.1374	-0.61104	0.84521	
P90-C10	13.52	0.083	-0.37181	0.77271	
P80-C20	12.64	0.088	-0.38882	0.59984	
P70-C30	11.14	0.13	-0.55484	0.84624	
P60-C40	9.33	0.057	-0.25739	0.43924	
P50-C50	5.51	0.20	-0.8951	0.84861	
P40-C60	7.99	0.18	-0.78488	0.8108	
P30-C70	7.12	0.16	-0.68983	0.85101	
P20-C80	6.21	0.176	-0.78915	0.89529	
P10-C90	5.69	0.148	-0.65428	0.81936	
C100	8.2	0.062	-0.27329	0.69185	

4.6 Biodegradability of PLF/COIR Fiber Reinforced Hybrid Epoxy Composites

Environmental policies set the boundary conditions for industries and commercial market regarding the maximum utilization of biodegradable material. In this context, the current section deals with the effect of relative fiber volume content and alkaline treatment of cellulosic fibers on the biodegradability of PALF/COIR filled epoxy composites in the natural soil environment. To accomplish the desired objectives, a total of 23 biocomposite specimens (untreated and alkali-treated) has been developed by hand lay-up molding technique and tested for tensile, flexural, impact, and weight loss properties according to ASTM standard. The description of developed specimens is reported in Table 4.26. The total of four samples for each composite specimen was tested and their average values were reported.

Table 4.26: Designation and composition of developed composites

Designation	Composition
EP	Epoxy matrix (100 vol.%)
P100	Epoxy (60 vol.%) + untreated pineapple leaf fiber (40 vol.%) + untreated coir fiber (0 vol.%)
P90-C10	Epoxy (60 vol.%) + untreated pineapple leaf fiber (36 vol.%) + untreated coir fiber (4 vol.%)
P80-C20	Epoxy (60 vol.%) + untreated pineapple leaf fiber (32 vol.%) + untreated coir fiber (8 vol.%)
P70-C30	Epoxy (60 vol.%) + untreated pineapple leaf fiber (28 vol.%) + untreated coir fiber (12 vol.%)
P60-C40	Epoxy (60 vol.%) + untreated pineapple leaf fiber (24 vol.%) + untreated coir fiber (16 vol.%)
P50-C50	Epoxy (60 vol.%) + untreated pineapple leaf fiber (20 vol.%) + untreated coir fiber (20 vol.%)
P40-C60	Epoxy (60 vol.%) + untreated pineapple leaf fiber (16 vol.%) + untreated coir fiber (24 vol.%)
P30-C70	Epoxy (60 vol.%) + untreated pineapple leaf fiber (12 vol.%) + untreated coir fiber (28 vol.%)
P20-C80	Epoxy (60 vol.%) + untreated pineapple leaf fiber (8 vol.%) + untreated coir fiber (32 vol.%)
P10-C90	Epoxy (60 vol.%) + untreated pineapple leaf fiber (4 vol.%) + untreated coir fiber (36 vol.%)
C100	Epoxy (60 vol.%) + untreated pineapple leaf fiber (0 vol.%) + untreated coir fiber (40 vol.%)
P100 (T)	Epoxy (60 vol.%) + NaOH treated pineapple leaf fiber (40 vol.%) + NaOH treated coir fiber (0 vol.%)
P90-C10 (T)	Epoxy (60 vol.%) + NaOH treated pineapple leaf fiber (36 vol.%) + NaOH treated coir fiber (4 vol.%)
P80-C20 (T)	Epoxy (60 vol.%) + NaOH treated pineapple leaf fiber (32 vol.%) + NaOH treated coir fiber (8 vol.%)
P70-C30 (T)	Epoxy (60 vol.%) + NaOH treated pineapple leaf fiber (28 vol.%) + NaOH treated coir fiber (12 vol.%)
P60-C40 (T)	Epoxy (60 vol.%) + NaOH treated pineapple leaf fiber (24 vol.%) + NaOH treated coir fiber (16 vol.%)
P50-C50 (T)	Epoxy (60 vol.%) + NaOH treated pineapple leaf fiber (20 vol.%) + NaOH treated coir fiber (20 vol.%)
P40-C60 (T)	Epoxy (60 vol.%) + NaOH treated pineapple leaf fiber (16 vol.%) + NaOH treated coir fiber (24 vol.%)
P30-C70 (T)	Epoxy (60 vol.%) + NaOH treated pineapple leaf fiber (12 vol.%) + NaOH treated coir fiber (28 vol.%)
P20-C80 (T)	Epoxy (60 vol.%) + NaOH treated pineapple leaf fiber (8 vol.%) + NaOH treated coir fiber (32 vol.%)
P10-C90 (T)	Epoxy (60 vol.%) + NaOH treated pineapple leaf fiber (4 vol.%) + NaOH treated coir fiber (36 vol.%)
C100 (T)	Epoxy (60 vol.%) + NaOH treated pineapple leaf fiber (0 vol.%) + NaOH treated coir fiber (40 vol.%)

4.6.1 Mechanical Properties

4.6.1.1 Tensile Strength

The deviation in strength of formulated composites as a function of burial time is depicted in Fig. 4.49. The thermoset matrix exhibits a very small decrement in tensile strength (about 2.35 MPa) after the 110 days of burial in the natural soil. This was credited to the cross-connected structure of a thermoset resin. The rate of reduction and total loss of tensile strength in the virgin epoxy matrix were increased with the incorporation of cellulosic fibers (PALF and COIR). It was due to the inherent characteristic of cellulosic fibers that they can biodegrade by the action of microorganisms. H. Kim *et al*. [254] also reported that the agro-flour filled PBS composite exhibits a higher rate of reduction in tensile strength than the unfilled PBS matrix. Fig. 4.49 revealed that the strength of pure PALF-Epoxy was reduced rapidly than the COIR-Epoxy in the natural soil environment. It can be explained by the fact that the COIR fiber contains high lignin content (40-45%) which provides higher stability against the attack of microorganisms. In all the formulated biocomposites, the natural fibers were hydrolyzed significantly which results in poor linkage among the reinforcement and polymeric resin. From Fig. 4.50, we can conclude that the hybrid composites possess a greater reduction in tensile strength as compared to the

pure PALF-Epoxy composite. This negative effect of hybridization in the natural soil environment is due to the penetration of water molecules at the interface between fiber-matrix and fiber-fiber which results in an easy fiber pull-out under mechanical loading conditions. The hybrid composite (P60-C40) drops 70% of tensile strength in the natural soil. This was due to the attack of microorganisms and the hydrolysis of lignocellulosic fibers. It can be observed that the NaOH treated Coir-Epoxy composite possess a higher rate of reduction in tensile strength than the untreated one. It was due to the subtraction of the lignin compound which results in rough and porous morphology of the surface (Fig. 4.51). Amongst all the developed composites, the NaOH treated P10-C90 possesses maximum reduction of tensile strength (75.12%) in the natural soil environment. However, the alkaline treated P80-C20 hybrid composite exhibits a 13% lower reduction in tensile strength than the unprocessed one. In most of the untreated and alkali-treated composites, the tensile strength of biocomposites was reduced significantly after 30 days of soil burial due to the substantial hydrolysis of cellulosic fibers. It is worth to note that the P60-C40 and P50-C50 composites exhibit a high rate of tensile strength reduction after 30 days.

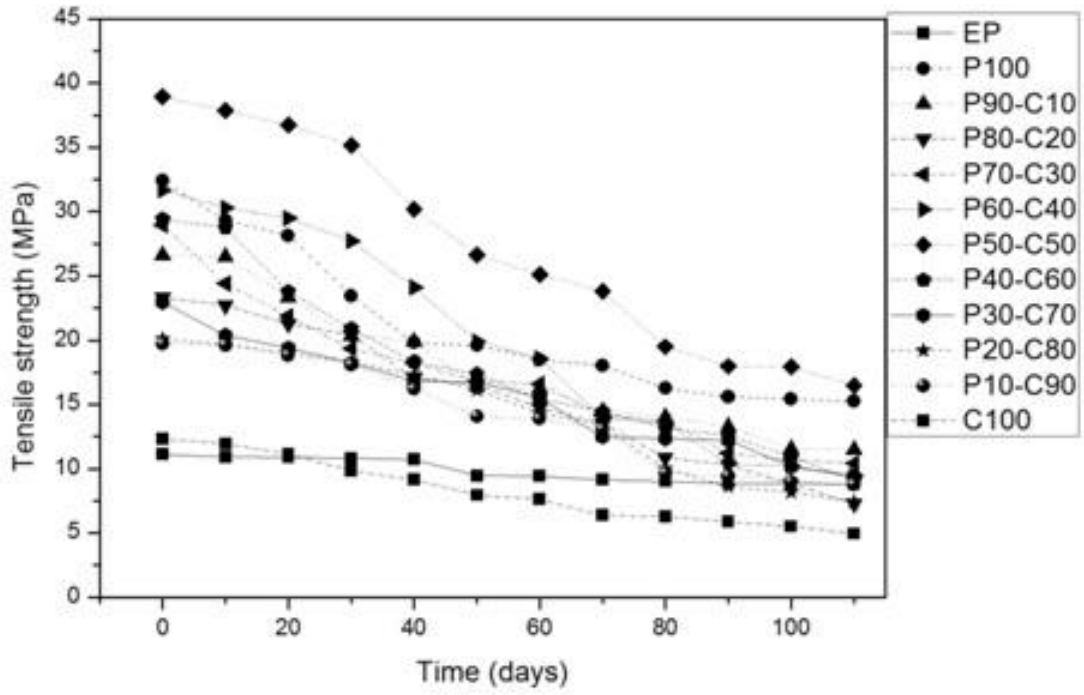

(a)

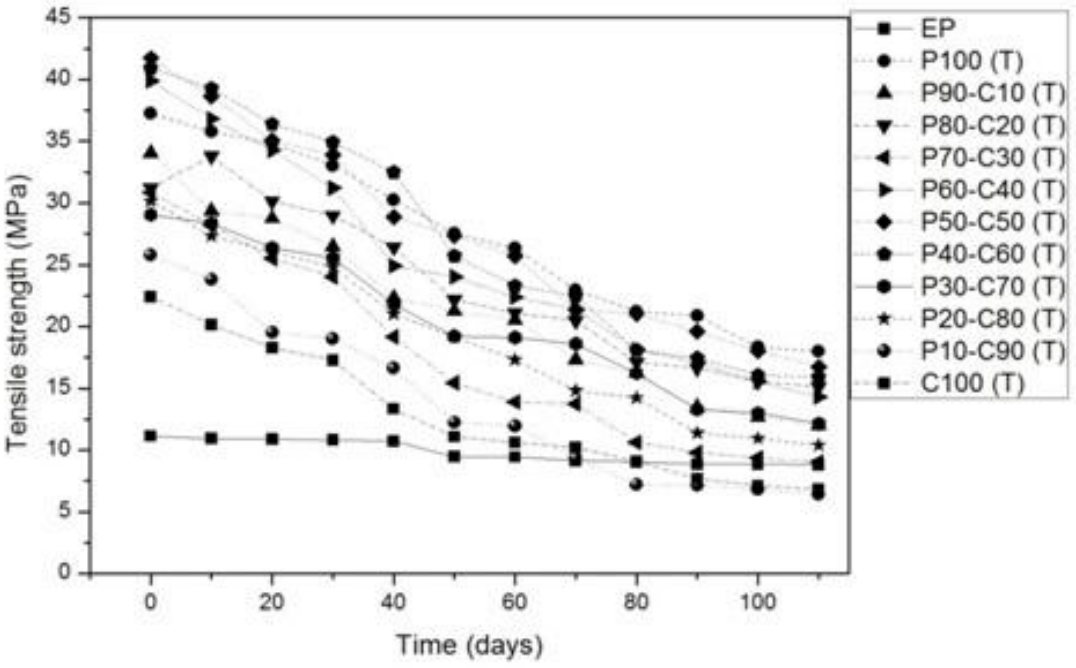

(b)

Fig. 4.49: Effect of the natural soil burial time on the tensile strength of (a) untreated biocomposites (b) alkali-treated biocomposites

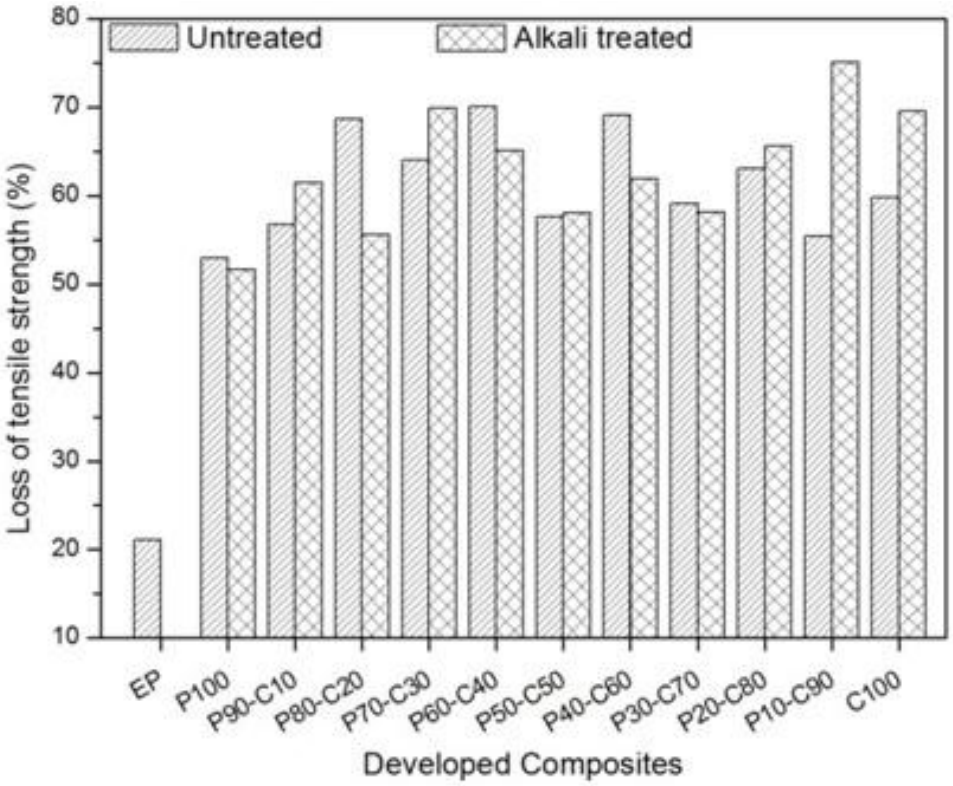

Fig. 4.50: Comparison of the maximum loss in tensile strength after 110 days of burial in the natural soil environment

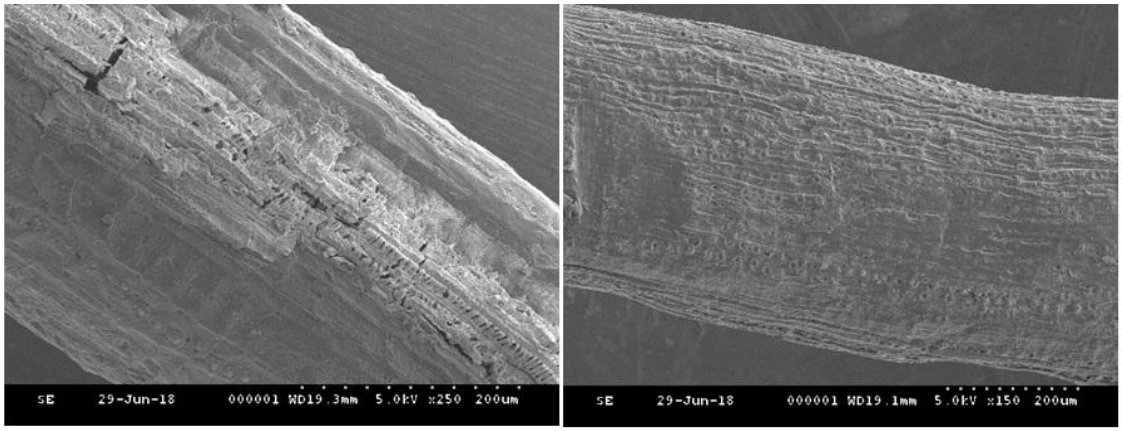

(a) **(b)**

Fig. 4.51: Surface morphology of (a) untreated COIR (b) 4% NaOH treated COIR

4.6.1.2 Flexural Strength

Fig. 4.52 (a)-(b) illustrates the bending strength of raw and mercerized biocomposites in response to natural soil burial time. It was observed that the bending strength of an epoxy thermoset was increased considerably after the addition of reinforcing PALF and COIR fibers. However, the fiber-reinforced composites exhibit a higher rate of reduction in flexural strength than the unfilled epoxy thermoset. This was attributed to the easy and selective hydrolysis of cellulosic fibers; entrapment of water molecules inside the pores, cavity, and an interfacial region between fiber and matrix; anisotropic nature of composites; scission and depolymerization of cellulosic chains; and localized stress concentration in micropores. The pure COIR fiber-reinforced composite possesses a slow rate of diminution in bending strength than the PALF-Epoxy. The bending strength of a hybrid material in the natural soil environment was reduced rapidly with the increase of coir fiber content. Amongst all the untreated hybrid composites, the P10-C90 one exhibits maximum reduction (%) in flexural strength. It was attributed to the poor stress transfer from PALF to COIR fiber and the presence of a large number of micropores and cavities at this particular composition which results in the absorption and adsorption of water molecules by capillary action. From Fig. 4.52, we can conclude that most of the composites revealed an accelerated rate of reduction after 30 days of burial in the natural soil environment. It is worth to note that the strength of developed specimens was reduced substantially in burial state after an alkaline treatment of cellulosic fibers (Fig. 4.53). This finding was because of the elimination of waxy substances from the surface of natural fibers. The flexural strength of NaOH treated P50-C50 composite

was reduced significantly after 10 days of burial in natural soil. Amongst all the developed composites, the alkaline treated Coir-Epoxy composite exhibits a maximum reduction in flexural strength after 110 days of burial. This was because of the significant removal of highly stable lignin compound after the mercerization process.

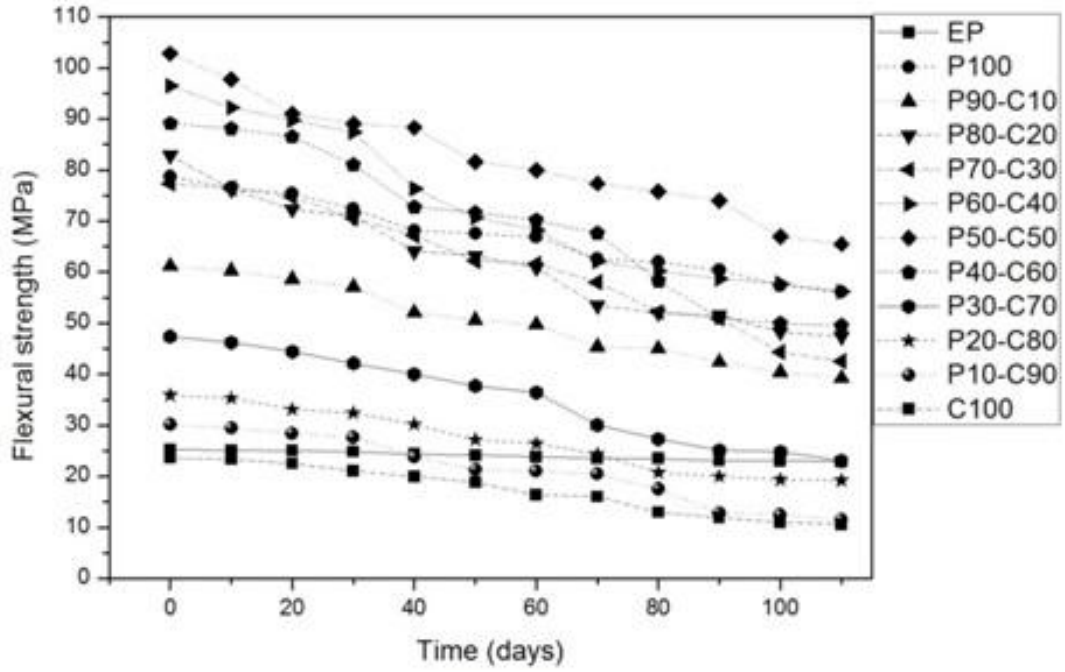

(a)

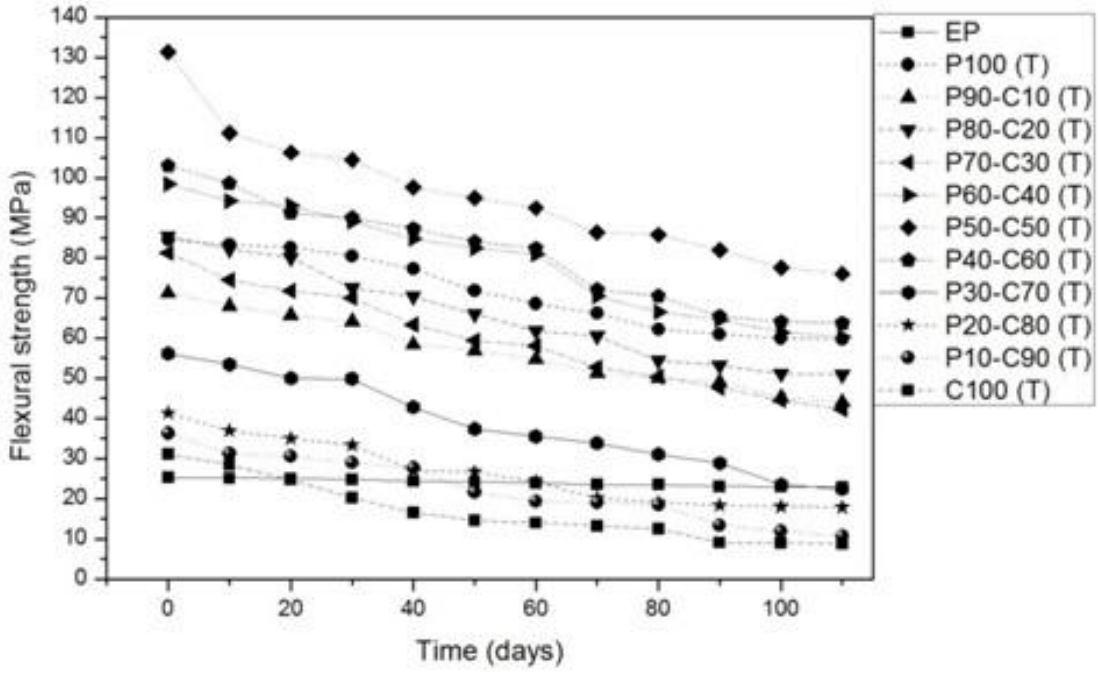

(b)

Fig. 4.52: Effect of the natural soil burial time on the flexural strength of (a) untreated biocomposites (b) alkali-treated biocomposites

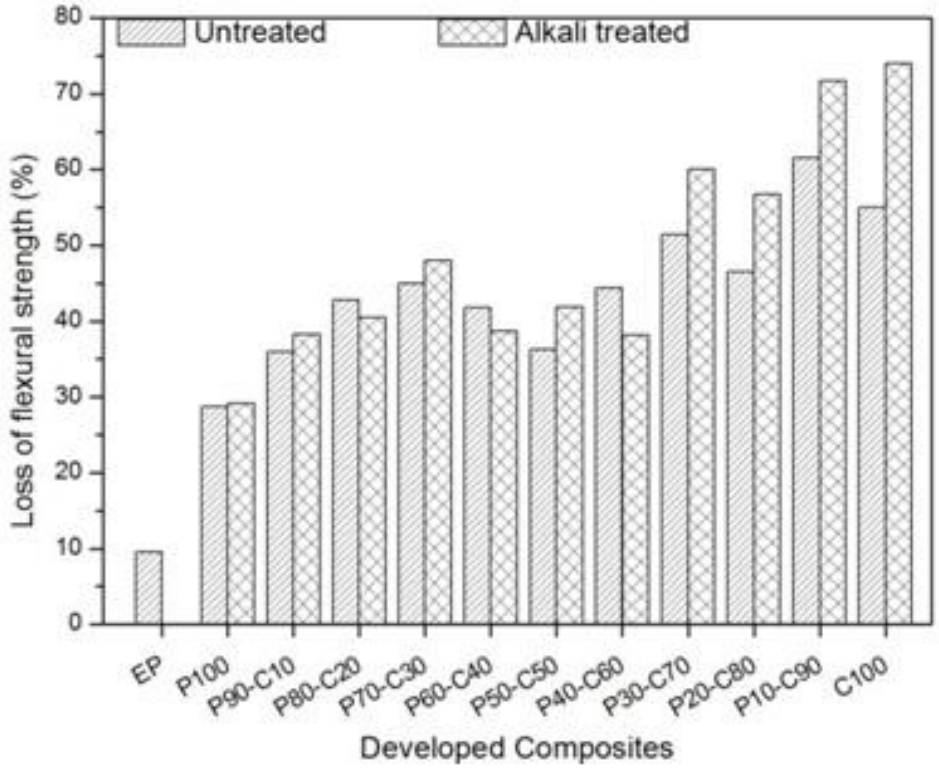

Fig. 4.53: Comparison of the maximum loss in flexural strength after 110 days of burial in the natural soil environment

4.6.1.3 Impact Strength

Fig. 4.54 (a)-(b) depicts the impact strength of formulated composites (untreated and alkali-treated) as a special function of natural soil burial time. The brittleness of an epoxy thermoset was reduced significantly by the incorporation of PALF and COIR fibers. The impact strength of developed composites was decreased in the natural soil environment. This kind of behavior is attributed to the entrapment of water molecules at the interfacial region which leads to easy and smooth fibers pull-out from the viscoelastic medium. Irrespective of the chemical composition of PALF and COIR fibers, the pure Coir-Epoxy composite exhibits a higher rate of reduction in impact strength after the 60 days of burial than that of the PALF-Epoxy composite. However, the total loss (%) in impact strength of the Coir-Epoxy composite was 15.9% less than the PALF-Epoxy (Fig. 4.55). It can be defined by the excellent characteristics of coir fiber to resist microbial and fungus attack. Fig. 4.54 revealed that the impact strength of hybrid material was reduced rapidly with the enhance of coir fiber content. This was attributed to the large penetration of water molecules in the interfacial region between coir fiber and the matrix resin. Amongst all the untreated hybrid composites, the P20-C80 revealed the maximum loss (%) of impact

strength in the natural soil environment. This was because of the localized stress concentration, substantial scission of polymeric chains, selective hydrolysis of reinforcing fibers, and avulsion of fiber bundles into individual fibers. From Fig. 4.55, we can conclude that the alkali treatment imparts a positive impact on the strength of a pure PALF-Epoxy. This was because of the removal of -OH group after the mercerization process which leads to a substantial reduction in the hydrolysis of pineapple leaf fiber. However, the NaOH treated COIR-Epoxy composite exhibits a higher rate of reduction in impact strength than the untreated one. It was due to the change in the chemical composition of coir fiber (removal of highly durable and stable lignin component) after alkaline treatment. From Fig. 4.54 (a)-(b), we can also conclude that the rate of reduction in impact strength was more accelerated after the 30 days of burial in the natural soil environment. The overall discussion revealed that the mechanical strength was reduced significantly due to the action of microorganisms.

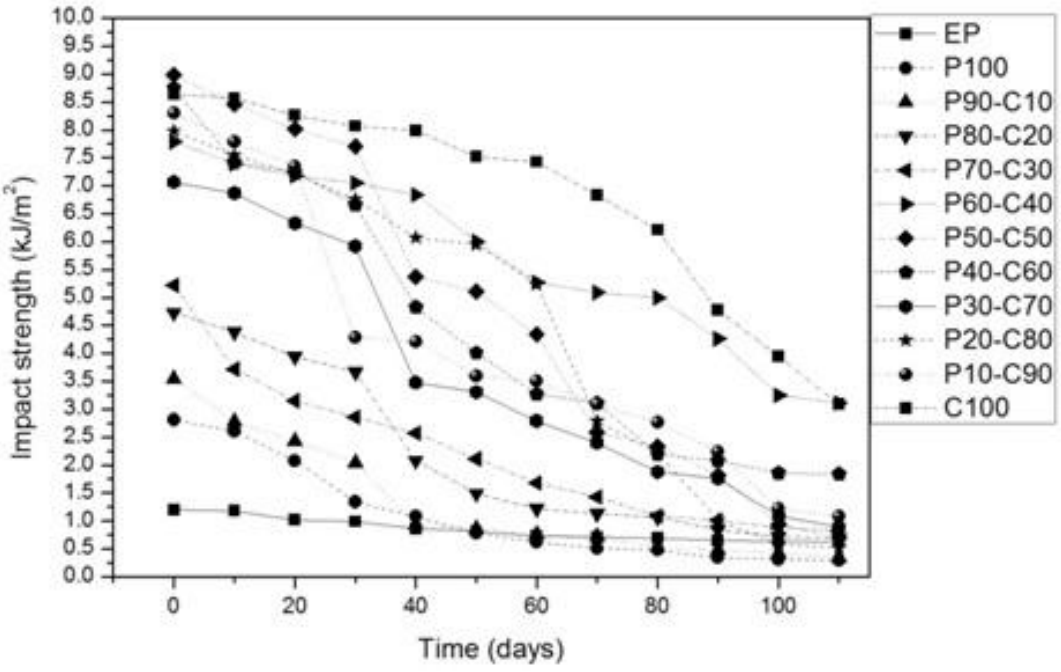

(a)

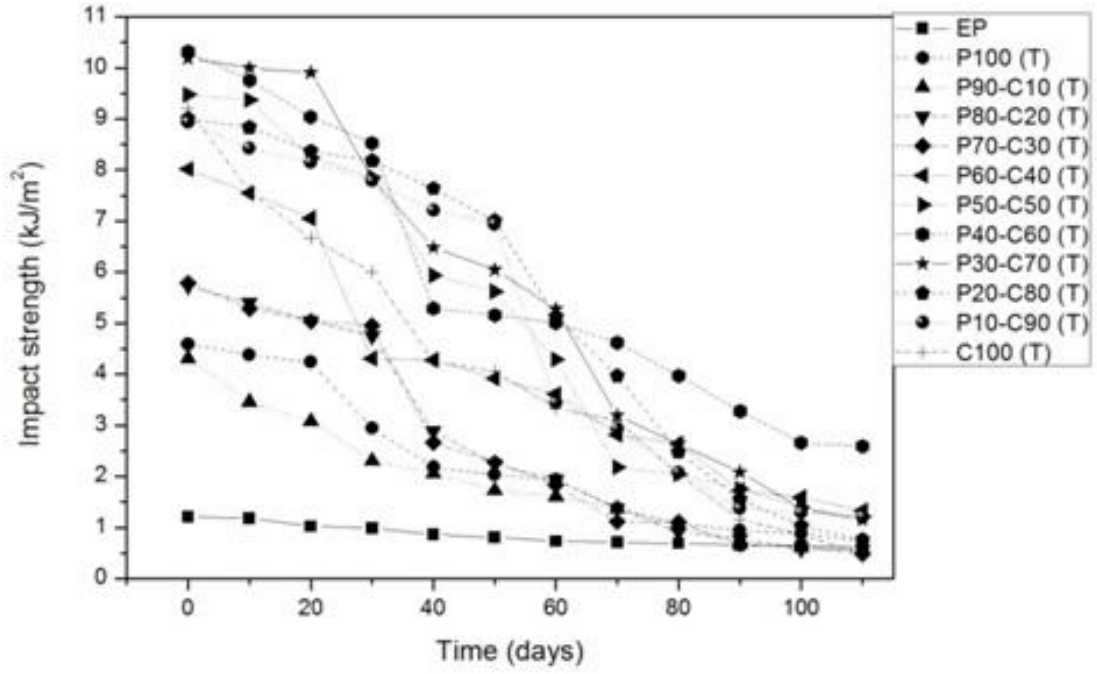

(b)

Fig. 4.54: Effect of the natural soil burial time on the impact strength of (a) untreated biocomposites (b) alkali-treated biocomposites

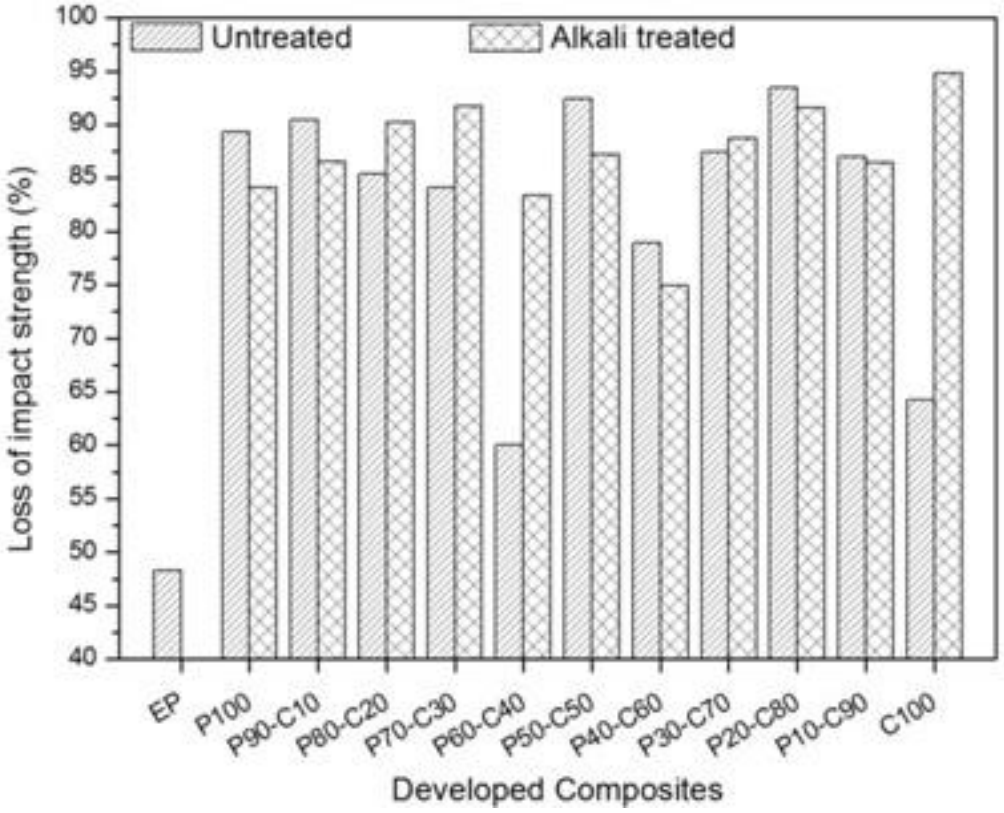

Fig. 4.55: Comparison of the maximum loss in flexural strength after 110 days of burial in the natural soil environment

4.6.2 Mass Loss

The mass loss of biocomposites in the response of natural soil burial time is shown in Fig. 4.56 respectively. The mass loss (%) of an epoxy thermoset was increased considerably in the natural soil environment after the incorporation of PALF and COIR fibers (As expectedly). Amongst all the developed materials, the pure PALF-Epoxy composite exhibits a maximum percentage of weight loss in the natural soil environment (Fig. 4.57). This result is attributed to the substantial hydrolysis of PALF which leads to the depolymerization and chain scission of cellulosic material into small monomer units. It was observed that the weight loss percentage of hybrid composites was reduced with the increase of coir fiber content. This was because of the high resisting power of COIR fiber to biodegrade. The coir fiber consists of high lignin content (40-45%) which makes it and their composites to resist the attack of bacteria, fungi, and microorganisms. Fig. 4.56 depicts that the single coir fiber-reinforced composite exhibits the least biodegradability in the natural soil environment. Moreover, the total mass loss (%) in the Coir-Epoxy composite was 51.1% less than that of the pure PALF-Epoxy composite. This result was attributed to the presence of high cellulose content in PALF which results in easy and fast absorption of water molecules. The mechanism of bio-degradation involves penetration of water molecules, breakage of strong covalent bonds, and deterioration of hemicellulose & cellulose by the action of microorganisms. Bharat K.N *et al*. [126] also reported that the biodegradation involves bond scission reactions in the backbone of polymers. The alkali-treated fiber-reinforced composites have a higher rate of biodegradation than the untreated. However, the NaOH treated composites (P100, P90-C10, and P80-C20) possess lower mass loss (%) than the untreated ones (Fig. 4.57) and it was due to the excess removal of –OH group after mercerization.

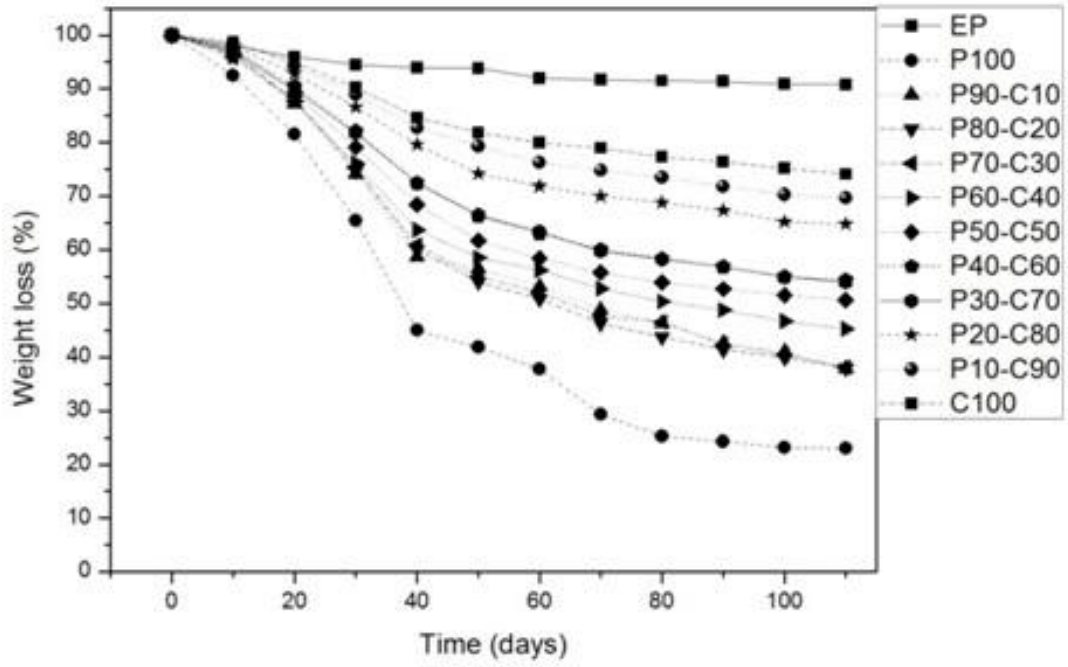

(a)

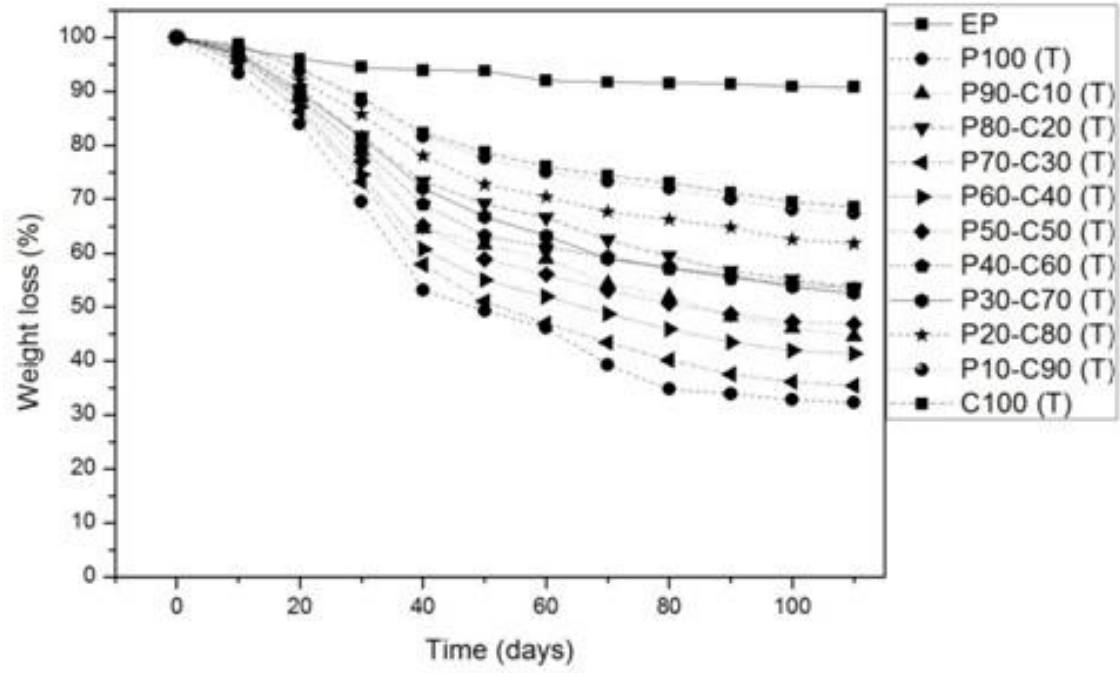

(b)

Fig. 4.56: Percentage weight loss of (a) untreated biocomposites (b) alkali-treated biocomposites in natural soil

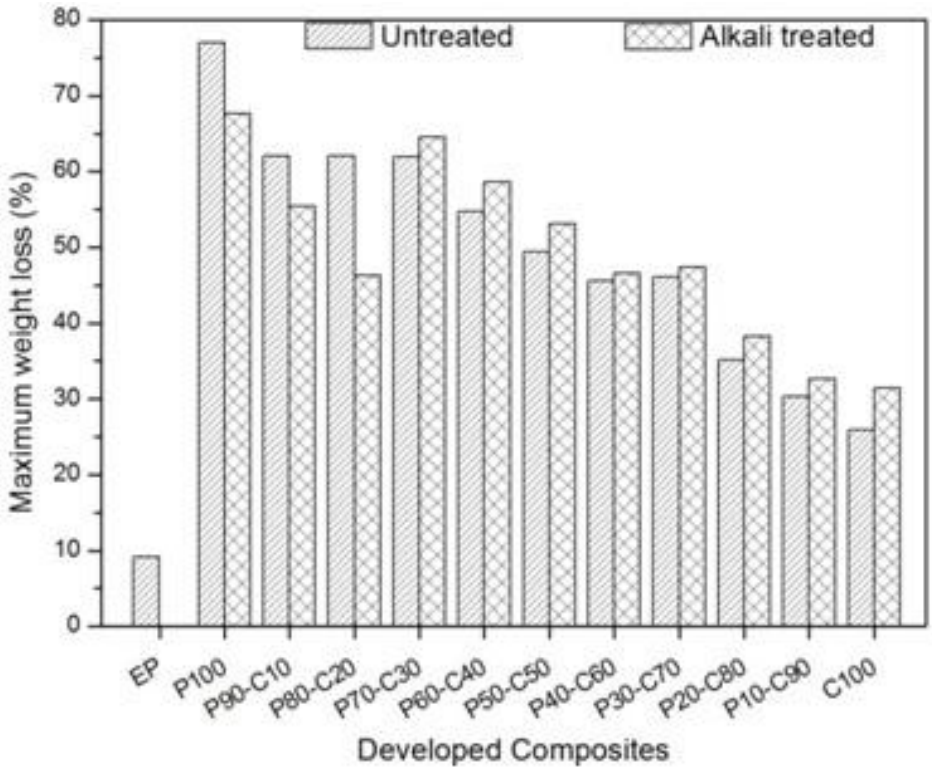

Fig. 4.57: Comparison of the maximum weight loss after 110 days of burial in the natural soil environment

CHAPTER 5 - APPLICATION OF THE DEVELOPED HYBRID COMPOSITE IN AUTOMOBILE SECTOR

The overall car creation rate is expanding and is assessed to arrive at 76 million vehicles every year by 2020. Government guidelines are driving vehicle makers to think about the ecological effect of their creation and conceivably move from the utilization of manufactured materials to the utilization of agro-based materials. It is assessed that a 25% decrease in car weight would be proportionate to saving 250 million barrels of unrefined petroleum. Therefore, it is necessitated that the makers will consider the expanding utilization of common filaments and bio-composites in their new items. In this regard, this chapter discusses the potential applications of cellulosic fiber based material in the automobile sector. The properties of a developed material were compared with typical bumper beam material and other biocomposites.

5.1 Application of a PALF/COIR Hybrid Material for Passenger Car Bumper Beam

This section examines the potential of a developed hybrid material for the passenger car bumper beam by comparing its properties with a typical bumper beam material called GMT. Fig. 5.1 compares the mechanical properties of P50-C50 hybrid material with GMT. It was observed that the mechanical properties of untreated PALF/COIR hybrid material are less than the GMT. This was because of the presence of voids and cavities which act as a stress raiser and leading to the reduction in mechanical strength and stiffness. Therefore, the current hybrid material needs some modifications to select in structural applications. To reduce void content and achieving strong bonding between ingredients, the SMC process can be employed instead of a hand layup technique.

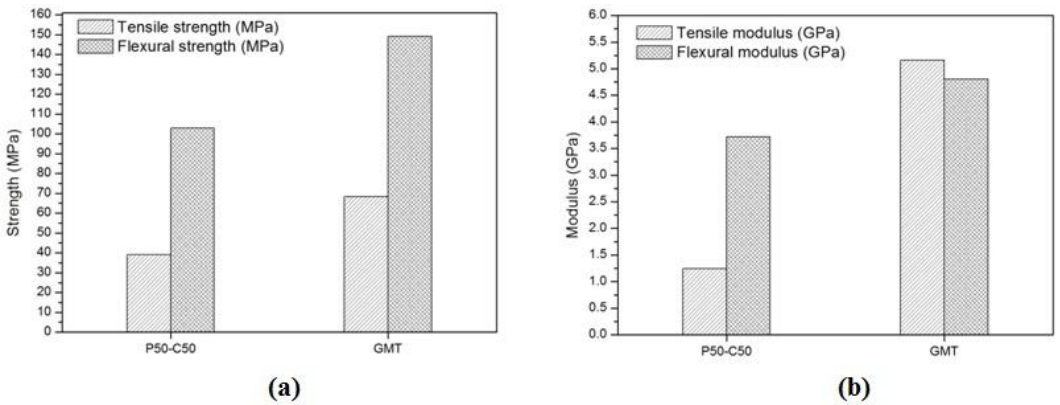

(a) (b)

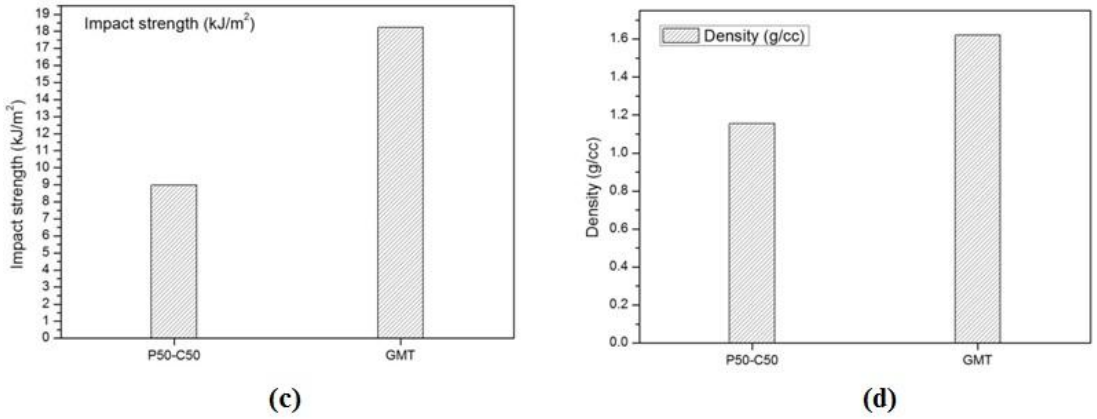

Fig. 5.1: Comparison between P50-C50 hybrid composite and GMT material in respect of (a) Tensile and Flexural strength (b) Tensile and Flexural modulus (c) Impact strength (d) Density

5.2 Application of a PALF/COIR Hybrid Epoxy Composite for Automotive Instrument Panel

Sapuan and Abdalla [255] reported that the tensile strength of at least 25 MPa is needed for composites developed for car dashboard panels. The alkaline treated P50-C50 developed hybrid biocomposite had an average strength of 41.73 MPa significantly higher than the strength required for interior automotive panel. The flexural strength of the developed composite was 134.4 MPa, is appropriate for the same application. Furthermore, the usage of such biocomposites rather than manufactured materials can contribute to lowering greenhouse gas emission thus combating climate change [256]. Due to all these aspects, we can conclude that the developed hybrid biocomposite can be utilized as an alternative material for interior automotive panels (Fig. 5.2).

Fig. 5.2: Automotive Instrument Panel

5.3 Comparison of Mechanical Properties between PALF/COIR Developed Composite with the PP/PS – xGnP for Automotive Applications

J. Parameswaranpillai *et al*. [257] have developed a hybrid composite PP/PS – xGnP and reported that the developed nanocomposite can be used for automotive applications. To analyze the potential of a developed PALF/COIR hybrid material in the same application, the mechanical properties of the hybrid were compared with PP/PS blend and PP/PS – xGnP composite in Table 5.1. The tensile strength of alkaline treated P50-C50 hybrid material is significantly higher than the strength of PP/PS blend and PP/PS – xGnP nanocomposite. However, the impact strength of P50-C50 (T) is little of low magnitude than that of the other two materials. Therefore, after some modifications for impact resistance, the developed PALF/COIR hybrid material can replace PP/PS blend for automobile components.

Table 5.1: Comparison between P50-C50 material with PP/PS blend and PP/PS – xGnP composite

Composite	Tensile strength	Impact strength
PP/PS blend	29.7	15
PP/PS – xGnP	32.3	14.16
P50-C50 (T)	41.76	9.54

5.4 Applications of a Developed PALF/COIR Hybrid Composite in the Interior of a Passenger Car

N. Ayrilmis *et al*. [258] suggest that the composite made with 60 wt% coir fiber, 37 wt% PP, and 3 wt% MAPP has significant potential for automotive interior applications. To investigate the ability of a hybrid PALF/COIR reinforced composite in an interior of passenger car, the properties of a developed hybrid material were compared with Coir/PP composite in Table 5.2. The observations show that the P50-C50 hybrid material exhibits considerably higher mechanical strength than the Coir/PP compatibilized composite. Therefore, the developed hybrid composite can be used for non-structural and semi-structural applications.

Table 5.2: Comparison between P50-C50 and Coir/PP materials

Composite	Density (g/cc)	Tensile strength (MPa)	Young's modulus (GPa)	Bending strength (MPa)
P50-C50	1.54	38.94	1.24	102.81
Coir/PP	0.8	17.8	0.78	30.6

5.5 Application of a PALF/COIR Hybrid Epoxy Composite for Door Panel

Mercedes-Benz used Jute-Epoxy material in the door panels in its E-class vehicles. Therefore, to evaluate the potential of a developed treated hybrid composite for the same application, the properties of hybrid were compared with Jute/Epoxy composite. Table 5.3 shows that the hybrid material offers better mechanical properties than the Jute/Epoxy composite. The density of treated P50-C50 composite is approximately equal to the density of Jute/Epoxy material. Therefore, it can be concluded that the developed hybrid material has the potential to use in the door panels of an automobile.

Table 5.3: Comparison of mechanical properties between P50-C50 and Jute/Epoxy composite

Composite	Density (g/cc)	Tensile strength (MPa)	Flexural strength (MPa)
P50-C50 (T)	1.21	41.76	102.81
Jute/Epoxy	1.196	40.5	72.32

CHAPTER 6 - CONCLUSIONS AND RECOMMENDATIONS

In this research work, a novel hybrid biocomposite material was developed and characterized. To develop a high-performance material using agricultural waste, the pineapple leaf and coconut husk fibers were selected as reinforcement in an epoxy thermoset matrix resin. For the development of an excellent hybrid biocomposite material, the following works have been done:

- Characterize the thermal stability, morphology, surface chemistry, and water absorption behavior of PALF and COIR fibers.
- Analyze the effect of alkaline treatment with various concentrated solutions (2%, 4%, 6%, 8%, and 10%) on the hydrophilic and thermal behavior of cellulosic fibers.
- Determine the optimum length and volume content of reinforcing fibers (PALF and COIR) at which the composites exhibit an optimum set of thermal and mechanical properties.
- Find out the best arrangement of fibers at which the composites show better flame retardancy, high resistance to moisture uptake, and excellent dynamic mechanical behavior.

After doing all these, the hybrid biocomposites were developed and characterized for mechanical and biodegradation properties.

On the basis of presented research work in this doctoral thesis, the following conclusions can be made:

6.1 Selection of Fibers and Matrix

Amongst all the commonly used natural fibers, the pineapple leaf (PALF) and coconut husk (COIR) have significant potential as a reinforcing agent in polymer-based composites which results in high strength, lightweight, and biodegradable biocomposite material. The PALF and COIR are multi-cellular fibers, extracted from the leaves of pineapple and the husk (mesocarp) of coconut fruit respectively. The primary reasons to select these fibers over the other are:

- PALF contains high cellulose content (70-85%) which results in it exhibits higher tensile and flexural properties than the flax, sisal, jute, OPEFB, and cotton fibers.
- The flexural and torsional rigidity of PALF is also comparable with jute fiber.
- Easy availability, low density, favorable aspect ratio, and low microfibrillar angle of PALF.
- COIR fiber has high lignin content (40-45%) which makes it more durable and stable under a wide range of temperature and humid conditions as well as provides excellent resistant properties against microbial and fungus attack.

6.2 Impact of Mercerization on Thermal, Morphological, and Hydrophilic Characteristics of Cellulosic Fibers

- An alkaline treatment increases the thermal stability of cellulosic fibers through physical and chemical changes.
- The alkali-treated fibers are rough with regularly placed pinholes than the untreated ones. This was caused by the removal of hemicellulose, binding agent, and gummy substances.
- The NaOH treated fillers absorb more water in the humid environment than the untreated one. Furthermore, the capillary and water diffusion action is more pronounced in alkali-treated fibers.
- The 4% NaOH treated COIR and 8% NaOH treated PALF absorb 5-8% and 9-15% more water than the untreated fibers respectively.
- Amongst the untreated and alkali-treated PALF and COIR fibers, the 4 wt% NaOH treated ones have maximum thermal stability.
- The thermal decomposition of PALF and COIR fibers proceeded in two steps. In 1^{st} step, a minor weight loss occurs due to evaporation of water and extraction of volatile compounds and in the 2^{nd} step, major degradation occurs because of the disintegration of hemicellulose, cellulose, and lignin components.
- PALF has a higher rate of decomposition (6.85 %/min) than COIR (4.85 %/min) but its main decomposition peak is higher (about 40 ^{0}C) than the coconut husk fiber. It was due to the presence of more cellulosic content in PALF

6.3 Impact of Reinforcement Geometry and Volume Fraction on the Characteristics of Biocomposites

- The tensile and bending strength of PALF/Epoxy were enlarged considerably with the increase of PALF length and content up to 15 mm and 34 vol. %. However, the maximum impact strength was achieved at 25 mm length and 43% PALF content.
- The Coir/Epoxy composite of 20 mm fiber span with 23% fiber volume content exhibits better mechanical properties than the other Coir/Epoxy composites. Beyond the addition of fibers and a further enlarge in length results in the improper wetting and an increase in void density.
- The moisture sorption affinity of composites was increased with the increase of fiber length and content. However, it is mainly affected by fiber content than the span. Amongst all the composites, the 43% fiber strengthened one absorbs maximum water.
- The thermal stability, E', E'', and T_g of the epoxy polymer was increased by the incorporation of coir and pineapple leaf fibers. It was due to the rigidity of polymeric chains and higher restrictions in molecular mobility.
- In context to the thermal stability of COIR/Epoxy and PALF/Epoxy composites, the optimum fiber volume content is 23%. The main degradation temperature of epoxy polymer was increased by 16.79 ^{0}C and 23.14 ^{0}C after the incorporation of 23% COIR and 23% PALF respectively.
- The order of thermal stability in COIR/Epoxy and PALF/Epoxy composites are: 23 CF-EP> 34 CF-EP> 17 CF-EP> EP> CF; 23 PF-EP> 34 PF-EP> 17 PF-EP> EP> PF respectively.
- The 23% COIR and 34% PALF reinforced composites have the lowest value of effectiveness coefficient 'C', obtained by the storage modulus analysis.
- The significant reduction in storage modulus (E') of epoxy and epoxy filled composites over the temperature range of 45-80 ^{0}C corresponds to the transition from the glassy phase to the rubbery phase.

6.4 Impact of Strands Layering Pattern on Performance Characteristics of Hybrid Material

- The ability of hybrid composites to retard flame and penetration of water molecules is not only a function of the kind of reinforcing filaments and adhesive resin but also depends on the pattern by which fibers are arranged in a viscoelastic matrix medium.
- Amongst all the developed hybrid composites [CPC, PCP, Bilayer (P/C), and IM], the CPC material exhibits the highest resistance to burning and flame penetration. This was due to the formation of more char at the surface which results in excellent resistance to thermal-oxidative decomposition.
- The IM absorbs 44.32% and 34.87% less water as compared to the PCP and bilayer (P/C) one respectively. It was due the better dispersion of filaments and improved interaction between constituent elements.
- The flame retardancy and hydrophobicity of hybrid biocomposites can be improved by layering the fibers in such a manner that the lignin enriched fiber acts as a skin and highly cellulose composed fiber act as a core material.
- The CPC layered hybrid composite has a lower value of effectiveness coefficient 'C' which leads to the higher activation energy required for transit glassy phase to the rubbery phase as compared to other hybrid composites.
- The bilayer and IM have nearly the same value of storage modulus and the glass transition temperature. But the intimately mixed composite has a lower 'C' value. It was due to the effective and uniform stress transfer from matrix to fiber and fiber to fiber.
- The dynamic modulus and glass transition temperature of pure COIR/Epoxy and PALF/Epoxy composites were increased by the synergistic hybridization of PALF with COIR fiber in an epoxy thermoset matrix. Moreover, the effectiveness coefficient 'C' and the peak value of the damping ratio (tan δ) for COIR/Epoxy composite were reduced after the hybridization with PALF.
- The trilayer CPC and bilayer (P/C) composites have maximum stiffness above and below T_g respectively.
- The storage modulus and the width of tan δ curve were elevated with the increase of frequency from 1 Hz to 5 Hz. This behavior assures the better adhesion at a higher frequency (short time).

6.5 Mechanical and Water Uptake Characteristics of Biocomposite Materials

- The tensile and bending strength and modulus of PALF/Epoxy composite are higher than the COIR/Epoxy. However, the composite reinforced with COIR fiber has a greater value of impact strength and dimensional stability as compared to the PALF reinforced composite.
- The mechanical properties and moisture sorption impedance of PALF/Epoxy and COIR/Epoxy composites have been improved by the incorporation of both types of fibers in a single polymeric resin.
- The optimum set of mechanical properties was obtained for the composite reinforced with an equal volume fraction of pineapple leaf fiber and coconut husk fiber. Moreover, the P50-C50 hybrid composite absorbs the least amount of water than the other composite samples.
- The moisture sorption affinity of hybrid material was diminished with enhance of COIR fiber volume. According to the water diffusion exponent (n), the large number of composites exhibits a Fickian diffusion mechanism.
- The PALF/COIR fiber reinforced hybrid composite has lower mechanical strength than the common car bumper beam material (GMT). Therefore, the developed material is far away to successfully employ in structural applications of an automobile. The developed hybrid composite can be used in non-structural and semi-structural applications. It can be used in different parts of an automobile such as door panels, headliner panel, package and floor trays, printed circuit boards, etc.
- In the natural soil environment, the PALF-Epoxy composite exhibits a higher rate of reduction in strength than the COIR-Epoxy. It was due to the substantial hydrolysis of PALF.
- Most of the developed composites revealed an accelerated rate of reduction in mechanical strength after 30 days of soil burial. This was attributed to the selective hydrolysis of reinforcing fibers and the substantial scission of polymeric chains.
- Amongst all the untreated and treated composites, the NaOH treated P10-C90 possess maximum reduction (%) in mechanical strength after 110 days of burial in the natural soil environment.

6.6 Biodegradation of Biocomposites

- In the natural soil environment, the weight loss (%) of an epoxy thermoset was amplified significantly after the inclusion of cellulosic strands.
- Amongst all the untreated and alkaline treated composites, the pure PALF/Epoxy possesses a maximum percentage of weight loss in the natural soil environment.
- The biodegradability and mechanical strength of COIR/Epoxy composite were increased significantly by the incorporation of pineapple leaf fibers and alkaline treatment of fibers. However, the NaOH treated PALF-Epoxy composite possesses higher stability against the attack of microorganisms than the untreated one.
- The biodegradability of a hybrid composite was reduced with the increase of coir fiber volume content. This was attributed to the high resistance power of a coir fiber against the microbial and fungus attack.
- The mechanism of bio-degradation involves penetration of water molecules, breakage of strong covalent bonds, and deterioration of hemicellulose & cellulose by the action of microorganisms.

Overall, we can conclude that the fiber hybridization and alkaline treatment of cellulosic fibers play a major role to affect the biodegradation. The experimental work proved that the developed hybrid composites are more environment-friendly and have good mechanical strength as compared to conventional plastics.

6.7 Recommendations for Future Work

The completion of this research has brought certain constraints, challenges, and consequently opportunities for future research directions. The following section outlines the recommendations for future research work.

6.7.1 Green composite Formulation

This research has utilized non-renewable epoxy synthetic resin for the fabrication of a composite material. To improve the sustainability of material, there is a need to replace synthetic resin with bio-resin which results in the formulation of 100% biobased composite material.

6.7.2 Fabrication Technique

In this work, a manual polymer processing technique was employed to formulate the biocomposite material. This technique is limited to low viscosity polymers. Moreover, the speed of production and uniform wetting of fibers with matrix resin are also major problems of this technique. Therefore, there is a need to utilize other production methods like spray layup, pultrusion, compression molding, resin transfer molding, pre-pregging, etc.

6.7.3 Fiber-Matrix Interfacial Adhesion

This work deals with the alkaline treatment of fibers to enhance the linkage between reinforcement and polymeric resin. Therefore, there is a need to examine the impact of other treatments on the performance of strengthened composites.

6.7.4 Life Cycle Predictions

Although the current research studied the biodegradation of biocomposites, it is of great importance to conduct a life cycle analysis (LCA) to ascertain life-cycle cost, production and transportation of the pineapple leaf and coir fibers.

6.7.5 Testing of Biocomposites

Although the thermo-mechanical properties of hybrid biocomposites were tested in this work, there is a need to evaluate the tribological, chemical, and electrical properties of PALF/COIR fiber-reinforced composite. It would be of great interest to obtain a data bank of the effect of different flame retardants on the flammability of PALF/COIR hybrid material.

6.7.6 Consistent Quality of Biocomposites

An important concern is the deficiency of standardized pineapple leaf and coir fibers. Climatic and geographical conditions affect the nature of strands. This is a main weakness if their composites are used in the automobile industry. Therefore, it is suggested that the filaments of consistent quality be used for the biocomposite.

REFERENCES

1. Nishino T, Hirao K, Kotera M, Nakamae K, and Inagaki H (2003) Kenaf reinforced biodegradable composite *Compos. Sci. Technol.* **63**(9): 1281-1286.
2. Nickel J and Riedel U (2003) Activities in biocomposites *Materials. Today.* 44-48.
3. Bledzki AK and Gassan J (2000) Composites reinforced with cellulose based fibers *Prog. Polym. Sci.* **24**(2): 221-274.
4. Bogoeva G, Avella M, Malinconico M, and Buzarovska A (2007) Natural fiber eco-composites *Polym. Compos.* **28**: 98-107.
5. Dicker M, Duckworth PF, Baker A, Francois G, Hazzard M, and Weaver, PM (2014) Green composites: A review of material attributes and complementary applications *Compos. Part A: Appl. Sci. Manuf.* **56**: 280-289.
6. X Li, Tabil LG, and Panigrahi S (2007) Chemical treatments of natural fiber for use in natural fiber reinforced composites: A Review *J. Polym. Environ.* **15**: 25-33.
7. Mukherjee PS and Satyanarayana KG (1986) Structure and properties of some vegetable fibers *J. Mater. Sci.* **21**(1): 51-56.
8. Satyanarayana KG, Ravikumar KK, Sukumaran K, Mukherjee PS, Pillai SGK, and Kukarni AG (1986) Structure and properties of some vegetable fibers *J. Mater. Sci.* **21**(1): 57-63.
9. Anuar H, Ahmad S, Rasid R, Ahmad A, and Busu W (2008) Mechanical properties and dynamic mechanical analysis of thermoplastic natural fiber reinforced short carbon fiber and kenaf fiber hybrid composites *J. Appl. Polym. Sci.* **107**(6): 4043-4052.
10. Barreto A, Esmeraldo M, Rosa D, Fechine P, and Mazzeto S (2010) Cardanol biocomposites reinforced with jute fiber: microstructure, biodegradability, and mechanical properties *Polym. Compos.* **31**(11): 1928-1937.
11. Statistical databases of " Food and agricultural organization of the united nations", www.fao.org/statistics/databases/en/
12. Wallenberger FT and Weston N (2004) Natural fibers, plastics, and composites *Kluwer Academics Publisher, New York.*
13. Mishra S, Mohanty AK, Drzal LT, Misra M, Parija S, Nayak SK, and Tripathy SS (2003) Studies on mechanical performance of biofibre/glass reinforced polyester hybrid composites *Compos. Sci. Technol.* **63**(10): 1377-1385.
14. Khalil HPS, Hanida S, Kang CW, and Fuaad NA (2007) Agro-hybrid composite: The effects on mechanical and physical properties of oil palm fiber (EFB)/Glass hybrid reinforced polyester composites *J. Reinf. Plast. Compos.* **26**(2): 203-218.
15. Mohanty AK and Misra M (1995) Studies on jute composites-A literature review *Polym. Plast. Technol. Eng.* **34**: 729-792.

16. Hirschler MM (2000) Chemical aspects of thermal decomposition of polymeric materials *Fire retardancy of polymeric materials, CRC Press, Boca Raton,* 28-79.
17. Dash BN, Rana, Mishra SC, Mishra HK, and Tripathy SS (2000) Novel low-cost Jute-Polyester composite *Polym. Plast. Technol. Eng.* **39**(2): 333-350.
18. Wang B, Panigrahi S, Tabil L, and Crerar W (2007) Pre-treatment of flax fiber for use in rotationally molded biocomposites *J. Reinf. Plast. Compos.* **26**(5): 447-463.
19. Mishra S, Mishra M, Tripathy SS, and Mohanty AK (2001) Potentiality of pineapple leaf fiber as reinforcement in PALF/Polyester composite: Surface modification and mechanical performance *J. Reinf. Plast. Compos.* **20**(4): 321-334.
20. Mohanty AK, Misra M, and Drzal LT (2012) Surface modifications of natural fibers and performance of the resulting biocomposites: An overview *Compos. Interf.* **8**(5): 313-343.
21. Kumar R, Obrai S, and Sharma A (2011) Chemical modification of natural fiber for composite material *Pelagia Research Library* **2**(4): 219-228.
22. http://en.m.wikipedia.org/wiki/composite_material
23. Mathews F and Rawlings R (1999) Composite materials: Engineering and science *Woodhead Publishing, Abington, England*.
24. Karbhari VM (2001) Materials considerations in FRP rehabilitation of concrete structures *J. Mater. Civil. Eng.* **13**(2): 90-97.
25. Fiber reinforced plastic use, *Plast. News.* August 2012.
26. Mapleston P (1999) Automakers see strong promise in natural fiber reinforcements (thermoplastic reinforced with natural fiber) *Mod. Plast.* 73-74.
27. Koronis G, Silva A, and Fontul M (2013) Green composites: A review of adequate materials for automotive applications **44**: 120-127.
28. Wedin R (2004) Chemistry on a High-Carb. Diet *American Chemical Society, Washington, D.C.* 30-35.
29. Mohanty AK, Misra M, and Drzal LT (2002) Sustainable bio-composites from renewable resources: opportunities and challenges in the green materials world *J. Polym. Environ.* **10**: 19-26.
30. Mohanty AK, Misra M, and Hinrichsen G (2000) Biofibers, biodegradable polymers, and biocomposites: an overview *Macromol. Mater. Eng.* **276**: 1-25.
31. Mohanty AK, Misra M, Drzal T (2002) Sutainable bio-composites from renewable resources: opportunities and challenges in the green materials world *J. Polym. Environ.* **10**: 19-26.
32. Akil HM, Omar, MF, Mazuki AAM, Safiee S, Ishak ZAM, and Bakar A (2011) Kenaf fiber reinforced composites: a review *Mater. Des.* **32**: 4107-4121.
33. Mohanty AK, Drzal LT, Ferguson KJ, Dale BE, Misra M, and Schalek R (2002) Explosion treatment of corn stalk fibers and their characterizations: a

new look at value added applications *Polym. Preprint – Polym. Chem. Div. Am. Chem. Soc.* **43**: 749-750.
34. Kalia S (2018) Lignocellulosic composite materials *Springer series on polymer and composite materials.*
35. George G, Joseph K, Boudenne A, and Thomas S (2010) Recent advances in green composite *Key. Eng. Mater.* **425**: 107-166.
36. Nakagaito AN and Yano H (2008) The effect of fiber content on the mechanical and thermal expansion properties of biocomposites based on micro fibrillated cellulose *Cellulose* **15**(4): 555-559.
37. Drzal LT, Mohanty AK, and Misra M Bio-composite material as alternatives to petroleum based composites for automotive applications.
38. Fowler PA, Hughes JM, and Elias RM (2006) Review biocomposites: technology, environmental, credentials, and market forces *J. Sci. Food. Agric.* **86**: 1781-1789.
39. Mohanty AK, Drzal LT, and Misra M (2002) Engineered natural fiber reinforced composites: Influence of surface modifications and novel powder impregnation processing *J. Adhes. Sci. Technol.* **16**: 999-1015.
40. Malkapuram R, Kumar V, and Negi Y (2009) Recent development in natural fiber reinforced polypropylene composites *J. Reinf. Plast. Compos.* **28:** 1169-1189.
41. Namvar F, Jawaid M, Tahir P, Mohamad R, Azizi S, Khodavandi A, Rahman H, and Nayeri M (2014) Potential use of plant fibers and their composites for biomedical applications *BioResources* **9**(3): 5688-5706.
42. Grown to fit the part (1999) DaimlerChrysler High Tech. Report 82-85.
43. Green door-trim panels use PP and natural fiber (2000) *Plast. Technol.***46**: 27.
44. Brouwer WD (2000) Natural fiber composites: where can flax compete with glass *SAMPE J*. **36**: 18-23.
45. Broge JL (2000) Natural fibers in automotive components *Automotive. Eng. Int.* **108**: 120.
46. Peijs T (2002) Composites turn green. Department of materials, Queen Mary, University of London; Available from: http://www.e-polymers.org.
47. Satyanarayana KG, Sukumaran K, Ravikumar KK, Brahmakumar M, Pillai SGK, Pavithran C, Mukherjee S, and Pai BC (1984) Possibility of using natural fiber polymer composites as building materials in low cost housing *CBRI Roorkee*, November 12-17.
48. Misra M, Mohanty AK, and Drzal LT (2000) Environmentally-friendly composites from jute and Mater-Bi, *Society for the advancement of material and process engineering (SAMPE)*, Dearborn, USA, Sept. 12-14.
49. Ozturk S (2010) Effect of fiber loading on the mechanical properties of kenaf and fiberfrax fiber reinforced phenol formaldehyde composites *J. Compos. Mater.* **44**: 2265-2288.
50. Maheshwari CU, Reddy K, Muzenda E, Shukla M, and Varada Rajulu A (2013) Mechanical properties and chemical resistance of short tamarind

fiber/unsaturated polyester composites: Influence of fiber modification and fiber content *Int. J. Polym. Anal. Ch.* **18**: 520-533.

51. Venkateshwaran N, ElayaPerumal A, and Jagatheeshwaran MS (2011) Effect of fiber length and fiber content on mechanical properties of banana fiber/Epoxy composite. *J. Reinf. Plast. Compos.* **30**(19): 1621-1627.
52. Zhao X, Li R, and Bai S (2014) Mechanical properties of sisal fiber reinforced high density polyethylene composites: Effect of fiber content, interfacial compatibilization, and manufacturing process *Composites: Part A* **65**: 169-174.
53. Mohanty S and Nayak SK (2010) Short bamboo fiber reinforced HDPE composites: Influence of fiber content and modification on strength of the composite *J. Reinf. Plast. Compos.* https://doi.org/10.1177/0731684409345618
54. Alvarez VA, Fraga AN, and Vazquez A (2003) Effect of the moisture and fiber content on the mechanical properties of biodegradable polymer-sisal fiber biocomposites *J. Appl. Polym. Sci.* **91**: 4007-4016.
55. Leblanc LJ, Furtado CRG, Leite MCAM, Visconte LLY, and Souza AMF (2006) Effect of the fiber content and plasticizer type on the rheological and mechanical properties of polyvinyl chloride/coconut fiber composites *J. Appl. Polym. Sci.* **106**: 3653-3665.
56. Sezgin H, Enis I, and Berkalp O (2016) Impact of biaxial square woven jute fabric reinforcement on mechanical performance of polyester based composites *Indian. J. Fibre. Text.* **43**: 252-256.
57. Yemele MCN, Koubaa A, Cloutier A, Soulounganga P, and Wolcott M (2010) Effect of bark fiber content and size on the mechanical properties of Bark/HDPE composites *Composites: Part A* **41**: 131-137.
58. Romhany G, Kocsis J, and Czigany T (2003) Tensile fracture and failure behavior of thermoplastic starch with unidirectional and cross-ply flax fiber reinforcements *Macromol. Mater. Eng.* **288**: 699-707.
59. Sbiai A, Kaddami H, Fleury E, Dufresne A, Soucy J, Koubaa A, Erchiqui F, and Maazouz A (2008) Effect of the fiber size on the physicochemical and mechanical properties of composites of epoxy and date palm fibers *Macromol. Mater. Eng.* **293**: 684-691.
60. Mohamed W, Baharum A, Ahmad I, Abdullah I, and Zakaria N (2018) Effect of fiber size and fiber content on mechanical and physical properties of Mengkuang reinforced thermoplastic natural rubber composites *BioResources* **13**(2): 2945-2959.
61. Rajeshkumar G, Hariharan V, Satishkumar TP, Fiore V, and Scalici T (2016) Synergistic effect of fiber content and length on mechanical and water absorption behaviours of Phoenix sp. fiber-reinforced epoxy composites *J. Ind. Text.* **0**(00): 1-22.
62. Capela C, Oliveira SE, Pestana J, and Ferreira JAM (2017) Effect of fiber length on the mechanical properties of high dosage carbon reinforced *2nd*

International Conference on Structural Integrity (ICSI), Funchal, Portugal **5**: 539-546.

63. Kumar K, Reddy K, and Rao D (2012) Evaluation of viscoelastic properties of some malvaceae fiber reinforced composites *Int. J. Appl. Eng. Res.* **7**(11).
64. Margem JI, Gomes VA, Margem FM, Ribeiro C, Braga F, and Monteiro S (2015) Flexural behavior of epoxy matrix composites reinforced with malva fiber *Mater. Res.* **18**: 114-120.
65. Gupta MK, and Srivastava RK (2017) Mechanical, thermal, and dynamic mechanical analysis of jute fiber reinforced epoxy composite *Indian. J. Fibre. Text. Res.* **42**: 64-71.
66. El-Shekeil YA, Sapuan SM, Abdan K, and Zainudin ES (2012) Influence of fiber content on the mechanical and thermal properties of kenaf fiber reinforced thermoplastic polyurethane composites *Mater. Des.* **40**: 299-303.
67. Varghese S, Kuriakose B, Thomas S, and Koshy A (2012) Mechanical and viscoelastic properties of short fiber reinforced natural rubber composites: effects of interfacial adhesion, fiber loading, and orientation *J. Adhes. Sci. Technol.* **8**(3): 235-248.
68. Botev M, Betchev H, Bikiaris D, and Panayiotou C (1999) Mechanical properties and viscoelastic properties of basalt fiber-reinforced polypropylene *J. Appl. Polym. Sci.* **74**: 523-531.
69. Teja MS, Ramana MV, Sriramulu D, and Rao CJ (2016) Experimental investigation of mechanical and thermal properties of sisal fiber reinforced composite and effect of SiC filler material *IOP Conf. Ser. Mater. Sci. Eng.* **149** http://doi.org/10.1088/1757-899X/149/1/012095.
70. Pickering KL, Efendy MG, and Le TM (2015) A review of recent developments in natural fibre composites and their mechanical performance *Composites: Part A* **83**: 98-112.
71. Ganesan C, Babu S, Pal Y, and Kaurase KP (2013) Effect of various fibers on mechanical properties of bio-composite materials *Int. J. Eng. Res. Dev.* **6**(2): 67-73.
72. El-Shekeil YA, Sapuan SM, Jawaid M, and Al-Shujaa O (2014) Influence of fiber content on mechanical, morphological, and thermal properties of kenaf fibers reinforced polyvinyl chloride/thermoplastic polyurethane poly-blend composites *Mater. Des.* http://doi.org/10.1016/j.matdes.2014.01.047.
73. Ray D, Sarkar BK, Rana AK, and Bose NR (2001) Mechanical properties of vinylester resin matrix composites reinforced with alkali-treated jute fibres *Composites: Part A* **32**(1): 119-127.
74. Yusefi M, Khalid M, Yasin F, Ketabchi M, Hajalilou A, and Abdullah L (2016) Physico-mechanical properties of polylactic acid biocomposites reinforced with cow dung *Mater. Res. Exp.* **4** http://doi.org/10.1088/2053-1591/aa5cdb
75. Mazharuddin KM, Reddy B, and Rao H (2015) Impact and chemical tests on natural fiber reinforced epoxy composite material *Int. J. Innov. Res. Sci. Eng. Tech.* **4**(9): 8489-8494.

76. Assarar M, Scida D, Mahi A, Poilane C, and Ayad R (2010) Influence of water ageing on mechanical properties and damage events of two reinforced composite materials: Flax-Fibres and Glass-Fibres *Mater. Des.* **32**: 788-795.
77. Giancaspro J, Papakonstantinou C, and Balaguru P (2009) Mechanical behavior of fire-resistant biocomposite *Composites: Part B* **40**: 206-211.
78. Leao A, Souza SF, Cherian BM, Frollini E, Thomas S, Pothan LA, and Kottaisamy M (2010) Pineapple leaf fibers for composites and cellulose *Mol. Cryst. Liq. Cryst.* **522**: 336-341.
79. Wisittanawat U, Thanawan S, and Amornsakchai T (2014) Mechanical properties of highly aligned short pineapple leaf fiber reinforced–Nitrile rubber composite: Effect of fiber content and bonding agent *Polym. Test.* **35:** 20-27.
80. Kalapakdee A and Amornsakchai T (2014) Mechanical properties of preferentially aligned short pineapple leaf fiber reinforced thermoplastic elastomer: Effects of fiber content and matrix orientation *Polym. Test.* **37**: 36-44.
81. Daramola OO, Adediran A, Adewuyi B, and Adewole O (2017) Mechanical properties and water absorption behavior of treated pineapple leaf fibre reinforced polyester matrix composites *Leonardo J. Sci.* **30**: 15-30.
82. Bahra M, Gupta VK, and Aggarwal L (2017) Effect of fiber content on mechanical properties and water absorption behavior of Pineapple/HDPE composite *5th International Conference of Materials Processing and Characterization (ICMPC)* **4**: 3207-3214.
83. Verma D, Gope PC, Shandilya A, Gupta A, and Maheshwari MK (2013) Coir fiber reinforcement and applications in polymer composites: A Review *J. Mater. Environ. Sci.* **4**(2): 263-276.
84. Naveen P and Yasaswi M (2013) Experimental analysis of coir fiber reinforced polymer composite materials *Int. J. Mech. Eng. Rob. Res.* **2**(1): 10-18.
85. Rout J, Misra M, Tripathy SS, Nayak SK, and Mohanty AK (2001) The influence of fiber treatment on the performance of coir-polyester composites *Comp. Sci. Technol.* **61**(9): 1303-1310.
86. Pradeep P and Dhas J (2015) Evaluation of mechanical property on Palm/Coir based polymer matrix composites *Adv. Mater. Sci. Eng.* **2**(3): 9-16.
87. Suardana NPG, Lokantara IP, and Lim J (2011) Influence of water absorption on mechanical properties of coconut coir fiber/poly lactic acid biocomposites *Mater. Phys. Mech.* **12**: 113-125.
88. Das G and Biswas S (2016) Effect of fiber parameters on physical, mechanical, and water absorption of coir fiber-epoxy composites *J. Reinf. Plast. Comp.* **0**(0): 1-10.
89. Nallusamy S, Rekha R, and Karthikeyan A (2017) Investigation on mechanical properties of coir fiber reinforced polymer resin composites saturated with different filling agents *IOP Conf. Series: Materials Science and Engineering* **225**: 1-9.

90. Das G and Biswas S (2016) Physical, mechanical, and water absorption behavior of coir fiber reinforced epoxy composites filled with Al_2O_3 particulates *IOP Conf. Series: Mater. Sci. Eng.* **115** http://doi.org/10.1088/1757-899X/115/012012.
91. Murlidhar BA (2013) Viscoelastic and thermal behavior of flax preforms reinforced epoxy composites *J. Ind. Text.* http://doi.org/10.1177/1528083713502999
92. Wan YZ, Luo H, He F, Liang H, Huang Y, and Li X (2009) Mechanical, moisture absorption, and biodegradation behavior of bacterial cellulose fiber-reinforced starch biocomposites *Comp. Sci. Tech.* **69**: 1212-1217.
93. Singh AA and Palsule S (2014) Effect of water absorption on coconut fibre reinforced functionalized polyethylene composites developed by palsule process *Appl. Polym. Comp.* **2**(4): 229-238.
94. Osman E, Vakhguelt A, Sbarski I, and Mutasher S Water absorption behavior and its effect on the mechanical properties of kenaf natural fiber unsaturated polyester composites *18th International Conference on Composite Materials.*
95. Munoz E and Manrique JA (2015) Water absorption behavior and its effect on the mechanical properties of flax fibre reinforced bioepoxy composites *Int. J. Polym. Sci.* http://dx.doi.org/10.1155/2015/390275.
96. Padal KTB, Srikiran S, and Nagendra P (2014) Dynamic mechanical and thermal properties of jute nano fibre reinforced polymer composite *5th International and 26th All-India Manufacturing Technology, Design and Research Conference (AIMTDR-2014), IIT Guwahati, India.*
97. Nishitani Y, Yamanaka T, Kajiyama T, and Kitano T (2016) Thermal properties of hemp fiber reinforced plant derived polyamide biomass composites and their dynamic viscoelastic properties in molten state *Intech* http://dx.doi.org/10.5772/64215.
98. Nakagaito AN and Yano H (2008) The effect of fiber content on the mechanical and thermal expansion properties of biocomposites based on microfibrillated cellulose *Cellulose* **15**: 555-559.
99. Song YS, Lee JT, Sunji D, Kim MW, and Lee SH (2011) The viscoelastic and thermal behavior of woven hemp fiber reinforced polylactic acid composites *Composites: Part B* **43**: 856-860.
100. John MJ and Anandjiwala RD Characterization of viscoelastic properties of flax reinforced polypropylene composites.
101. Niu P, Liu B, Wei X, Wang X, and Yang J (2011) Study on mechanical properties and thermal stability of polypropylene/hemp fiber composites *J. Reinf. Plast. Comp.* **30**: 36-44.
102. Costa C, Fonseca AC, Serra AC, and Coelho J (2016) Dynamic mechanical thermal analysis of polymer composites reinforced with natural fibers *Polym. Review.* **56**(2): 362-383.
103. Salazar M and Correa J (2017) Mechanical and thermal properties of biocomposites from nonwoven industrial fique fiber mats with epoxy resin and linear low density polyethylene *Results in Physcics.* **8**: 461-467.

104. Tajvidi M and Takemura A (2009) Effect of fiber content and type, compatibilizer, and heating rate on thermogravimetric properties of natural fiber high density polyethylene composites *Polym. Comp.* http://dx.doi.org/10.1002/pc.20682.
105. Tajvidi M and Takemura A (2010) Thermal degradation of natural fiber reinforced polypropylene composites *J. Thermoplast. Comp.* **23**: 281-298.
106. Hshieh FY and Beeson HD (1996) Flammability testing of flame-retarded epoxy composites and phenolic composites *In: Proceedings of the International Conference on Fire Safety, San Francisco* **21**: 189-205.
107. Brown JR, Fawell PD, and Mathys Z (1994) Fire-hazard assessment of extended chain polyethylene and aramid composites by cone calorimetry *Fire. Mater.* **18**: 167-172.
108. Schindler WD and Hauser PJ (2004) Flame-retardant finishes *In: Chemical Finishing of Textiles* 98-116, Woodhead, Cambridge.
109. Helwig M and Paukszta D (2000) Flammability of composites based on polypropylene and flax fibres *Mol. Cryst. Liq. Cryst.* **354**: 373-380.
110. Borysiak S, Paukszta D, nad Helwig M (2006) Flammability of wood-polypropylene composites *Polym. Degrad. Stab.* **91**: 3339-3343.
111. Kandola BK and Kandare E (2008) Composites having improved fire resistance *Adv. Fire. Retard. Mater.* 398-442, Woodhead, Cambridge.
112. Bharat KN and Basavarajappa S (2014) Flammability characteristics of chemically treated woven natural fabric reinforced phenol formaldehyde composites *Procedia Mater. Sci.* **5**: 1880-1886.
113. Waldman WR and De Paoli MA (2008) Thermal properties of high density polyethylene composites with natural fibers: coupling agent effect *Polym. Degrad. Stab.* **93**: 1770-1775.
114. Albano C, Gonzalez J, Ichazo M, and Kaiser D (1990) Thermal stability of blends of polyolefins and sisal fiber *Polym. Degrad. Stab.* **66**: 179-190.
115. Schartel B and Hull TR (2007) Development of fire-retardant materials-Interpretation of cone calorimeter data *Fire. Mater.* **31**: 327-354.
116. Karlsson B and Quintiere JG (2000) A qualitative description of enclosed fires *Enclosed Fire Dynamics* 17-18, CRC Press, Boca Raton.
117. Fitzgerald RW (2004) Design fires *In: Building Fire Performance Analysis* 95-130 John Wiley & Sons, New York.
118. Rejeesh CR and Saju KK (2017) Effect of chemical treatment on fire-retardant properties of medium density coir fiber boards *Wood. Fiber. Sci.* **49**(3): 1-6.
119. Suardana NPG, Ku MS, and Lim JK (2011) Effects of diammonium phosphate on the flammability and mechanical properties of biocomposites *Mater. Des.* **32**: 1990-1999.
120. Mark HF, Atlas SM, Shalaby SW, and Pearce EM (1975) Combustion of polymers and its retardation *Flame Retardant Polymeric Materials* 1-17, Plenum Press, New York.

121. Mouritz AP and Gibson AG (2006) Flame retardant composites *Fire Properties of Polymer Composite Materials* 237-286, Springer, London.
122. Hirschler MM (2000) Chemical aspects of thermal decomposition of polymeric materials *Fire Retardancy of Polymeric Materials* 28-79, CRC Press, Boca Raton.
123. Fakhrul T and Islam MA (2013) Degradation behavior of natural fiber reinforced polymer matrix composites *5th BSME International Conference on Thermal Engineering* **56**: 795-800.
124. Takagi H (2010) Mechanical and biodegradation behavior of natural fiber composites *Adv. Mater. Res.* **123:** 1163-1166.
125. Kumar R, Yakubu MK, and Anandjiwala RD (2010) Biodegradation of flax fiber reinforced polylactic acid *eXpress. Polym. Letters.* **4**(7): 423-430.
126. Bharat KN, Swamy RP, and Mohan GC (2010) Experimental studies on biodegradable and swelling characteristics of natural fiber composites *Int. J. Agr. Sci.* **2**(1): 1-4.
127. Lee SH and Wang S (2006) Biodegradable polymers/bamboo fiber biocomposite with bio-based coupling agent *Composites: Part A* **37**: 80-91.
128. Pons N, Benezet JC, Ferry L, and Bergeret A Biodegradation kinetics of biopolymers and biocomposites.
129. Azwa ZN, Yousif BF, Manalo AC, and Karunasena W (2012) A review on the degradability of polymeric composites based on natural fibres *Mater. Des.* **47**: 424-442.
130. Sinha NK and Sinha S (2005) Stress relaxation at high temperatures and the role of delayed elasticity *Mater. Sci. Eng.* **393**: 179-190.
131. John MJ and Thomas S (2008) Biofibres and biocomposites *Carbohydr. Polym.* **71**(3): 343-364.
132. Shah AN and Lakkad SC (1981) Mechanical properties of jute reinforced plastics *Fiber Sci. Technol.* **15**(1): 41-46.
133. Clark RA and Ansell MP (1986) Jute and glass fibre hybrid laminates *J. Mater. Sci.* **21**(1): 269-276.
134. Ghosh P, Bose NR, Mitra BC, and Das S (1997) Dynamic mechanical analysis of FRP composites based on different fiber reinforcement and epoxy resin as the matrix material *J. Appl. Polym. Sci.* **64**: 2467-2472.
135. Pothan LA, Potschke P, and Thomas S (2001) The static and dynamic mechanical properties of banana and glass fibre woven fabric reinforced polyester composites *Proceedings of the AUCN-3, University of New South Wales*, 452-460.
136. Rahman M, Das S, and Hasan M (2018) Mechanical properties of chemically treated banana and pineapple leaf fiber reinforced hybrid polypropylene composites *Adv. Mater. Process. Technol.* http://doi.org/10.1080/2374068X.2018.1468972.
137. Arumugaprabhu V, Uthayakumar M, Cardona F, and Sultan MTH (2016) Mechanical characterization of Coir/Palmyra waste fiber hybrid composites,

IOP Conf. Series; Mater. Sci. Eng. **152** http://doi.org/10.1088/1757-899X/152/1/012054.

138. Sharba MJ, Leman Z, Sultan MTH, Ishak MR, and Hanim MA (2016) Effect of kenaf fiber orientation on mechanical properties and fatigue life of Glass/Kenaf hybrid composites *BioResources* **11**(1): 1448-1465.
139. Sharba MJ, Leman Z, Sultan MTH, Ishak MR, and Hanim M (2016) Partial replacement of glass fiber by woven kenaf in hybrid composites and its effect on monotonic and fatigue properties *BioResources* **11**(1): 2665-2683.
140. Atiqah A, Maleque MA, Jawaid M, and Iqbal M (2014) Development of kenaf-glass reinforced unsaturated polyester hybrid composite for structural applications *Composites: Part B* **56**: 68-73.
141. Fong AL, Khandoker N, and Debnath S (2018) Development and characterization of sugarcane bagasse fiber and nano-silica reinforced epoxy hybrid composites *IOP Conf. Series; Mater. Sci. Eng.* **344** http://doi.org/10.1088/1757-899X/344/1/012029.
142. Manoj R, Thulasikanath V, Senkathir S, Arun AC, Geethapriyan T (2016) Development of hybrid E-glass fibre reinforced polymer matrix composite and study of mechanical properties *J. Chem. Pharma. Sci.* **9**(4): 2770-2774.
143. Khalil HPS, Masri M, Saurabh CK, Fazita MRN, Azniwati AA, Aprilla NA, Rosamah E, and Dungani R (2017) Incorporation of coconut shell based nanoparticles in kenaf/coconut fibers reinforced vinyl ester composites *Mater. Res. Exp.* http://doi.org/10.1088/2053-1591/aa62ec.
144. Nurazzi, N.M., Khalina, A., Sapuan, S., Rahmah, M. (2018). Development of sugar palm yarn/glass fiber reinforced unsaturated polyester hybrid composites, *Materials Research Express*, http://doi.org/10.1088/2053-1591/aabc27.
145. Shrivastava R, Telang A, Rana RS, and Purohit R (2017) Mechanical properties of Coir/Glass fiber epoxy resin hybrid composite *Materials Today: Proceedings* **4**: 3477-3483.
146. Bhagat VK, Biswas S, and Dehury J (2013) Physical, Mechanical, and Water absorption behavior of Coir/Glass fiber reinforced epoxy based hybrid composites *Polym. Compo.* http://doi.org/10.1002/pc.22736.
147. Devi LU, Bhagawan SS, Nair K, and Thomas S (2011) Water absorption behavior of PALF/GF hybrid polyester composites *Polym. Compo.* http://doi.org/10.1002/pc.21034.
148. Cheng F, Hu Y, and Yuan J (2014) Preparation and characterization of glass fiber-coir hybrid composites by a novel and facile prepreg/press process *Fibers Polym.* **15**(8): 1715-1721.
149. Uppin VS, Ashok, Joshi A, Sridhar I, and Gouda PS (2016) Interlaminar fracture toughness in Glass-Cellulose reinforced epoxy hybrid composites *IOP Conf. Series; Mater. Sci. Eng.* **149** http://doi.org/10.1088/1757-899X/149/1/012113.

150. Saw SK, Akhtar K, Yadav N, and Singh AK (2014) Hybrid composites made from Jute/Coir fibers: Water absorption, Thickness swelling, Density, Morphology, and Mechanical Properties *J. Nat. Fibers* **11**: 39-53.
151. Satishkumar TP, Navaneethakrishnan P, Shankar S, and Kumar J (2012) Mechanical properties of randomly oriented snake grass fiber with banana and coir fiber-reinforced hybrid composites *J. Compos. Mater.* http://doi.org/10.1177/0021998312454903.
152. Khanam PN, Reddy GR, Raghu K, and Naidu SV (2009) Tensile, flexural, and compressive properties of Coir/Silk fiber reinforced hybrid composites *J. Reinf. Plast. Compo.* http://doi.org/10.1177/0731684409345413.
153. Nunna S, Chandra P, Shrivastava S, and Jalan AK (2012) A review on mechanical behavior of natural fiber based hybrid composites *J. Reinf. Plast. Compos.* http://doi.org/10.1177/0731684412444325.
154. Kakou C, Essabir H, Bensalah M, Bouhfid R, Rodrigue D, and Qaiss A (2015) Hybrid composites based on polyethylene and coir/oil palm fibers *J. Reinf. Plast. Compos.* http://doi.org/10.1177/0731684415596235.
155. Zhang L and Hu Y (2013) Novel lignocellulosic hybrid particleboard composites made from rice straws and coir fibers *Mater. Des.* http://dx.doi.org/10.1016/j.matdes.2013.09.066.
156. Siddika S, Mansura F, Hasan M, and Hassan A (2014) Effect of reinforcement and chemical treatment of fiber on the properties of jute-coir fiber reinforced hybrid polypropylene composites *Fiber Polym.* **15**(5): 1023-1028.
157. Siakeng R, Jawaid M, Ariffin H, and Sapuan S M (2018) Thermal properties of coir and pineapple leaf fiber reinforced polylactic acid hybrid composites *IOP Conf. Ser. Mater. Sci. Eng.* **368**, http://doi.org/10.1088/1757-899X/368/1/0120319.
158. Ramesh M, Logesh R, Manikandan M, Pratap D, and Kumar N (2017) Mechanical and water intake properties of banana-carbon hybrid fiber reinforced polymer composites *Mater. Res.* http://dx.doi.org/10.1590/1980-5373-MR-2016-0760
159. Alexander J and Elphej SJ (2017) Mechanical characterization of basalt based natural hybrid composites for aerospace applications *IOP Conf. Ser. Mater. Sci. Eng.* **197**, http://doi.org/10.1088/1757-899X/197/1/012008.
160. Idicula M, Malhota SK, Joseph K, and Thomas S (2005) Effect of layering pattern on dynamic mechanical properties of randomly oriented short banana/sisal hybrid fiber-reinforced polyester composites *J. Appl. Polym. Sci.* **97**: 2168-2174.
161. Chee SS, Jawaid M, and Sultan MTH (2017) Thermal stability and dynamic mechanical properties of Kenaf/Bamboo fibre reinforced epoxy composites *BioResources* **12**(4): 7118-7132.
162. Baghaei B, Skrifvars M, Rissanen M, and Ramamoorthy S (2014) Mechanical and thermal characterization of compression moulded polylactic

acid natural fiber composites reinforced with hemp and lyocell fibers *J. Appl. Polym. Sci.* http://dx.doi.org/10.1002/app.40534.

163. Aji Is, Zainudin Edi, Sapuan S, Khalina A, and Khairul M (2013) Mechanical properties and water absorption of hybridized kenaf/pineapple leaf fibre-reinforced high-density polyethylene composite *J. Compos. Mater.*
164. Bakri B, Chandrabakty S, and Putra KA (2017) Evaluation of mechanical properties of Coir-Angustifolia Haw Agave fiber reinforced hybrid epoxy composite *Jurnal Mekanikal* **8**(1): 679-685.
165. Yahaya R, Sapuan SM, Jawaid M, Leman Z, and Zainudin ES (2016) Water absorption behavior and impact strength of kenaf-kevlar reinforced epoxy hybrid composites *Adv. Compo. Lett.* **25**(4): 98-102.
166. Akash, Girisha KG, Gupta NS, and Rao KV (2017) A study on flammability and water absorption behavior of sisal/coir fiber reinforced hybrid composites *IOP Conf. Ser. Mater. Sci. Eng.* **19**, http://doi.org/10.1088/1757-899X/191/1/0120083.
167. Jawaid M, Khalil HPS, and Alattas OS (2011) Woven hybrid biocomposites: Dynamic mechanical and thermal properties *Composites: Part A* **43**: 288-293.
168. Mansor MR, Sapuan SM, Zainudin ES, Nuraini AA, and Hambali A (2013) Hybrid natural and glass fibers reinforced polymer composites material selection using analytical hierarchy process for automotive brake lever design *Mater. Des.* **51**: 484-492.
169. Davoodi MM, Sapuan SM, Ahmad D, Ali A, Khalina A, and Jonoobi M (2010) Mechanical properties of hybrid kenaf/glass reinforced epoxy composite for passenger car bumper beam *Mater. Des.* **31**: 4927-4932.
170. Sreekala MS, George J, Kumaran MG, and Thomas S (2002) The mechanical performance of hybrid phenol-formaldehyde based composites reinforced with glass and oil palm fibres *Compos. Sci. Technol.* **62**: 339-353.
171. Mishra S, Mohanty AK, Drzal LT, Misra M, Parija S, Nayak SK, and Tripathy SS (2003) Studies on mechanical performance of biofibre/glass reinforced polyester hybrid composites *Compos. Sci. Technol.* **63**: 1377-1385.
172. Burgueno R, Quagliata M J, Mohanty A K, Mehta G, Drzal L T, and Misra M (2005) Hybrid biofiber-based composites for structural cellular plates *Composite: Part A* **36**: 581-593.
173. Ranganathan N, Oksman K, Nayak SK, and Sain M (2015) Structure-property relation of hybrid biocomposites based on jute, viscose, and polypropylene: The effect of the fiber content and the length on the fracture toughness and the fatigue properties *Composites: Part A* http://dx.doi.org/10.1016/j.compositesa.2015.10.037.
174. Kaiser MR, Anuar H, and Abdul Razak SB (2014) Improvement in thermomechanical properties of injection molded nano-modified hybrid biocomposite *J. Thermoplast. Compos. Mater.* **27**(7): 992-1009.
175. Davoodi MM, Sapuan SM, Ahmad D, Aidy A, Khalina A, and Jonoobi M (2011) Concept selection of car bumper beam with developed hybrid bio-composite material *Mater. Des.* **32**: 4857-4865.

176. Chevali VS, Nerenz BA, Ulven CA, and Kandare E (2015) Mechanical properties of hybrid lignocellulosic fiber-filled acrylonitrile butadiene styrene (ABS) biocomposites *Polym. Plast. Technol. Eng.* **54**: 375-382.
177. Haq M, Burgueno R, Mohanty A K, and Misra M (2008) Hybrid bio-based composites from blends of unsaturated polyester and soybean oil reinforced with nanoclay and natural fibers *Compos. Sci. Technol.* **68**: 3344-3351.
178. Murugan R, Ramesh R, and Padmanabhan K (2014) Investigation on static and dynamic mechanical properties of epoxy based woven fabric Glass/Carbon hybrid composite laminates *Procedia Engineering* **97**: 459-468.
179. Ranjan R, Bajpai PK, and Tyagi RK (2013) Mechanical characterization of banana/sisal fibre reinforced PLA hybrid composites for structural applications *Eng. Int.* **1**(1): 39-48.
180. Jawaid M, Khalil HPS, Hassan A, and Abdallah E (2012) Bi-layer hybrid biocomposites: Chemical resistant and physical properties *BioResources* **7**(2): 2344-2355.
181. Jawaid M and Khalil HPS (2011) Cellulosic/synthetic fibre reinforced polymer hybrid composites: A review *Carbohydr. Polym.* **86**: 1-18.
182. Bledzki AK and Gassan J (1999) Composites reinforced with cellulose based fibres *Prog. Polym. Sci.* **24**(2): 221-274.
183. Brett C and Waldron K (1996) Physiology and biochemistry of plant cell walls *2nd ed., Chapman & Hall, London.*
184. Hiesh YL, Thompson J, and Miller A (1996) Water wetting and retention of cotton assemblies as affected by alkaline and bleaching treatment *Textile Res. J.* **66**(7): 456-464.
185. Ribitsch V, Stana-Kleinschek K, and Jeler S (1996) The influence of classical and enzymatic treatment on the surface charge of cellulose fibres *Colloid. Polym. Sci.* **274**: 388-394.
186. Saheb DN and Jog JP (1999) Natural fibre polymer composites: a review *Adv. Polym. Technol.* **18**: 351-363.
187. Dhakal HN, Zhang ZY, and Richardson MOW (2007) Effect of water absorption on the mechanical properties of hemp fibre reinforced unsaturated polyester composites *Compos. Sci. Technol.* **67**: 1674-1683.
188. Symington MC, Banks WM, David West O, and Pethrick RA (2009) Tensile testing of cellulose based natural fibers for structural composite applications *J. Compos. Mater.* **43**: 1083-1108.
189. Placet V, Cisse O, and Boubakar L (2012) Influence of environmental relative humidity on the tensile and rotational behavior of hemp fibres *J. Mater. Sci.* **47**: 3435-3446.
190. Pejic BM, Kostic MM, Skundric PD, and Praskalo JZ (2008) The effects of hemicelluloses and lignin removal on water uptake behaviour of hemp fibers *Bioresource Technology* **99**: 7152-7159
191. Frederick TW and Norman W (2004) Natural fibers plastics and composites *Kluwer Academics Publishers, New York.*

192. Nakamura K, Hatakeyama T, and Hatakeyama H (1981) Studies of bound water of cellulose by differential scanning calorimetry *Text. Res. J.* **51**: 607-613.
193. Davies GC and Bruce DM (1988)Effect of environmental relative humidity and damage on the tensile properties of flax and nettle fibers *Text. Res. J.* **68**: 623-629.
194. Stamboulis A, Baillie CA, Garkhail SK, Melick HGH, and Pejis T (2000) Environmental durability of flax fibres and their composites based on polypropylene matrix *Appl. Compos. Mater.* **7**: 273-294.
195. Xie Y, Hill C, Jalaludin Z, Curling S, Anandjiwala R, Norton A, and Newman G (2011) The dynamic water vapour sorption behavior of natural fibres and kinetic analysis using the parallel kinetics exponential model *J. Mater. Sci.* **46**: 479-489.
196. Bismarck A, Aranberri I, and Springer J (2002) Surface characterization of flax, hemp, and cellulose fibres: surface properties and water uptake behavior *Polym. Compos.* **23**(5): 872-894.
197. Wielage B, Lampke T, Marx G, Nestler K, and Starke D (1999) Thermogravimetric and differential scanning calorimetric analysis of natural fibres and polypropylene *Thermochimica Acta* **337**: 169-177.
198. Stevulova N, Hospodarova V, and Estokova A (2016) Study of thermal analysis of selected cellulosic fibres *Geo Sci. Eng.* **62**: 18-21.
199. Varma IK, Krishnan SRA, and Krishnamurthy S (1988) Effect of chemical treatment on thermal behavior of jute fibers *Text. Res. J.* http://doi.org/10.1177/004051758805800810.
200. Mortari DA, Britto MC, and Crnkovic P (2014) Correlation between activation energy and thermal decomposition yield of sugar cane bagasse under CO_2/O_2 and N_2/O_2 *Chem. Eng. Trans.* **37**: 31-36.
201. Ndazi S, Nyahumwa C, and Joseph T (2007) Chemical and thermal stability of rice husks against alkali treatment *BioResources* **3**(4): 1267-1277.
202. Rachini A, Troedec Le, Peyratout C, and Smith A (2009) Comparison of the thermal degradation of natural, alkali treated, and silane treated hemp fibers under air and an inert atmosphere *J. Appl. Polym. Sci.* **112**: 226-234.
203. White JE, Catallo WJ, and Legendre BL (2011) Biomass pyrolysis kinetics: A comparative critical review with relevant agricultural residue case studies *J. Anal. Appl. Pyrol.* **91**(1): 1-33.
204. Yao Fei, Qinglin W, Yong L, Weihong G, and Yanjun X (2008) Thermal decomposition of natural fibers: Global kinetic modeling with nonisothermal thermogravimetric analysis *Polym Degr Stab.* **93**: 90-98.
205. Na Lu and Oza S (2013) Effect of surface treatment of hemp fibers on the thermal stability of Hemp-PLA composites *Adv Mat Res*. **651**: 499-504.
206. Elammaran J, Sinin H, Rahman Md., Khusairy M, and Bakri B (2014) Investigation of fiber surface treatment on mechanical, acoustical, and thermal properties of belnut fiber polyester composites *Proceedings of the GCMM* **97**: 545-554.

207. Drzal T, Misra M, and Mohanty AK (2001) Surface modifications of natural fibers and performance of the resulting biocomposites: An overview *Compos. Interf.* **8**(5): 313-343.
208. Barkakaty BC (1976) Some structural aspects of sisal fibers *J. Appl. Polym. Sci.* **20**: 2921-2940.
209. Cazaurang MN, Peraza S, and Cruz-Ramos CA (1990) Dissoving-grade pulps from henequen fibers *Cellulose. Chem. Tech.* **24**: 629-638.
210. Sreekala MS, Kumaran MG, and Thomas S (1998) Oil palm fibers: Morphology, chemical composition, surface modification, and mechanical properties *J. Appl. Polym. Sci.* **66**: 821-835.
211. Ramadevi P, Sampathkumar D, Srinivasa C, and Bennehalli B (2012) Effect of alkali treatment on water absorption of single cellulosic abaca fiber *BioResources* **7**(3): 3515-3524.
212. Bismarck A, Mohanty AK, Askargorta I, Czapla S, Misra M, Hinrichsen G, and Springer J (2001) Surface characterization of natural fibers; surface properties and water uptake behavior of modified sisal and coir fibers *Green Chem.* **3**: 100-107.
213. Sgriccia N, Hawley MC, and Misra M (2008) Characterization of natural fiber surfaces and natural fiber composites *Composites: Part A* **39**: 1632-1637.
214. Ramanaiah K, Prasad AV, and Reddy K (2011) Thermal and mechanical properties of sansevieria green fiber reinforcement *Int. J. Polym. Anal. Charact.* **16**: 602-608.
215. Samal R and Bhuyan L (1994) Chemical modification of lignocellulosic fibers I. Functionality changes and graft copolymerization of acrylonitrile onto pineapple leaf fibers, their characterization and behavior *J. Appl. Polym. Sci.* **52**: 1675-1685.
216. Ray D, Sarkar BK, Rana AK, and Bose NR (2001) The mechanical properties of vinylester resin matrix composites reinforced with alkali treated jute fibers *Compos: Part A* **32**: 119-127.
217. Rachini A, Troedec Le, Peyratout C, and Smith A (2009) Comparison of the thermal degradation of natural, alkali treated, and silane treated hemp fibers under air and an inert atmosphere *J. Appl. Polym. Sci.* **112**: 226-234.
218. Maheshwari CU, Obi Reddy K, Muzenda E, Shukla M, and Varada Rajulu A (2013) Mechanical properties and chemical resistance of short tamarind fiber/unsaturated polyester composites: Influence of fiber modification and fiber content *Int. J. Polym. Anal. Charact.* **18**: 520-533.
219. Venkateshappa SC, Jayadevappa SY, and Puttiah PKW (2011) Mechanical behaviour of areca fiber reinforced epoxy composites *Advances in Polymer Technology* **31**(4): 319-330.
220. Shanmugam and Thiruchitrambalam M (2013) Static and dynamic mechanical properties of alkali treated unidirectional continuous Palmyra palm leaf stalk fiber/Jute fiber reinforced hybrid polyester composites *Mater. Des.* **97**: 533-542.

221. Shanmugam D and Thiruchitrambalam M (2013) Static and dynamic mechanical properties of alkali treated unidirectional continuous Palmyra palm leaf stalk fiber/Jute fiber reinforced hybrid polyester composites *Mater. Des.* **97**: 533-542.
222. Pandey JK, Ahn SH, Lee C, Mohanty AK, and Misra M (2010) Recent advances in the application of natural fiber based composites *Macromol. Mater. Eng.* **295**: 975-989.
223. Doan TTL, Gao SL, and Mader E (2006) Jute/Polypropylene composites I. Effect of matrix modification *Compos. Sci. Technol.* **66**: 952-963.
224. Herrera-Franco PJ and Valadez A (2005) A study of the mechanical properties of short natural fiber reinforced composites *Compos: Part B* **36**: 597-608.
225. Lopez E, Lopez M, Fonseca A, Nunez R, Rodrigue D, and Ortiz R (2016) Effect of fiber content and surface treatment on the mechanical properties of natural fiber composites produced by rotomolding *Compos. Interf.* http://dx.doi.org/10.1080/09276440.2016.1184556.
226. Chung TJ, Park JW, Lee HJ, Kwon HJ, Kim HJ, Lee YK, and Yin Tze W (2018) The improvement of mechanical properties, thermal stability, and water absorption resistance of an eco-friendly PLA/Kenaf biocomposite using acetylation, *Appl. Sci.* **8**: 1-13.
227. Jandas PJ, Mohanty S, Nayak SK, and Srivastava H (2011) Effect of surface treatments of banana fiber on the mechanical, thermal, and biodegradability properties of PLA/Banana fiber biocomposites *Polym. Compos.* 1689-1700 http://do.org/10.1002/pc.
228. Panyasart K, Chaiyut N, Amornsakchai T, and Santawitee O (2014) Effect of surface treatment on the properties of pineapple leaf fibers reinforced polyamide 6 composites *Energy Procedia,* **56**: 406-413.
229. Lu Na and Oza, S (2013) Effect of surface treatment of hemp fibers on the thermal stability of Hemp-PLA composites *Adv. Mater. Res.* **651**: 499-504.
230. Oza S, Ning H, Ferguson I, and Lu Na (2014) Effect of surface treatment on thermal stability of the hemp-PLA composites: Correlation of activation energy with thermal degradation *Compos: Part B* **67**: 227-232.
231. Jayamani E, Hamdan S, Rahman R, Khusairy M, and Bakri B (2014) Investigation of fiber surface treatment on mechanical, acoustical, and thermal properties of betelnut fiber polyester composites *Proceedings of the GCMM* **97**: 545-554.
232. Zhang K, Wang F, Liang W, Wang Z, Duan Z, Duan Z, and Yang B (2018). Thermal and mechanical properties of bamboo fiber reinforced epoxy composites *Polym.* **10**: 1-18.
233. Niu P, Liu B, Wei X, Wang X, and Yang J (2011) Study on mechanical properties and thermal stability of polypropylene/hemp fiber composites *J. Reinf. Plast. Compos.* **30**: 36-44.

234. Khalil HPS and Suraya NL (2011) Anhydride modification of cultivated kenaf bast fibers: morphological, spectroscopic, and thermal studies *BioResources* **6**(2): 1122-1135.
235. Misra RK, Saw SK, and Datta C (2011) The influence of fiber treatment on the mechanical behavior of Jute-Coir reinforced epoxy resin hybrid composite plate *Mech. Adv. Mater. Struc.* **18**: 431-445.
236. Goud G and Rao RN (2011) Effect of fiber content and alkali treatment on mechanical properties of *Roystonea regia*-reinforced epoxy partially biodegradable composites, *B. Mater. Sci.* **34**(7): 1575-1581.
237. Holbery J and Houston D (2006) Natural fiber reinforced polymer composites in automotive applications *J. Miner. Mater. Char. Eng.* **58**(11): 80-86.
238. http://www.ncsresins.com/unsaturated-polyester-resin.
239. Ferry JD (1980) Viscoelastic properties of polymers *Wiley: NY.*
240. Ray D, Sarkar BK, Das S, and Rana AK (2002) Dynamic mechanical and thermal analysis of vinyl-ester resin matrix composites reinforced with untreated and alkali treated jute fibers *Compos. Sci. Technol.* **62**: 911-917.
241. Clark RL, Craven MD, and Kander RG (1990) Nylon 66/poly(vinyl pyrrolidone) reinforced composites: 2: Bulk mechanical properties and moisture effects *Compos: Part A,* **30**: 37-48.
242. Mallarino S, Chailan J, and Vernet JL (2009) Interphase study in cyanate/glass fiber composites using thermomechanical analysis and micro-thermal analysis, *Composites Science and Technology,* **69**: 28-32.
243. Agarwal BD and Broutman LJ (1990) Analysis and performance of fiber composites *Wiley, New York* 2nd ed.
244. Ndazi B, Tesha J, and Bisanda E (2006) Some opportunity and challenges of producing bio-composites from non-wood residues *J. Mater. Sci.* **41**(21): 6984-6990.
245. Alwani MS, Khalil HPS, Sulaiman O, Islam Md, and Dungani R (2014) An approach to using agricultural waste fibres in biocomposite application: Thermogravimetric analysis and activation energy study *BioResources* **9**: 218-230.
246. Nasar MN and Mackay GDM (1984) Mechanism of thermal decomposition of lignin *Wood Fib. Sci.* **16**(3): 441-453.
247. Paiva JM and Frollini E (2006) Unmodified and modified surface sisal fibers as reinforcement of phenolic and lignophenolic matrices composites: thermal analysis of fibers and composites *Macromol. Mater. Eng.* **291**: 405-417.
248. Yang H, Yang R, Chen H, Lee DH, and Zheng C (2007) Characteristics of hemicellulose, cellulose, and lignin pyrolysis *Fuel* **86**(12): 1781-1788.
249. Ornaghi HL, Bolner AS, Fiorio R, Zattera AJ, and Amico SC (2010). Mechanical and dynamic mechanical analysis of hybrid composites molded by resin transfer molding *J. Appl. Polym. Sci.* **118**: 887-896.
250. Obaid N, Kortschot MT, and Sain M (2017) Understanding the stress relaxation behavior of polymers reinforced with short elastic fibers *Materials* http://doi.org/10.3390/ma10050472.

251. Manfredi LB, Rodriguez ES, Wladyka-Przbylak M, and Vaquez A (2006) Thermal degradation and fire resistance of unsaturated polyester modified acrylic resins and their composites with natural fibers *Polym. Degrad. Stab.* **91**: 255-261.
252. Pothan LA, Oommen Z, and Thomas S (2003) Dynamic mechanical analysis of banana fiber reinforced polyester composites *Compos. Sci. Technol.* **63:** 283-293.
253. Romanzini D, Lavoratti A, Ornagahi HL, Amico SC, and Zattera AJ (2013) Influence of fiber content on the mechanical and dynamic mechanical properties of glass/ramie polymer composites *Mater. Des.* **47**: 9-15.
254. Kim H, Yang H, and Kim H (2005) Biodegradability and mechanical properties of agro-flour filled polybutylene succinate biocomposites *J. Appl. Polym. Sci.* **97:** 1513-1521.
255. Sapuan SM and Abdalla HS A prototype knowledge-based system for the material selection of polymeric based composites for automotive components *Compos: Part A* **29**: 731-742.
256. Rwawiire S, Okello J, Habbi G (2014) Comparative evaluation of dynamic mechanical properties of epoxy composites reinforced with woven fabrics from Sanvieria fibres and banana fibres *Tekstilec* **57**: 315-320.
257. Parameswaranpillai J, Joseph G, Shinu KP, Jose S, Salim NV, and Hameed N (2015) Development of hybrid composites for automotive applications: effect of addition of SEBS on the morphology, mechanical, viscoelastic, crystallization, and thermal degradation properties of PP/PS – xGnP composites *RSC Adv.* **5**: 25634-25641.
258. Ayrilmis N, Jausombuti S, Fueangvivat V, Bauchongkaol P, and White R (2011) Coir fiber reinforced polypropylene composite panel for automotive interior applications *Fiber Polym.* **12**(7): 919-926.